

**EXTENDED HAAR WAVELET QUASILINEARIZATION  
METHOD FOR SOLVING BOUNDARY VALUE PROBLEMS**

**NOR ARTISHAM BINTI CHE GHANI**

**FACULTY OF SCIENCE  
UNIVERSITY OF MALAYA  
KUALA LUMPUR**

**2018**

**EXTENDED HAAR WAVELET QUASILINEARIZATION  
METHOD FOR SOLVING BOUNDARY VALUE  
PROBLEMS**

**NOR ARTISHAM BINTI CHE GHANI**

**THESIS SUBMITTED IN FULFILMENT OF THE  
REQUIREMENTS FOR THE DEGREE OF  
DOCTOR OF PHILOSOPHY**

**INSTITUTE OF MATHEMATICAL SCIENCES  
FACULTY OF SCIENCE  
UNIVERSITY OF MALAYA  
KUALA LUMPUR**

**2018**

UNIVERSITY OF MALAYA

ORIGINAL LITERARY WORK DECLARATION

Name of Candidate: **Nor Artisham Binti  
Che Ghani**

Matric No: **SHB130004**

Name of Degree: **Doctor of Philosophy (Mathematics and Science Philosophy)**

Title of ~~Project Paper/Research Report/Dissertation~~/Thesis ("this Work"):

**Extended Haar Wavelet Quasilinearization Method for Solving Boundary Value Problems**

Field of Study: **Numerical Methods**

I do solemnly and sincerely declare that:

- (1) I am the sole author/writer of this Work;
- (2) This Work is original;
- (3) Any use of any work in which copyright exists was done by way of fair dealing and for permitted purposes and any excerpt or extract from, or reference to or reproduction of any copyright work has been disclosed expressly and sufficiently and the title of the Work and its authorship have been acknowledged in this Work;
- (4) I do not have any actual knowledge nor do I ought reasonably to know that the making of this work constitutes an infringement of any copyright work;
- (5) I hereby assign all and every rights in the copyright to this Work to the University of Malaya ("UM"), who henceforth shall be owner of the copyright in this Work and that any reproduction or use in any form or by any means whatsoever is prohibited without the written consent of UM having been first had and obtained;
- (6) I am fully aware that if in the course of making this Work I have infringed any copyright whether intentionally or otherwise, I may be subject to legal action or any other action as may be determined by UM.

Candidate's Signature

Date

Subscribed and solemnly declared before,

Witness's Signature

Date

Name:

Designation:

# EXTENDED HAAR WAVELET QUASILINEARIZATION METHOD FOR SOLVING BOUNDARY VALUE PROBLEMS

## ABSTRACT

Several computational methods have been proposed to solve single nonlinear ordinary differential equations. In spite of the enormous numerical effort, however yet numerically accurate and robust algorithm is still missing. Moreover, to the best of our knowledge, only a few works are dedicated to the numerical solution of coupled nonlinear ordinary differential equations. Hence, a robust algorithm based on Haar wavelets and the quasilinearization process is provided in this study for solving both numerical solutions; single nonlinear ordinary differential equations and systems of coupled nonlinear ordinary differential equations, including two of them are the new problems with some additional related parameters. In this research, the generation of Haar wavelets function, its series expansion and one-dimensional matrix for a chosen interval  $[0, B)$  is introduced in detail. We expand the usual defined interval  $[0, 1)$  to  $[0, B)$  because the actual problem does not necessarily involve only limit  $B$  to one, especially in the case of coupled nonlinear ordinary differential equations. To achieve the target, quasilinearization technique is used to linearize the nonlinear ordinary differential equations, and then the Haar wavelet method is applied in the linearized problems. Quasilinearization technique provides a sequence of function which monotonic quadratically converges to the solution of the original equations. The highest derivatives appearing in the differential equations are first expanded into Haar series. The lower order derivatives and the solutions can then be obtained quite easily by using multiple integration of Haar wavelet. All the values of Haar wavelet functions are substituted into the quasilinearized problem. The wavelet coefficient can be calculated easily by using MATLAB software. The universal subprogram is introduced to calculate the integrals of Haar wavelets. This will provide small computational time. The initial

approximation can be determined from mathematical or physical consideration. In the demonstration problem, the performance of Haar wavelet quasilinearization method (HWQM) is compared with the existing numerical solutions that showed the same basis found in the literature. For the beginning, the computation was carried out for lower resolution. As expected, the more accurate results can be obtained by increasing the resolution and the convergence are faster at collocation points. For systems of coupled nonlinear ordinary differential equations, the equations are obtained through the similarity transformations. The transformed equations are then solved numerically. This is contrary to Runge-Kutta method, where the boundary value problems of HWQM need not to be reduced into a system of first order ordinary differential equations. Besides in terms of accuracy, efficiency and applicability in solving nonlinear ordinary differential equations for a variety of boundary conditions, this method also allow simplicity, fast and small computation cost since most elements of the matrices of Haar wavelet and its integration are zeros, it were contributed to the speeding up of the computation. This method can therefore serve as very useful tool in many physical applications.

**Keywords:** Haar wavelet, quasilinearization, single nonlinear ordinary differential equations, coupled nonlinear ordinary differential equations, boundary conditions

**PENAMBAHBAIKAN KAEDAH GELOMBANG KECIL HAAR  
PENGLINEARAN KUASI BAGI MENYELESAIKAN MASALAH NILAI  
SEMPADAN**

**ABSTRAK**

Beberapa kaedah pengiraan telah dicadangkan untuk menyelesaikan persamaan pembezaan biasa tak linear tunggal. Walaupun banyak usaha berangka, namun, algoritma berangka yang tepat dan mantap masih tiada. Selain itu, sepanjang pengetahuan kami, hanya beberapa kajian sahaja yang menyelesaikan penyelesaian berangka persamaan pembezaan biasa tak linear gandingan. Oleh itu, algoritma mantap berdasarkan gelombang kecil Haar dan proses penglinearan kuasi diselidiki dalam kajian ini bagi menyelesaikan kedua-dua penyelesaian berangka; persamaan pembezaan biasa tak linear tunggal dan sistem persamaan pembezaan biasa tak linear gandingan; ini termasuklah dua daripadanya merupakan masalah baharu dengan beberapa parameter tambahan yang bersesuaian. Dalam kajian ini, penjanaan gelombang fungsi Haar, pengembangan siri dan matriks dalam satu dimensi untuk selang  $[0, B)$  diperkenalkan secara terperinci. Selang dikembangkan daripada  $[0, 1)$  kepada  $[0, B)$  kerana masalah sebenar tidak semestinya melibatkan hanya had  $B$  kepada satu, terutama dalam kes persamaan pembezaan biasa tak linear gandingan. Untuk mencapai sasaran itu, teknik penglinearan kuasi digunakan bagi melinearkan persamaan pembezaan biasa tak linear, dan kemudian kaedah gelombang kecil Haar digunakan dalam masalah yang telah dilinearkan. Teknik penglinearan kuasi menyediakan turutan fungsi yang menumpu secara kuadratik berekanada kepada penyelesaian persamaan asal. Pembezaan tertinggi yang terdapat dalam persamaan pembezaan pada mulanya dikembangkan ke bentuk siri Haar. Pembezaan yang lebih rendah dan penyelesaiannya boleh diperolehi dengan mudah dengan menggunakan pelbagai kamiran gelombang kecil Haar. Semua nilai fungsi gelombang kecil Haar digantikan ke dalam masalah yang telah dilinearkan.

Pekali gelombang kecil boleh dihitung dengan mudah dengan menggunakan perisian MATLAB. Sub aturcara umum diperkenalkan untuk mengira kamiran gelombang kecil Haar. Ini akan memberikan masa pengiraan yang singkat. Penghampiran awal boleh ditentukan daripada pertimbangan matematik atau fizikal. Dalam masalah yang didemonstrasikan, prestasi kaedah gelombang kecil Haar penglinearan kuasi (HWQM) dibandingkan dengan penyelesaian berangka sedia ada menunjukkan asas yang sama seperti terdapat dalam literatur. Sebagai permulaan, pengiraan dijalankan dengan resolusi yang lebih rendah. Seperti yang dijangkakan, hasil yang lebih tepat diperolehi dengan meningkatkan resolusi dan penumpuan yang lebih cepat berlaku pada titik terpilih. Bagi sistem persamaan pembezaan biasa tak linear gandingan pula, persamaan diperolehi melalui transformasi persamaan. Persamaan yang dijelmakan kemudiannya diselesaikan secara berangka. Ini adalah bertentangan dengan kaedah Runge-Kutta, iaitu masalah nilai sempadan HWQM tidak perlu dijelmakan ke dalam sistem persamaan pembezaan biasa peringkat pertama. Selain dari segi ketepatan, kecekapan dan kesesuaian dalam menyelesaikan persamaan pembezaan biasa tak linear untuk pelbagai keadaan sempadan, kaedah ini mudah, kos pengiraan cepat dan kecil kerana kebanyakan unsur matriks gelombang kecil Haar dan kamirannya adalah sifar, ianya menyumbangkan kepada pengiraan yang cepat. Oleh itu, kaedah ini boleh menjadi perlaksanaan yang sangat berguna dalam banyak aplikasi fizikal.

**Kata kunci:** gelombang kecil Haar, penglinearan kuasi, persamaan pembezaan biasa tak linear tunggal, persamaan pembezaan biasa tak linear gandingan, keadaan sempadan

## ACKNOWLEDGEMENTS

Alhamdulillah, praise to Allah for the completion of this study.

I would like to express my profound sense of reverence and gratitude to my supervisors, Dr. Amran Hussin and Dr. Zailan Siri for guided me and had shown great dedication in helping me through the completion of this study. Their kindness and patience in supplementing my knowledge is unparalleled. From them, I have learn that doing research required as much as painful endeavor as a feeling of achievement.

A special thanks to my beloved family especially to my husband, my parents, siblings and all my family members for their pray, deepest love, continued support and endless patience in pursuit my aspirations through the years of study.

Not forget to my friends; late Dr. Nuradhiathy Abd. Razak from Universiti Malaysia Pahang and Dr. Ruhaila Kasmani from Pusat Asasi Sains, University of Malaya and others for their valuable advice.

I also would like to gratefully acknowledge the support given by the staff members of Institute of Mathematical Sciences, especially Mrs. Budiyah Yeop and Mr. Abd. Malek Osman for their support and assistance.

Last but not least, I would like to pay high regards to Ministry of Higher Education Malaysia, Financial Department and Human Resources Department from University of Malaya for their assistance and sponsorship during three years of study and Postgraduate Research Grant (RG397-17AFR) for aiding me to carry out my research smoothly.

## TABLE OF CONTENTS

Abstract .....	iii
Abstrak .....	v
Acknowledgements .....	vii
Table of Contents .....	viii
List of Figures .....	xii
List of Tables .....	xv
List of Symbols and Abbreviations .....	xviii
<b>CHAPTER 1: INTRODUCTION .....</b>	<b>1</b>
1.1 Overview of Thesis .....	1
1.2 Motivation .....	2
1.3 Scope of the Study .....	3
1.4 Research Objectives .....	4
1.5 Thesis Organization .....	5
<b>CHAPTER 2: LITERATURE REVIEW .....</b>	<b>8</b>
2.1 Literature Review on Haar Wavelet .....	8
2.2 Literature Review on Quasilinearization Technique .....	13
2.3 Literature Review on Haar Wavelet Quasilinearization Method .....	14
<b>CHAPTER 3: HAAR WAVELET QUASILINEARIZATION METHOD ...</b>	<b>15</b>
3.1 The Haar Wavelets .....	15
3.1.1 Introduction .....	15
3.1.2 Haar Wavelet Functions .....	16

3.1.3	Expanding Functions Into The Haar Wavelet Series .....	19
3.1.4	Haar Wavelet Matrix .....	21
3.1.5	Integration of Haar Wavelet Functions .....	22
3.2	Quasilinearization Technique .....	25
3.3	Numerical Method of Haar Wavelet Quasilinearization .....	27

**CHAPTER 4: SINGLE NONLINEAR ORDINARY DIFFERENTIAL**

	<b>EQUATION .....</b>	<b>31</b>
4.1	The Bratu Equation .....	31
4.1.1	Introduction .....	31
4.1.2	Numerical Solution .....	33
4.1.3	Results and Discussion .....	34
4.2	The Falkner-Skan Equation .....	43
4.2.1	Introduction .....	43
4.2.2	Numerical Solution .....	44
4.2.3	Results and Discussion .....	46
4.3	The Blasius Equation .....	57
4.3.1	Introduction .....	57
4.3.2	Numerical Solution .....	59
4.3.3	Results and Discussion .....	60
4.4	Conclusions.....	65

**CHAPTER 5: COUPLED NONLINEAR ORDINARY DIFFERENTIAL**

	<b>EQUATIONS .....</b>	<b>66</b>
5.1	Boundary Layer Flow and Heat Transfer Due to a Stretching Sheet .....	66
5.1.1	Introduction .....	66

5.1.2	Problem Formulation .....	68
5.1.3	Numerical Solution .....	70
5.1.4	Results and Discussion .....	74
5.2	Laminar Film Condensation .....	78
5.2.1	Introduction .....	78
5.2.2	Problem Formulation .....	79
5.2.3	Numerical Solution .....	81
5.2.4	Results and Discussion .....	83
5.3	Natural Convection Boundary Layer Flow .....	87
5.3.1	Introduction .....	87
5.3.2	Problem Formulation .....	87
5.3.3	Numerical Solution .....	89
5.3.4	Results and Discussion .....	91
5.4	Conclusions.....	97
<b>CHAPTER 6: COUPLED NONLINEAR ORDINARY DIFFERENTIAL EQUATIONS WITH SOME ADDITIONAL PARAMETERS .....</b>		<b>98</b>
6.1	Heat Transfer and Boundary Layer Flow of a Viscoelastic Fluid Above a Stretching Plate with Velocity Slip Boundary .....	98
6.1.1	Introduction .....	98
6.1.2	Problem Formulation .....	100
6.1.3	Numerical Solution .....	103
6.1.4	Results and Discussion .....	105

6.2	Convective Heat Transfer in Maxwell Fluid with Cattaneo-Christov Heat Flux Model Past a Stretching Sheet in the Presence of Suction and Injection .....	112
6.2.1	Introduction .....	112
6.2.2	Problem Formulation .....	113
6.2.3	Numerical Solution .....	115
6.2.4	Results and Discussion .....	118
6.3	MHD Flow of Cattaneo-Christov Heat Flux Model for Maxwell Fluid Past a Stretching Sheet with Heat Generation/Absorption .....	124
6.3.1	Introduction .....	124
6.3.2	Problem Formulation .....	125
6.3.3	Numerical Solution .....	126
6.3.4	Results and Discussion .....	129
6.4	Conclusions.....	136
	<b>CHAPTER 7: CONCLUSIONS AND FUTURE WORK .....</b>	<b>140</b>
7.1	Conclusions.....	140
7.2	Future Work .....	142
	References .....	144
	List of Publications and Papers Presented .....	162
	Appendix A: Haar Wavelet Functions and Repeated Integration of Haar Wavelet..	163

## LIST OF FIGURES

Figure 3.1	: First four Haar functions .....	18
Figure 3.2	: The integration of Haar wavelet functions for $m = 4$ .....	24
Figure 3.3	: Algorithm for solving nonlinear ODE by using HWQM .....	29
Figure 4.1	: Comparison of absolute errors for (a) $\lambda = 1$ , (b) $\lambda = 2$ and (c) $\lambda = 3.51$ .....	40
Figure 4.2	: Comparison of exact solution and numerical solution by HWQM for (a) first, (b) second (c) third iterations at $m = 2^{11}$ when $\lambda = 1$ .....	41
Figure 4.3	: HWQM solution for (a) $f(\eta)$ and (b) $f'(\eta)$ when $\beta = 0.5$ at different iterations .....	48
Figure 4.4	: Comparison of $ \log_{10}(\text{absolute errors}) $ for (a) $f(\eta)$ and (b) $f'(\eta)$ with $\beta = 0.5$ .....	49
Figure 4.5	: HWQM solution for (a) $f(\eta)$ and (b) $f'(\eta)$ when $\beta = 1$ at different iterations .....	51
Figure 4.6	: Comparison of $ \log_{10}(\text{absolute errors}) $ for (a) $f(\eta)$ and (b) $f'(\eta)$ with $\beta = 1$ .....	52
Figure 4.7	: HWQM solution for (a) $f(\eta)$ and (b) $f'(\eta)$ when $\beta = 1.6$ at different iterations .....	54
Figure 4.8	: Comparison of $ \log_{10}(\text{absolute errors}) $ for (a) $f(\eta)$ and (b) $f'(\eta)$ with $\beta = 1.6$ .....	55
Figure 4.9	: HWQM solution of $f(\eta)$ for different iterations .....	62
Figure 4.10	: HWQM solution for $f(\eta)$ , $f'(\eta)$ and $f''(\eta)$ .....	64
Figure 5.1	: Physical model of boundary layer flow and heat transfer due to a stretching sheet .....	69
Figure 5.2	: HWQM for (a) $f'(\eta)$ and (b) $\theta(\eta)$ case of BLFHTSS with different values of $A$ when $m = 512$ , $L = 10$ and $\text{Pr} = 1$ .....	75
Figure 5.3	: HWQM for $\theta(\eta)$ , case of BLFHTSS with different values of $\text{Pr}$ when $A = 0.8$ , $m = 512$ and $L = 10$ .....	76
Figure 5.4	: Physical model and coordinate system of laminar film condensation of saturated steam .....	80

Figure 5.5	: HWQM for $f(\eta)$ , case of LFC when $m = 128$ and $L = 7$ at different values of Pr .....	85
Figure 5.6	: HWQM for $\theta(\eta)$ , case of LFC when $m = 128$ and $L = 6$ at different values of Pr .....	86
Figure 5.7	: HWQM for $f'(\eta)$ , case of LFC when $m = 128$ and $L = 7$ at different values of Pr .....	86
Figure 5.8	: HWQM for $\theta'(\eta)$ , case of LFC when $m = 128$ and $L = 7$ at different values of Pr .....	87
Figure 5.9	: Physical model of natural convection boundary layer flow .....	88
Figure 5.10	: HWQM for $f(\eta)$ and $\theta(\eta)$ , case of NCBLF when $m = 256$ , $L = 7$ and Pr = 1500 .....	93
Figure 5.11	: HWQM for (a) $f(\eta)$ and (b) $\theta(\eta)$ , case of NCBLF when $m = 256$ and $L = 1$ at Pr = 40,000 and Pr = 100,000 .....	94
Figure 5.12	: HWQM for (a) $f(\eta)$ and (b) $f'(\eta)$ , case of NCBLF when $m = 256$ and $L = 7$ for different values of Pr .....	95
Figure 5.13	: HWQM for (a) $\theta(\eta)$ and (b) $\theta'(\eta)$ , case of NCBLF when $m = 256$ and $L = 7$ for different values of Pr .....	96
Figure 6.1	: Profiles of $f(\eta)$ and $f'(\eta)$ for different values of $\beta$ when $\gamma = \text{Pr} = b = 1$ , $m = 256$ and $L = 6$ .....	107
Figure 6.2	: Profiles of $\theta(\eta)$ for different values of $\beta$ when $\gamma = \text{Pr} = b = 1$ , $m = 256$ and $L = 7$ .....	107
Figure 6.3	: Profiles of $f'(\eta)$ for different values of $b$ when $\gamma = \text{Pr} = \beta = 1$ , $m = 256$ and $L = 8$ .....	108
Figure 6.4	: Profiles of $\theta(\eta)$ for different values of $b$ when $\gamma = \text{Pr} = \beta = 1$ , $m = 256$ and $L = 8$ .....	108
Figure 6.5	: Profiles of $\theta(\eta)$ for different values of $\gamma$ when $\beta = b = \text{Pr} = 1$ , $m = 256$ and $L = 8$ .....	109
Figure 6.6	: Profiles of $\theta(\eta)$ for different values of Pr when $\beta = b = \gamma = 1$ , $m = 256$ and $L = 12$ .....	110
Figure 6.7	: Velocity and temperature profiles for different values of $\gamma$ when $f_w = 0$ , $m = 512$ , $L = 7$ , Pr = 1 and $\beta = 0.1$ .....	121
Figure 6.8	: Velocity and temperature profiles for different values of $\beta$ when $f_w = 0$ , $m = 512$ , $L = 7$ , Pr = 1 and $\gamma = 0.5$ .....	122
Figure 6.9	: Velocity and temperature profiles for different values of Pr when $f_w = 0$ , $m = 512$ , $\beta = \gamma = 1$ and $L = 7$ .....	122

Figure 6.10	: Velocity and temperature profiles for different values of $f_w$ when $m = 512, L = 7, \beta = 0.2, \gamma = 0.1$ and $Pr = 1$ .....	123
Figure 6.11	: Velocity and temperature profiles for different values of $\beta$ when $m = 512, L = 7, M = 0.2, f_w = 0, Q = 0.2, \gamma = 0.3$ and $Pr = 1.4$ .....	131
Figure 6.12	: Velocity and temperature profiles for different values of $M$ when $m = 512, L = 7, \beta = 0.4, f_w = 0, Q = 0.2, \gamma = 0.3$ and $Pr = 1.4$ .....	132
Figure 6.13	: Velocity and temperature profiles for different values of $Q$ when $m = 512, L = 7, \beta = 0.2, f_w = 1, M = 0.2, \gamma = 0.2$ and $Pr = 1$ .....	133
Figure 6.14	: Velocity and temperature profiles for different values of $\gamma$ when $m = 512, L = 7, \beta = 0.4, f_w = 0, M = 0.2, Q = 0.2$ and $Pr = 1$ .....	134
Figure 6.15	: Velocity and temperature profiles for different values of $Pr$ when $m = 512, L = 7, \beta = 0.4, f_w = 0, M = 0.2, Q = 0.2$ and $\gamma = 0.3$ .....	135
Figure 6.16	: Velocity and temperature profiles for different values of $f_w$ when $m = 512, L = 7, \beta = 0.4, M = 0.2, Q = 0.2, Pr = 1$ and $\gamma = 0.3$ .....	136

## LIST OF TABLES

Table 4.1	: Comparison between HWQM with exact solutions for different values of $\lambda$ .....	36
Table 4.2	: Comparison of absolute errors between HWQM with other methods for $\lambda = 1$ .....	37
Table 4.3	: Comparison of absolute errors between HWQM with other methods for $\lambda = 2$ .....	38
Table 4.4	: Comparison of absolute errors between HWQM with other methods for $\lambda = 3.51$ .....	39
Table 4.5	: Convergence error at three iterations when $\lambda = 1$ and $m = 2^{11}$ ...	42
Table 4.6	: Comparison of CPU time (sec) between RKHSM and HWQM when $L = 1$ and $m = 8$ .....	42
Table 4.7	: Comparison between HWQM with RKM and OHAM for $f(\eta)$ and $f'(\eta)$ when $\beta = 0.5$ .....	47
Table 4.8	: Comparison of absolute errors between OHAM and HWQM for $f(\eta)$ and $f'(\eta)$ when $\beta = 0.5$ .....	47
Table 4.9	: Comparison between HWQM with RKM and OHAM for $f(\eta)$ and $f'(\eta)$ when $\beta = 1$ .....	50
Table 4.10	: Comparison of absolute errors between OHAM and HWQM for $f(\eta)$ and $f'(\eta)$ when $\beta = 1$ .....	50
Table 4.11	: Comparison between HWQM with RKM and OHAM for $f(\eta)$ and $f'(\eta)$ when $\beta = 1.6$ .....	53
Table 4.12	: Comparison of absolute errors between OHAM and HWQM for $f(\eta)$ and $f'(\eta)$ when $\beta = 1.6$ .....	53
Table 4.13	: Comparison of $f''(0)$ between HWQM with RKM and OHAM for different values of $\beta$ .....	56
Table 4.14	: Comparison of CPU time (sec) between CCF and HWQM for different values of $\beta$ when $L = 6$ and $m = 8$ .....	56
Table 4.15	: Comparison between HPM, LTNHPM, Howarth and HWQM for $f(\eta)$ .....	61
Table 4.16	: Comparison between Howarth, LTNHPM and HWQM for the velocity profile, $f'(\eta)$ at the selected values of $\eta$ .....	63
Table 4.17	: Comparison between Howarth (1938) and HWQM for $f''(\eta)$ .....	64

Table 4.18	: Comparison between HWQM, Mohammed (2014), Asaithambi (2005) and Howarth (1938) results for the wall shear stress, $f''(0)$ with $m = 128$ and $L = 8$ .....	64
Table 5.1	: Comparison between HWQM with RKM and HWCM for $f(\eta)$ and $\theta(\eta)$ of BLFHTSS with $m = 256$ , $A = 20$ , $Pr = 1$ and $L = 1$ ...	74
Table 5.2	: The values of the heat transfer $-\theta'(0)$ for $A = 0$ at steady-state flow when $L = 10$ and $Pr = 1$ .....	77
Table 5.3	: Comparison of values between HWQM with quasilinearization technique and Keller-box method for skin friction coefficient $-f''(0)$ and heat transfer $-\theta'(0)$ of BLFHTSS when $L = 10$ .....	77
Table 5.4	: CPU time (sec) for different values of $Pr$ when $L = 1$ , $A = 0$ and $m = 8$ .....	78
Table 5.5	: Comparison between HWQM with RKM and HWCM for $f(\eta)$ and $\theta(\eta)$ of LFC with $m = 128$ , $Pr = 100$ and $L = 1$ .....	84
Table 5.6	: Comparison of CPU time (sec) between HWCM, RKM and HWQM for different values of $Pr$ when $L = 1$ and $m = 8$ .....	84
Table 5.7	: Comparison between HWQM with RKM and HWCM for $f(\eta)$ and $\theta(\eta)$ of NCBLF with $m = 256$ , $Pr = 3$ and $L = 1$ .....	91
Table 5.8	: Comparison between HWQM with FDM and HWCM for $f''(0)$ of NCBLF when $Pr = 0.72$ .....	92
Table 5.9	: Comparison of CPU time (sec) between HWCM, RKM and HWQM for different values of $Pr$ when $L = 1$ and $m = 8$ .....	92
Table 6.1	: Comparison the values of $-f''(0)$ between exact solution and HWQM at $\beta = 0$ , $b = 0$ , $m = 512$ and $L = 6$ .....	111
Table 6.2	: Comparison of local Nusselt number $-\theta'(0)$ in the case of Newtonian fluid ( $\beta = \gamma = b = 0$ ) with $m = 512$ and $L = 6$ for different values of $Pr$ .....	111
Table 6.3	: The values of $-f''(0)$ for HWQM with different values of $\beta$ when $Pr = 1$ , $b = 1$ , $\gamma = 0.1$ , $m = 512$ and $L = 6$ .....	111
Table 6.4	: The values of $-\theta'(0)$ for HWQM with different values of $\beta$ and $\gamma$ when $Pr = 1$ , $b = 1$ , $m = 512$ and $L = 6$ .....	112
Table 6.5	: Comparison the values of $-f''(0)$ between exact solution and HWQM for different values of $f_w$ at $\beta = 0$ , $Pr = 1$ , $L = 5$ , $\gamma = 0.1$ and $m = 512$ .....	118
Table 6.6	: The values of HWQM for $-f''(0)$ with different values of $\beta$ when $Pr = 1$ , $L = 5$ , $f_w = 0$ , $\gamma = 0.1$ and $m = 512$ .....	119

Table 6.7	: The values of HWQM for $-\theta'(0)$ with different values of $\beta$ and $\gamma$ when $Pr = 1, L = 5, f_w = 0$ and $m = 512$ .....	119
Table 6.8	: The values of HWQM for $-f''(0)$ and $-\theta'(0)$ with different values of $\beta$ and $f_w$ (impermeable surface and suction) when $Pr = 1, \gamma = 0.5, L = 5$ and $m = 512$ .....	120
Table 6.9	: The values of HWQM for $-f''(0)$ and $-\theta'(0)$ with different values of $\beta$ and $f_w$ (injection) when $Pr = 1, \gamma = 0.5, L = 5$ and $m = 512$ .....	120
Table 6.10	: Comparison the values of $-f''(0)$ with previous studies for different values of $\beta$ when $f_w = 0, M = 0, L = 7, Pr = 1, Q = 0, \gamma = 0.2$ and $m = 512$ .....	129
Table 6.11	: Comparison the values of $-\theta'(0)$ with previous study when $f_w = 0, M = 0, Q = 0, Pr = 1, \beta = 0.5, \gamma = 0.3, L = 7$ and $m = 512$ .....	129
Table 6.12	: Comparison the values of $-f''(0)$ with previous study for different values of $M$ when $f_w = 0, \beta = 0, \gamma = 0.2, Pr = 1, L = 8$ and $m = 512$ .....	130
Table 6.13	: The values of HWQM for $-f''(0)$ and $-\theta'(0)$ when $Pr = 2, \beta = 0.1, \gamma = 0.2, m = 512$ and $L = 5$ .....	130

## LIST OF SYMBOLS AND ABBREVIATIONS

$A$	:	Dimensionless measure of the unsteadiness
$B_0$	:	Transverse magnetic field
$b$	:	Slip coefficient
$c$	:	Stretching rate
$c_f$	:	Skin friction coefficient
$c_i$	:	Haar wavelet coefficient
$c_p$	:	Specific heat
$\mathbf{c}_m^T$	:	Haar coefficient vector
$e_m$	:	Error of approximation
$\mathbf{H}_m(x)$	:	Haar function vector
$h_0(x)$	:	Haar wavelet scaling function
$h_1(x)$	:	Haar mother wavelet function
$k$	:	Thermal conductivity
$L$	:	Large positive number
$M$	:	Magnetic field parameter
$m$	:	Level of Haar wavelet
Pr	:	Prandtl number
$p_{i,v}$	:	Repeated integration of Haar wavelet
$Q_0$	:	Heat generation/absorption coefficient
$\mathbf{q}$	:	Heat flux vector
$q_w$	:	Heat flux at the surface of the sheet
$q_{w_0}$	:	Characteristic wall heat flux
$T$	:	Temperature of fluid

$T_w$	:	Temperature of surface
$T_s$	:	Saturated temperature of the film
$T_\infty$	:	Temperature of ambient
$t$	:	Time
$u$	:	Velocity component along $x$ -axis
$u_w$	:	Velocity of the moving sheet
$\mathbf{V}$	:	Velocity vector
$v$	:	Velocity component along $y$ -axis
$x_j$	:	Collocation points

### **Greek Symbols**

$\alpha$	:	Thermal diffusivity of the fluid
$\beta$	:	Elasticity number
$\gamma$	:	Non-dimensional heat flux relaxation time
$\eta$	:	Similarity variable
$\theta$	:	Non-dimensional temperature
$\psi$	:	Stream function
$\nu$	:	Kinematic viscosity
$\lambda_1$	:	Fluid relaxation time
$\lambda_2$	:	Thermal relaxation time
$f_w$	:	Suction parameter
$\sigma_v$	:	Tangential momentum
$\rho$	:	Density of the fluid

### **Abbreviations**

ADM	:	Adomian decomposition method
BLFHTSS	:	Boundary layer flow and heat transfer due to a stretching sheet

BVP	:	Boundary value problem
CCF	:	Chebyshev cardinal functions
FDM	:	Finite difference method
HAM	:	Homotopy analysis method
HPM	:	Homotopy perturbation method
HWCM	:	Haar wavelet collocation method
HWQM	:	Haar wavelet quasilinearization method
LFC	:	Laminar film condensation
LTNHPM	:	Laplace transform with new homotopy perturbation method
MATLAB	:	Matrix laboratory
MHD	:	Magnetohydrodynamic
NCBLF	:	Natural convection boundary layer flow
ODE	:	Ordinary differential equation
OSOMRI	:	One-shot operational matrix for repeated integration
PDE	:	Partial differential equation
QLM	:	Quasilinearization method
RKHSM	:	Reproducing kernel Hilbert space method
RKM	:	Runge-kutta method
UCM	:	Upper-convected Maxwell
VIM	:	Variational iteration method

## CHAPTER 1: INTRODUCTION

### 1.1 Overview of Thesis

There are several well-known numerical methods for solving boundary value problems (BVPs) in ordinary differential equations (ODEs) such as homotopy perturbation method (HPM), finite difference method (FDM), shooting method and collocation method. The most popular numerical method for solving BVPs is shooting method. It is a successive substitution method by guessing the initial condition which satisfies the desired boundary condition. Unfortunately, shooting method is inefficient as they may often converge quite slowly and increases the computer time because of the wrong guess (Al-Bayati et al., 2011). Furthermore, the numerical errors can be enlarged. On the other hand, shooting method is not always computationally suitable for the whole range of practical BVPs, particularly those on a very long or infinite intervals. Hence, it seems to offer less hope for some of the practical engineering problems (Lee & Kim, 2005; Michalik et al., 2009).

Alternatively, BVPs can be solved by using collocation method since it often gives a better performance than other numerical methods (Boyd, 2000). However, the choice of the collocation points greatly influence the effectiveness of this method. Ghani et al. (2014) have tested three different Haar wavelet collocation methods to solve ODEs, namely repeated application of Haar operational matrix, one-shot operational matrix for repeated integration (OSOMRI) and collocation method. It turn out that the collocation method by Lepik (2005) is superior in terms of accuracy. To apply this method, it consist of reducing the problem to a set of algebraic equations by first expanding the terms, which have maximum derivatives, given in the equation as Haar function with unknown coefficients. Subsequent integration give the lower derivatives and  $f(x)$ . Substituting the values in the given equation gives the coefficients and hence the solution.

Many numerical methods have been used for solving nonlinear system of second order boundary value problems, such as FDM and adjoint operator methods (Na, 1979), reproducing Kernal space (Geng & Cui, 2007), variational iteration method (Lu, 2007), third degree B-spline (Caglar & Caglar, 2009), sinc-collocation method (Dehghan & Saadatmandi, 2007) and Chebyshev finite difference method (Saadatmandi & Farsangi, 2007). Furthermore, there continuous to be interest in solving higher order as indicated by the recent appearance (Mandelzweig & Tabakin, 2001; Sharidan et al., 2006; Ahmed et al., 2010; Rashidi & Pour, 2010; Islam et al., 2011; Kaur et al., 2011; Aminikhah, 2012; Kaur et al., 2013).

In numerical analysis, the discovery of Haar wavelet method has proven to be a useful tool for solving a variety of ODEs, partial differential equations (PDEs), integral and fractional order differential equations. But, Haar wavelets or rather piecewise constant functions in general, are not widely used for solving system of coupled nonlinear ODEs. In view of successful application of Haar wavelet quasilinearization method (HWQM) in numerical solution of single nonlinear ODEs (Kaur et al., 2011; Jiwari, 2012; Kaur et al., 2013), we now extend the method to solve system of coupled nonlinear ODEs arising in natural convection boundary layer flows problems with high Prandtl ( $Pr$ ) number and heat and mass transfer problems related to the Cattaneo-Christov heat flux model for boundary layer flow of Maxwell fluid. The quasilinearization procedure replaces the original nonlinear equation by a sequence of linear equations and Haar wavelets procedure is exploited to solve these linear boundary value problems.

## 1.2 Motivation

- a. Most of the studies on Haar wavelet collocation method are based on the interval  $[0, 1)$ . This give limitations to our ultimate goal as the integration involved in

differential equation does not necessarily limited to the interval between zero to one. Therefore, it is convenient to derive the Haar wavelet functions that can generalized the whole domain of Haar series expansion. On the other hand, the boundary layer fluid flow problems and heat and mass transfer problems deal with sufficiently large number of infinite intervals.

- b. Haar wavelets are made up of pairs of piecewise constant functions and are mathematically the simplest among all the wavelet families. One of good feature of the Haar wavelets is the possibility to integrate them analytically arbitrary times. This feature is required for solving differential equations.
- c. Numerous applications of ODEs and PDEs have appeared in many areas of physics and engineering. For most nonlinear system of ODEs, the exact solutions are not known. Therefore, different numerical methods have been applied for providing approximate solutions. However, most of the existing methods such as homotopy perturbation method (HPM), the variational iteration method (VIM), the Adomian decomposition method (ADM), finite difference method (FDM) and shooting method have their own limitations and weaknesses. Therefore, the capability of HWQM is introduced in this study, since no literature discussed the analytical solutions for solving systems of coupled nonlinear ODEs by using HWQM.
- d. The beauty of the mathematical construction of Haar wavelets and its utility in practical applications attract nowadays researchers from both pure and applied science. Hence, this research may help practitioners in science and engineering for finding an alternative formulation to solve problem in boundary value problems.

### **1.3 Scope of the Study**

The main focus on this work is to solve single nonlinear ODEs and systems of coupled nonlinear ODEs arising in natural convection boundary layer flows problems with high

Pr number and heat and mass transfer problems related to the Cattaneo-Christov heat flux model for boundary layer flow of Maxwell fluid by using HWQM. These two types of nonlinear ODEs extensively used in a large variety of applications.

In the process of constructing a new algorithm for this method, we have derived generalized Haar wavelet functions and their integration for a chosen domain, numerically and graphically. We also set up a universal subprogram for Haar wavelet functions and repeated integration of Haar wavelet by using matrix laboratory (MATLAB) software. According to the HWQM, the nonlinear ODE is converted into linear discretized equation with the help of quasilinearization technique and apply the Haar wavelet method at each iteration of quasilinearization technique to get the solution.

The derivation of generalized Haar wavelet and the multiple integration for solving the two types of nonlinear ODEs are extended. The numerical stability and error analysis of this method has been given in the literature. Hence, to justify the accuracy of these numerical results, a comparison with analytical solution given by others is being employed. For single nonlinear ODEs, the difference between the proposed method and the exact solution is shown by absolute error.

#### **1.4 Research Objectives**

The objectives of this research are;

- a. to study the Haar wavelets collocation method in extended interval  $[0, B)$ ,
- b. to develop a simple algorithm combining the method of Haar wavelet and quasilinearization to solve nonlinear two-point boundary value problems,
- c. to validate the effectiveness of HWQM in solving single nonlinear ODEs and coupled nonlinear ODEs,

- d. to compare the efficiency of HWQM with the existing numerical methods found in the literature,
- e. to apply HWQM to solve single nonlinear ODEs and systems of coupled nonlinear ODEs arising in natural convection boundary value problems

## 1.5 Thesis Organization

This thesis consists of seven chapters including this chapter and is organized as follows:

Chapter 1 introduced in brief some of well known numerical method for solving BVPs in ODEs including nonlinear systems of second order BVPs that found in the literature. An overview of the method that we used throughout the thesis is also given. Then, we list down what inspired us to study or get involved in this research, and a rough description of our scope of research are listed. Lastly, the research objectives are highlighted.

Chapter 2 consists of three parts. The overview of Haar wavelet, quasilinearization technique and combination of method Haar wavelet and quasilinearization are discussed in this chapter. A few well known orthogonal function that has been used by some scholars are listed. Then, a specific orthogonal function namely Haar basis function is focused. This selection of orthogonal function is justified by listing down a few of its advantages compared to other orthogonal functions. Some of the successful applications of Haar wavelets by some researchers also discussed in this part. Further, reviewed on quasilinearization technique by giving explanation of the previous work lies in the application of quasilinearization technique. At the end of this chapter, review on HWQM is provided.

In Chapter 3, the mathematical background of Haar wavelet method, quasilinearization technique and combination of HWQM are illustrated which are needed to understand the concept followed in this thesis. Most of the literature defined

Haar wavelet and its integration within the interval  $[0, 1)$ . Therefore, the generalized of Haar wavelet and its integration are derived which could cater the Haar series expansion domain greater than one. On the other hand, the detail of quasilinearization formula is also provided. The remainder of the chapter presents an efficient new algorithm and step by step for easy understanding the concept of HWQM for solving nonlinear ordinary differential equations.

In Chapter 4, the proposed method that discussed in Chapter 3 is applied to three problems of single nonlinear ordinary differential equation, namely; Bratu equation, Falkner-Skan equation and Blasius equation. The usage of generalized Haar basis and its integration together with new algorithm are very helpful hence enable us in finding the solution quickly. Their numerical results are shown and compared with the existing numerical methods and exact solution given numerically and displayed graphically. The discussion of these findings are also written in this chapter.

Chapter 5 presents a methodology for applying HWQM to three different types of coupled nonlinear differential equations related to the natural convection boundary layer fluid flow problems with high Pr number, namely; boundary layer flow and heat transfer due to a stretching sheet (BLFHTSS), laminar film condensation (LFC) and natural convection boundary layer flow (NCBLF). The ordinary differential equations are obtained based on similarity transformations as introduced in the literature. The effects of variation of Pr on heat transfer are investigated. Simulation results were compared with those obtained by another researcher's work.

Numerical solutions for three different types of coupled nonlinear differential equations with some additional parameters that are related the Cattaneo-Christov heat flux model for boundary layer flow of Maxwell fluid are shown in Chapter 6. The first problem is in the presence of velocity slip boundary and while the last two problems are new problems in the presence of suction, injection and heat generation/absorption. The

numerical solutions of three different problems are discussed numerically and graphically.

Finally, Chapter 7 concludes the overall works and contributions of the study in numerical analysis of fluid flow problems and heat and mass transfer problems. Some recommendations for future work are proposed at the end of this thesis.

University of Malaya

## CHAPTER 2: LITERATURE REVIEW

### 2.1 Literature Review on Haar Wavelet

The approximation of orthogonal functions played an important role in the solution of problem such as parameter identification analysis or optimal control in the last two decades. Subsequently, the set of orthogonal functions widely applied in solving bilinear systems (Cheng & Hsu, 1982), the parameter identification of linear lumped time invariant systems (Mouroutsos & Paraskevopoulos, 1985) and multi-input and multi-output systems (Hwang, 1997). The main feature of this technique is it converts the differential equation into a set of algebraic equations. Among orthogonal basis functions that have been given special attention are Walsh function (Chen & Hsiao, 1975), cosine-sine and exponential function (Paraskevopoulos, 1987), block pulse function (Chi-Hsu, 1983), Legendre mother wavelets (Khellat & Yousefi, 2006), Chebyshev wavelet (Babolian & Fattahzadeh, 2007) and Haar wavelet (Gu & Jiang, 1996; Chen & Hsiao, 1997). However, wavelet basis is the most attractive method due to good approximation and fast convergence of the wavelet sequence.

Most of the orthogonal wavelet systems are defined recursively and generated with two operations; translations and dilations of a single function, known as the mother wavelet. Wavelet systems with fast transform algorithm, such as Daubechies wavelet (Daubechies, 1988) do not have explicit expression, and as such, analytical differentiation or integration is not possible. Therefore, any attempt to solve differential equations with this orthogonal wavelet usually will be complicated and difficult to apply. Meanwhile Legendre multi-wavelets are the alteration of Haar's wavelet. They are piecewise linear and have short support, however they lack of smoothness and are discontinuous. On the other hand, they also localized in time but not in the frequency due to their discontinuity. Chebyshev wavelets had been applied by Ghasemi and Tavassoli Kajani (2011) to obtain the solution of time-varying delay systems. They

proved that the Chebyshev wavelets provide an exact solution only for the cases when the exact solutions are polynomials.

However, all these numerical computations share a number of advantages. One of them is the ability of finding the solution with only matrices manipulation rather than performing integration or differentiation in a conventional ways. Another advantage is the capability of transforming the matrices into a sparse matrix and small number of significant coefficients (Hariharan & Kannan, 2011). This is the main factor that reduces computational time. This advantage remains even if big matrix size is involved whereby big matrix size usually requires large computer storage and enormous number of arithmetic operations (Lepik & Tamme, 2004).

Wavelets became a requisite mathematical tool in many investigations and have numerous applications. The main field of applications of wavelet analysis is analysis and processing of different class of non-stationary (in time) or inhomogeneous (in space) signals. On the other hand, physics applications of wavelets are so numerous. It has been used in theoretical studies in functional calculus, renormalization in gauge theories, conformal field theories, nonlinear chaoticity and in practical fields such as quasicrystals, meteorology, acoustics, seismology, nonlinear dynamics of accelerators, turbulence, structure of surfaces and many more (Dremin et al., 2001).

Wavelets also proved to be an extremely useful mathematical method for analyzing complicated physical signals at various scales and definite locations. In medicine and biology fields, the discovery of wavelets have proven to be a useful tool for decoding information hidden in one dimensional function especially in analysis of heartbeat intervals, electrocardiogram (ECG), electroencephalogram (EEG) and deoxyribonucleic acid (DNA). Recognition of different shapes of biological objects is another problem which can be solved with the help of wavelet analysis (Dremin et al., 2001).

Another use of wavelets is in application of data compression (Dremin et al., 2001). It help to store the data spending as low memory capacity as possible or to transfer it at a low cost using smaller packages. This is commonly used by Federal Bureau of Investigation (FBI), United State of America for pattern recognition and saving a lot of money on computer storage of fingerprints. Related to pattern recognition is the problem of microscope focusing. This can be solved by resolving well focused image from that with diffused contours.

In this study, Haar wavelet basis function and its integral will be considered. Among the wavelet families, which are defined by an analytical expression, special attention deserves the Haar wavelets since they are the simplest possible wavelet function with a compact support, which means that it vanishes outside of a finite interval. In numerical analysis, the discovery of compactly supported wavelets have proven to be a useful tool for the approximation of functions, where a short support makes approximation analysis local. However, the technical disadvantage of the Haar wavelet is it contains piecewise constant functions which means that it is not continuous and hence at the points of discontinuity the derivatives does not exist.

Since Haar wavelets are not continuous, there are two strategies to fix this situation. One way is proposed by Cattani (2001) where he regularized the Haar wavelets with interpolating splines. But this step complicates the solution, thus the simplicity of Haar wavelets are no longer beneficial. Another strategy is introduced by Chen and Hsiao (1997) where the highest derivatives appearing in the differential equations are first expanded into Haar series. The lower order derivatives and the solutions can be obtained quite easily by using Haar operational matrix of integration.

Another advantageous features of Haar wavelet method at the chosen collocation points that can be summarized in the previous literature. Some of them are;

- a. it provide high accuracy solution for a small number of grid points,

- b. less time consuming is needed since the calculation for the integrals of the wavelet functions can be calculated at once (universal subprograms can be build together) and are used in the subsequent computations repeatedly. Here the matrix programs of MATLAB are very effective,
- c. this method is very convenient for solving boundary value problems defined on a very long interval,
- d. this method does not require conversion of a boundary value problem into initial value problem where it is not integrated as an initial value problem with guesses for the unknown initial values. Hence, this property eliminates the possibility of unstable solution due to wrong guesses,
- e. a variety of boundary conditions can be handled with equal ease,
- f. this method is very effective for treating singularities since they can be interpreted as intermediate boundary conditions, and
- g. it is simple and direct applicability with no need other intermediate technique.

The literature devoted to Haar wavelets method is very voluminous. The ideas from Chen and Hsiao (1997) were later used by Hsiao (1997), Hsiao and Wang (2001), Razzaghi and Ordokhani (2001), Maleknejad and Mirzaee (2005), Lepik (2005, 2007), Shi et al. (2007), Hsiao (2008), Babolian and Shamsavaran (2009), Derili et al. (2012) and Sunmonu (2012) to solve integral and differential equations. Their ideas were also applied by Hsiao (2004), Dai and Cochran (2009) and Swaidan and Hussin (2013) for solving variational and optimal control problems. Haar wavelets method also had been applied successfully for numerical solution of linear ordinary differential equations by Chang and Piau (2008), nonlinear differential equations by Hariharan et al. (2009), Lepik (2005, 2007), fractional order differential equations by Geng et al. (2011) and Li and Zhao (2010) and boundary layer fluid flow problems by Islam et al. (2011).

Moreover, Haar wavelets method have been applied for solving partial differential equations (PDEs) from beginning of the early 1990s. In the last two decades, PDEs problem has attracted great attention and numerous papers in this problem have been published. The pioneering work for solving PDEs was led by Cattani (2004) is very important. Wu (2009) had solved for first order fractional PDEs numerically using Haar wavelet operational method. Rashidi Kouchi et al. (2011) proposed an adaptive wavelet algorithms for elliptic PDEs on product domains. Ghani (2012) solved the two dimensions space elliptic PDEs by using Haar wavelet operational matrix method. Lepik (2011) introduced numerical solution of differential equations with high order, integral equations and two dimensional PDEs using Haar wavelet method. Islam et al. (2013) solved parabolic PDE using Haar and Legendre wavelets.

Some of the studies related to boundary value problems which based on Haar wavelets are found in the literature. Islam et al. (2010) introduced a numerical method based on uniform Haar wavelets for solving different types of linear and nonlinear second order boundary value problems. Later, a collocation method based on Haar wavelet for the numerical solution of eight-order two-point boundary value problems and initial value problems in ordinary differential equations is proposed by Fazal-i-Haq et al. (2010). They also performed a new method based on non-uniform Haar wavelets for the numerical solution of singularly perturbed two-point boundary value problems (Fazal-i-Haq et al., 2011). Al-Bayati et al. (2011) designed a new algorithm for boundary value problems with an infinite number of boundary conditions. Fazal-i-Haq et al. (2011) had solved numerical solution of multi-point fourth-order boundary value problems related to the two dimensional channel with the porous walls and a special type of parameterized boundary value problems by using uniform Haar wavelets.

## 2.2 Literature Review on Quasilinearization Technique

In this study, Haar wavelet method with quasilinearization technique will be focused since quasilinearization technique offers sufficient approach to obtain approximate solutions to nonlinear problems. Nonlinear differential equations are playing crucial role in both theory and applications. The quasilinearization method (QLM) is designed to confront the nonlinear aspects of physical processes. The origin of quasilinearization lies in the theory of dynamic programming (Bellmann & Kalaba, 1965; Lee, 1968). Their ideas were later used to study many real-world problems such as the motion of a spinning rocket in a smooth bore launcher (Bellmann & Roth, 1983), the growth of a pathogenic bacteria (Murty et al., 1990) and solving nonlinear differential systems including problems of atmospheric flight mechanics (Miele & Wang, 1993). In numerical analysis, the discovery of quasilinearization method has proven to be a useful tool for solving a variety of initial and boundary value problems for different types of differential equations such as the work by Mandelzweig and Tabakin (2001). Their earlier work have proved that quasilinearization approach can be solved to nonlinear problems in physics with application to nonlinear ODEs. Some important features of the QLM can be found in Mandelzweig and Tabakin (2001).

The quasilinearization method is essentially a generalized Newton-Raphson method for functional equations. Both methods based on the same principle; Newton's method for solving nonlinear algebraic equations whilst quasilinearization method for solving functional equations by constructing the solution of nonlinear problems in an iterative way. They all possesses the same two important properties of monotone convergence and quadratic convergence. Hence, for most problems, Newton's method or quasilinearization method is equally efficient. The QLM linearized the nonlinear boundary value problems and provides a sequence of functions which in general converges quadratically to the solution of the original equation, if there is convergence

at all and in general has monotone convergence. The solution of original nonlinear boundary value problem can be obtained through a sequence of successive iterations of the dependent variable. The quasilinearization approach has been proven applicable to a general nonlinear ordinary or partial  $n$ -th order differential equations in  $N$ -dimensional space (Mandelzweig & Tabakin, 2001). This technique is easily understandable since there is no useful technique for obtaining the general solution of a nonlinear equations in terms of a finite set of particular solutions.

### **2.3 Literature Review on Haar Wavelet Quasilinearization Method**

In recent years, the Haar wavelet applications in dealing with QLM provide an efficient tool for solving nonlinear differential equations with two-point boundary conditions have been discussed by many researchers. One of the study that used this great combination of techniques is by Kaur et al. (2011). They presented the Haar wavelet based solutions of BVPs by using Haar wavelet collocation method and utilized the quasilinearization technique to resolve quadratic nonlinearity of unknown function. They also have proposed the same technique to solve the Blasius equation by using the transformation for converting the problem on a fixed computational domain (Kaur et al., 2013). The same approach used by Jiwari (2012) for the numerical simulation of time dependent nonlinear Burger's equation. Since the QLM is suitable to a general nonlinear ordinary or partial differential equations of any order, Saeed and Rehman (2013) have proved that this technique also can be solved for nonlinear functional order with initial and boundary value problems over a uniform grids based on the Haar wavelets. However, most of the previous work on HWQM only defined in the interval  $[0, 1)$ .

## CHAPTER 3: HAAR WAVELET QUASILINEARIZATION METHOD

In this chapter, the generation of Haar wavelet functions, its series expansion, Haar wavelet matrix and the integration of Haar wavelet functions are introduced. Many literature have defined the Haar wavelet and its integration on the interval  $[0, 1)$ . Here we expand the usual defined interval to  $[0, B)$  as actual problem does not necessarily hold up to one only. In addition, the detail of quasilinearization formula is provided. At the end of this chapter, we establish a novelty algorithm and step by step of Haar wavelet quasilinearization technique for solving nonlinear ODEs. Mathematical consideration to find the initial approximation is also provided.

### 3.1 The Haar Wavelets

#### 3.1.1 Introduction

The Haar wavelets were first introduced by Alfred Haar in 1909 in the form of a regular pulse pair. Then, many other wavelet functions were generated and introduced, including the Shannon, Daubechies, Legendre wavelets and many others (Lepik, 2011). However, among those forms, which are defined by an analytical expression, special attention deserves the Haar wavelets since they can be interpreted as intermediate boundary conditions; this circumstance will led to a great extent simplifies the solution. Moreover, Haar wavelets are the simplest among all the wavelet families and are made up of pairs of piecewise constant functions.

The initial theory by Alfred Haar has been expanded recently into a wide variety of applications, including the representation of various functions with a combination of step functions and wavelets over a specified interval.

### 3.1.2 Haar Wavelet Functions

The simplest basis of Haar wavelet family is the Haar scaling function that appears in the form of a square wave over the interval  $[0, B)$  as expressed in Equation (3.1),

$$h_0(x) = \begin{cases} 1, & 0 \leq x < B \\ 0, & \text{elsewhere.} \end{cases} \quad (3.1)$$

The Equation (3.1) is known as Haar father wavelet, where the zeroth level wavelet has no displacement and dilation of unit magnitude. Correspondingly, define

$$h_1(x) = \begin{cases} 1, & 0 \leq x < \frac{B}{2} \\ -1, & \frac{B}{2} \leq x < B \\ 0, & \text{elsewhere.} \end{cases} \quad (3.2)$$

Equation (3.2) is called a Haar mother wavelet where all the other subsequent functions are generated from  $h_1(x)$  with two operations; translation and dilation. For example, the third subplot in Figure 3.1 was drawn by the compression  $h_1(x)$  to left half of its original interval and the fourth subplot is the same as the third plot plus translating to the right side by  $\frac{1}{2}$ . Generally, we can write out the Haar wavelet family as

$$h_i(x) = \begin{cases} 1, & \frac{kB}{2^\alpha} \leq x < \frac{(k+0.5)B}{2^\alpha} \\ -1, & \frac{(k+0.5)B}{2^\alpha} \leq x < \frac{(k+1)B}{2^\alpha} \\ 0, & \text{elsewhere in } [0, B) \end{cases} \quad (3.3)$$

where  $i = 1, 2, \dots, m-1$  is the series index number and the resolution  $m = 2^J$  is a positive integer. An  $\alpha$  and  $k$  represent the integer decomposition of the index  $i$ , i.e.  $i = 2^\alpha + k$  in which  $\alpha = 0, 1, \dots, J-1$  and  $k = 0, 1, 2, \dots, 2^\alpha - 1$ .

If the maximal level of resolution  $J$  is prescribed then, it follows from Equation (3.3) that

$$\int_0^B h_r(x)h_s(x)dt = \begin{cases} B 2^{-\alpha}, & \text{if } r = s \\ 0, & \text{if } r \neq s. \end{cases} \quad (3.4)$$

So that we can see that the Haar wavelet functions are also orthogonal to each other.

Equation (3.4) can be proven as follows. If  $r = s$ , then we have

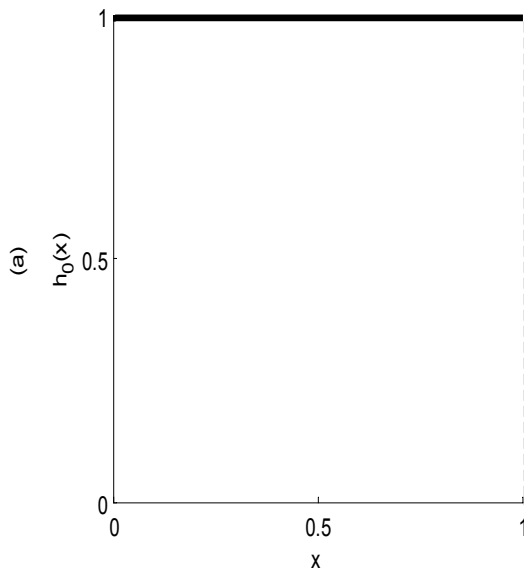
$$\begin{aligned} (h_r(x), h_s(x)) &= \int_0^B h_r(x)h_s(x)dt \\ &= \int_0^B h_n^2(x)dx \\ &= \|h_n(x)\|^2 \end{aligned} \quad (3.5)$$

$$\begin{aligned} &= \int_{\frac{kB}{2^\alpha}}^{\frac{(k+0.5)B}{2^\alpha}} dx + \int_{\frac{(k+0.5)B}{2^\alpha}}^{\frac{(k+1)B}{2^\alpha}} dx \\ &= \frac{B/2}{2^\alpha} + \frac{B/2}{2^\alpha} \\ &= B 2^{-\alpha} \end{aligned} \quad (3.6)$$

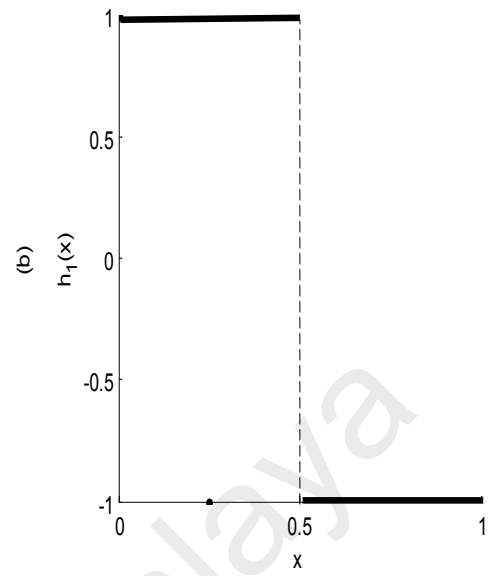
and if  $r \neq s$ , then we have

$$\int_0^B h_r(x)h_s(x)dt = 0, \quad (3.7)$$

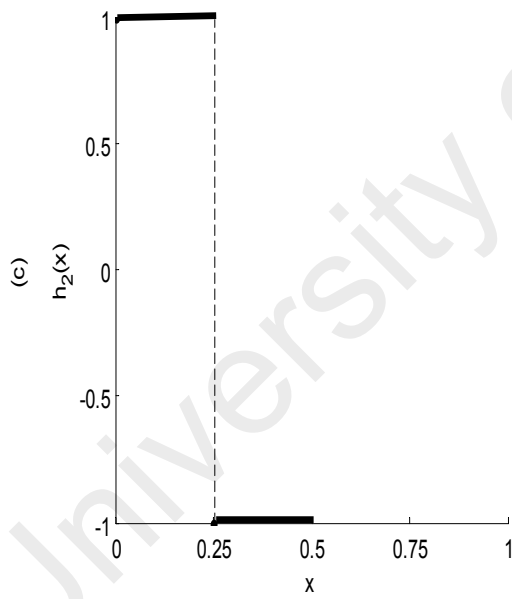
as all integrals in Equation (3.4) are zeros. The orthogonal set of the first four Haar function ( $m = 4$ ) in the interval  $0 \leq x < 1$  can be shown in Figure 3.1, where the bold line represent the Haar function.



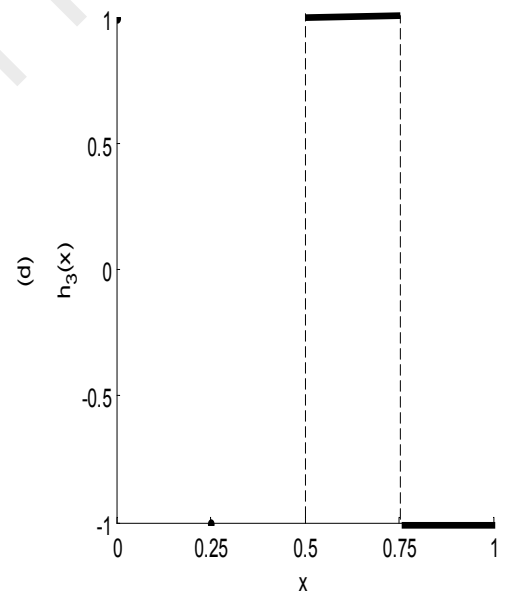
(a) Haar function of  $h_0(x)$



(b) Haar function of  $h_1(x)$



(c) Haar function of  $h_2(x)$



(d) Haar function of  $h_3(x)$

**Figure 3.1:** First four Haar functions

### 3.1.3 Expanding Functions Into The Haar Wavelet Series

Any function of  $L^2([0, B])$  can be expanded into the Haar wavelet series with an infinite number of terms,

$$f(x) = \sum_{i=0}^{\infty} c_i h_i(x). \quad (3.8)$$

The symbol  $c_i$  denotes the Haar wavelet coefficients. If the function  $f(x)$  is approximated as piecewise constant, then the sum in Equation (3.8) will be terminated after  $m$  terms, then it can be compactly written in the form,

$$f_m(x) \approx \sum_{i=0}^{m-1} c_i h_i(x). \quad (3.9)$$

Suppose that  $\{h_i(x)\}$  is an orthogonal set of functions on an interval  $[0, B]$ . It is possible to determine a set of coefficients  $c_i$ , for which

$$f(x) = c_0 h_0(x) + c_1 h_1(x) + \dots + c_n h_n(x) + \dots \quad (3.10)$$

where the coefficient  $c_i$  can be determined by utilizing the inner product in Equation (3.4). Multiplying Equation (3.10) by  $h_r(x)$  and integrating over the interval  $[0, B]$  gives,

$$\begin{aligned} \int_0^B f(x) h_r(x) dx &= c_0 \int_0^B h_0(x) h_r(x) dx + c_1 \int_0^B h_1(x) h_r(x) dx + \dots \\ &\quad \dots + c_n \int_0^B h_n(x) h_r(x) dx + \dots \\ &= c_0 (h_0, h_r) + c_1 (h_1, h_r) + \dots + c_n (h_n, h_r) + \dots + \dots \end{aligned} \quad (3.11)$$

By orthogonality, the value of each term on the right side of Equation (3.11) is equal to zero except when  $r = n$ . For this case, we obtain,

$$\int_0^B f(x)h_n(x)dx = c_n \int_0^B h_n^2(x)dx. \quad (3.12)$$

The required coefficients are

$$c_n = \frac{\int_0^B f(x)h_n(x)dx}{\int_0^B h_n^2(x)dx}, \quad n = 0, 1, 2, \dots \quad (3.13)$$

Equation (3.13) can be written as

$$c_n = \frac{\int_0^B f(x)h_n(x)dx}{\|h_n(x)\|^2}, \quad n = 0, 1, 2, \dots \quad (3.14)$$

From Equation (3.6), the norm  $\|h_n(x)\|^2 = \frac{B}{2^\alpha}$ , therefore the Haar wavelet coefficient is

$$c_n = \frac{2^\alpha}{B} \int_0^B f(x)h_n(x)dx, \quad n = 0, 1, 2, \dots \quad (3.15)$$

Thus, the Haar wavelet coefficient in Equation (3.9) can be determined as

$$c_i = \frac{2^\alpha}{B} \int_0^B f_m(x)h_i(x)dx. \quad (3.16)$$

If  $f(x)$  in Equation (3.8) is an exact solution and satisfies a Lipschitz condition and  $f_m(x)$  in Equation (3.9) is an approximate solution, then the error of approximation  $f(x)$  with  $f_m(x)$  is given as

$$e_m(x) = f(x) - f_m(x). \quad (3.17)$$

According to Saedi et al. (2011), they have shown that the square of the error norm for Haar wavelet approximation is written as

$$\|e_m\|_{L^2} \leq \frac{K}{m\sqrt{3}}, \quad (3.18)$$

where  $K$  is the Lipschitz constant.

From Equation (3.18) it is shown that the error is inversely proportional to the level of resolution of Haar wavelet function. This implies that Haar wavelet approximation method is converge when  $m \rightarrow \infty$ .

### 3.1.4 Haar Wavelet Matrix

The sum in Equation (3.9) can be compactly written in the form,

$$f_m(x) = \mathbf{c}_m^T \mathbf{H}_m(x), \quad (3.19)$$

where  $\mathbf{c}_m^T$  is called Haar coefficient vector and  $\mathbf{H}_m(x)$  is the Haar function vector.

They are defined as

$$\mathbf{c}_m^T = [c_0 \quad c_1 \quad \dots \quad c_{m-1}], \quad (3.20)$$

and

$$\mathbf{H}_m(x) = [h_0(x) \quad h_1(x) \quad \dots \quad h_{m-1}(x)]^T. \quad (3.21)$$

The superscript  $T$  is denotes the transpose and the subscript  $m$  denotes the dimension of vectors and matrices. Taking the collocation points as following,

$$x_j = \frac{(j+0.5)B}{m}, \quad j = 0, 1, 2, \dots, m-1. \quad (3.22)$$

The Haar function vectors can be expressed in matrix form as

$$(\mathbf{H}_m)_{i,j} = h_i(x_j). \quad (3.23)$$

For illustration, consider the case  $0 \leq x < 1$ , with  $m = 4$ . By calculating the coordinate of collocation points from Equation (3.22), we find  $x_0 = 0.125$ ,  $x_1 = 0.375$ ,  $x_2 = 0.625$  and  $x_3 = 0.875$ . The first four Haar function vectors can be expressed in a matrix form as the following,

$$\mathbf{H}_4\left(\frac{1}{8}\right) = [1 \ 1 \ 1 \ 0]^T, \quad (3.24)$$

$$\mathbf{H}_4\left(\frac{3}{8}\right) = [1 \ 1 \ -1 \ 0]^T, \quad (3.25)$$

$$\mathbf{H}_4\left(\frac{5}{8}\right) = [1 \ -1 \ 0 \ 1]^T, \quad (3.26)$$

$$\mathbf{H}_4\left(\frac{7}{8}\right) = [1 \ -1 \ 0 \ -1]^T. \quad (3.27)$$

Altogether from Equation (3.24)-(3.27), we have,

$$\mathbf{H}_4 = \begin{bmatrix} H_4\left(\frac{1}{8}\right) & H_4\left(\frac{3}{8}\right) & H_4\left(\frac{5}{8}\right) & H_4\left(\frac{7}{8}\right) \end{bmatrix}$$

$$H_4 = \begin{bmatrix} 1 & 1 & 1 & 1 \\ 1 & 1 & -1 & -1 \\ 1 & -1 & 0 & 0 \\ 0 & 0 & 1 & -1 \end{bmatrix}. \quad (3.28)$$

### 3.1.5 Integration of Haar Wavelet Functions

Multiple integration of  $h_i(x)$  are required when solving differential equation using Haar wavelet method. For  $m = 4$ , the integration of the Haar wavelet function,  $H_m(\tau)$  in the interval  $(0, x)$  can be expressed as following,

$$\int_0^x h_0(\tau) d\tau = x \quad 0 \leq x < B, \quad (3.29)$$

$$\int_0^x h_1(\tau) d\tau = \begin{cases} x & 0 \leq x < \frac{1}{2}B \\ B-x & \frac{1}{2}B \leq x < B \end{cases} \quad (3.30)$$

$$\int_0^x h_2(\tau) d\tau = \begin{cases} x & 0 \leq x < \frac{1}{4}B \\ \frac{1}{2}B - x & \frac{1}{4}B \leq x < \frac{1}{2}B \\ 0 & \text{elsewhere.} \end{cases} \quad (3.31)$$

$$\int_0^x h_3(\tau) d\tau = \begin{cases} x - \frac{1}{2}B & \frac{1}{2}B \leq x < \frac{3}{4}B \\ B - x & \frac{3}{4}B \leq x < B \\ 0 & \text{elsewhere.} \end{cases} \quad (3.32)$$

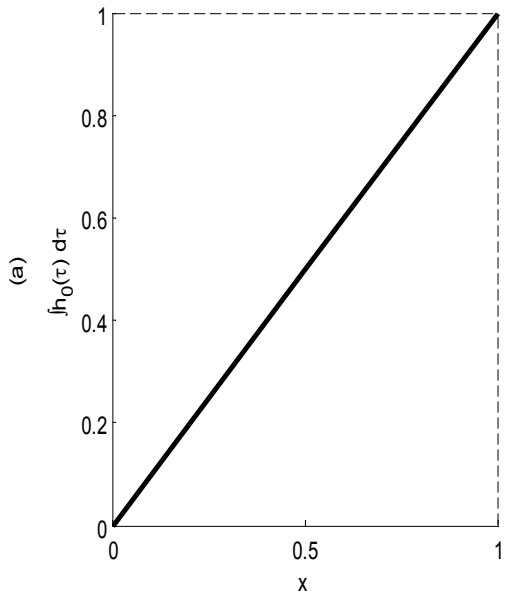
In general, the integral of Equation (3.3) for  $i = 1, 2, \dots, m-1$  can be written as

$$p_{i,v}(x) = \int_0^x \int_0^x \dots \int_0^x h_i(t) (dt)^v = \frac{1}{\Gamma(v)} \int_0^x (x-t)^{v-1} h_i(t) dt, \quad v > 0. \quad (3.33)$$

Similar as Haar matrix, integration of Haar wavelet also can be expressed into matrix form as

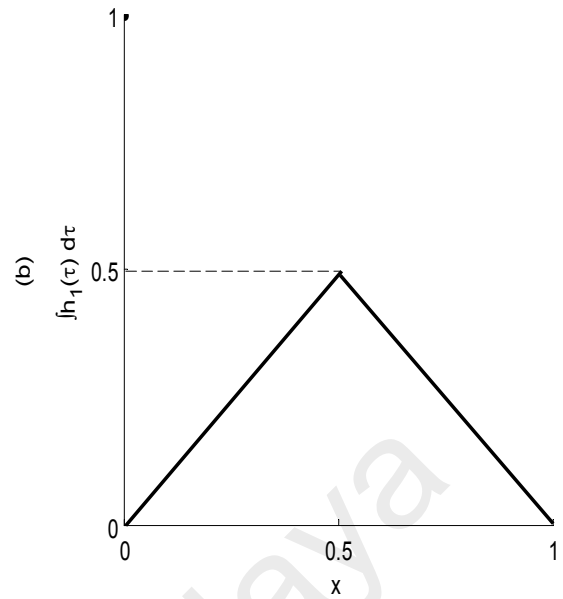
$$(P_v)_{i,j} = p_{i,v}(x_j), \quad v = 1, 2, \dots \quad (3.34)$$

For illustration, the integration for  $H_4$  from 0 to  $x$  can be represented as in Figure 3.2 below.



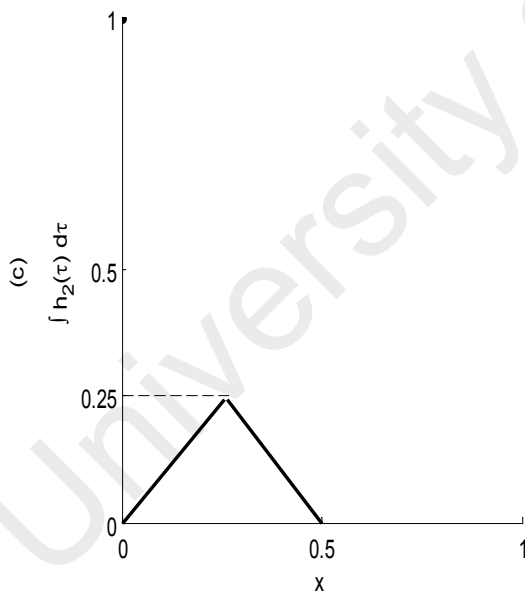
a) Integration of first haar function,

$$\int_0^x h_0(\tau) d\tau .$$



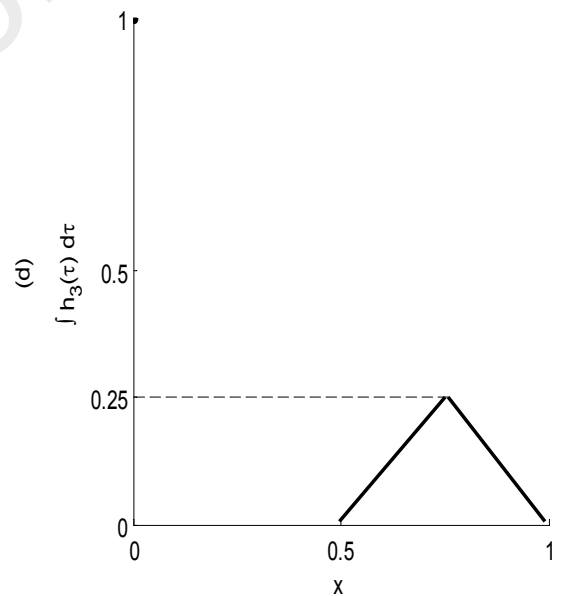
b) Integration of second haar function,

$$\int_0^x h_1(\tau) d\tau .$$



c) Integration of third haar function,

$$\int_0^x h_2(\tau) d\tau .$$



d) Integration of fourth haar function,

$$\int_0^x h_3(\tau) d\tau .$$

**Figure 3.2:** The integration of Haar wavelet functions for  $m = 4$

In matrix form, first integration of Haar wavelet, at collocation points,  $x_0 = 1/8$ ,  $x_1 = 3/8$ ,  $x_2 = 5/8$  and  $x_3 = 7/8$ ,  $P_1$  is given as

$$P_1 = \int_0^x H_4(\tau) d\tau = \frac{1}{8} \begin{bmatrix} 1 & 3 & 5 & 7 \\ 1 & 3 & 3 & 1 \\ 1 & 1 & 0 & 0 \\ 0 & 0 & 1 & 1 \end{bmatrix}. \quad (3.35)$$

The expression in Equation (3.35) is the transformation of the integrals from  $h_0(\tau)$  to  $h_3(\tau)$  into matrix form at the collocation points. The averaged values are taken to represent these triangular functions. The integral of  $h_0(\tau)$  is a ramp function and the integral of  $h_1(\tau)$  is a triangular function consisting of a rising ramp and a falling ramp. It is noted that the absolute value of the slopes of these ramps is the same. The integral of  $h_2(\tau)$  and  $h_3(\tau)$  also are triangular functions. However, it spans the first and the second half intervals.

### 3.2 Quasilinearization Technique

The quasilinearization method is essentially a generalized Newton-Raphson method for functional equations. It inherits the two important properties of the method, namely quadratic convergence and often monotone convergence. This technique linearized the nonlinear boundary value problem and provides a sequence of functions which in general converges quadratically to the solution of the original equation, if there is convergence at all and in general has monotone convergence. The solution of original nonlinear boundary value problem can be obtained through a sequence of successive iterations of the dependent variable.

For illustrative purpose, let consider a nonlinear second-order differential equation,

$$y''(x) = \tilde{f}(y(x), x), \quad (3.36)$$

with the boundary conditions,

$$y(A) = \alpha, \text{ and } y(B) = \beta, \quad A \leq x \leq B \quad (3.37)$$

where  $\tilde{f}$  may be a function of  $x$  or  $y(x)$ . Let  $y_0(x)$  be an initial approximation of the function  $y(x)$ . The Taylor's series expansion of  $f$  about  $y_0(x)$  is

$$\tilde{f}(y(x), x) = \tilde{f}(y_0(x), x) + (y(x) - y_0(x))\tilde{f}_{y_0}(y_0(x), x) + O((y(x) - y_0(x))^2) \quad (3.38)$$

Ignoring second and higher order terms of Equation (3.38) and replacing into Equation (3.36), we get

$$y''(x) = \tilde{f}(y_0(x), x) + (y(x) - y_0(x))\tilde{f}_{y_0}(y_0(x), x) \quad (3.39)$$

solving Equation (3.39) and called the solution  $y_1(x)$ . Using  $y_1(x)$  and again expanding Equation (3.36) about  $y_1(x)$ . Ignore the second and higher order of the expanding, we have

$$y''(x) = \tilde{f}(y_1(x), x) + (y(x) - y_1(x))\tilde{f}_{y_1}(y_1(x), x). \quad (3.40)$$

After simplification we get  $y_2(x)$ , second approximation to  $y(x)$ . Hence, we can conclude the sequence of functions  $\{y_r(x)\}$  are continuous and we obtain the desired accuracy if the problem converges. If the sequence  $\{y_r\}$  converges, Mandelzweig and Tabakin (2001) have proved that the sequence converge quadratically to the solution.

In general, the recurrence relation for second order nonlinear differential equation can be written as

$$y''_{r+1}(x) = \tilde{f}(y_r(x), x) + (y_{r+1}(x) - y_r(x))\tilde{f}_{y_r}(y_r(x), x), \quad r = 0, 1, 2, \dots \quad (3.41)$$

in which  $y_r(x)$  is known and it is used to obtain  $y_{r+1}(x)$ . Equation (3.41) is always be a linear differential equation. The boundary condition for Equation (3.41) is given as

$$y_{r+1}(A) = \alpha, \text{ and } y_{r+1}(B) = \beta. \quad (3.42)$$

The same procedure can also be applied on other higher order nonlinear problem. The general quasilinear iteration to solve  $n$ th order nonlinear differential equation,

$$L^{(n)}y(x) = \tilde{f}(y', y'', \dots, y^{(n-1)}, x), \quad (3.43)$$

subject to the boundary conditions,

$$y(A) = \alpha_1, y'(A) = \alpha_2, y''(A) = \alpha_3, \dots, y^{(n-1)}(A) = \alpha_n, \quad (3.44)$$

$$y(B) = \beta_1, y'(B) = \beta_2, y''(B) = \beta_3, \dots, y^{(n-1)}(B) = \beta_n, \quad (3.45)$$

is given by Mandelzweig and Tabakin (2001),

$$L^{(n)}y_{r+1}(x) = \tilde{f}(y_r(x), y_r'(x), \dots, y_r^{(n-1)}(x), x) + \sum_{s=0}^{n-1} (y_{r+1}^{(s)}(x) - y_r^{(s)}(x)) \tilde{f}_{y^{(s)}}(y_r(x), y_r'(x), \dots, y_r^{(n-1)}(x), x), \quad (3.46)$$

where  $\tilde{f}$  is a continuous function and  $y_r^{(0)}(x) = y_r(x)$ . Equation (3.46) is always linear differential equation and can be solved recursive easily by using Haar wavelet method.

### 3.3 Numerical Method of Haar Wavelet Quasilinearization

Here we suggest an algorithm for easy understanding of HWQM for solving nonlinear differential equation(s).

Step 1 : Apply the quasilinearization technique to the nonlinear problems.

Step 2 : Apply the Haar wavelet method to the quasilinearized equation by approximating the higher order derivatives term by Haar wavelet series as

$$y_{r+1}^{(n)}(x) = \sum_{i=0}^{m-1} a_i h_i(x), \quad (3.47)$$

where  $h$  is the Haar matrix,  $a_i$  is the wavelet coefficients and  $n$  is the highest derivative appearing in the differential equation(s).

Step 3 : Integrate Equation (3.47) from 0 to  $x$ ,  $n$ th times,

$$y_{r+1}^{(n-1)}(x) = \sum_{i=0}^{m-1} a_i p_{i,1}(x) + y_{r+1}^{(n-1)}(0) \quad (3.48)$$

⋮  
⋮

$$y_{r+1}^{(v)}(x) = \sum_{i=0}^{m-1} a_i p_{i,n-v}(x) + \sum_{\sigma=0}^{n-v-1} \frac{1}{\sigma!} (x-A)^\sigma y_0^{(v+\sigma)}, \quad (3.49)$$

where  $v$  is the lowest derivative.

Step 4 : Substitute  $y_{r+1}^{(v)}(x)$  and all the related values into the quasilinearized problem(s).

Step 5 : Calculate the wavelet coefficient,  $a_i$ . The initial approximation  $y_0(x)$  is calculated when  $r = 0$ . It is used for obtaining  $y_{r+1}(x)$ .

Step 6 : Obtain the numerical solution for  $y_{r+1}(x)$ . For solving  $y_1, y_2$  and  $y_3$  iteratively, the iterations described above will continue until

$$\|y_{r+1} - y_r\| < \varepsilon, \quad (3.50)$$

for some prescribed error tolerance,  $\varepsilon$ .

All the steps are illustrated in Figure 3.3.

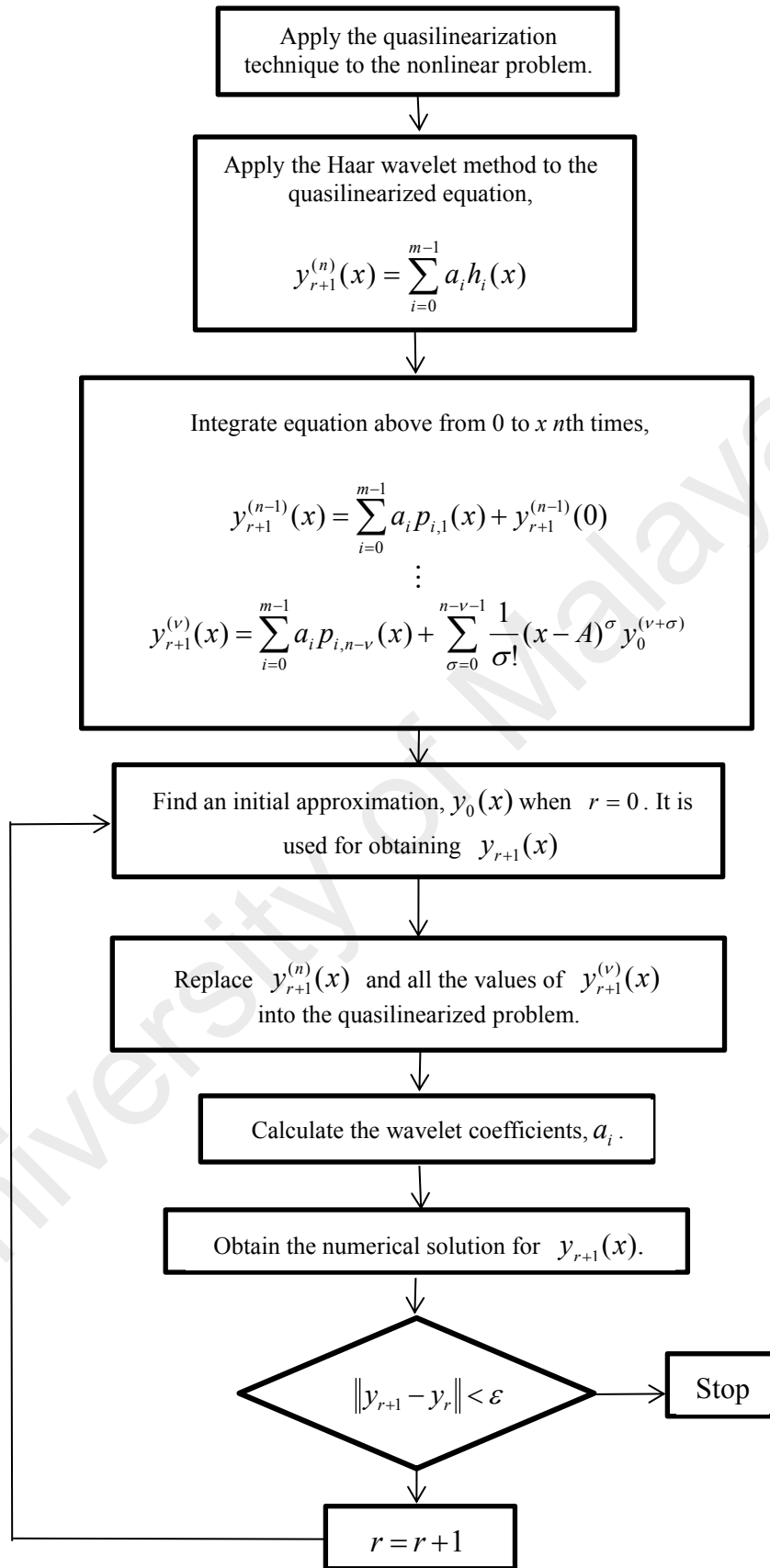


**Figure 3.3:** Algorithm for solving nonlinear ODE by using HWQM.

The following is the mathematical consideration to find the initial approximation function by using HWQM;

Step 1: Find a trivial function that satisfy the boundary condition.

Step 2: If the trivial function cannot be obtained, find a function such that we can solve for  $y_0(x)$  in Equation (3.46).

University of Malaya

## CHAPTER 4: SINGLE NONLINEAR ORDINARY DIFFERENTIAL EQUATION

In this chapter, the solution using HWQM will be tested to single nonlinear ODEs namely; Bratu equation (Boyd, 2011), Falkner-Skan equation (Falkner & Skan, 1931) and Blasius equation (Blasius, 1950). Numerical solutions of these problems have always been of great interest for scientist and engineers. However, there is no study available on the HWQM for these problems especially on the infinite intervals. Hence, this is a great opportunity to validate and compare the present method with the previous methods that available in the literature. This work may be useful in science and engineering applications for finding an alternative formulation in boundary value problems.

### 4.1 The Bratu Equation

#### 4.1.1 Introduction

Bratu's problem is known as "Liouville-Gelfand-Bratu" problem in honor of Gelfand and nineteenth century work of great French mathematician Liouville (Buckmire, 2004; Mounim & de Dormale, 2006; Boyd, 2011). This problem is extensively used in a large variety of applications such as the model of thermal reaction process, nanotechnology, chemical reaction theory, radiative heat transfer and Chandrasekhar model of the expansion of universe (Boyd, 2011).

The boundary value problem of Bratu's equation in one-dimensional planar coordinates is considered. It can be written as

$$f''(\eta) + \lambda e^{f(\eta)} = 0, \quad 0 < \eta < 1, \quad (4.1)$$

with the boundary conditions  $f(0) = f(1) = 0$ . For  $\lambda > 0$  is a constant, the exact solution of Equation (4.1) is given by

$$f(\eta) = -2 \ln \left( \frac{\cosh(0.5\theta(\eta - 0.5))}{\cosh(0.25\theta)} \right), \quad (4.2)$$

where  $\theta$  satisfies

$$\theta = \sqrt{2\lambda} \cosh(0.25\theta). \quad (4.3)$$

The Bratu's problem has zero, one or two solutions when  $\lambda > \lambda_c$ ,  $\lambda = \lambda_c$  and  $\lambda < \lambda_c$  respectively, where the critical value  $\lambda_c$  satisfies the equation

$$1 = \frac{1}{4} \sqrt{2\lambda_c} \sinh(\theta_c / 4), \quad (4.4)$$

and it was evaluated by Aregbesola (2003) and Boyd (2003). They reported that the critical value is

$$\lambda_c = 3.513830719. \quad (4.5)$$

Several numerical methods have been done for the study of Bratu's problem, for example, Adomian decomposition method (ADM) (Wazwaz, 2005; Rach, 2008; Ghazanfari & Sefvanzadeh, 2014), modified decomposition method (Wazwaz, 1999), variational iteration method (VIM) (Batiha, 2010; Saravi et al., 2013; He et al., 2014), modified variational iteration method (Ghazanfari & Sefvanzadeh, 2015a), the homotopy perturbation method (HPM) (Feng et al., 2008; Ahmet, 2009; Ghazanfari & Sefvanzadeh, 2015b), nonstandard finite-difference schemes (Buckmire, 2004), artificial neural network (ANN) (Raja & Islam, 2012; Kumar & Yadav, 2015), decomposition method (Deeba et al., 2000), Laplace method (Khuri, 2004), B-Spline method (Caglar et al., 2010), the Lie-group shooting method (LGSM) (Abbasbandy et al., 2011), differential transformation method (DTM) (Abel-Helim Hassan & Erturk, 2007), Chebyshev wavelets method (Changqing & Jianhua, 2013), non-polynomial spline method (Jalilian, 2010), parametric cubic spline method (Zarebnia & Sarvari, 2013) and successive differentiation method (Wazwaz, 2016).

In the next section, we will apply HWQM to Bratu's equation. All the numerical

results display graphically and their error will be calculated.

#### 4.1.2 Numerical Solution

Consider the nonlinear Bratu's ODE from Equation (4.1). The first step is to apply quasilinearization technique, we have

$$f_{r+1}'' = -\lambda e^{f_r} + (f_{r+1} - f_r) \tilde{f}_{f_r}(-\lambda e^{f_r}), \quad (4.6)$$

where the subscript  $r$  represents the number of iteration. Solving and rearranging Equation (4.6), we obtain

$$f_{r+1}'' + \lambda e^{f_r} f_{r+1} = \lambda e^{f_r} (-1 + f_r). \quad (4.7)$$

The boundary conditions are

$$f_{r+1}(0) = f_{r+1}(1) = 0. \quad (4.8)$$

Haar wavelet method is applied to Equation (4.7) by approximating the higher order derivative term by Haar wavelet series as

$$f_{r+1}''(\eta) = \sum_{i=0}^{m-1} a_i h_i(\eta). \quad (4.9)$$

The lower order derivatives are obtained by integrating Equation (4.9) and by using the boundary conditions (4.8). Hence, we get

$$f_{r+1}'(\eta) = \sum_{i=0}^{m-1} a_i p_{i,1}(\eta) + f_{r+1}'(0), \quad (4.10)$$

and

$$f_{r+1}(\eta) = \sum_{i=0}^{m-1} a_i p_{i,2}(\eta) + \eta f_{r+1}'(0) + f_{r+1}(0). \quad (4.11)$$

The purpose now is to find the missing boundary condition,  $f_{r+1}'(0)$ . This unknown value can be obtained from Equation (4.11) by substituting  $\eta = 1$ , implies that

$$f_{r+1}'(0) = -\sum_{i=0}^{m-1} a_i p_{i,2}(1) - f_{r+1}(0) + f_{r+1}(1). \quad (4.12)$$

Hence, the new equations for (4.10) and (4.11) are

$$f'_{r+1}(\eta) = \sum_{i=0}^{m-1} a_i (p_{i,1}(\eta) - p_{i,2}(1)), \quad (4.13)$$

and

$$f_{r+1}(\eta) = \sum_{i=0}^{m-1} a_i (p_{i,2}(\eta) - \eta p_{i,2}(1)). \quad (4.14)$$

Substitute Equations (4.9), (4.13) and (4.14) into Equation (4.7), we obtain

$$\sum_{i=0}^{m-1} a_i (h_i(\eta) + \lambda e^{f_r(\eta)} (p_{i,2}(\eta) - \eta p_{i,2}(1))) = \lambda e^{f_r(\eta)} (-1 + f_r(\eta)). \quad (4.15)$$

Haar coefficients,  $a_i$  can be calculated easily from Equation (4.15). The efficiency and accuracy of HWQM, was tested for several different values of  $\lambda$ 's for Equation (4.15).

### 4.1.3 Results and Discussion

The numerical solutions of Equation (4.15) are obtained for the case of  $\lambda = 1, 2$  and  $3.51$ . By following the suggested algorithm as discussed in Section 3.3, we get the initial approximations for  $\lambda = 1, 2$  and  $3.51$  as follows,

$$f_0(\eta) = \cos \eta + \tan\left(\frac{1}{2}\right) \sin \eta - 1, \quad (4.16)$$

$$f_0(\eta) = -2 \sec\left(\frac{1}{\sqrt{2}}\right) \sin\left(\frac{\eta-1}{\sqrt{2}}\right) \sin\left(\frac{\eta}{\sqrt{2}}\right), \quad (4.17)$$

and

$$f_0(\eta) = 1.35993 \sin(1.8735\eta) + \cos(1.8735\eta) - 1, \quad (4.18)$$

respectively. All computations of HWQM and exact solutions are performed by MATLAB software with high resolution,  $m = 2^{11}$ .

The numerical result can be compared with exact result as shown in Table 4.1 for different values of  $\lambda$ 's. The following tabulated values in Tables 4.2 - 4.4 are set up for comparison of absolute errors with other methods that available in the literature such as VIM (Saravi et al., 2013), ANN (Kumar & Yadav, 2015), decomposition method (Deeba

et al., 2000), Laplace method (Khuri, 2004), B-Spline method (Caglar & Caglar, 2009), LGSM (Abbasbandy et al., 2011), DTM (Abel-Halim Hassan & Erturk, 2007), Chebyshev wavelet method (Changqing & Jianhua, 2013) and NPSM (Jalilian, 2010).

In Table 4.1 the exact solutions for the case  $\lambda = 1, 2$  and  $3.51$  derived from Equation (4.2) are compared with the numerical solution obtained by the HWQM. It is clear that HWQM produces numerical solutions which are closer to the exact solutions. The results have shown that solving single nonlinear ODEs using this method could give encouraging results with  $m = 2^{11}$ . The analytical and graphical representation for comparison of absolute errors between proposed method and other existing methods are shown in Tables 4.2 - 4.4 and Figure 4.1 for different values of  $\lambda$ 's. According to Tables 4.2 and 4.3, it is observed that the Decomposition method give less accuracy compare to others. Meanwhile HWQM produced better estimation with absolute error around  $1 \times 10^{-9}$ .

**Table 4.1:** Comparison between HWQM with exact solutions for different values of  $\lambda$ 

$\eta$	Exact Solutions			HWQM		
	$\lambda = 1$	$\lambda = 2$	$\lambda = 3.51$	$\lambda = 1$	$\lambda = 2$	$\lambda = 3.51$
0.0	0	0	0	0	0	0
0.1	0.0498467912	0.1144107433	0.3643358036	0.0498467907	0.1144107400	0.3643353858
0.2	0.0891899346	0.2064191165	0.6778697057	0.0891899336	0.2064191103	0.6778688893
0.3	0.1176090958	0.2738793118	0.9222141971	0.1176090944	0.2738793033	0.9222130389
0.4	0.1347902539	0.3150893642	1.0786342408	0.1347902523	0.3150893541	1.0786328469
0.5	0.1405392144	0.3289524213	1.1326179783	0.1405392127	0.3289524107	1.1326164996
0.6	0.1347902539	0.3150893642	1.0786342408	0.1347902523	0.3150893541	1.0786328469
0.7	0.1176090958	0.2738793118	0.9222141971	0.1176090944	0.2738793033	0.9222130389
0.8	0.0891899346	0.2064191165	0.6778697057	0.0891899336	0.2064191103	0.6778688893
0.9	0.0498467912	0.1144107433	0.3643358036	0.0498467907	0.1144107400	0.3643353858
1.0	0	0	0	0	0	0

**Table 4.2:** Comparison of absolute errors between HWQM with other methods for  $\lambda = 1$

$\eta$	Decomposition (Deeba et al., 2000)	ANN (Kumar & Yadav, 2015)	VIM (Saravi et al., 2013)	Laplace (Khuri, 2004)	B-Spline (Caglar & Caglar, 2009)	LGSM (Abbasbandy et al., 2011)	HWQM (Present)
0.0	0	0	0	0	0	0	0
0.1	$2.69 \times 10^{-3}$	$2.75 \times 10^{-4}$	$6.46 \times 10^{-5}$	$1.98 \times 10^{-6}$	$2.98 \times 10^{-6}$	$7.51 \times 10^{-7}$	$5.69 \times 10^{-10}$
0.2	$2.02 \times 10^{-3}$	$3.29 \times 10^{-4}$	$1.29 \times 10^{-4}$	$3.94 \times 10^{-6}$	$5.47 \times 10^{-6}$	$1.02 \times 10^{-6}$	$1.04 \times 10^{-9}$
0.3	$1.52 \times 10^{-4}$	$2.13 \times 10^{-3}$	$1.94 \times 10^{-4}$	$5.85 \times 10^{-6}$	$7.34 \times 10^{-6}$	$9.05 \times 10^{-7}$	$1.40 \times 10^{-9}$
0.4	$2.20 \times 10^{-3}$	$1.32 \times 10^{-3}$	$2.65 \times 10^{-4}$	$7.70 \times 10^{-6}$	$8.50 \times 10^{-6}$	$5.24 \times 10^{-7}$	$1.62 \times 10^{-9}$
0.5	$3.02 \times 10^{-3}$	$3.75 \times 10^{-4}$	$3.51 \times 10^{-4}$	$9.47 \times 10^{-6}$	$8.89 \times 10^{-6}$	$5.07 \times 10^{-9}$	$1.70 \times 10^{-9}$
0.6	$2.20 \times 10^{-3}$	$8.63 \times 10^{-4}$	$4.76 \times 10^{-4}$	$1.11 \times 10^{-5}$	$8.50 \times 10^{-6}$	$5.14 \times 10^{-7}$	$1.62 \times 10^{-9}$
0.7	$1.52 \times 10^{-4}$	$3.20 \times 10^{-3}$	$6.78 \times 10^{-4}$	$1.26 \times 10^{-5}$	$7.34 \times 10^{-6}$	$8.95 \times 10^{-7}$	$1.40 \times 10^{-9}$
0.8	$2.02 \times 10^{-3}$	$1.29 \times 10^{-3}$	$1.02 \times 10^{-3}$	$1.35 \times 10^{-5}$	$5.47 \times 10^{-6}$	$1.01 \times 10^{-6}$	$1.04 \times 10^{-9}$
0.9	$2.69 \times 10^{-3}$	$4.66 \times 10^{-6}$	$1.59 \times 10^{-3}$	$1.20 \times 10^{-5}$	$2.98 \times 10^{-6}$	$7.42 \times 10^{-7}$	$5.69 \times 10^{-10}$
1.0	0	0	0	0	0	0	0

**Table 4.3:** Comparison of absolute errors between HWQM with other methods for  $\lambda = 2$

$\eta$	Decomposition (Deeba et al., 2000)	VIM (Saravi et al., 2013)	Laplace (Khuri, 2004)	ANN (Kumar & Yadav, 2015)	B-Spline (Caglar & Caglar, 2009)	DTM (Abel-Halim Hassan & Erturk, 2007)	LGSM (Abbasbandy et al., 2011)	Chebyshev (Changqing & Jianhua, 2013)	HWQM (Present)
0.0	0	0	0	0	0	0	0	0	0
0.1	$1.52 \times 10^{-2}$	$3.66 \times 10^{-3}$	$2.13 \times 10^{-3}$	$2.35 \times 10^{-3}$	$1.72 \times 10^{-5}$	$1.30 \times 10^{-6}$	$4.03 \times 10^{-6}$	$5.01 \times 10^{-7}$	$3.28 \times 10^{-9}$
0.2	$1.47 \times 10^{-2}$	$7.23 \times 10^{-3}$	$4.21 \times 10^{-3}$	$1.56 \times 10^{-3}$	$3.26 \times 10^{-5}$	$2.56 \times 10^{-6}$	$5.70 \times 10^{-6}$	$1.17 \times 10^{-6}$	$6.22 \times 10^{-9}$
0.3	$5.89 \times 10^{-3}$	$1.39 \times 10^{-3}$	$6.17 \times 10^{-3}$	$3.52 \times 10^{-3}$	$4.49 \times 10^{-5}$	$3.77 \times 10^{-6}$	$5.22 \times 10^{-6}$	$2.34 \times 10^{-6}$	$8.57 \times 10^{-9}$
0.4	$3.25 \times 10^{-3}$	$1.79 \times 10^{-2}$	$8.00 \times 10^{-3}$	$4.95 \times 10^{-3}$	$5.28 \times 10^{-5}$	$4.87 \times 10^{-6}$	$3.07 \times 10^{-6}$	$5.49 \times 10^{-6}$	$1.01 \times 10^{-8}$
0.5	$5.99 \times 10^{-3}$	$2.11 \times 10^{-2}$	$9.60 \times 10^{-3}$	$4.09 \times 10^{-3}$	$5.56 \times 10^{-5}$	$5.85 \times 10^{-6}$	$1.46 \times 10^{-8}$	$1.34 \times 10^{-6}$	$1.06 \times 10^{-8}$
0.6	$3.25 \times 10^{-3}$	$2.32 \times 10^{-2}$	$1.09 \times 10^{-2}$	$5.13 \times 10^{-3}$	$5.28 \times 10^{-5}$	$6.66 \times 10^{-6}$	$3.05 \times 10^{-6}$	$2.41 \times 10^{-6}$	$1.01 \times 10^{-8}$
0.7	$5.89 \times 10^{-3}$	$2.37 \times 10^{-2}$	$1.19 \times 10^{-2}$	$3.77 \times 10^{-3}$	$4.49 \times 10^{-5}$	$7.29 \times 10^{-6}$	$5.19 \times 10^{-6}$	$3.73 \times 10^{-6}$	$8.57 \times 10^{-9}$
0.8	$1.47 \times 10^{-2}$	$2.19 \times 10^{-2}$	$1.24 \times 10^{-2}$	$1.70 \times 10^{-3}$	$3.26 \times 10^{-5}$	$7.71 \times 10^{-6}$	$5.68 \times 10^{-6}$	$7.19 \times 10^{-6}$	$6.22 \times 10^{-9}$
0.9	$1.52 \times 10^{-2}$	$1.68 \times 10^{-2}$	$1.09 \times 10^{-2}$	$1.28 \times 10^{-3}$	$1.72 \times 10^{-5}$	$7.41 \times 10^{-6}$	$4.01 \times 10^{-6}$	$1.47 \times 10^{-6}$	$3.28 \times 10^{-9}$
1.0	0	0	0	0	0	0	0	0	0

**Table 4.4:** Comparison of absolute errors between HWQM with other methods for  $\lambda = 3.51$

$\eta$	B-Spline (Caglar & Caglar, 2009)	ANN (Kumar & Yadav, 2015)	LGSM (Abbasbandy et al., 2011)	NPSM (Jalilian, 2010)	HWQM (Present)
0.0	0	0	0	0	0
0.1	$3.84 \times 10^{-2}$	$2.98 \times 10^{-4}$	$4.45 \times 10^{-5}$	$6.61 \times 10^{-6}$	$4.18 \times 10^{-7}$
0.2	$7.48 \times 10^{-2}$	$6.88 \times 10^{-3}$	$7.12 \times 10^{-5}$	$5.83 \times 10^{-6}$	$8.16 \times 10^{-7}$
0.3	$1.06 \times 10^{-1}$	$2.72 \times 10^{-3}$	$7.30 \times 10^{-5}$	$6.19 \times 10^{-6}$	$1.16 \times 10^{-6}$
0.4	$1.27 \times 10^{-1}$	$1.76 \times 10^{-2}$	$4.47 \times 10^{-5}$	$6.89 \times 10^{-6}$	$1.39 \times 10^{-6}$
0.5	$1.35 \times 10^{-1}$	$1.04 \times 10^{-2}$	$6.76 \times 10^{-7}$	$7.31 \times 10^{-6}$	$1.48 \times 10^{-6}$
0.6	$1.27 \times 10^{-1}$	$1.37 \times 10^{-2}$	$4.56 \times 10^{-5}$	$6.89 \times 10^{-6}$	$1.39 \times 10^{-6}$
0.7	$1.06 \times 10^{-1}$	$4.32 \times 10^{-3}$	$7.20 \times 10^{-5}$	$6.19 \times 10^{-6}$	$1.16 \times 10^{-6}$
0.8	$7.48 \times 10^{-2}$	$6.68 \times 10^{-3}$	$7.05 \times 10^{-5}$	$5.83 \times 10^{-6}$	$8.16 \times 10^{-7}$
0.9	$3.84 \times 10^{-2}$	$1.66 \times 10^{-3}$	$4.41 \times 10^{-5}$	$6.61 \times 10^{-6}$	$4.17 \times 10^{-7}$
1.0	0	0	0	0	0

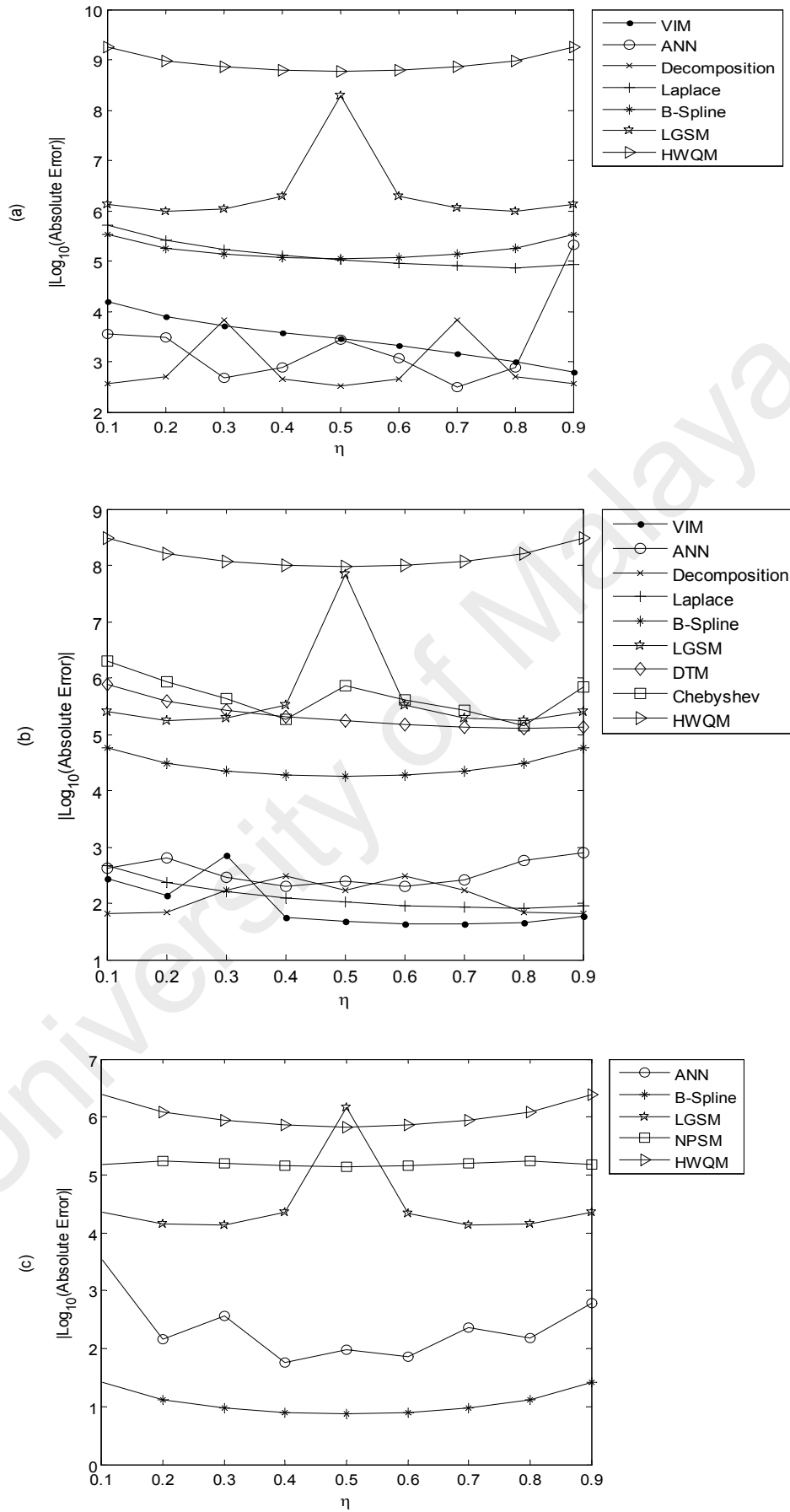


**Figure 4.1:** Comparison of absolute errors for (a)  $\lambda = 1$ , (b)  $\lambda = 2$  and (c)  $\lambda = 3.51$

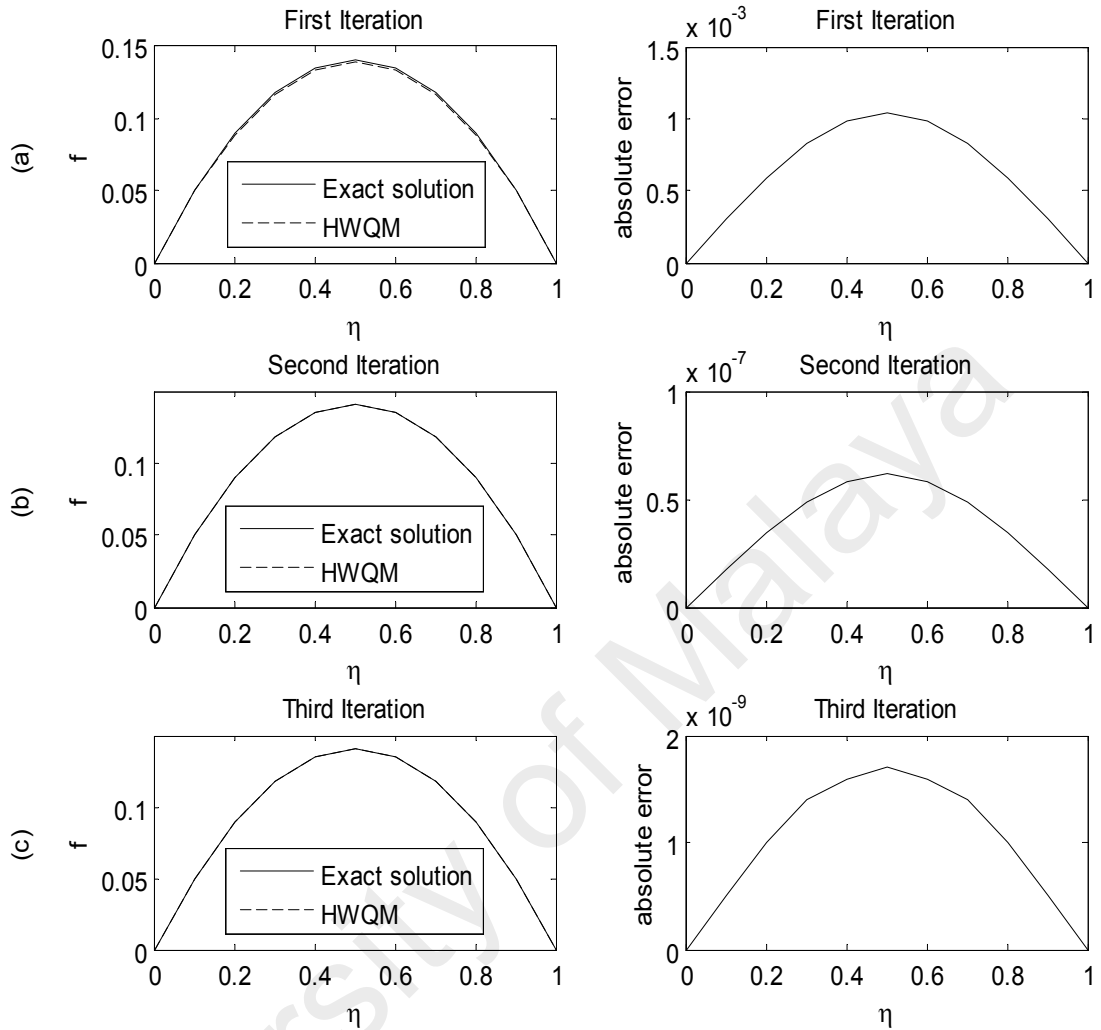


**Figure 4.2:** Comparison of exact solution and numerical solution by HWQM for (a) first, (b) second (c) third iterations at  $m = 2^{11}$  when  $\lambda = 1$

Figure 4.2 and Table 4.5 show the exact solution and approximate solution, respectively at three iterations. It shows that the absolute error reduces with increasing iterations, hence the sequence  $\{f_r\}$  defined by Equation (4.14) converges monotonically to the solution of Equation (4.1) in an interval  $0 \leq \eta \leq 1$ .

**Table 4.5:** Convergence error at three iterations when  $\lambda = 1$  and  $m = 2^{11}$ 

$\eta$	$f_0$	$f_1$	$f_2$	$ f_1 - f_0 $	$ f_2 - f_1 $
0.0	0	0	0	0	0
0.1	0.04954341	0.04984677	0.04984679	$3.0336 \times 10^{-4}$	$2.0 \times 10^{-8}$
0.2	0.08860013	0.08918990	0.08918999	$5.8977 \times 10^{-4}$	$9.0 \times 10^{-8}$
0.3	0.11677991	0.11760905	0.11760909	$8.2914 \times 10^{-4}$	$4.0 \times 10^{-8}$
0.4	0.13380120	0.13479020	0.13479025	$9.8900 \times 10^{-4}$	$5.0 \times 10^{-8}$
0.5	0.13949393	0.14053915	0.14053921	$1.0452 \times 10^{-3}$	$6.0 \times 10^{-8}$
0.6	0.13380120	0.13479020	0.13479025	$9.8900 \times 10^{-4}$	$5.0 \times 10^{-8}$
0.7	0.11677991	0.11760905	0.11760909	$8.2914 \times 10^{-4}$	$4.0 \times 10^{-8}$
0.8	0.08860013	0.08918990	0.08918993	$5.8977 \times 10^{-4}$	$9.0 \times 10^{-8}$
0.9	0.04954341	0.04984677	0.04984679	$3.0336 \times 10^{-4}$	$2.0 \times 10^{-8}$
1.0	0	0	0	0	0

**Table 4.6:** Comparison of CPU time (sec) between RKHSM and HWQM when  $L = 1$  and  $m = 2^3$ 

$\eta$	$\lambda = 1$		$\lambda = 2$		$\lambda = 3.51$	
	RKHSM (Inc et al., 2015)	HWQM (Present)	RKHSM (Inc et al., 2015)	HWQM (Present)	RKHSM (Inc et al., 2015)	HWQM (Present)
0.1	0.593	0.023	0.656	0.040	0.593	0.091
0.2	0.577	0.023	0.655	0.040	0.718	0.091
0.3	0.577	0.023	0.624	0.040	0.702	0.091
0.4	0.593	0.023	0.577	0.040	0.546	0.091
0.5	0.546	0.023	0.624	0.040	0.624	0.091
0.6	0.593	0.023	0.577	0.040	0.546	0.091
0.7	0.577	0.023	0.624	0.040	0.702	0.091
0.8	0.577	0.023	0.578	0.040	0.718	0.091
0.9	0.593	0.023	0.562	0.040	0.593	0.091

Table 4.6 is tabulated for a comparison of CPU time between reproducing kernel Hilbert space method (RKHSM) (Inc et al., 2015) with present method. The efficiency analysis of HWQM is performed by using ‘Run and Time’ command in MATLAB software version R2015a, while the RKHSM is calculated by employing Maple 16

software. It is observed that HWQM provides smaller CPU time compared to RKHSM, in which differs in a range -96% to -87%, since universal subprogram is applied to calculate Haar wavelet functions and their integrals.

## 4.2 The Falkner-Skan Equation

### 4.2.1 Introduction

The Falkner-Skan equation was first obtained for the boundary layer flow with stream-wise pressure gradient (Falkner & Skan, 1931),

$$f'''(\eta) + \gamma f(\eta)f''(\eta) + \beta(1 - f'^2(\eta)) = 0, \quad (4.19)$$

subject to the boundary conditions,

$$\begin{aligned} \eta = 0 & : f(0) = f'(0) = 0, \\ \eta \rightarrow \infty & : f' \rightarrow 1. \end{aligned} \quad (4.20)$$

where  $\gamma$  and  $\beta$  are constants. In this present work, we let  $\gamma$  in Equation (4.19) as  $\gamma = 1$ .

Numerical solutions of this problem has always been of interest for scientists and engineers. Some interesting characteristics of the Falkner-Skan equation were observed by some early researchers. The first analytical treatment for the Falkner-Skan equation was given by Hartree (1937), who found that in the region  $-0.19884 < \beta < 0$ , there exists a family of unique solutions whose first order derivative  $f'(\eta)$  tends to 1 exponentially. Weyl (1942) initiated the mathematically rigorous analysis for this equation for  $\beta = 0$ , namely the Blasius equation. He also proved that for  $\beta > 0$ , the problem has a solution  $f(\eta)$  whose first derivative  $f'(\eta)$  increases with  $\eta$  and whose second derivative  $f''(\eta)$  tends decreasing to zero as  $\eta$  approaches infinity. Coppel (1960) pointed out that the restriction on the first derivative can be omitted when  $0 \leq \beta \leq 1$ . The extension for  $\beta < 0$  was discussed and the properties of solutions were investigated further (Veldman & Vooren, 1980; Oskam & Veldman,

1982).

Several numerical techniques have been done for the study of Falkner-Skan equation. For example, finite difference method (Hartree, 1937; Oskam & Veldman, 1982; Becket, 1983; Asaithambi, 1998, 2004a), finite element method (Asaithambi, 2004b), shooting method (Cebici & Keller, 1971; Asaithambi, 1997, 2005; Sher & Yakhot, 2001; Chang et al., 2006; Liu & Chang, 2008), Adomian decomposition method (Elgazery, 2008; Alizadeh et al., 2009), homotopy analysis method (Abbasbandy & Hayat, 2009a; Yao, 2009; Hendi & Hussain, 2012), Hankel-Pade method (Abbasbandy & Hayat, 2009b), collocation method (Parand et al., 2011; Allame et al., 2014; Kajani et al., 2014), group invariance theory (Fazio, 1994, 1996), Chebyshev spectral method (Nasr et al., 1990; Elbarbary, 2005), differential transformation method (Kuo, 2003), optimal homotopy asymptotic method (OHAM) (Marinca et al., 2014) and quasilinearization method (Zhu et al., 2009).

#### 4.2.2 Numerical Solution

Consider the nonlinear Falkner-Skan equation as in Equation (4.19). Apply quasilinearization technique to Equation (4.19), we have

$$f_{r+1}''' + f_r'' f_{r+1} + f_r f_{r+1}'' - 2\beta f_r' f_{r+1}' = -\beta(1 + f_r'^2) + f_r'' f_r. \quad (4.21)$$

The boundary conditions are

$$\begin{aligned} \eta = 0 & : f_{r+1} = f_{r+1}' = 0, \\ \eta \rightarrow \infty & : f' \rightarrow 1, \end{aligned} \quad (4.22)$$

where  $0 \leq \eta \leq L$ , with  $L$  is sufficiently large number. The Haar wavelet method is applied to Equation (4.21), by approximating the higher order derivative term by Haar wavelet series as

$$f_{r+1}'''(\eta) = \sum_{i=0}^{m-1} a_i h_i(\eta). \quad (4.23)$$

The lower order derivatives are obtained by integrating Equation (4.23) three times and by using the boundary conditions (4.22), we get

$$f_{r+1}''(\eta) = \sum_{i=0}^{m-1} a_i p_{i,1}(\eta) + f_{r+1}''(0), \quad (4.24)$$

$$f_{r+1}'(\eta) = \sum_{i=0}^{m-1} a_i p_{i,2}(\eta) + \eta f_{r+1}''(0) + f_{r+1}'(0), \quad (4.25)$$

$$f_{r+1}(\eta) = \sum_{i=0}^{m-1} a_i p_{i,3}(\eta) + \frac{\eta^2}{2} f_{r+1}''(0) + \eta f_{r+1}'(0) + f_{r+1}(0). \quad (4.26)$$

To find the missing boundary condition,  $f_{r+1}''(0)$ ; it can be obtained from Equation (4.25), by letting  $\eta = L$ , implies that

$$f_{r+1}''(0) = \frac{1}{L} \left( - \sum_{i=0}^{m-1} a_i p_{i,2}(L) - f_{r+1}'(0) + f_{r+1}'(L) \right). \quad (4.27)$$

Now, Equations (4.24), (4.25) and (4.26) become,

$$f_{r+1}''(\eta) = \sum_{i=0}^{m-1} a_i \left( p_{i,1}(\eta) - \frac{1}{L} p_{i,2}(L) \right) + \frac{1}{L}, \quad (4.28)$$

$$f_{r+1}'(\eta) = \sum_{i=0}^{m-1} a_i \left( p_{i,2}(\eta) - \frac{\eta}{L} p_{i,2}(L) \right) + \frac{\eta}{L}, \quad (4.29)$$

$$f_{r+1}(\eta) = \sum_{i=0}^{m-1} a_i \left( p_{i,3}(\eta) - \frac{\eta^2}{2L} p_{i,2}(L) \right) + \frac{\eta^2}{2L}. \quad (4.30)$$

Substitute Equations (4.23) and (4.28) - (4.30) into Equation (4.21), we obtain

$$\begin{aligned} & \sum_{i=0}^{m-1} a_i \left( \begin{aligned} & h_i(\eta) + f_r''(\eta) p_{i,3}(\eta) - \frac{\eta^2}{2L} f_r''(\eta) p_{i,2}(L) - 2\beta f_r'(\eta) p_{i,2}(\eta) \\ & + \frac{2\beta}{L} \eta f_r'(\eta) p_{i,2}(L) - f_r(\eta) p_{i,1}(\eta) - \frac{1}{L} f_r(\eta) p_{i,2}(L) \end{aligned} \right) \\ & = -\beta(1 + f_r'^2(\eta)) + f_r''(\eta) f_r(\eta) - \frac{\eta^2}{2L} f_r''(\eta) + \frac{2\beta}{L} \eta f_r'(\eta) - \frac{1}{L} f_r(\eta). \end{aligned} \quad (4.31)$$

The initial approximation is

$$f_0(\eta) = -\frac{\beta}{6} \eta^3 + \left( \frac{2 + \beta L^2}{4L} \right) \eta^2. \quad (4.32)$$

Haar coefficients,  $a_i$  can be calculated easily from Equation (4.31). To see the efficiency and accuracy of this method, this problem is tested for three different values of  $\beta$ 's. The efficiency and accuracy of the present method will be discussed in the following section.

### 4.2.3 Results and Discussion

In this section, numerous  $\beta$  of the Falkner-Skan equation are solved numerically by using HWQM with the help MATLAB software. In order to see the accuracy of the results for  $\beta = 0.5, 1$  and  $1.6$ , we illustrate the accuracy of the HWQM by comparing with the previously obtained approximate solutions reported by Marinca et al. (2014), where the numerical integration results computed by means of the shooting method combined with fourth-order Runge-Kutta method (RKM4) using Wolfram Mathematica 6.0 software.

The numerical results of HWQM at  $m = 2^8$  obtain for different values of  $\beta$  corresponding to the values of  $f(\eta)$  and  $f'(\eta)$  are listed in Tables 4.7, 4.9 and 4.11. From these tables, it is clear that HWQM produces stable results and the results are more closer to RKM compared to optimal homotopy asymptotic method (OHAM). Absolute errors are shown in Tables 4.8, 4.10 and 4.12 and Figures 4.4, 4.6 and 4.8 for each  $f(\eta)$  and  $f'(\eta)$  along with different values of  $\beta$ . It is observed that HWQM gives the smallest absolute error compared to OHAM.

Figures 4.3, 4.5 and 4.7 show the variation of iterations for  $f(\eta)$  and its derivative. It can be seen that as we increased the iterations, the result is getting closed to the desired approximation, hence it is satisfied the boundary conditions given. In order to verify the accuracy and rapid convergence of our present method, we have listed the values of  $f''(0)$  for different values of  $\beta$  as shown in Table 4.13. It is evident that

there is excellent agreement between the previous and present results.

**Table 4.7:** Comparison between HWQM with RKM and OHAM for  $f(\eta)$  and  $f'(\eta)$  when  $\beta = 0.5$

$\eta$	RKM (Marinca et al., 2014)		OHAM (Marinca et al., 2014)		HWQM (Present)	
	$f(\eta)$	$f'(\eta)$	$f(\eta)$	$f'(\eta)$	$f(\eta)$	$f'(\eta)$
4/5	0.254348	0.583305	0.254315	0.583315	0.254348	0.583305
8/5	0.855027	0.876098	0.855062	0.875965	0.855027	0.876098
12/5	1.604527	0.976069	1.604359	0.975952	1.604528	0.976069
16/5	2.396313	0.997192	2.396240	0.997377	2.396314	0.997192
4	3.195500	0.999808	3.195378	0.999469	3.195501	0.999808
24/5	3.995453	0.999993	3.994961	0.999522	3.995453	0.999993
28/5	4.795451	1.000000	4.794697	0.999833	4.795452	1.000000
32/5	5.595451	1.000000	5.594653	1.000005	5.595452	1.000000
36/5	6.395451	1.000000	6.394624	0.999883	6.395452	1.000000
8	7.195451	1.000000	7.194427	0.999617	7.195452	1.000000

**Table 4.8:** Comparison of absolute errors between OHAM and HWQM for  $f(\eta)$  and  $f'(\eta)$  when  $\beta = 0.5$

$\eta$	$f(\eta)$		$f'(\eta)$	
	$ \text{OHAM}^1 - \text{RKM} $	$ \text{HWQM}^2 - \text{RKM} $	$ \text{OHAM}^1 - \text{RKM} $	$ \text{HWQM}^2 - \text{RKM} $
4/5	$3.313410 \times 10^{-5}$	$7.700000 \times 10^{-9}$	$1.013370 \times 10^{-5}$	$3.550000 \times 10^{-8}$
8/5	$3.534730 \times 10^{-5}$	$7.700000 \times 10^{-8}$	$1.324243 \times 10^{-4}$	$1.355000 \times 10^{-7}$
12/5	$1.685673 \times 10^{-4}$	$2.100000 \times 10^{-7}$	$1.167979 \times 10^{-4}$	$1.674000 \times 10^{-7}$
16/5	$7.294670 \times 10^{-5}$	$3.060000 \times 10^{-7}$	$1.848228 \times 10^{-4}$	$6.830000 \times 10^{-8}$
4	$1.220981 \times 10^{-4}$	$3.350000 \times 10^{-7}$	$3.388907 \times 10^{-4}$	$1.350000 \times 10^{-8}$
24/5	$4.918840 \times 10^{-4}$	$3.390000 \times 10^{-7}$	$4.702794 \times 10^{-4}$	$1.800000 \times 10^{-9}$
28/5	$7.541605 \times 10^{-4}$	$3.390000 \times 10^{-7}$	$1.666808 \times 10^{-4}$	$4.000000 \times 10^{-10}$
32/5	$7.987450 \times 10^{-4}$	$3.400000 \times 10^{-7}$	$5.028974 \times 10^{-6}$	$3.000000 \times 10^{-10}$
36/5	$8.271670 \times 10^{-4}$	$3.400000 \times 10^{-7}$	$1.167343 \times 10^{-4}$	$5.000000 \times 10^{-10}$
8	$1.023896 \times 10^{-3}$	$3.410000 \times 10^{-7}$	$3.825046 \times 10^{-4}$	$5.000000 \times 10^{-10}$

<sup>1</sup> Marinca et al. (2014)      <sup>2</sup> Present

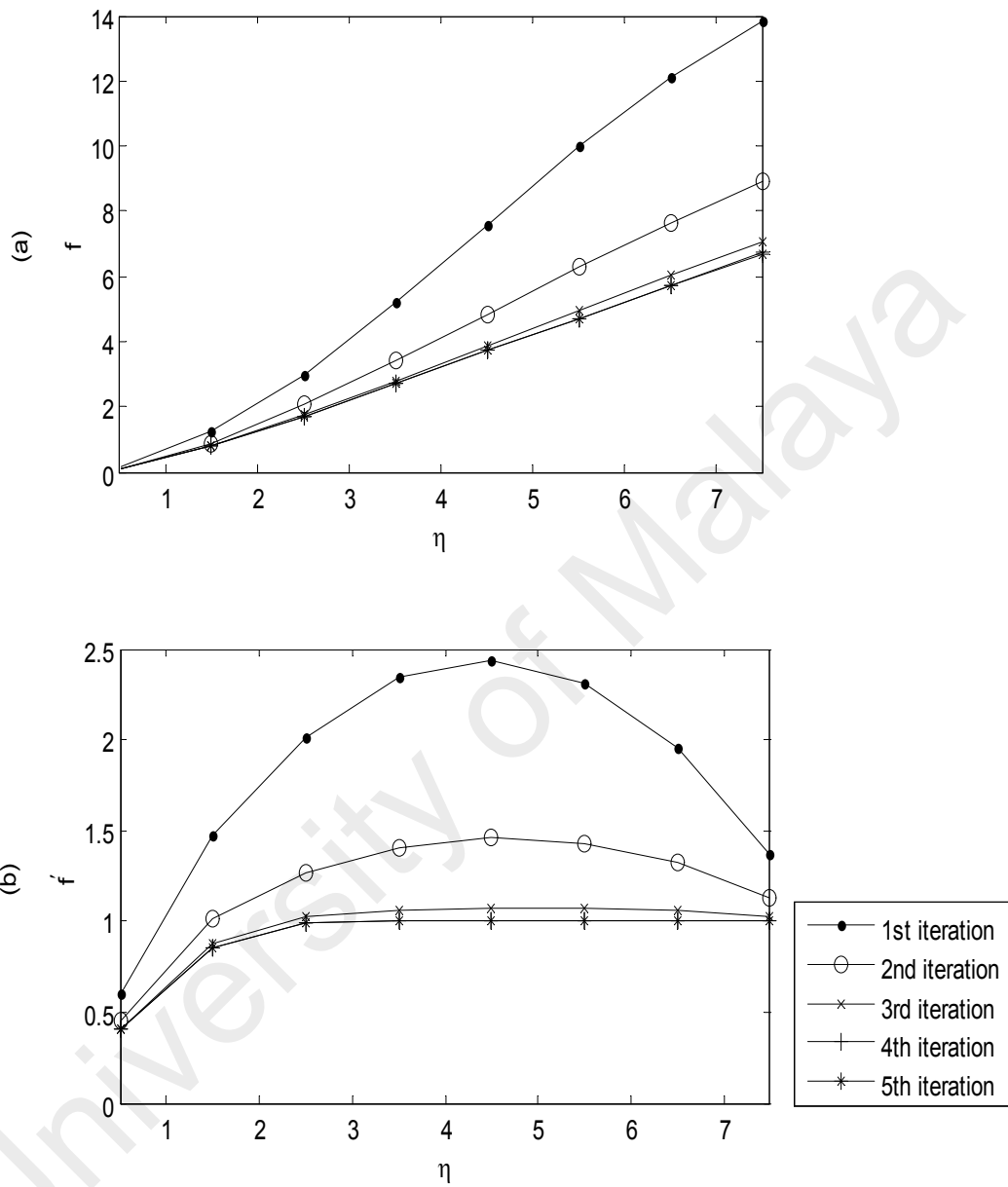


**Figure 4.3:** HWQM solution of (a)  $f(\eta)$  and (b)  $f'(\eta)$  when  $\beta = 0.5$  at different iterations

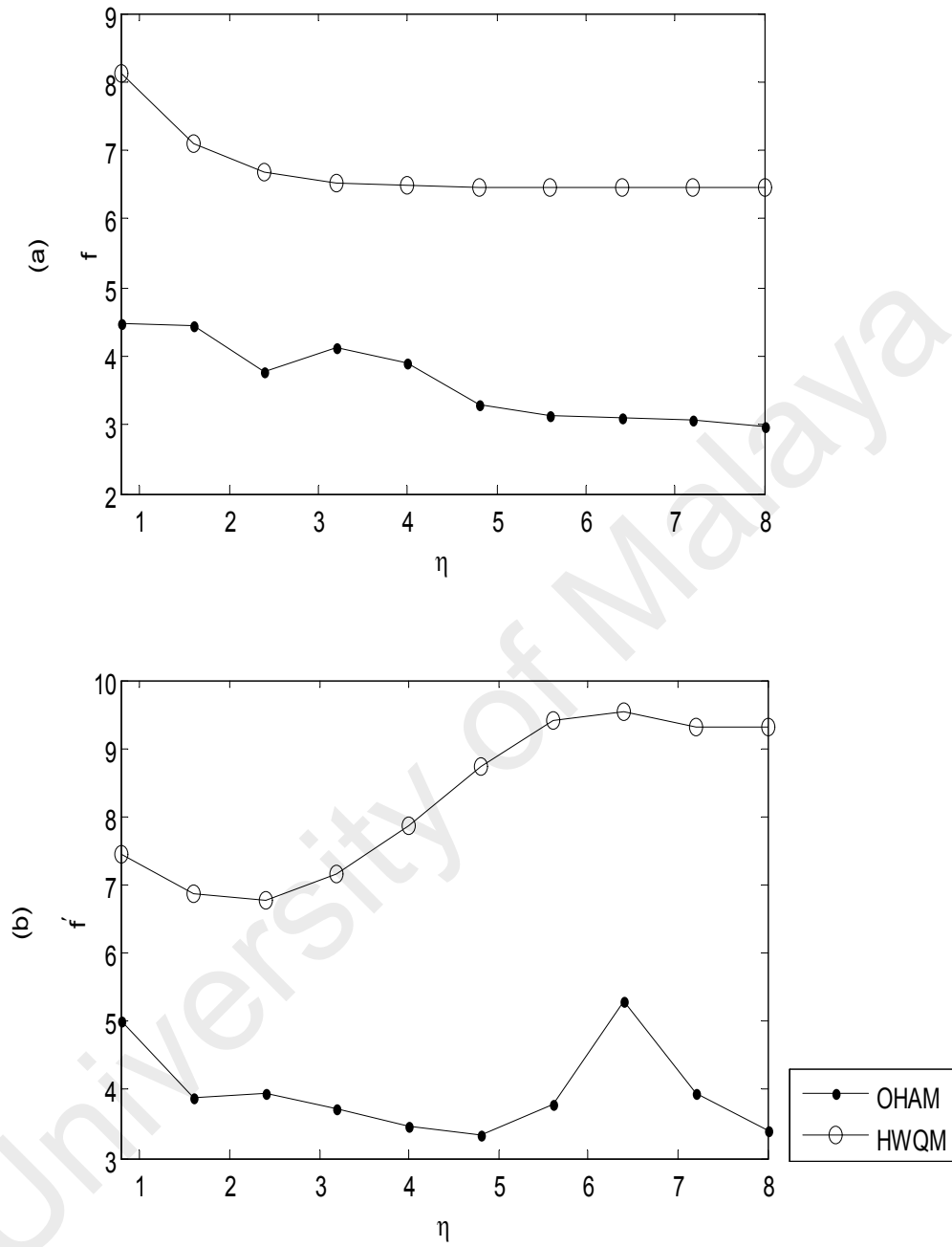


**Figure 4.4:** Comparison of  $|\log_{10}(\text{absolute errors})|$  for (a)  $f(\eta)$  and (b)  $f'(\eta)$  with  $\beta = 0.5$

**Table 4.9:** Comparison between HWQM with RKM and OHAM for  $f(\eta)$  and  $f'(\eta)$  when  $\beta = 1$

$\eta$	RKM		OHAM		HWQM	
	(Marinca et al., 2014)		(Marinca et al., 2014)		(Present)	
	$f(\eta)$	$f'(\eta)$	$f(\eta)$	$f'(\eta)$	$f(\eta)$	$f'(\eta)$
4/5	0.312423	0.685937	0.312422	0.685935	0.312423	0.685938
8/5	0.979780	0.932348	0.979781	0.932347	0.979780	0.932348
12/5	1.755254	0.990549	1.755257	0.990568	1.755254	0.990550
16/5	2.552325	0.999186	2.552347	0.999197	2.552326	0.999186
4	3.352109	0.999958	3.352131	0.999962	3.352110	0.999958
24/5	4.152100	0.999999	4.152144	1.000055	4.152100	0.999999
28/5	4.952100	1.000000	4.952202	1.000080	4.952100	1.000000
32/5	5.752100	1.000000	5.752260	1.000062	5.752100	1.000000
36/5	6.552100	1.000000	6.552299	1.000036	6.552100	1.000000
8	7.352100	1.000000	7.352319	1.000017	7.352100	1.000000

**Table 4.10:** Comparison of absolute errors between OHAM and HWQM for  $f(\eta)$  and  $f'(\eta)$  when  $\beta = 1$

$\eta$	$f(\eta)$		$f'(\eta)$	
	$ \text{OHAM}^1 - \text{RKM} $	$ \text{HWQM}^2 - \text{RKM} $	$ \text{OHAM}^1 - \text{RKM} $	$ \text{HWQM}^2 - \text{RKM} $
	4/5	$1.133942 \times 10^{-6}$	$3.800000 \times 10^{-9}$	$2.696657 \times 10^{-6}$
8/5	$1.783054 \times 10^{-6}$	$9.370000 \times 10^{-8}$	$1.371273 \times 10^{-6}$	$1.924000 \times 10^{-7}$
12/5	$3.364056 \times 10^{-6}$	$2.120000 \times 10^{-7}$	$1.893000 \times 10^{-5}$	$1.262000 \times 10^{-7}$
16/5	$2.117940 \times 10^{-5}$	$2.790000 \times 10^{-7}$	$1.072000 \times 10^{-5}$	$5.260000 \times 10^{-8}$
4	$2.146329 \times 10^{-5}$	$2.940000 \times 10^{-7}$	$3.683007 \times 10^{-6}$	$2.100000 \times 10^{-9}$
24/5	$4.456650 \times 10^{-5}$	$2.940000 \times 10^{-7}$	$5.601120 \times 10^{-5}$	$3.000000 \times 10^{-9}$
28/5	$1.022586 \times 10^{-4}$	$2.910000 \times 10^{-7}$	$7.953890 \times 10^{-5}$	$4.000000 \times 10^{-9}$
32/5	$1.605945 \times 10^{-4}$	$2.860000 \times 10^{-7}$	$6.218900 \times 10^{-5}$	$6.200000 \times 10^{-9}$
36/5	$1.995199 \times 10^{-4}$	$2.800000 \times 10^{-7}$	$3.567310 \times 10^{-5}$	$8.000000 \times 10^{-9}$
8	$2.198750 \times 10^{-4}$	$2.730000 \times 10^{-7}$	$1.688180 \times 10^{-5}$	$1.000000 \times 10^{-8}$

<sup>1</sup> Marinca et al. (2014)

<sup>2</sup> Present

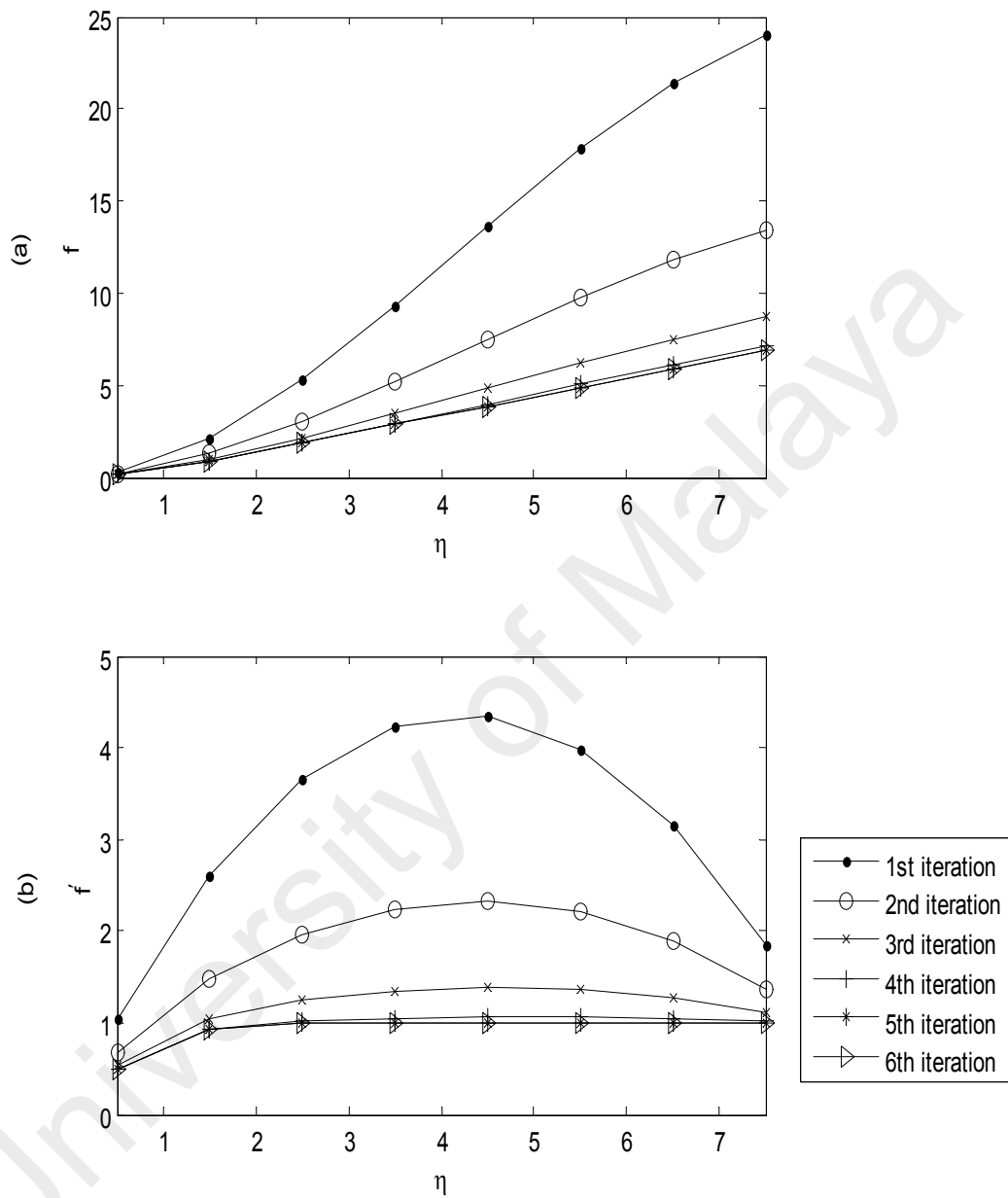


**Figure 4.5:** HWQM solution for (a)  $f(\eta)$  and (b)  $f'(\eta)$  when  $\beta = 1$  at different iterations

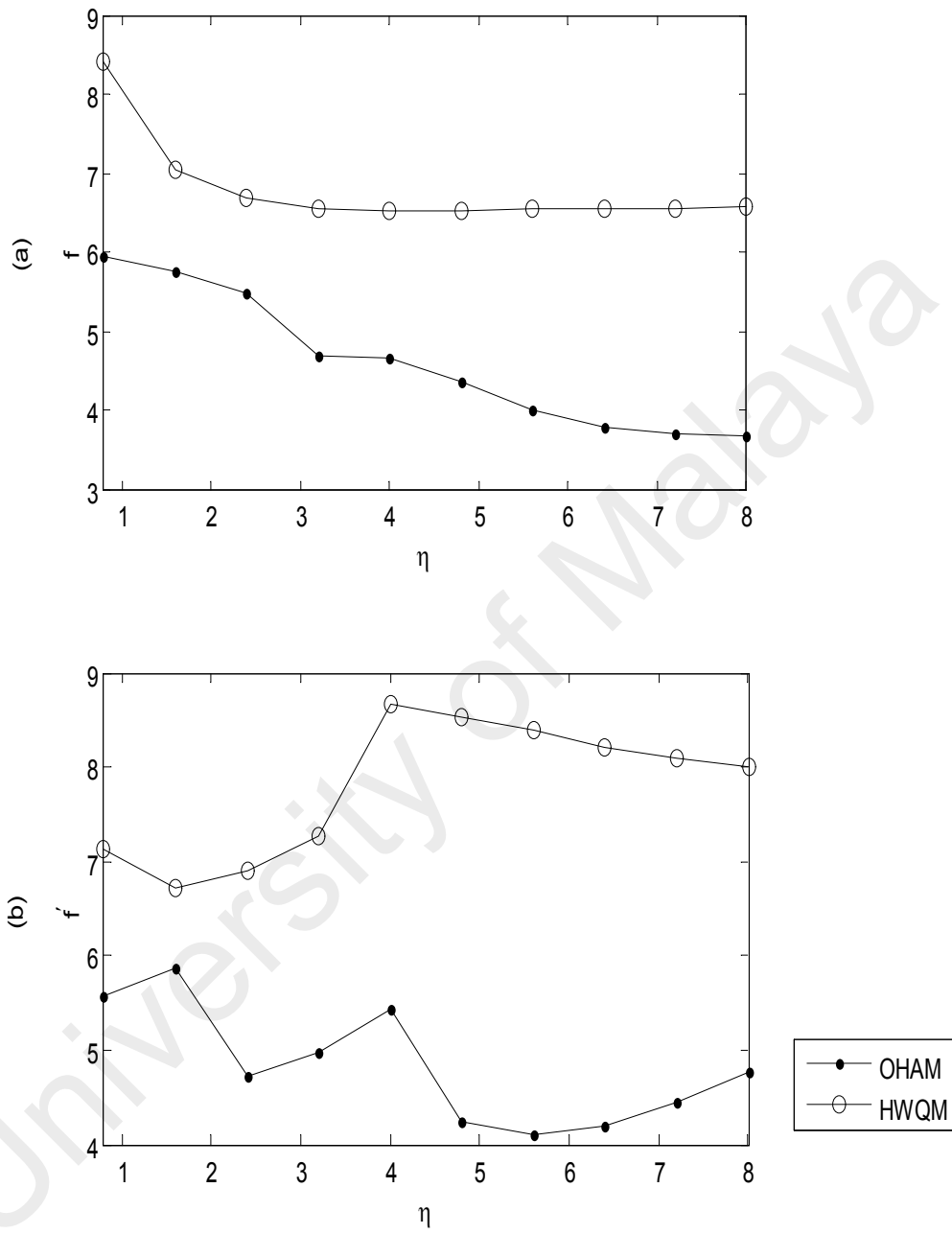


**Figure 4.6:** Comparison of  $|\log_{10}(\text{absolute errors})|$  for (a)  $f(\eta)$  and (b)  $f'(\eta)$  with  $\beta = 1$

**Table 4.11:** Comparison between HWQM with RKM and OHAM for  $f(\eta)$  and  $f'(\eta)$  when  $\beta = 1.6$

$\eta$	RKM (Marinca et al., 2014)		OHAM (Marinca et al., 2014)		HWQM (Present)	
	$f(\eta)$	$f'(\eta)$	$f(\eta)$	$f'(\eta)$	$f(\eta)$	$f'(\eta)$
4/5	0.359978	0.760923	0.359978	0.760924	0.359979	0.760923
8/5	1.069615	0.961978	1.069616	0.961971	1.069615	0.961978
12/5	1.857162	0.996057	1.857163	0.996066	1.857163	0.996057
16/5	2.656043	0.999744	2.656046	0.999737	2.656044	0.999744
4	3.455980	0.999990	3.455977	0.999987	3.455981	0.999990
24/5	4.255978	1.000000	4.255978	1.000008	4.255979	1.000000
28/5	5.055978	1.000000	5.055983	1.000001	5.055979	1.000000
32/5	5.855978	1.000000	5.855980	0.999992	5.855979	1.000000
36/5	6.655978	1.000000	6.655972	0.999989	6.655979	1.000000
8	7.455978	1.000000	7.455964	0.999991	7.455979	1.000000

**Table 4.12:** Comparison of absolute errors between OHAM and HWQM for  $f(\eta)$  and  $f'(\eta)$  when  $\beta = 1.6$

$\eta$	$f(\eta)$		$f'(\eta)$	
	$ \text{OHAM}^1 - \text{RKM} $	$ \text{HWQM}^2 - \text{RKM} $	$ \text{OHAM}^1 - \text{RKM} $	$ \text{HWQM}^2 - \text{RKM} $
4/5	$2.160525 \times 10^{-7}$	$1.760000 \times 10^{-8}$	$1.486624 \times 10^{-6}$	$1.835000 \times 10^{-7}$
8/5	$9.093019 \times 10^{-7}$	$2.140000 \times 10^{-7}$	$7.352687 \times 10^{-6}$	$2.451000 \times 10^{-7}$
12/5	$9.977941 \times 10^{-7}$	$3.480000 \times 10^{-7}$	$9.018419 \times 10^{-6}$	$8.830000 \times 10^{-8}$
16/5	$2.878145 \times 10^{-6}$	$3.840000 \times 10^{-7}$	$7.413383 \times 10^{-6}$	$7.000000 \times 10^{-9}$
4	$3.436309 \times 10^{-6}$	$3.830000 \times 10^{-7}$	$2.724280 \times 10^{-6}$	$6.600000 \times 10^{-9}$
24/5	$1.038556 \times 10^{-8}$	$3.750000 \times 10^{-7}$	$8.360731 \times 10^{-6}$	$1.420000 \times 10^{-8}$
28/5	$4.685640 \times 10^{-6}$	$3.600000 \times 10^{-7}$	$1.338446 \times 10^{-6}$	$2.300000 \times 10^{-8}$
32/5	$1.582358 \times 10^{-6}$	$3.360000 \times 10^{-7}$	$8.223935 \times 10^{-6}$	$3.600000 \times 10^{-8}$
36/5	$6.516027 \times 10^{-6}$	$3.000000 \times 10^{-7}$	$1.086350 \times 10^{-5}$	$5.400000 \times 10^{-8}$
8	$1.450440 \times 10^{-5}$	$2.480000 \times 10^{-7}$	$8.665844 \times 10^{-6}$	$7.640000 \times 10^{-8}$

<sup>1</sup> Marinca et al. (2014)

<sup>2</sup> Present

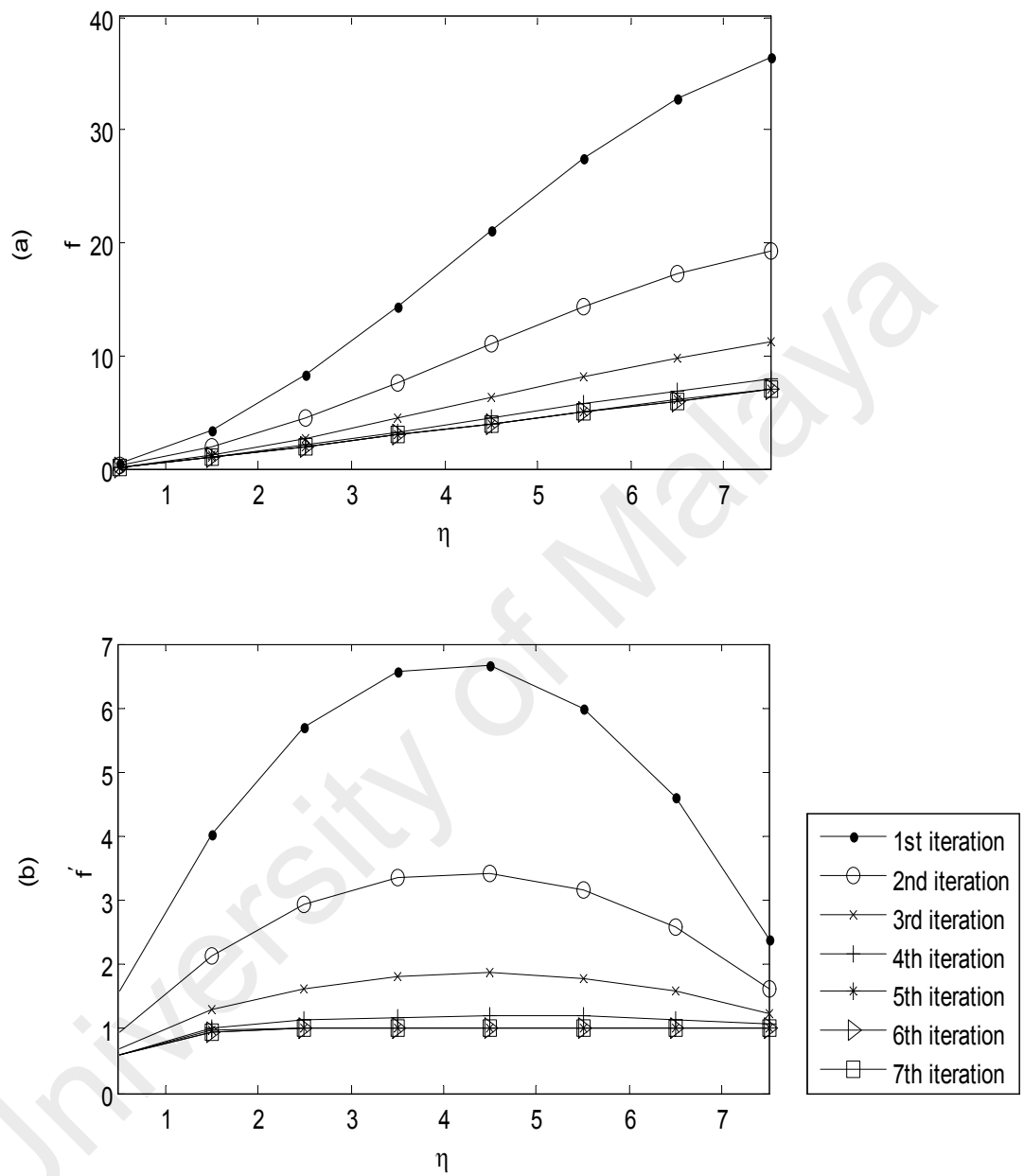


**Figure 4.7:** HWQM solution for (a)  $f(\eta)$  and (b)  $f'(\eta)$  when  $\beta = 1.6$  at different iterations

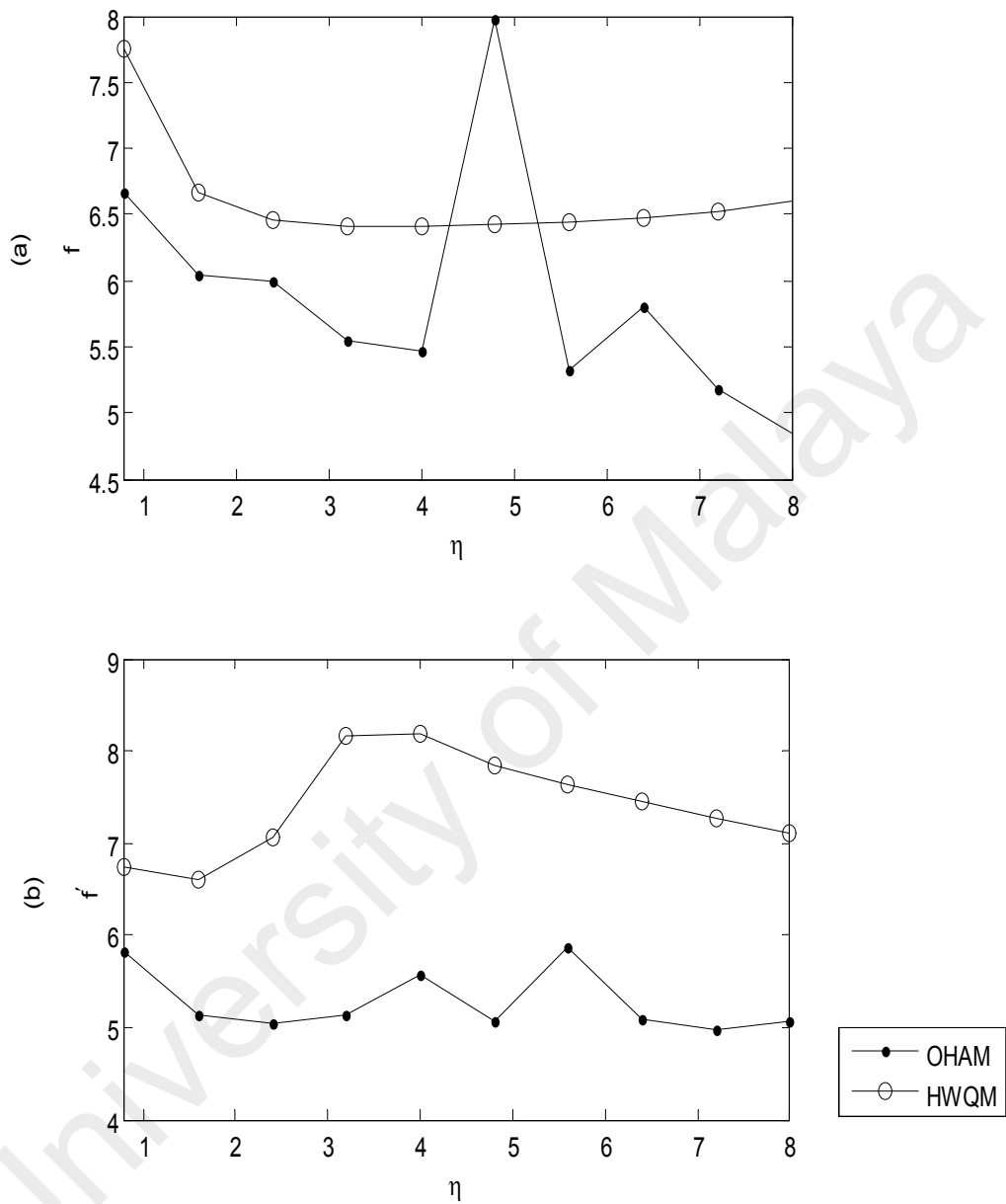


**Figure 4.8:** Comparison of  $|\log_{10}(\text{absolute errors})|$  for (a)  $f(\eta)$  and (b)  $f'(\eta)$  with  $\beta = 1.6$

**Table 4.13:** Comparison of  $f''(0)$  between HWQM with RKM and OHAM for different values of  $\beta$

$\beta$	RKM (Marinca et al., 2014)	OHAM (Marinca et al., 2014)	HWQM (Present)
0.5	0.92768	0.92779	0.92768
1.0	1.23259	1.23257	1.23258
1.6	1.52151	1.52151	1.52151

**Table 4.14:** Comparison of CPU time (sec) between CCF and HWQM for different values of  $\beta$  when  $L = 6$  and  $m = 8$

$\beta$	CCF (Lakestani, 2011)	HWQM (Present)
2.0	31.97	0.193
1.0	32.09	0.196
0.5	31.41	0.244
0.0	24.13	0.206
-0.10	31.56	0.195
-0.12	31.95	0.196
-0.15	31.96	0.193
-0.18	33.06	0.198
-0.1988	60.02	0.234

From Table 4.14, the Chebyshev cardinal functions (CCF) (Lakestani, 2011) method was selected to show the computational accuracy for solving Falkner-Skan equation. It shows that HWQM provides better results with less computing time, in which differs in a range of -99.6% to -99%. This is because it did not faced with necessity of large computer memory and time.

### 4.3 The Blasius Equation

#### 4.3.1 Introduction

The Blasius equation is used to model the boundary layer growth over a surface when the flow field is slender in nature. The Blasius equation (Blasius, 1950) is given as

$$\alpha f'''(\eta) + f(\eta)f''(\eta) = 0, \quad (4.33)$$

where  $\alpha$  is a constant parameter. The boundary conditions are

$$\begin{aligned} \eta = 0 & : f(0) = a, \quad f'(0) = b, \\ \eta \rightarrow \infty & : f' \rightarrow c. \end{aligned} \quad (4.34)$$

The original problem for the Blasius equation is associated with  $a = b = 0$  and  $c = 1$ . This equation has been studied for many different conditions. For  $\alpha = 1$  and  $\alpha = 2$ , this equation is a form of the Blasius relation for the flat plate flow in fluid mechanics. Several methods have been obtained for  $\alpha = 1$  that found in the literature. Klemp and Acrivos (1976) considered  $f'(0)$  being negative for a moving plate. Hussaini and Lakin (1986) showed that the solutions of such boundary layer problems exist only up to a certain critical value of the velocity ratio parameter. Vajravelu and Mohapatra (1990) analyzed the problem of boundary layer flow on a flat plate with injection and a constant velocity opposite in direction to that of the uniform mainstream.

Fang (2003a) extended the previous works to the general situations including mass injection as well as suction on the wall and the case of the wall moving in the same direction as the free stream velocity. He also studied the heat transfer problem for a moving wall boundary layer (Fang, 2003b). Cortell (2007) presented a numerical analysis of the momentum and heat transfer of an incompressible fluid past a parallel moving sheet. Gahan et al. (2000) constructed a new finite difference method for computing numerical solutions to the Blasius equation arising from incompressible laminar flow past a thin flat plate with mass transfer by both suction and blowing. Another class of boundary layer problem for a stretching sheet relevant to the Blasius

equation was studied by Sakiadis (1961), in which the boundary conditions become  $f'(0) = 1$ ,  $f'(\infty) = 0$  with  $f(0) = 0$  for an impermeable plate and  $f(0) \neq 0$  for mass transfer across a permeable plate.

In this study, we considered  $\alpha = 2$ . Within boundary layer theory, Blasius equation is given as,

$$2f'''(\eta) + f(\eta)f''(\eta) = 0, \quad (4.35)$$

subject to the boundary conditions

$$\begin{aligned} \eta = 0 & : f(0) = f'(0) = 0, \\ \eta \rightarrow \infty & : f' \rightarrow 1. \end{aligned} \quad (4.36)$$

Several methods also have been obtained for  $\alpha = 2$  that found in the literature. Ahmad (2007) solved this problem in the case of constant flow in a boundary layer and replaced the second condition by negative value. Aminikhah (2009) introduced a new modification of homotopy perturbation method (HPM) for solving Blasius equation. He also presented Laplace transform and new homotopy perturbation methods to study Blasius' viscous flow equation (Aminikhah, 2012). Esmailpour and Ganji (2007) applied He's homotopy perturbation method (He, 1999b) to the problem of forced convection over a horizontal flat plate for finding the approximate solution. Fang et al. (2006) obtained the solution of the extended Blasius equation from the original Blasius equation with a variable transformation technique and discussed for an arbitrary real parameter or complex parameter. A comparison between homotopy perturbation method and homotopy analysis method is made by He (2004). Liao (1997) proposed the homotopy analysis method by introducing a non-zero parameter into the classical way of constructing a homotopy for solving laminar viscous flow over an infinite flat plate. Later, Liao (1998) applied homotopy analysis method to give an explicit solution of the laminar viscous flow over a semi-infinite flat plate.

He (1999a) solved Blasius equation via VIM and compared the analytical solution

with Howarth's numerical solution (Howarth, 1938). The VIM also applied for a reliable treatment of two forms third order nonlinear Blasius equation which comes from boundary layer equations as reported by Wazwaz (2007). Abbasbandy (2007) proposed ADM and compared with HPM and Howarth's numerical solution. Wang (2004) introduced a new algorithm based on the ADM to the transformation of the Blasius equation. Cortell (2005) obtained numerical solutions of the classical Blasius flat plate problem by using well-known fourth order Runge-Kutta algorithm. The parameter iteration method was used by Lin (1999) to solve similar problem. Mohammed et al. (2014) proposed the successive linearization method (SLM) for solving some boundary layer problems. A modified rational Legendre method for solving classical Blasius equation was given by Tajvidi et al. (2008).

Although solution for this problem had been obtained by Kaur et al. (2013) by using Haar wavelet quasilinearization method, but they only considered the problem defined over the interval  $[0, 1]$  and used the transformation for converting the problem on a fixed computational domain. This will limit the study because the boundary layer fluid flow problems deal with sufficiently large number of infinite intervals.

#### 4.3.2 Numerical Solution

The quasilinearization equation is

$$2f_{r+1}''' + f_r'' f_{r+1} + f_r f_{r+1}'' = f_r'' f_r. \quad (4.37)$$

The new boundary conditions are

$$\begin{aligned} \eta = 0 & : f_{r+1} = f_{r+1}' = 0, \\ \eta \rightarrow \infty & : f_{r+1}' \rightarrow 1, \end{aligned} \quad (4.38)$$

where  $0 \leq \eta \leq L$ , whereas  $L$  is sufficiently large number. After simplification and substitution, we get

$$f_{r+1}''(\eta) = \sum_{i=0}^{m-1} a_i \left( p_{i,1}(\eta) - \frac{1}{L} p_{i,2}(L) \right) + \frac{1}{L}, \quad (4.39)$$

$$f_{r+1}'(\eta) = \sum_{i=0}^{m-1} a_i \left( p_{i,2}(\eta) - \frac{\eta}{L} p_{i,2}(L) \right) + \frac{\eta}{L}, \quad (4.40)$$

$$f_{r+1}(\eta) = \sum_{i=0}^{m-1} a_i \left( p_{i,3}(\eta) - \frac{\eta^2}{2L} p_{i,2}(L) \right) + \frac{\eta^2}{2L}. \quad (4.41)$$

The coefficient  $a_i$  can be computed as follows,

$$\begin{aligned} \sum_{i=0}^{m-1} a_i \left( \begin{aligned} & h_i(\eta) + \frac{1}{2} f_r''(\eta) p_{i,3}(\eta) - \frac{\eta^2}{4L} f_r''(\eta) p_{i,2}(L) \\ & + \frac{1}{2} f_r'(\eta) p_{i,1}(\eta) - \frac{1}{2L} f_r'(\eta) p_{i,2}(L) \end{aligned} \right) \\ = \frac{1}{2} f_r''(\eta) f_r(\eta) - \frac{\eta^2}{4L} f_r''(\eta) - \frac{1}{2L} f_r'(\eta). \end{aligned} \quad (4.42)$$

Equation (4.42) is solved by using initial approximation as follows,

$$f_0(\eta) = \frac{\eta^2}{2L}. \quad (4.43)$$

### 4.3.3 Results and Discussion

Some of the computed results for the variations of  $\eta$  belong to the functions  $f(\eta)$ ,  $f'(\eta)$  and  $f''(\eta)$  are tabulated in Tables 4.15 - 4.17.

All the results obtained via HWQM with  $m = 256$  are compared with the numerical solutions in the literature such as HPM (Esmailpour & Ganji, 2007), combination of Laplace transform and new homotopy perturbation method (LTNHPM) (Aminikhah, 2012) and Howarth method (Howarth, 1938) which confirms the validity of the proposed methods and shared similar interval  $[0, 5]$ . It is evident that there is excellent agreement between the previous and present results.

**Table 4.15:** Comparison between HPM, LTNHPM, Howarth and HWQM for  $f(\eta)$ 

$\eta$	HPM (Esmailpour & Ganji, 2007)	LTNHPM (Aminikhah, 2012)	Howarth (Howarth, 1938)	HWQM (Present)
0	0	0	0	0
0.2	0.00697	0.00664	0.00664	0.0066410686
0.4	0.02788	0.02656	0.02656	0.0265601477
0.6	0.06270	0.05973	0.05974	0.0597352037
0.8	0.11137	0.10611	0.10611	0.1061091794
1.0	0.17380	0.16557	0.16557	0.1655731493
1.2	0.24980	0.23795	0.23795	0.2379506634
1.4	0.33912	0.32298	0.32298	0.3229840873
1.6	0.44140	0.42032	0.42032	0.4203238833
1.8	0.55618	0.52952	0.52952	0.5295217939
2.0	0.68288	0.65002	0.65003	0.6500288006
2.2	0.82082	0.78119	0.78120	0.7811984868
2.4	0.96919	0.92228	0.92230	0.9222960509
2.6	1.12708	1.07250	1.07252	1.0725127485
2.8	1.29350	1.23098	1.23099	1.2309850055
3.0	1.46741	1.39681	1.39682	1.3968169615
3.2	1.64776	1.56909	1.56911	1.5691048197
3.4	1.83352	1.74695	1.74696	1.7469611824
3.6	2.02379	1.92952	1.92954	1.9295375767
3.8	2.21787	2.11602	2.11605	2.1160436149
4.0	2.41534	2.30575	2.30576	2.3057616561
4.2	2.61623	2.49805	2.49806	2.4980563622
4.4	2.82115	2.69242	2.69238	2.6923790941
4.6	3.03145	2.88859	2.88826	2.8882675734
4.8	3.24946	3.08718	3.08534	3.0853416143
5.0	3.47866	3.29272	3.28329	3.2832959341

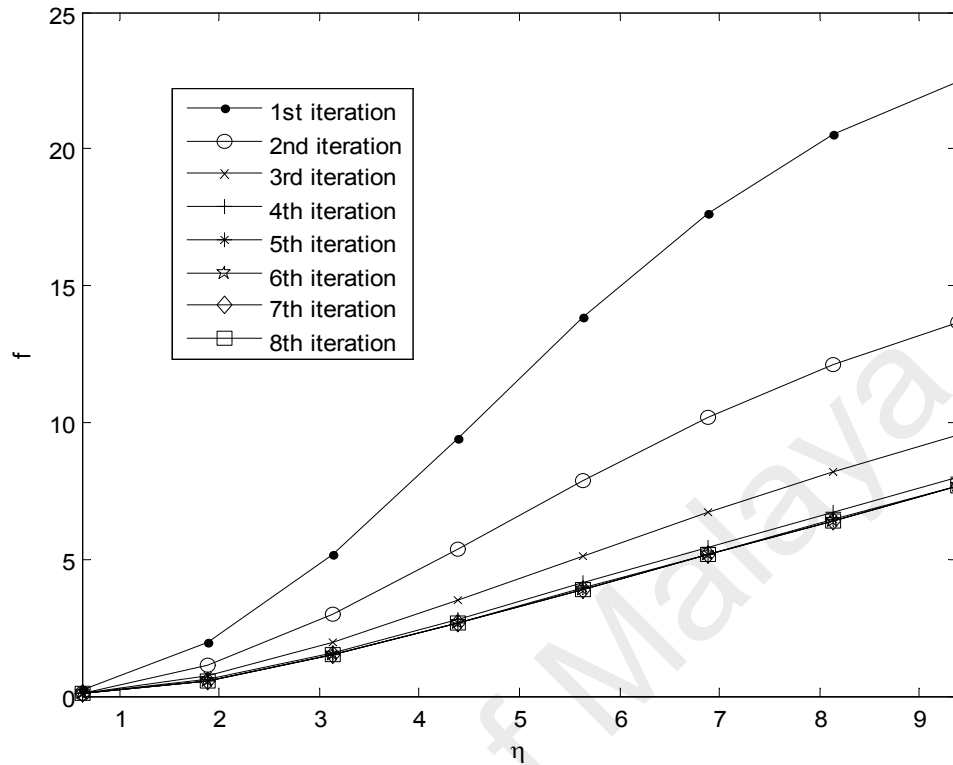


**Figure 4.9:** HWQM solution of  $f(\eta)$  for different iterations

The Blasius boundary layer problem of Equation (4.35) is a special case of Equation (4.33) with  $\alpha = 2$ . Table 4.18 shows the value of the wall shear stress  $f''(0)$  obtained by the HWQM compared with those obtained in the literature. The solutions obtained presently are in excellent agreement with those reported previously. The graph in Figure 4.9 shows the approximate solution by HWQM at eight iterations. In Figure 4.10, we plot the curves of  $f(\eta)$ ,  $f'(\eta)$  and  $f''(\eta)$  against  $\eta$  for the Blasius boundary layer problem at eighth order of the HWQM approximation. We chose  $\eta = 8$  because it satisfy with the boundary condition in Equation (4.38).

**Table 4.16:** Comparison between Howarth, LTNHPM and HWQM for the velocity profile  $f'(\eta)$  at the selected values of  $\eta$

$\eta$	LTNHPM (Aminikhah, 2012)	Howarth (Howarth, 1938)	HWQM (Present)
0	0	0	0
0.2	0.06641	0.06641	0.0664084675
0.4	0.13276	0.13277	0.1327654138
0.6	0.19894	0.19894	0.1989390124
0.8	0.26471	0.26471	0.2647112907
1.0	0.32978	0.32979	0.3297825119
1.2	0.39378	0.39378	0.3937788449
1.4	0.45626	0.45627	0.4562646838
1.6	0.51676	0.51676	0.5167599065
1.8	0.57476	0.57477	0.5747614141
2.0	0.62977	0.62977	0.6297692120
2.2	0.68131	0.68132	0.6813141081
2.4	0.72898	0.72899	0.7289859691
2.6	0.77245	0.77246	0.7724594598
2.8	0.81151	0.81152	0.8115145129
3.0	0.84604	0.84605	0.8460498330
3.2	0.87608	0.87609	0.8760873517
3.4	0.90176	0.90177	0.9017676101
3.6	0.92333	0.92333	0.9233364453
3.8	0.94112	0.94112	0.9411251010
4.0	0.95553	0.95552	0.9555255073
4.2	0.96704	0.96696	0.9669643868
4.4	0.97639	0.97587	0.9758780736
4.6	0.98564	0.98269	0.9826905109
4.8	1.00322	0.98779	0.9877962550
5.0	1.06671	0.99155	0.9915482668

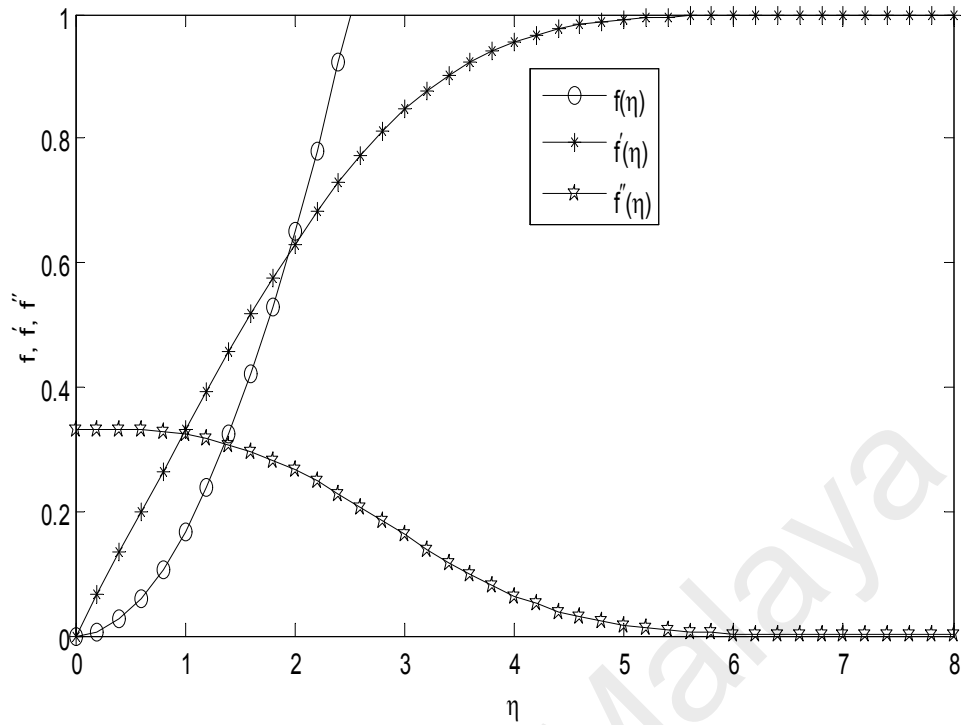


**Figure 4.10:** HWQM solution for  $f(\eta)$ ,  $f'(\eta)$  and  $f''(\eta)$

**Table 4.17:** Comparison between Howarth (1938) and HWQM for  $f''(\eta)$

$\eta$	Howarth (Howarth, 1938)	HWQM (Present)
0	0.33206	0.33206
1	0.32301	0.32301
2	0.26675	0.26676
3	0.16136	0.16136
4	0.06424	0.06423
5	0.01591	0.01590

**Table 4.18:** Comparison between the HWQM, Mohammed (2014), Asaithambi (2005) and Howarth (1938) results for the wall shear stress,  $f''(0)$  with  $m = 128$  and  $L = 8$

Howarth method (Howarth, 1938)	Recursive evaluation (Asaithambi, 2005)	SLM (Mohammed et al., 2014)	HWQM (Present)
0.33206	0.33206	0.33206	0.33206

#### 4.4 Conclusions

In this chapter, the HWQM is employed to solve three types of single nonlinear ODEs. Some comparison are made between the results of the present method and other numerical methods. It is found that the present results agree well with those obtained by other methods and exact solution. The validity of this method is based on the assumption that it converges by increasing the number of resolution. The choice of the collocation points and initial approximation are also greatly influence the effectiveness of this method.

The amount of computational effort used by the present method is significantly less compared to the other methods. For each fixed value of  $L$ , the method required on average 5 - 8 iterations in order to get the desired accuracy. Even though the exact solution is available in a first problem, the use of numerical Haar wavelet method is to test the capability of present method for solving nonlinear ODE in infinite domain, where the former used the domain within the interval  $[0, 1]$  only. As a result, this method is much simpler and it can be easily coded. This factor gives Haar wavelet a reason to be ventured further as numerical tools. Additionally, few benefits come from its great features such as faster computation and attractiveness. This work is going to be a stepping stone in solving coupled nonlinear ODE in the next chapter.

## CHAPTER 5: COUPLED NONLINEAR ORDINARY DIFFERENTIAL EQUATIONS

In this chapter, the HWQM is proposed for the numerical solution of system of coupled nonlinear ODEs related to the natural convection boundary layer fluid flow problems with high Prandtl number,  $Pr$ . The effects of variation  $Pr$  on heat transfer are investigated. The three problems involved in this flows are:

- (a) boundary layer flow and heat transfer due to a stretching sheet (BLFHTSS),
- (b) laminar film condensation of a saturated stream on an isothermal vertical plate (LFC),
- (c) natural convection boundary layer flow (NCBLF).

### 5.1 Boundary Layer Flow and Heat Transfer Due to a Stretching Sheet

#### 5.1.1 Introduction

The steady flow and heat transfer of a viscous and incompressible fluid induced by a continuously moving or stretching surface in an inactive fluid has a significant importance in engineering applications, especially in manufacturing processes such as hot rolling, wire drawing, glass fiber, paper production (Ahmed et al., 2010), geophysical and insulating engineering, modeling of packed sphere beds and solar power collector (Hayat et al., 2010).

The boundary layer flow due to a stretching surface in an ambient fluid was first studied by Crane (1970). He obtained similarity solutions for the velocity and temperature fields of a two dimensional steady state viscous flow over a linearly stretching sheet. The problem was extended afterwards by different research groups to include other aspects. Carragher and Crane (1982) investigated the influence of heat transfer in the flow over a stretching surface when the temperature difference between the surface and the ambient fluid is proportional to a power of distance from the fixed

point. Dutta et al. (1985) and Grubka and Bobba (1985) analyzed the temperature distribution in the flow of a viscous incompressible fluid caused by a stretching surface subject to a uniform heat flux.

Furthermore, Elbashbeshy (1998) examined heat transfer over a stretching surface with variable surface heat flux and uniform surface heat flux subject to injection and suction. From the findings, he concluded that the suction increases the heat transfer from the surface, whereas injection cause a decrease in the heat transfer. Lin and Chen (1998) constructed an exact expression of the temperature distribution for the heat transfer from a stretching surface with prescribed power law heat flux. Gupta and Gupta (1977) examined the heat and mass transfer for the boundary layer flow over a stretching sheet in the presence of suction and blowing. An analysis has been carried out by Chen and Char (1988) to determine the heat transfer occurring in the laminar boundary layer on a linearly stretching, continuous surface subject to suction or blowing.

Magyari and Keller (1999) used similarity solutions to examine the steady plane boundary layers on an exponentially stretching continuous surface with an exponential temperature distribution. They also obtained analytical solutions for the case when the sheet is permeable in the presence of suction or injection (Magyari & Keller, 2000). Liao and Pop (2004) applied the HAM to give two kinds of explicit analytic solutions of the boundary layer equations, valid for the convective viscous flow past a suddenly heated vertical plate in a porous medium and viscous flow over a stretching wall.

All the above mentioned studies deal with the case of heat transfer and steady flow only. In view of the previous work of Elbashbeshy (1998), Elbashbeshy and Bazid (2004) extended this work to unsteady flow and heat transfer over a stretching sheet in laminar boundary layer by using similarity solution. Further, Sharidan et al. (2006) were first to present the similarity solutions to investigate the unsteady boundary layer flow

and heat transfer due to a stretching sheet by using Keller-box method. Moreover, Ishak et al. (2009) presented the solution of the unsteady mixed convection boundary layer flow and heat transfer problem due to a stretching vertical surface, including the discussion on the effects of unsteadiness parameter, bouyancy parameter and Pr number on the flow characteristic. Rashidi and Pour (2010) used HAM to find the totally analytic solutions of the system of nonlinear ordinary differential equations derived from similarity transform for unsteady boundary layer flow and heat transfer due to a stretching sheet. The same problem also has been solved by Ibrahim and Shankar (2011) using quasilinearization technique. They presented the numerical results for the local skin friction coefficient and local Nusselt number. Islam et al. (2011) developed Haar wavelet collocation method with Newton method for the numerical solution of boundary layer fluid flow problems with high Pr number. They investigated the effects of variation of Pr on heat transfer and the performance of their proposed method is compared with the FDM, RKM and HAM.

### 5.1.2 Problem Formulation

From the physical model as shown in Figure 5.1, the origin is kept fixed, while two equal and opposite forces are suddenly applied along the  $x$ -axis. As a result, the sheet is stretched and the flow is generated. The wall temperature of the sheet  $T_w$  is suddenly raised from  $T_\infty$  to  $T_w$  as such it is suddenly generated a heat flux  $q_w$  at the wall. The mathematical formulation of the boundary layer governing the flow and heat transfer due to the stretching sheet are given by (Sharidan et al., 2006),

$$\frac{\partial u}{\partial x} + \frac{\partial v}{\partial y} = 0 \quad , \quad (5.1)$$

$$\frac{\partial u}{\partial t} + u \frac{\partial u}{\partial x} + v \frac{\partial u}{\partial y} = \nu \left[ \frac{\partial^2 u}{\partial y^2} \right] \quad , \quad (5.2)$$

$$\frac{\partial T}{\partial t} + u \frac{\partial T}{\partial x} + v \frac{\partial T}{\partial y} = \alpha \frac{\partial^2 T}{\partial y^2}, \quad (5.3)$$

subject to the initial and boundary conditions

$$\begin{aligned} t < 0 & : u = v = 0, \quad T = T_\infty, \quad \text{for any } x, y \\ t \geq 0 & : u = u_w(t, x), \quad v = 0, \\ & T = T_w(t, x) \\ y \rightarrow \infty & : u \rightarrow 0, \quad T \rightarrow T_\infty, \end{aligned} \quad (5.4)$$

where  $u$  and  $v$  are the velocity components along the  $x$ - and  $y$ - axes respectively,  $t$  is the time,  $\alpha$  is the thermal diffusivity,  $\nu$  is the kinematic viscosity,  $T$  is the temperature and  $k$  is the thermal conductivity. The velocity of sheet,  $u_w(t, x)$ , the temperature of sheet,  $T_w(t, x)$  and the heat flux,  $q_w(t, x)$  are defined as in the following form (Sharidan et al., 2006)

$$\begin{aligned} u_w(t, x) &= \frac{cx}{1-\gamma t}, \\ T_w(t, x) &= T_\infty + \frac{c}{2\nu x^2 (1-\gamma t)^{3/2}}, \\ q_w(t, x) &= \frac{q_{w_0}}{2x^2} \left( \frac{c}{\nu} \right)^{3/2} \frac{1}{(1-\gamma t)^2}. \end{aligned} \quad (5.5)$$

$c$  is subjected to positive constant stretching rate,  $\gamma$  is a positive constant, in which measures the unsteadiness and  $q_{w_0}$  is a characteristic of heat transfer quantity.

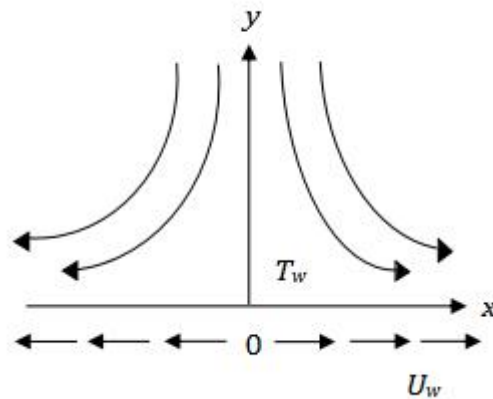


**Figure 5.1:** Physical model of boundary layer flow and heat transfer due to a stretching sheet

The new variables after transformations as proposed by Sharidan et al. (2006) are

$$\eta = \sqrt{\frac{c}{\nu(1-\gamma t)}}y, \quad \psi = \sqrt{\frac{c\nu}{1-\gamma t}}xf(\eta), \quad (5.6)$$

$$T = T_\infty + \frac{c}{2\nu x^2(1-\gamma t)^{3/2}}\theta(\eta),$$

where  $\psi$  is the stream function and it is defined as  $u = \partial\psi/\partial y$  and  $v = -\partial\psi/\partial x$ .

Using these transformations, with respect to  $\eta$ , Equations (5.1) - (5.3) can be reduced to the following nonlinear ODEs,

$$f''' + ff'' - f'^2 - A\left(f' + \frac{1}{2}\eta f''\right) = 0 \quad (5.7)$$

and

$$\frac{1}{Pr}\theta'' + f\theta' + 2f'\theta - \frac{A}{2}(3\theta + \eta\theta') = 0. \quad (5.8)$$

The new boundary conditions are given as

$$\begin{aligned} \eta = 0 & : f = 0, \quad f' = 1, \quad \theta = 1, \\ \eta \rightarrow \infty & : f' \rightarrow 0, \quad \theta \rightarrow 0. \end{aligned} \quad (5.9)$$

where Pr is Prandtl number and  $A = \frac{\gamma}{c}$  is a non-dimensional constant measures the flow and heat transfer unsteadiness.

### 5.1.3 Numerical Solution

All the steps remain the same as for single nonlinear ODE as discussed in Chapter 4.

The quasilinearization technique is applied to Equations (5.7) and (5.8) implies

$$\begin{aligned} f_{r+1}''' &= -f_r f_r'' + f_r'^2 + Af_r' + \frac{A}{2}\eta f_r'' + (f_{r+1} - f_r) \\ &\quad \tilde{f}_{f_r} \left( -f_r f_r'' + f_r'^2 + Af_r' + \frac{A}{2}\eta f_r'' \right) + (f_{r+1}' - f_r') \\ &\quad \tilde{f}_{f_r'} \left( -f_r f_r'' + f_r'^2 + Af_r' + \frac{A}{2}\eta f_r'' \right) + (f_{r+1}'' - f_r'') \\ &\quad \tilde{f}_{f_r''} \left( -f_r f_r'' + f_r'^2 + Af_r' + \frac{A}{2}\eta f_r'' \right). \end{aligned} \quad (5.10)$$

Solving and rearranging Equation (5.10), we obtain

$$\begin{aligned} f_{r+1}''' + f_{r+1}f_r'' - 2f_r'f_{r+1}' - Af_{r+1}' + f_{r+1}''f_r - \frac{1}{2}A\eta f_{r+1}'' \\ = -f_r'^2 + f_rf_r'' , \end{aligned} \quad (5.11)$$

and

$$\begin{aligned} \theta_{r+1}'' + 2\Pr f_r'\theta_{r+1}' - \frac{3}{2}A\Pr \theta_{r+1}' + \Pr f_r\theta_{r+1}' \\ - \frac{1}{2}A\Pr \eta\theta_{r+1}' + \Pr \theta_r'f_{r+1}' + 2\Pr \theta_r f_{r+1}' \\ = 2\Pr f_r'\theta_r + \Pr f_r\theta_r' , \end{aligned} \quad (5.12)$$

respectively, where  $0 \leq \eta \leq L$ ,  $L$  is a sufficiently large number. The boundary conditions are

$$\begin{aligned} \eta = 0 & : f_{r+1} = 0, \quad f_{r+1}' = 1, \quad \theta_{r+1} = 1, \\ \eta \rightarrow \infty & : f_{r+1}' \rightarrow 0, \quad \theta_{r+1} \rightarrow 0. \end{aligned} \quad (5.13)$$

Now, we apply the Haar wavelet method to Equations (5.11) and (5.12), then approximate the higher order derivative term by Haar wavelet series as

$$f_{r+1}'''(\eta) = \sum_{i=0}^{m-1} a_i h_i(\eta) \quad (5.14)$$

and

$$\theta_{r+1}''(\eta) = \sum_{i=0}^{m-1} b_i h_i(\eta) \quad (5.15)$$

respectively. The lower order derivatives are obtained by integrating Equations (5.14) and (5.15) three times and twice, respectively with respect to  $\eta$ , hence we obtain

$$f_{r+1}''(\eta) = \sum_{i=0}^{m-1} a_i p_{i,1}(\eta) + f_{r+1}''(0), \quad (5.16)$$

$$f_{r+1}'(\eta) = \sum_{i=0}^{m-1} a_i p_{i,2}(\eta) + \eta f_{r+1}''(0) + f_{r+1}'(0), \quad (5.17)$$

$$f_{r+1}(\eta) = \sum_{i=0}^{m-1} a_i p_{i,3}(\eta) + \frac{\eta^2}{2} f_{r+1}''(0) + \eta f_{r+1}'(0) + f_{r+1}(0), \quad (5.18)$$

$$\theta'_{r+1}(\eta) = \sum_{i=0}^{m-1} b_i p_{i,1}(\eta) + \theta'_{r+1}(0), \quad (5.19)$$

$$\theta_{r+1}(\eta) = \sum_{i=0}^{m-1} b_i p_{i,2}(\eta) + \eta \theta'_{r+1}(0) + \theta_{r+1}(0). \quad (5.20)$$

The values for  $f''_{r+1}(0)$  and  $\theta'_{r+1}(0)$  can be obtained from Equations (5.17) and (5.20) respectively, by substituting  $\eta = L$ , we obtain

$$f''_{r+1}(0) = \frac{1}{L} \left( - \sum_{i=0}^{m-1} a_i p_{i,2}(L) - f'_{r+1}(0) + f'_{r+1}(L) \right), \quad (5.21)$$

and

$$\theta'_{r+1}(0) = \frac{1}{L} \left( - \sum_{i=0}^{m-1} b_i p_{i,2}(L) - \theta_{r+1}(0) + \theta_{r+1}(L) \right). \quad (5.22)$$

Hence, the new equations for (5.16) - (5.20) are

$$f''_{r+1}(\eta) = \sum_{i=0}^{m-1} a_i \left( p_{i,1}(\eta) - \frac{1}{L} p_{i,2}(L) \right) - \frac{1}{L}, \quad (5.23)$$

$$f'_{r+1}(\eta) = \sum_{i=0}^{m-1} a_i \left( p_{i,2}(\eta) - \frac{\eta}{L} p_{i,2}(L) \right) - \frac{\eta}{L} + 1, \quad (5.24)$$

$$f_{r+1}(\eta) = \sum_{i=0}^{m-1} a_i \left( p_{i,3}(\eta) - \frac{\eta^2}{2L} p_{i,2}(L) \right) - \frac{\eta^2}{2L} + \eta, \quad (5.25)$$

$$\theta'_{r+1}(\eta) = \sum_{i=0}^{m-1} b_i \left( p_{i,1}(\eta) - \frac{1}{L} p_{i,2}(L) \right) - \frac{1}{L}, \quad (5.26)$$

$$\theta_{r+1}(\eta) = \sum_{i=0}^{m-1} b_i \left( p_{i,2}(\eta) - \frac{\eta}{L} p_{i,2}(L) \right) - \frac{\eta}{L} + 1. \quad (5.27)$$

Substitute Equations (5.14), (5.15) and (5.23) - (5.27) into (5.11) and (5.12), we obtain

$$\begin{aligned}
& \sum_{i=0}^{m-1} a_i \left( \begin{aligned} & h_i + f_r'' p_{i,3}(\eta) - (2f_r' + A) p_{i,2}(\eta) + \left( f_r - \frac{1}{2} A \eta \right) p_{i,1}(\eta) \\ & - \left( \frac{\eta^2}{2L} f_r'' - \frac{2\eta}{L} f_r' - \frac{1}{L} A \eta + \frac{1}{L} f_r - \frac{1}{2L} A \eta \right) p_{i,2}(L) \end{aligned} \right) \\
& = - \left( f_r' + \frac{2\eta}{L} - 2 \right) f_r' + \left( f_r + \frac{\eta^2}{2L} - \eta \right) f_r'' + \frac{1}{L} f_r - \frac{A\eta}{L} \\
& \quad + A - \frac{A\eta}{2L}, \tag{5.28}
\end{aligned}$$

and

$$\begin{aligned}
& \sum_{i=0}^{m-1} a_i \left( \begin{aligned} & \Pr \theta_r' p_{i,3}(\eta) + \left( -\frac{1}{2L} \Pr \eta^2 \theta_r' - \frac{2}{L} \Pr \eta \theta_r \right) p_{i,2}(L) \\ & + 2 \Pr \theta_r p_{i,2}(\eta) \end{aligned} \right) + \\
& \sum_{i=0}^{m-1} b_i \left( \begin{aligned} & h_i + \left( 2 \Pr f_r' - \frac{3A}{2} \right) p_{i,2}(\eta) + \left( \Pr f_r - \frac{A}{2} \Pr \eta \right) p_{i,1}(\eta) \\ & + \left( -\frac{2\eta}{L} \Pr f_r' - \frac{1}{L} \Pr f_r + \frac{3A}{2L} \Pr \eta + \frac{A}{2L} \Pr \eta \right) p_{i,2}(L) \end{aligned} \right) \\
& = \left( 2 \Pr \theta_r + \frac{2}{L} \Pr \eta - 2 \Pr \right) f_r' + \left( \Pr f_r + \frac{1}{2L} \Pr \eta^2 \right) \theta_r' \\
& \quad + \left( -\frac{3A}{2L} \eta + \frac{3A}{2} + \frac{1}{L} f_r - \frac{A}{2L} \eta \right) \Pr. \tag{5.29}
\end{aligned}$$

The Equations (5.28) and (5.29) can be solved simultaneously to obtain Haar coefficients,  $a_i$  and  $b_i$ . We chose the initial approximation which satisfy the boundary conditions (5.13) as follows

$$\begin{aligned}
f_0(\eta) = \frac{1}{2} \left( -\sqrt{\pi A \eta} e^{A\eta^2/4} \operatorname{erf} \left( \frac{\sqrt{A} L}{2} \right) + \sqrt{\pi A \eta} e^{A\eta^2/4} \operatorname{erf} \left( \frac{\sqrt{A}}{2} \eta \right) \right. \\
\left. - \frac{2\pi}{L} e^{-A(L^2-\eta^2)/4} + 2 \right), \tag{5.30}
\end{aligned}$$

and

$$\theta_0(\eta) = 1 - \frac{1}{L} \eta. \tag{5.31}$$

where  $\operatorname{erf}$  is an error function.

### 5.1.4 Results and Discussion

The transformed Equations (5.7) and (5.8) with boundary conditions (5.9) were numerically solved with the help of MATLAB. The results are given for some values of the unsteady parameter  $A$  and the Prandtl number, Pr. The accuracy of this numerical method was validated for the case of VWT by a comparison with the previous study of Islam et al. (2011), Grubka and Bobba (1985), Elbashbeshy and Bazid (2004), Sharidan et al. (2006) and Ibrahim and Shankar (2011).

A comparison of numerical results between HWQM with Haar wavelet collocation method (HWCM) and RKM corresponding to the two dimensional boundary layer flow and heat transfer due to a stretching sheet (BLFHTSS) is shown in Table 5.1. This comparison is made for small values of Pr. It is clear that from this table, the Haar wavelets based algorithm agrees well with RKM round up to five decimal places.

**Table 5.1:** Comparison between HWQM with RKM and HWCM for  $f(\eta)$  and  $\theta(\eta)$  of BLFHTSS with  $m = 256$ ,  $A = 20$ , Pr = 1 and  $L = 1$

$\eta$	$f(\eta)$			$\theta(\eta)$		
	HWCM (Islam et al., 2011)	RKM (Islam et al., 2011)	HWQM (Present)	HWCM (Islam et al., 2011)	RKM (Islam et al., 2011)	HWQM (Present)
0	0	0	0	1.0000000	1.0000000	1.0000000
0.1	0.0826274	0.0826354	0.0826353	0.6216970	0.6218480	0.6218452
0.2	0.1397660	0.1397880	0.1397880	0.4005150	0.4006900	0.4006869
0.3	0.1807370	0.1807720	0.1807714	0.2668020	0.2669500	0.2669481
0.4	0.2110510	0.2110960	0.2110955	0.1832610	0.1833700	0.1833686
0.5	0.2340860	0.2341390	0.2341379	0.1293600	0.1294310	0.1294297
0.6	0.2519680	0.2520240	0.2520227	0.0933950	0.0934326	0.0934320
0.7	0.2660280	0.2660820	0.2660815	0.0683056	0.0683103	0.0683102
0.8	0.2770030	0.2770490	0.2770480	0.0491161	0.0497810	0.0490787
0.9	0.2849340	0.2849630	0.2849623	0.0303333	0.0302495	0.0302509
1	0.2884160	0.2884290	0.2884287	0	0	0

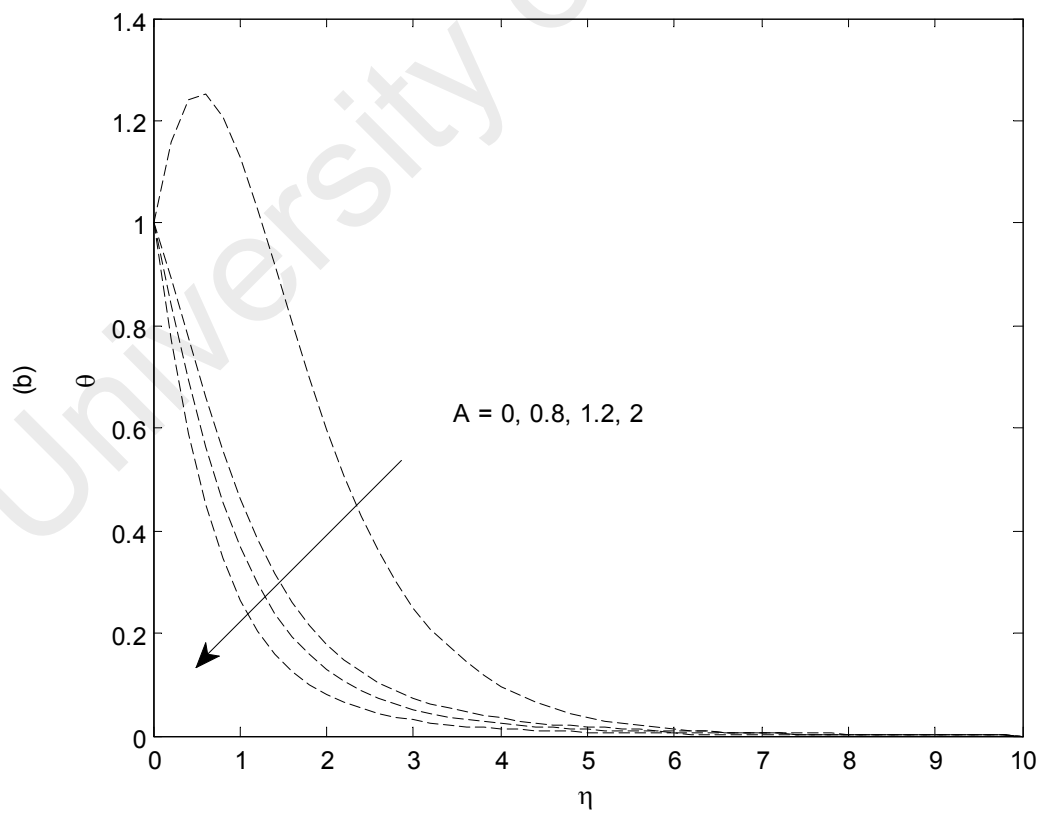
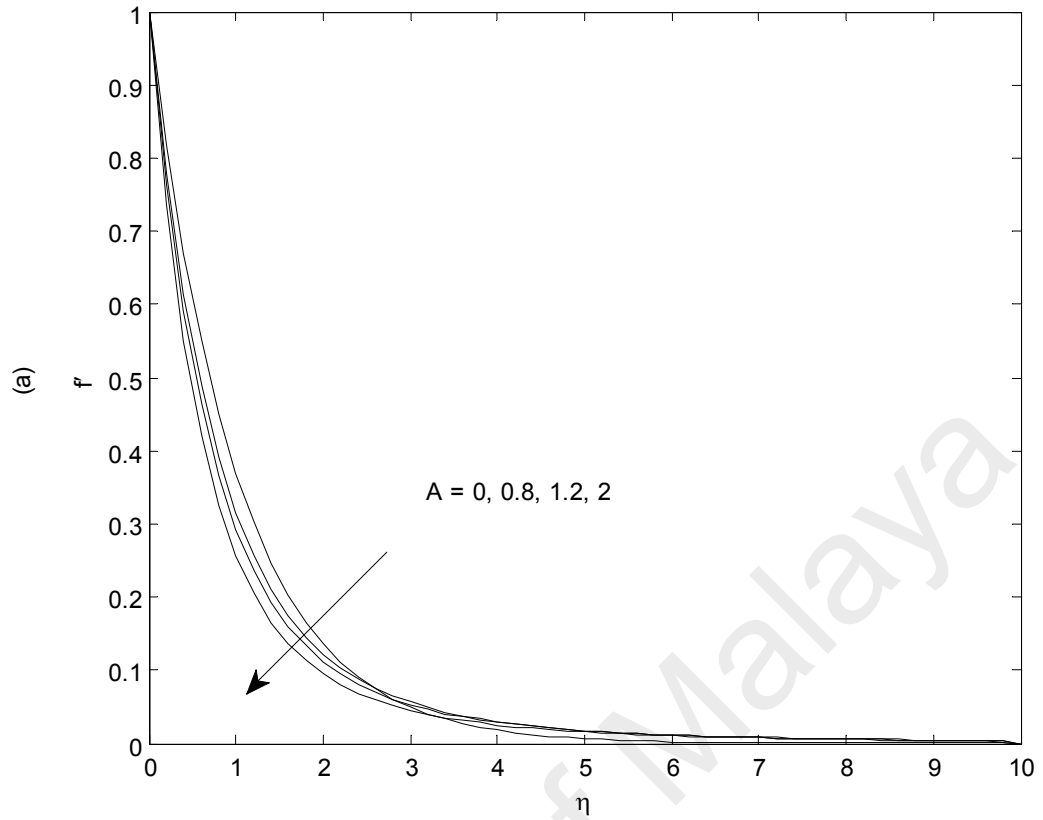


**Figure 5.2:** HWQM for (a)  $f'(\eta)$  and (b)  $\theta(\eta)$  case of BLFHTSS with different values of  $A$  when  $m = 512$ ,  $L = 10$  and  $Pr = 1$

Figures 5.2 and 5.3 show the variation of the velocity,  $f'(\eta)$  and temperature,  $\theta(\eta)$  for different values of the parameter  $A$  and the Pr. It can be seen from Figure 5.2(a) that the velocity profiles decrease with an increase in unsteadiness parameter  $A$ . It also shows that the boundary layer thickness decreases monotonically when parameter  $A$  increases. Figure 5.2(b) shows the temperature profiles also decrease monotonically with the increase of  $A$ , except for  $A = 0$ . The temperature profiles overshoot its value at the surface of the sheet in the case when  $A = 0$ . This flow of behaviour is in agreement with the results of Sharidan et al. (2006) and Grubka and Bobba (1985) but it is contrary with the results of Elbashbeshy and Bazid (2004).

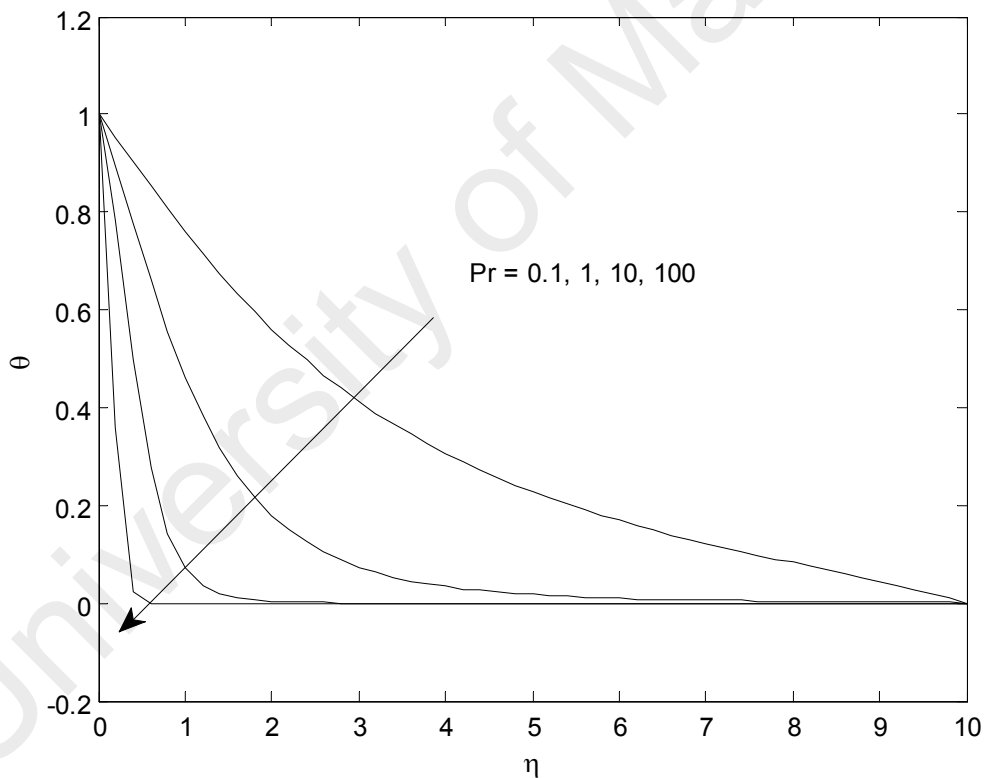


**Figure 5.3:** HWQM for  $\theta(\eta)$ , case of BLFHTSS with different values of Pr when  $A = 0.8$ ,  $m = 512$  and  $L = 10$

The effects of Pr on the non-dimensional temperature profile is illustrated in Figure 5.3 for some values of Pr. It is possible to see that the temperature decreases as the Pr increases while keeping  $A$  fixed at 0.8. This is due to the fact that a higher Pr fluid has a thinner thermal boundary layer which increases the gradient of the temperature.

Consequently, the surface of the heat transfer increases as Pr increases.

**Table 5.2:** The values of the heat transfer rate  $-\theta'(0)$  for  $A = 0$  at steady-state flow when  $L = 10$  and  $Pr = 1$

Grubka and Bobba (1985)	Elbashbeshy and Bazid (2004)	Sharidan et al. (2006)	HWQM (Present)
1.00000	0.99999	0.99999	1.00000

**Table 5.3:** Comparison of values between HWQM with quasilinearization technique and Keller-box method for skin friction coefficient  $-f''(0)$  and heat transfer rate  $-\theta'(0)$  of BLFHTSS when  $L = 10$

$A$	$Pr$	Quasilinearization (Ibrahim & Shankar, 2011)		Keller-box method (Sharidan et al., 2006)		HWQM (Present)	
		$-f''(0)$	$-\theta'(0)$	$-f''(0)$	$-\theta'(0)$	$-f''(0)$	$-\theta'(0)$
0.8	0.01	1.938800	0.250200	1.261042	0.092274	1.261034	0.093761
	0.1	1.938800	0.247600	1.261042	0.229433	1.261034	0.229458
	1	1.938800	0.047200	1.261042	0.471190	1.261034	0.471198
1.2	0.01	2.032700	0.258400	1.377722	0.114053	1.377710	0.152838
	0.1	2.032700	0.317600	1.377722	0.311720	1.377710	0.313179
	1	2.032700	0.420900	1.377722	0.788173	1.377710	0.788181
2	0.01	2.208400	0.274500	1.587362	0.150317	1.587342	0.176854
	0.1	2.208400	0.439100	1.587362	0.438750	1.587342	0.438955
	1	2.208400	0.965100	1.587362	1.243741	1.587342	1.243744

Table 5.2 represents the results for the heat transfer rate from the sheet,  $-\theta'(0)$  for different method of previous studies. It can be seen from this table that a very good agreement between the results exists. The numerical solution of skin friction coefficient  $-f''(0)$  and heat transfer rate  $-\theta'(0)$  for various values of Pr and unsteadiness parameter  $A$  generated through HWQM is given in Table 5.3 alongside quasilinearization technique and Keller-box method. From the table, it is noticed that

the skin friction coefficient and heat transfer rate increase as the Pr and unsteadiness parameter are increased.

Table 5.4 is represented CPU time (in seconds) needed for HWQM in solving BLFHTSS for different values of Pr. The CPU time is calculated by employing ‘Run and Time’ command in MATLAB software.

**Table 5.4:** CPU time in (sec) for different values of Pr when  $L = 1$ ,  $A = 0$  and  $m = 8$

Pr	HWQM (Present)
1	0.236
10	0.124
50	0.124
100	0.124
200	0.124
500	0.124
1000	0.124

## 5.2 Laminar Film Condensation

### 5.2.1 Introduction

The investigation about laminar film condensation has received considerable attention over the past several decades after the pioneering work by Nusselt (1916). It is widely used in engineering and industry such as heat and fluid flows for some industrial drying and cooling processes, enhanced recovery of petroleum resources, packed-bed heat exchangers, solidification of castings, geothermal reservoirs and so on (Eckert, 1963).

Nusselt (1916) formulated a theory of laminar film condensation considered in condensation onto an isothermal flat plate maintained at a constant temperature below the saturation temperature of the surrounding inactive vapor. According to the basic Nusselt theory, thermal convection and interfacial shear were neglected due to inertia

forces. Many investigations have subsequently refined Nusselt's theory to include some of the omissions. Bromley (1952) examined the effects of thermal convection and then Rohsenow (1956) proposed modifications to the latent heat of condensation to be used in assessing heat transfer at the plate but the inertia effects were ignored.

Later, Sparrow and Gregg (1959) recognized the close parallels between natural convection boundary layers and laminar film condensation. They introduced a set of similarity transformation of the governing parabolic equations and reduced the PDEs to a set of ODEs, including the detailed numerical solutions were obtained for a wide range of Pr and condensation rates. As a result, it showed that if the Pr is not less than 10, the inertia effects on heat transfer are limited. Chen (1961) used the retarding effect of vapor shear stress on the condensate film by perturbation method and modified integral boundary-layer equations. Theoretical heat-transfer coefficients are computed and it found that the influence of surface shear stress is negligible at high Pr.

Koh et al. (1961) realized that if the condensation rate is sufficiently high, the effect of the shear stress is significant. Rose (1988) reviewed basic theoretical studies of laminar film condensation since Nusselt (1916) and gave a more accurate expression for the Nusselt number. The study of the problems related to laminar film condensation are discussed by many researchers such as Bromely (1952), Patankar and Sparrow (1979), Wilkins (1980), Brouwers (1989), Méndez and Treviño (1996), Shang (1997), Pop et al. (2004), Xu (2004), White (2005), Xu et al. (2008), Ariel (2009), Ahmed et al. (2010), Dinarvand et al. (2010), Hayat et al. (2010), Shu (2012).

### **5.2.2 Problem Formulation**

In this study, a laminar film condensation of a saturated stream is considered on an isothermal vertical flat plate. Let  $x$  and  $y$  are the measures of the distances in the downward direction parallel and perpendicular to the plate, respectively. The leading

edge of the plate is located at  $x = y = 0$ . The physical model to be examined is illustrated in Figure 5.4, under assumptions that the change of pressure across the film is negligible and the velocity gradient in the cross-film direction ( $y$ -direction) is much greater than the one in the flow direction ( $x$ -direction).

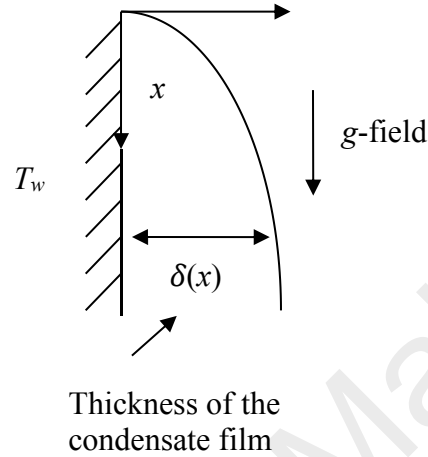


**Figure 5.4:** Physical model and coordinate system of laminar film condensation of saturated steam

The governing equations expressing conservation of mass, momentum and energy in the liquid phase are given as follows,

$$\frac{\partial u}{\partial x} + \frac{\partial v}{\partial y} = 0, \quad (5.32)$$

$$u \frac{\partial u}{\partial x} + v \frac{\partial u}{\partial y} = g \left( \frac{\rho - \rho^*}{\rho} \right) + \nu_1 \frac{\partial^2 u}{\partial y^2}, \quad (5.33)$$

$$u \frac{\partial T}{\partial x} + v \frac{\partial T}{\partial y} = \frac{k_1}{\rho c_p} \frac{\partial^2 T}{\partial y^2}, \quad (5.34)$$

respectively, where  $u$  and  $v$  are the velocity components associated with increasing coordinates  $(x, y)$  measured along and normal to the plate from the leading edge of the plate and  $T$  is temperature within the condensate film. The physical properties  $g$  is the acceleration due to gravity,  $\rho^*$  the vapor density,  $\rho, \nu_1, k_1$  and  $c_p$  are the density,

the kinematic viscosity, the thermal conductivity and the specific heat at constant pressure of the liquid.

The Equations (5.32) - (5.34) are subjected to the boundary conditions,

$$y = 0: \quad u = 0, \quad v = 0, \quad T = T_w, \quad (5.35)$$

$$y = \delta: \quad \frac{\partial u}{\partial y} = 0, \quad T = T^*, \quad (5.36)$$

where  $\delta$  is the thickness of the condensate film,  $T_w$  is the plate temperature and  $T^*$  is the saturation temperature of the vapor. By using the similarity transformations (Oosthuizen & Naylor, 1999),

$$\begin{aligned} \psi &= \left[ \left( \frac{\rho - \rho^*}{\rho} \right) g v_1^2 x^3 \right]^{\frac{1}{4}} f(\eta), \\ \theta(\eta) &= \frac{T - T^*}{T_w - T^*}, \\ \eta &= \frac{y}{x^{\frac{1}{4}}} \left[ \left( \frac{\rho - \rho^*}{v_1^2 \rho} \right) g \right]^{\frac{1}{4}}. \end{aligned} \quad (5.37)$$

Equations (5.32) - (5.34) can be reduced to the following system of nonlinear ODEs,

$$f''' + \frac{3}{4} f f'' - \frac{f'^2}{2} + 1 = 0, \quad (5.38)$$

$$\theta'' + \frac{3}{4} \text{Pr} f \theta' = 0, \quad (5.39)$$

subject to the boundary conditions,

$$\begin{aligned} \eta = 0 &: \quad f = f' = 0, \quad \theta = 1, \\ \eta \rightarrow \infty &: \quad f'' \rightarrow 0, \quad \theta \rightarrow 0, \end{aligned} \quad (5.40)$$

where  $\text{Pr} = \rho c_p / k_1$  is the Prandtl number.

### 5.2.3 Numerical Solution

Quasilinearization technique is applied to Equations (5.38) and (5.39) implies

$$f_{r+1}''' + \frac{3}{4} f_r'' f_{r+1} - f_r' f_{r+1}' + \frac{3}{4} f_r f_{r+1}'' = -\frac{1}{2} f_r'^2 + \frac{3}{4} f_r'' f_r - 1, \quad (5.41)$$

and

$$\theta_{r+1}'' + \frac{3}{4} \text{Pr} f_r \theta_{r+1}' + \frac{3}{4} \text{Pr} \theta_r' f_{r+1} = \frac{3}{4} \text{Pr} f_r \theta_r', \quad (5.42)$$

respectively. The boundary conditions are

$$\begin{aligned} \eta = 0 & : f_{r+1} = 0, \quad f_{r+1}' = 0, \quad \theta_{r+1} = 1, \\ \eta \rightarrow \infty & : f_{r+1}'' \rightarrow 0, \quad \theta_{r+1} \rightarrow 0. \end{aligned} \quad (5.43)$$

The lower order derivatives are obtained similar as previous problem, since both problems have similar higher order but with different boundary conditions for  $f_{r+1}'(0)$ .

Hence, the new Haar wavelets integration of higher order derivatives in both (5.14) and (5.15) gives

$$f_{r+1}''(\eta) = \sum_{i=0}^{m-1} a_i (p_{i,1}(\eta) - p_{i,1}(L)), \quad (5.44)$$

$$f_{r+1}'(\eta) = \sum_{i=0}^{m-1} a_i (p_{i,2}(\eta) - \eta p_{i,1}(L)), \quad (5.45)$$

$$f_{r+1}(\eta) = \sum_{i=0}^{m-1} a_i \left( p_{i,3}(\eta) - \frac{\eta^2}{2} p_{i,1}(L) \right), \quad (5.46)$$

$$\theta_{r+1}'(\eta) = \sum_{i=0}^{m-1} b_i \left( p_{i,1}(\eta) - \frac{1}{L} p_{i,2}(L) \right) - \frac{1}{L}, \quad (5.47)$$

$$\theta_{r+1}(\eta) = \sum_{i=0}^{m-1} b_i \left( p_{i,2}(\eta) - \frac{\eta}{L} p_{i,2}(L) \right) - \frac{\eta}{L} + 1. \quad (5.48)$$

where the unknown value for  $f_{r+1}''(0)$  and  $\theta_{r+1}'(0)$  are,

$$f_{r+1}''(0) = -\sum_{i=0}^{m-1} a_i p_{i,1}(L), \quad (5.49)$$

and

$$\theta_{r+1}'(0) = \frac{1}{L} \left( -\sum_{i=0}^{m-1} b_i p_{i,2}(L) - 1 \right), \quad (5.50)$$

respectively. Substitute (5.44)-(5.48) and the highest order derivatives into (5.41) and (5.42), we obtain

$$\sum_{i=0}^{m-1} a_i \left( \begin{array}{l} h_i + \frac{3}{4} f_r'' p_{i,3}(\eta) - f_r' p_{i,2}(\eta) + \frac{3}{4} f_r p_{i,1}(\eta) \\ - \left( \frac{3}{8} \eta^2 f_r'' - \eta f_r' + \frac{3}{4} f_r \right) p_{i,1}(L) \end{array} \right) = -\frac{1}{2} f_r'^2 + \frac{3}{4} f_r'' f_r - 1, \quad (5.51)$$

and

$$\begin{aligned} & \sum_{i=0}^{m-1} a_i \left( \frac{3}{4} \text{Pr } \theta_r' p_{i,3}(\eta) - \frac{3}{8} \text{Pr } \eta^2 \theta_r' p_{i,1}(L) \right) + \\ & \sum_{i=0}^{m-1} b_i \left( h_i + \frac{3}{4} \text{Pr } f_r p_{i,1}(\eta) - \frac{3}{4L} \text{Pr } f_r p_{i,2}(L) \right) \\ & = \frac{3}{4L} \text{Pr } f_r + \frac{3}{4} \text{Pr } f_r \theta_r'. \end{aligned} \quad (5.52)$$

The Equations (5.51) and (5.52) can be solved simultaneously to obtain Haar coefficients,  $a_i$  and  $b_i$ . We chose the initial approximation which satisfy the boundary conditions (5.43) as follows

$$f_0(\eta) = \frac{L}{2} \eta^2 - \frac{1}{6} \eta^3, \quad (5.53)$$

and

$$\theta_0(\eta) = 1 - \frac{1}{L} \eta. \quad (5.54)$$

#### 5.2.4 Results and Discussion

The numerical results corresponding to this case are shown in Figures 5.5 - 5.8 and Table 5.5. In Table 5.5, we found that excellent agreement between HWQM with RKM and HWCM for both,  $f$  and  $\theta$  for  $\text{Pr} = 100$ . Table 5.6 is tabulated for a comparison of CPU time between HWCM, RKM and present method. The efficiency analysis of HWQM is performed by using 'Run and Time' command in MATLAB software version

R2015a, while the HWCM and RKM are calculated by employing Timing command in Mathematica 7.0 software and ODE solver NDSolve, respectively. Besides provides better results, it is observed that HWQM provides smaller CPU time compared to HWCM and RKM.

**Table 5.5:** Comparison between HWQM with RKM and HWCM for  $f(\eta)$  and  $\theta(\eta)$  of LFC with  $m = 128$ ,  $Pr = 100$  and  $L = 1$

$\eta$	$f(\eta)$			$\theta(\eta)$		
	HWCM (Islam et al., 2011)	RKM (Islam et al., 2011)	HWQM (Present)	HWCM (Islam et al., 2011)	RKM (Islam et al., 2011)	HWQM (Present)
0	0	0	0	1	1	1
0.1	0.0046446	0.0046444	0.0046444	0.7548670	0.7549480	0.7549459
0.2	0.0179122	0.0179114	0.0179114	0.5194270	0.5194960	0.5194953
0.3	0.0388057	0.0388040	0.0388040	0.3143650	0.3143050	0.3143049
0.4	0.0663328	0.0663297	0.0663297	0.1606550	0.1608700	0.1608672
0.5	0.0995078	0.0995028	0.0995029	0.0664569	0.0670163	0.0670075
0.6	0.1373540	0.1373470	0.1373471	0.0212199	0.0219129	0.0219024
0.7	0.1789080	0.1788970	0.1788975	0.0050076	0.0054431	0.0054359
0.8	0.2232160	0.2232020	0.2232026	0.0007970	0.0009936	0.0009906
0.9	0.2693450	0.2693260	0.2693266	0.0000813	0.0001220	0.0001214
1	0.3163740	0.3163510	0.3163512	0	0	0

**Table 5.6:** CPU time in (sec) for HWCM, RKM and HWQM when  $L = 1$  and  $m = 8$

Pr	HWCM (Islam et al., 2011)	RKM (Islam et al., 2011)	HWQM (Present)
1	0.29	0.2	0.071
10	0.11	0.4	0.098
50	0.11	0.6	0.099
100	0.11	2.4	0.095
200	0.11	6.4	0.104
500	0.11	26.6	0.104
1000	0.11	Solution diverges	0.104

In Figure 5.5, there is no effect of changing the values of  $Pr$  on  $f$  even though the high value of  $Pr$  involved. It is similar to the derivative of  $f$  as shown in Figure 5.7. From Figure 5.6, the variation of mean temperature field  $\theta$  with respect to  $Pr$  is shown. It is clear that with increase of  $Pr$  the thickness of the thermal boundary layer decreases within the dynamical region  $[0, 6]$ . Figure 5.8 depicts the variable  $\theta'$  changes rapidly in the middle as  $Pr$  changes values from 1 to 100.

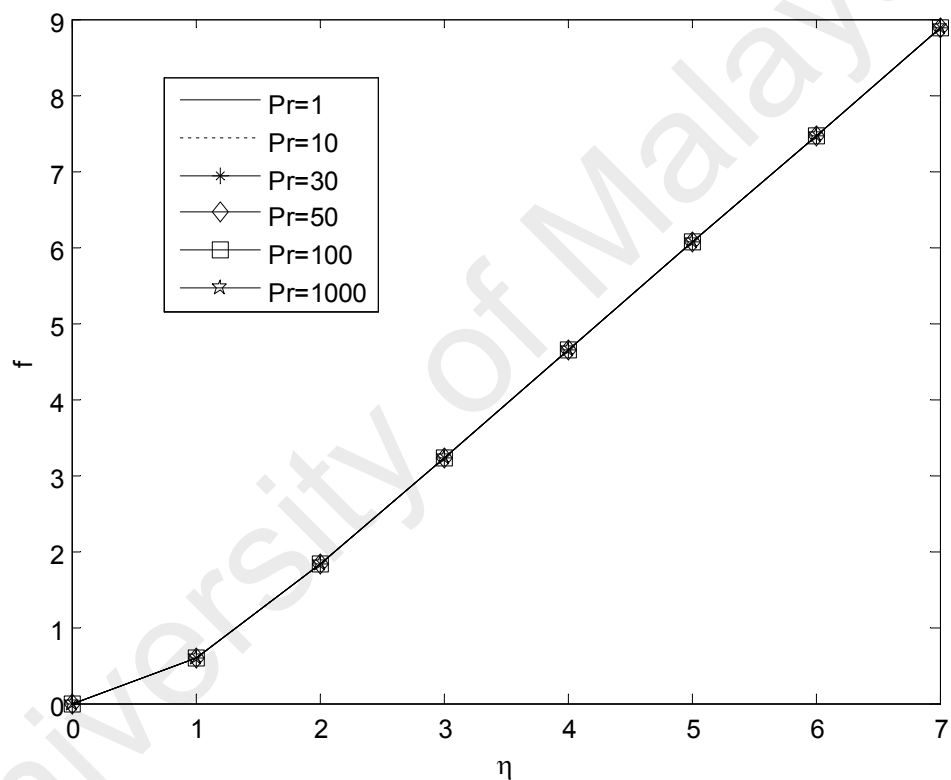


**Figure 5.5:** HWQM for  $f(\eta)$ , case of LFC when  $m = 128$  and  $L = 7$  at different values of  $Pr$

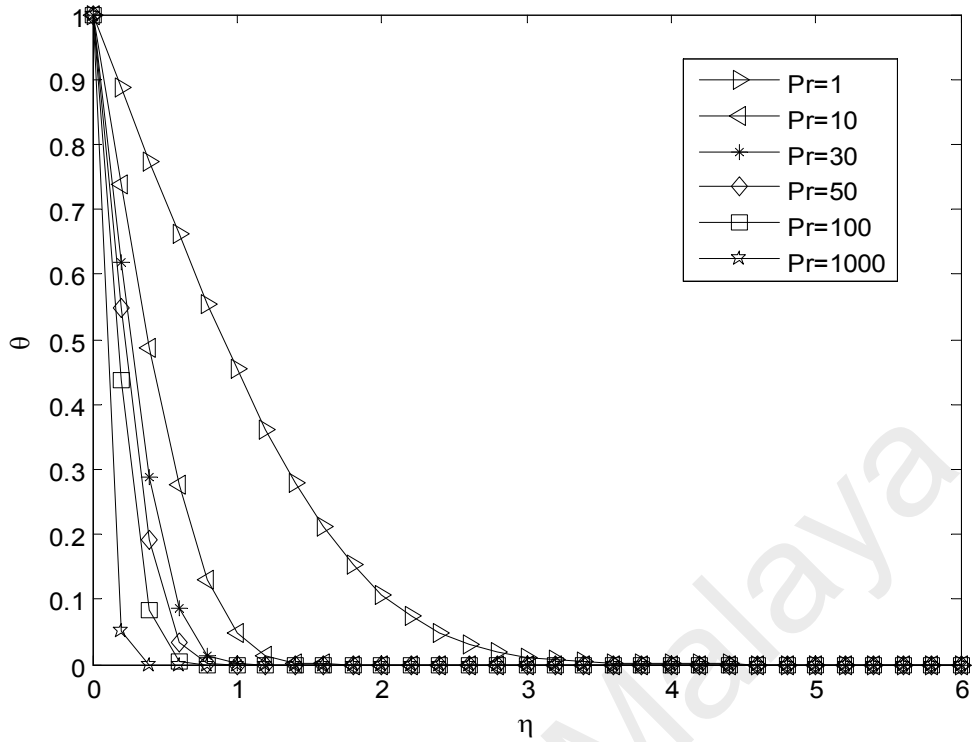


**Figure 5.6:** HWQM for  $\theta(\eta)$ , case of LFC when  $m = 128$  and  $L = 6$  at different values of Pr

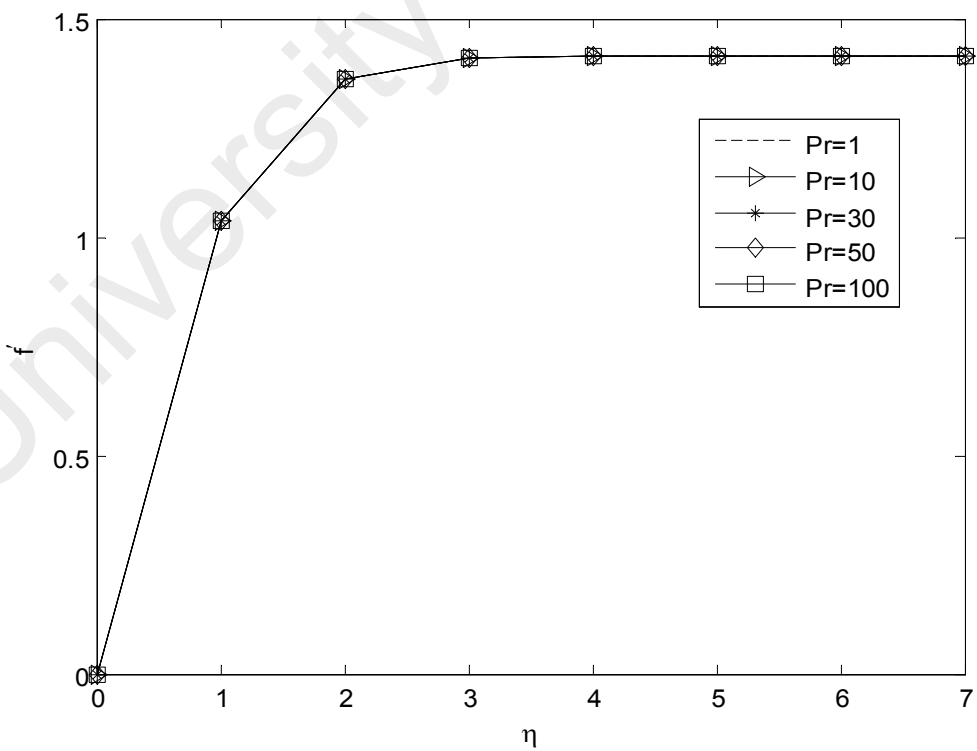


**Figure 5.7:** HWQM for  $f'(\eta)$ , case of LFC when  $m = 128$  and  $L = 7$  at different values of Pr

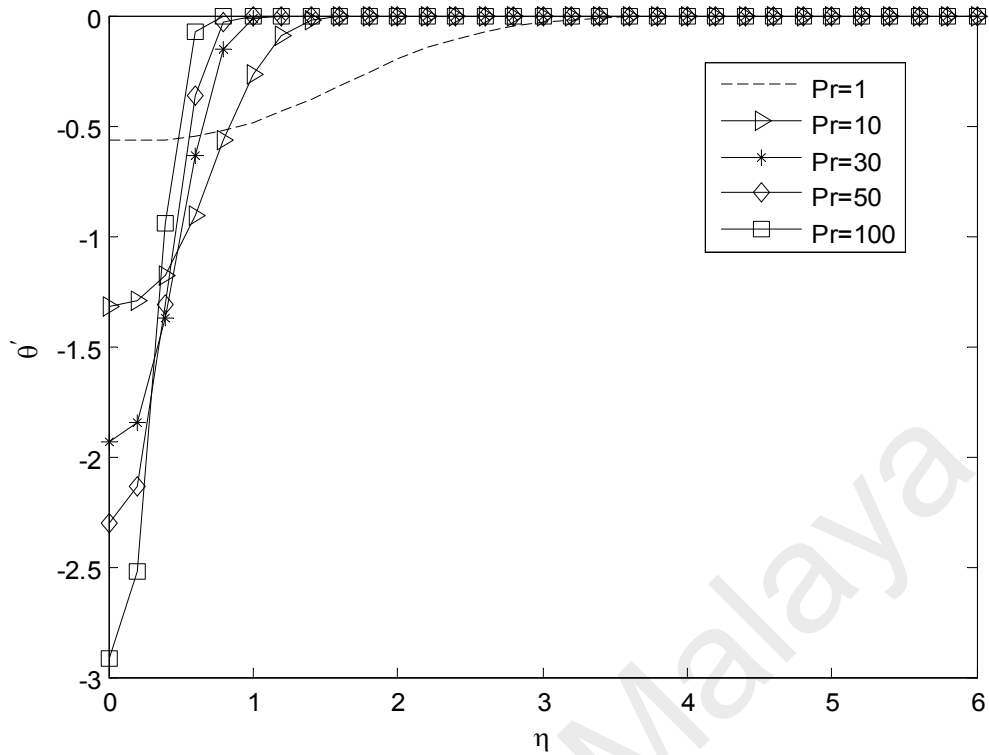


**Figure 5.8:** HWQM for  $\theta'(\eta)$ , case of LFC when  $m = 128$  and  $L = 7$  at different values of Pr

### 5.3 Natural Convection Boundary Layer Flow

#### 5.3.1 Introduction

Boundary layer flows of viscous fluids are of the highest industrial importance. Most of them can be modeled mathematically by systems of nonlinear ordinary differential equations on an unbounded domain. The theoretical, experimental and numerical analysis for the natural convection boundary layer flow related to isothermal, vertical flat plates have been carried out widely by many authors (Eckert & Soehngen, 1948; Ostrach, 1953; Stewart, 1971; Suwono, 1980; Merkin, 1985). Some of the method found in the literature that used similar case but with small values of Pr are HAM (Ghotbi et al., 2009) and FDM (Na, 1979; Mahdy & Hady, 2009).

#### 5.3.2 Problem Formulation

The natural convection flows are caused due to the density differences coming from

temperature gradients. These flows are generated in the vicinity of external surfaces and within channels in which the fluid flows.

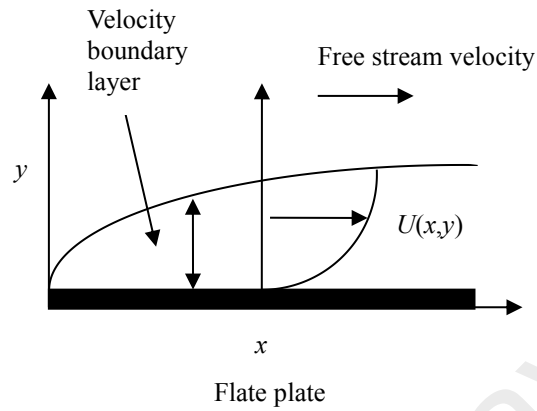


**Figure 5.9:** Physical model of natural convection boundary layer flow

The two dimensional flow over a horizontal flat plate with uniform surface temperature are governed by the continuity, momentum and energy equations as follows:

$$\frac{\partial u}{\partial x} + \frac{\partial v}{\partial y} = 0, \quad (5.55)$$

$$u \frac{\partial u}{\partial x} + v \frac{\partial u}{\partial y} = \nu \frac{\partial^2 u}{\partial y^2} + \theta \beta \left[ \frac{T - T_\infty}{T_w - T_\infty} \right], \quad (5.56)$$

$$u \frac{\partial T}{\partial x} + v \frac{\partial T}{\partial y} = \alpha \frac{\partial^2 T}{\partial y^2}, \quad (5.57)$$

subject to the boundary conditions

$$\begin{aligned} y = 0 & : u = 0, \quad v = 0, \quad T = T_w(x), \\ y \rightarrow \infty & : u = 0, \quad T = T_\infty, \end{aligned} \quad (5.58)$$

where  $x, y$  are the coordinates measured parallel and perpendicular to the plate. The

stream function  $\psi$  is defined as  $u = \frac{\partial \psi}{\partial y}$  and  $v = -\frac{\partial \psi}{\partial x}$ . The transformations below

are introduced (Na, 1979).

$$\eta = y \left[ \frac{\theta\beta}{4\nu^2 x} \right]^{\frac{1}{4}}, \quad \theta(\eta) = \frac{T - T_\infty}{T_w - T_\infty}, \quad \psi = 4\nu \left[ \frac{\theta\beta}{4\nu^2 x} \right]^{\frac{1}{4}} f(\eta). \quad (5.59)$$

By using the transformations, the Equations (5.55) - (5.57) are reduced to the following equations,

$$f''' + 3ff'' - 2f'^2 + \theta = 0, \quad (5.60)$$

and

$$\theta'' + 3\text{Pr} f\theta' = 0. \quad (5.61)$$

The boundary conditions are

$$\begin{aligned} \eta = 0 & : f = 0, \quad f' = 0, \quad \theta = 1, \\ \eta \rightarrow \infty & : f' \rightarrow 0, \quad \theta \rightarrow 0. \end{aligned} \quad (5.62)$$

### 5.3.3 Numerical Solution

Applying the quasilinearization technique to Equations (5.60) and (5.61), we get

$$f_{r+1}''' + 3f_r'' f_{r+1} - 4f_r' f_{r+1}' + 3f_r f_{r+1}'' + \theta_{r+1} = -2f_r'^2 + 3f_r'' f_r, \quad (5.63)$$

and

$$\theta_{r+1}'' + 3\text{Pr} f_r \theta_{r+1}' + 3\text{Pr} \theta_r' f_{r+1} = 3\text{Pr} \theta_r' f_r \quad (5.64)$$

respectively. The boundary conditions are

$$\begin{aligned} \eta = 0 & : f_{r+1} = 0, \quad f_{r+1}' = 0, \quad \theta_{r+1} = 1, \\ \eta \rightarrow \infty & : f_{r+1}' \rightarrow 0, \quad \theta_{r+1} \rightarrow 0. \end{aligned} \quad (5.65)$$

After simplification and substitution of boundary conditions given, the unknown value for  $f_{r+1}''(0)$  and  $\theta_{r+1}'(0)$  can be obtained as follows,

$$f_{r+1}''(0) = -\frac{1}{L} \sum_{i=0}^{m-1} a_i p_{i,2}(L), \quad (5.66)$$

and

$$\theta_{r+1}'(0) = \frac{1}{L} \left( -\sum_{i=0}^{m-1} b_i p_{i,2}(L) - 1 \right), \quad (5.67)$$

respectively. The Haar wavelets integration of higher order derivatives gives

$$f_{r+1}''(\eta) = \sum_{i=0}^{m-1} a_i \left( p_{i,1}(\eta) - \frac{1}{L} p_{i,2}(L) \right), \quad (5.68)$$

$$f_{r+1}'(\eta) = \sum_{i=0}^{m-1} a_i \left( p_{i,2}(\eta) - \frac{\eta}{L} p_{i,2}(L) \right), \quad (5.69)$$

$$f_{r+1}(\eta) = \sum_{i=0}^{m-1} a_i \left( p_{i,3}(\eta) - \frac{\eta^2}{2L} p_{i,2}(L) \right), \quad (5.70)$$

$$\theta_{r+1}'(\eta) = \sum_{i=0}^{m-1} b_i \left( p_{i,1}(\eta) - \frac{1}{L} p_{i,2}(L) \right) - \frac{1}{L}, \quad (5.71)$$

$$\theta_{r+1}(\eta) = \sum_{i=0}^{m-1} b_i \left( p_{i,2}(\eta) - \frac{\eta}{L} p_{i,2}(L) \right) - \frac{\eta}{L} + 1. \quad (5.72)$$

Substitute Equations (5.68) - (5.72) and higher order derivatives into Equations (5.63)

and (5.64), we obtain

$$\begin{aligned} & \sum_{i=0}^{m-1} a_i \left( h_i + 3f_r'' p_{i,3}(\eta) - \frac{3}{2L} \eta^2 f_r'' p_{i,2}(\eta) - 4f_r' p_{i,2}(\eta) \right. \\ & \quad \left. + \frac{4}{L} \eta f_r' p_{i,2}(L) + 3f_r p_{i,1}(\eta) - \frac{3}{L} f_r p_{i,2}(L) \right) \\ & \quad + \sum_{i=0}^{m-1} b_i \left( p_{i,2}(\eta) - \frac{1}{L} \eta p_{i,2}(L) \right) \\ & = -2f_r'^2 + 3f_r f_r'' + \frac{1}{L} \eta - 1, \end{aligned} \quad (5.73)$$

and

$$\begin{aligned} & \sum_{i=0}^{m-1} a_i \left( 3 \Pr \theta_r' p_{i,3}(\eta) - \frac{3}{2L} \Pr \eta^2 \theta_r' p_{i,2}(L) \right) + \\ & \sum_{i=0}^{m-1} b_i \left( h_i + 3 \Pr f_r p_{i,1}(\eta) - \frac{3}{L} \Pr f_r p_{i,2}(L) \right) \\ & = 3 \Pr \theta_r' f_r + \frac{3}{L} \Pr f_r. \end{aligned} \quad (5.74)$$

The Equations (5.73) and (5.74) are solved simultaneously to obtain Haar coefficient  $a_i$  and  $b_i$ . The initial approximation which satisfy the boundary conditions (5.65) as follows

$$f_0(\eta) = 0, \quad (5.75)$$

and

$$\theta_0(\eta) = 1 - \frac{1}{L}\eta. \quad (5.76)$$

### 5.3.4 Results and Discussion

The numerical results for natural convection boundary layer flow problem (NCBLF) are discussed in this section.

**Table 5.7:** Comparison between HWQM with RKM and HWCM for  $f(\eta)$  and  $\theta(\eta)$  of NCBLF with  $m = 256$ ,  $Pr = 3$  and  $L = 1$

$\eta$	$f(\eta)$			$\theta(\eta)$		
	HWCM (Islam et al., 2011)	RKM (Islam et al., 2011)	HWQM (Present)	HWCM (Islam et al., 2011)	RKM (Islam et al., 2011)	HWQM (Present)
0	0	0	0	1	1	1
0.1	0.0014533	0.0014766	0.0014733	0.8940570	0.8979760	0.8938646
0.2	0.0051997	0.0052909	0.0053123	0.7882710	0.7960030	0.7878979
0.3	0.0103994	0.0105972	0.0106511	0.6829970	0.6941960	0.6824494
0.4	0.0163197	0.0166537	0.0167465	0.5787050	0.5927130	0.5780227
0.5	0.0223356	0.0228227	0.0229778	0.4759360	0.4917370	0.4751769
0.6	0.0279277	0.0285706	0.0287724	0.3752060	0.3914480	0.3744298
0.7	0.0326819	0.0334676	0.0337273	0.2769670	0.2920130	0.2762398
0.8	0.0362856	0.0371863	0.0374877	0.1815650	0.1935690	0.1809780
0.9	0.0385254	0.0395007	0.0398222	0.0892148	0.0962128	0.0888726
1	0.0392829	0.0402840	0.0406231	0	0	0

Comparison of the present method with RKM and HWCM for small value of  $Pr$  is shown in Table 5.7. According to that, good agreement is found between HWQM with RKM and HWCM for both  $f$  and  $\theta$  at the collocation points between  $[0, 1]$ . Some of the method found in the literature that used similar case but with small values of  $Pr = 0.72$

are FDM (Na, 1979) and Haar wavelet collocation method (HWCM) combined with Newton method (Islam et al., 2011) as shown in Table 5.8. The result shows that good agreement between HWQM with FDM and HWCM at two decimal places. Table 5.9 is constructed for a comparison of CPU time to run a program between HWQM with previously reported methods. It shows that HWQM offers less computing time compared to the others.

**Table 5.8:** Comparison between HWQM with FDM and HWCM for  $f''(0)$  of NCBLF when  $Pr = 0.72$

$f''(0)$		
FDM (Na, 1979)	HWCM (Islam et al., 2011)	HWQM (Present)
0.6742	0.6739	0.6751

**Table 5.9:** Comparison of CPU time (sec) between HWCM, RKM and HWQM for different values of  $Pr$  when  $L = 1$  and  $m = 8$

Pr	HWCM (Islam et al., 2011)	RKM (Islam et al., 2011)	HWQM (Present)
1	0.321	0.21	0.131
10	0.124	0.37	0.128
100	0.141	0.89	0.133
150	0.141	1.25	0.136
170	0.141	1.36	0.138
300	0.141	1.59	0.138
400	0.141	2.00	0.138
600	0.141	2.30	0.138
800	0.141	14.21 (Solution diverges)	0.138
1000	0.141	21.8 (Solution diverges)	0.138
1500	0.141	24.6 (Solution diverges)	0.138

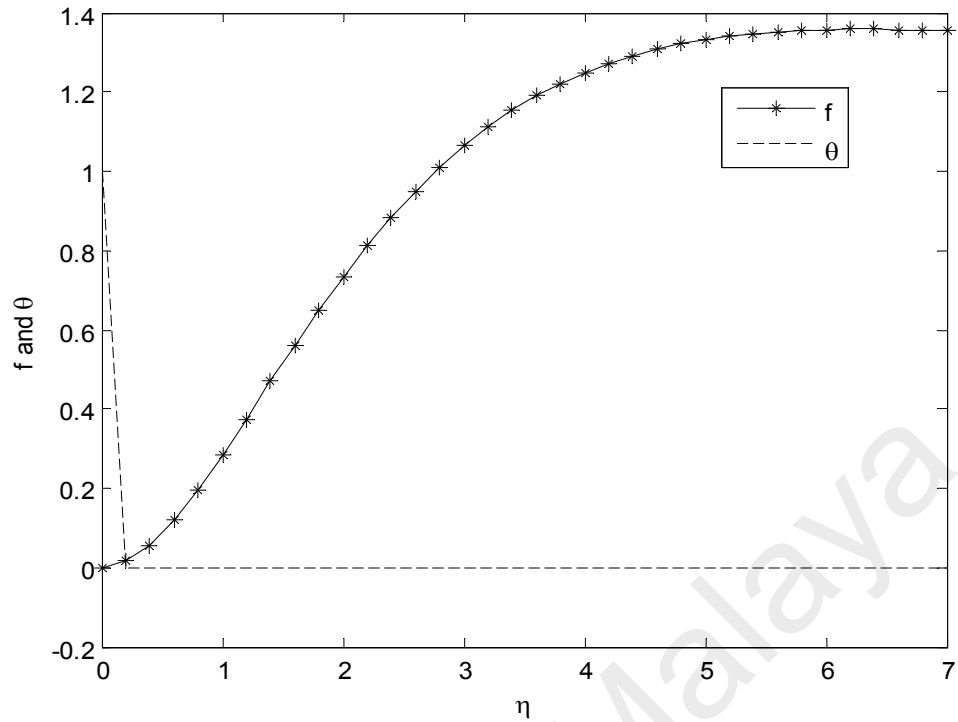


**Figure 5.10:** HWQM for  $f(\eta)$  and  $\theta(\eta)$ , case of NCBLF when  $m = 256$ ,  $L = 7$  and  $Pr = 1500$

Figures 5.10 and 5.11 show that HWQM produces stable results for larger values of  $Pr$  either for small interval or large interval. According to Figure 5.12(a), with the increase in  $Pr$ , the thickness of the layer is not effected. This similar to the Figure 5.12(b) in which represents the variations of the velocity distribution in the boundary layer profiles for various values of  $Pr$ . Moreover, from Figure 5.13(a), it is obvious that the thermal boundary layer decreases as well with the increase of  $Pr$ . Figure 5.13(b) shows that the rate of change of the thermal boundary layer decreases at the beginning, but it tends to approach zero level in the middle.

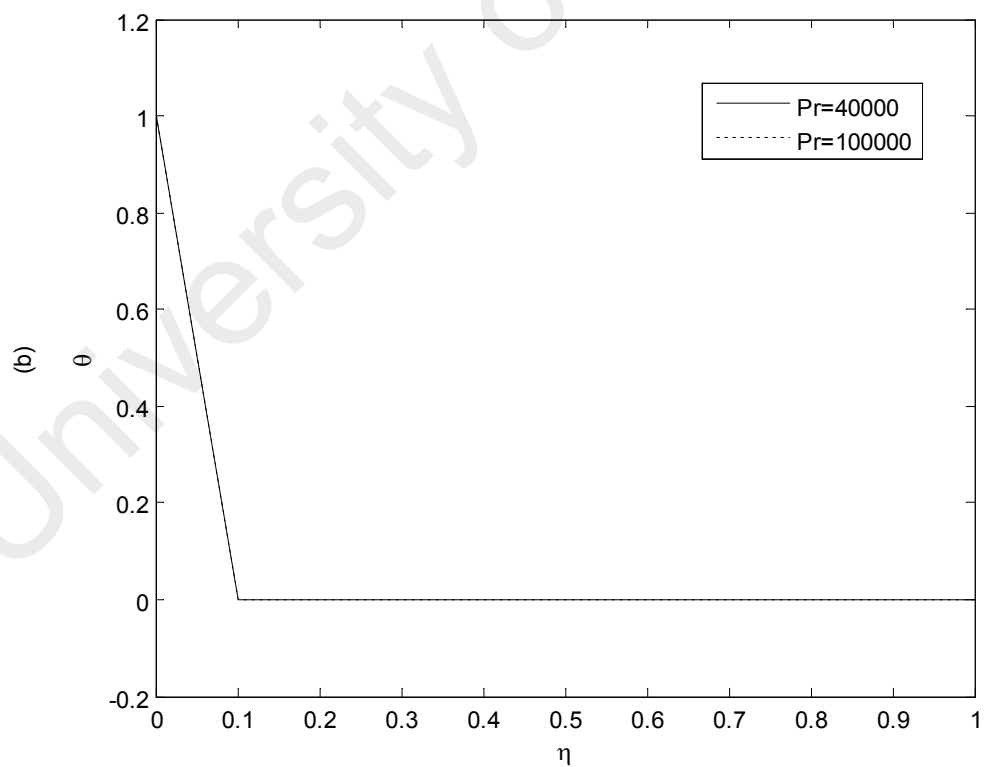
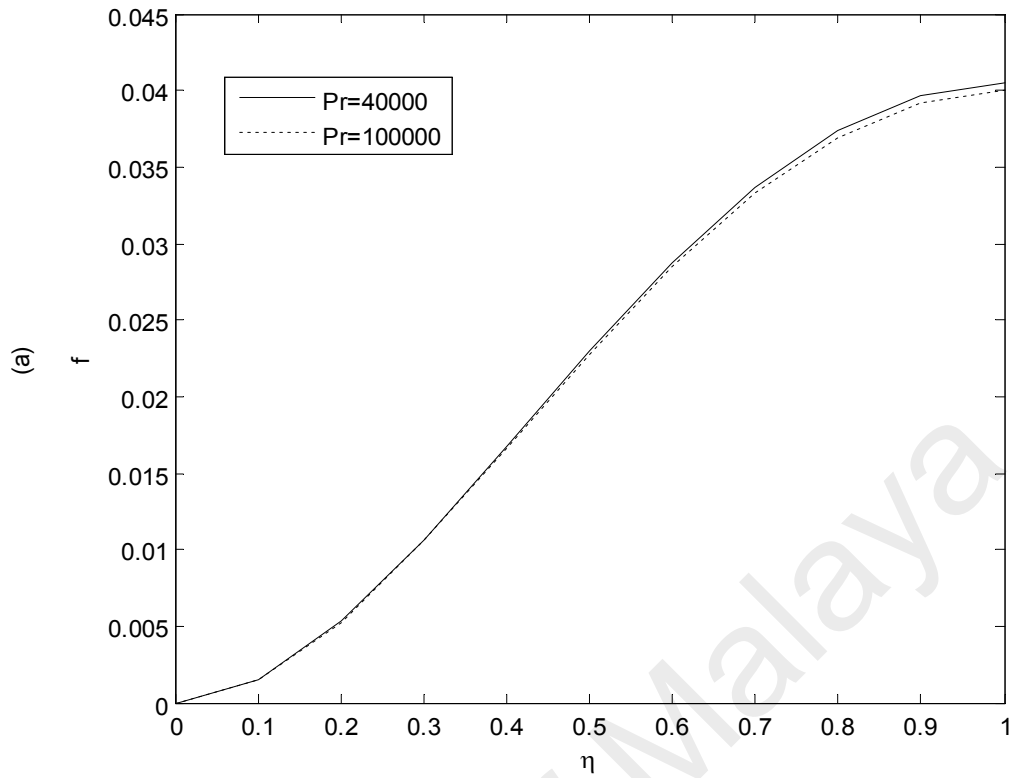


**Figure 5.11:** HWQM for (a)  $f(\eta)$  and (b)  $\theta(\eta)$  case of NCBLF when  $m = 256$  and  $L = 1$  at  $Pr = 40,000$  and  $Pr = 100,000$

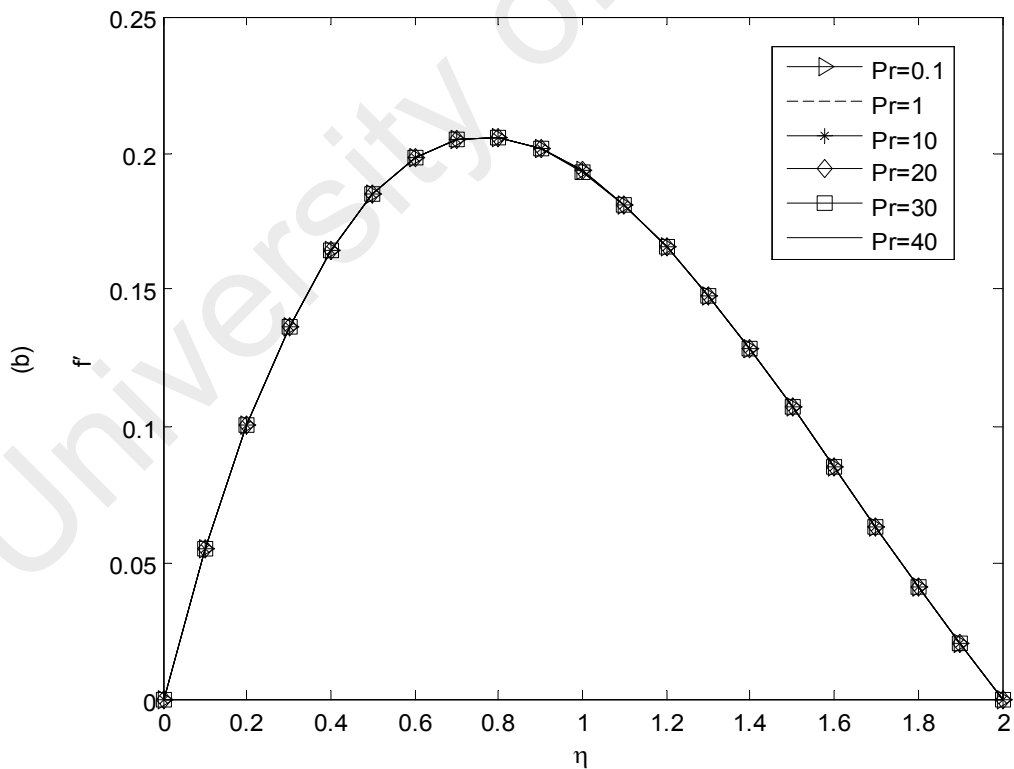
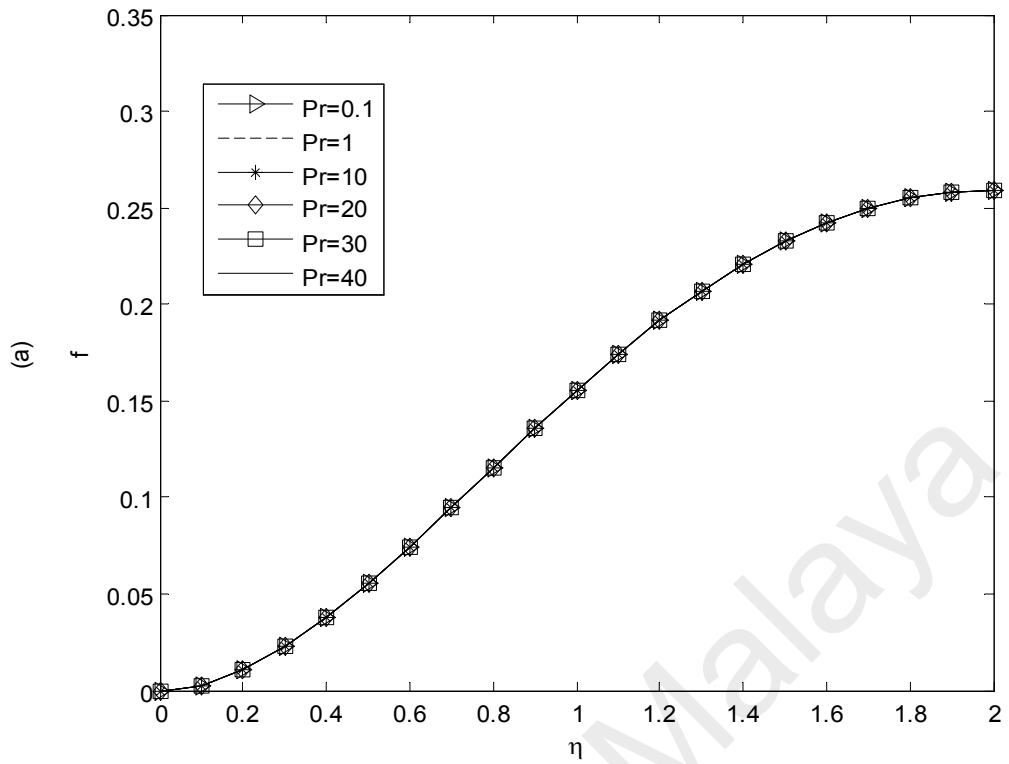


**Figure 5.12:** HWQM for (a)  $f(\eta)$  and (b)  $f'(\eta)$ , case of NCBLF when  $m = 256$  and  $L = 7$  for different values of Pr

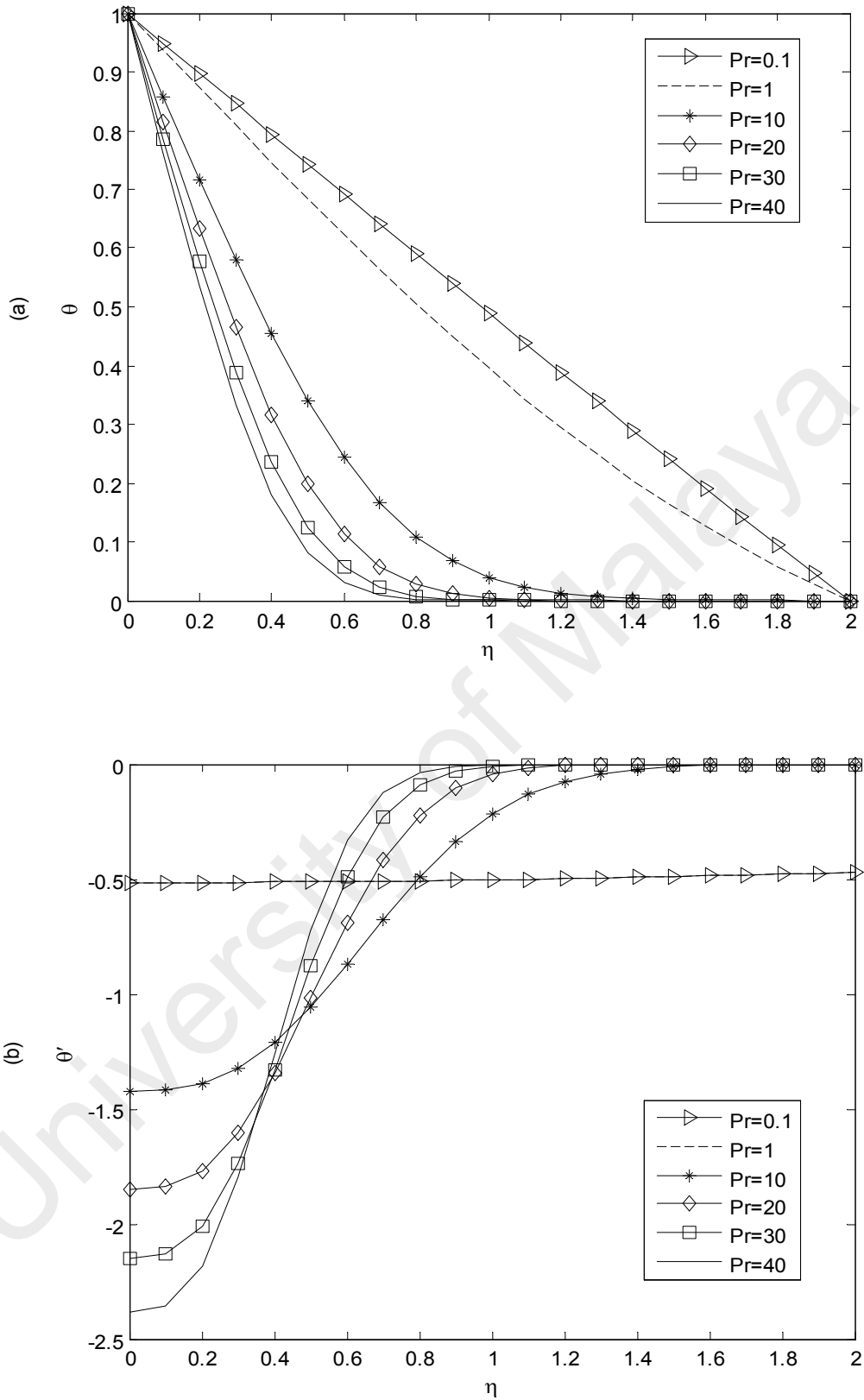


**Figure 5.13:** HWQM for (a)  $\theta(\eta)$  and (b)  $\theta'(\eta)$ , case of NCBLF when  $m = 256$  and  $L = 7$  for different values of Pr

## 5.4 Conclusions

Detailed examination on variety of systems of boundary value problems arising in natural convection boundary layer flows without exact solution have been performed by using Haar wavelet quasilinearization method. The quasilinearization procedure replaces the original nonlinear equation by a sequence of linear equations and Haar wavelets procedure is exploited to solve these linear boundary value problems.

Present results are compared with the available experimental results. It has been found that the results of HWQM provides excellent approximations to the solution and its derivatives with high accuracy. Based on the findings presented in the previous sections, HWQM can be handled in the case of flows with low Pr. HWQM based algorithm also produces stable numerical solution for fluid flows with larger values of Pr, which is quite challenging for asymptotic methods like homotopy analysis method (HAM), HPM and differential transformation method (DTM).

This method also suitable for the numerical solution of boundary value problems defined on small and long intervals. HWQM provides smaller CPU time since universal subprogram is applied to calculate integrals of Haar wavelets. Similar to HWCM, HWQM does not require conversion of a boundary value problem into initial value problem. This is unlike the procedure of RKM where this method require conversion by using shooting technique. In order for achieving a very accurate solution, HWQM ensured a very rapid convergence after only one iteration and by increasing the level of resolution.

## **CHAPTER 6: COUPLED NONLINEAR ORDINARY DIFFERENTIAL EQUATIONS WITH SOME ADDITIONAL PARAMETERS**

In this chapter, the Haar wavelet quasilinearization method is proposed for the numerical solution of system of coupled nonlinear ODEs related to the Cattaneo-Christov heat flux model for boundary layer flow of Maxwell fluid in the presence of,

- (a) velocity slip boundary,
- (b) suction and injection,
- (c) heat generation/absorption.

### **6.1 Heat Transfer and Boundary Layer Flow of a Viscoelastic Fluid Above a Stretching Plate with Velocity Slip Boundary**

#### **6.1.1 Introduction**

The phenomenon of heat transfer exist due to difference of temperature between objects or between different parts of the same object. The well-known heat conduction law or known as Fourier's law proposed by Fourier (1822) provides an insight to examine the heat transfer analysis. However, this law causes a parabolic energy equation, means that any initial disturbance is instantly felt through the medium under consideration. Due to this limitation, Cattaneo (1948) revised this law by adding a relaxation time term. Later, Christov (2009) made some modification on Cattaneo model by replacing the ordinary derivative with the Oldroyd's upper-convected derivative. This model is recognized as Cattaneo-Christov heat flux model in the literature. Straughan (2010) studied the thermal convection in horizontal layer of incompressible Newtonian fluid by using Cattaneo-Christov model. Ciarletta and Straughan (2010) proved the uniqueness and stability of the solutions for the Cattaneo-Christov equations. By using Cattaneo-Christov model, Tibullo and Zampoli (2011) studied the uniqueness of the

solutions for an incompressible fluid.

The Maxwell fluid model is one of the simplest viscoelastic models and can address the influence of the fluid relaxation time. Due to these reasons, this model has received remarkable attention of the researchers. Han et al. (2014) employed the upper-convected Maxwell (UCM) model and Cattaneo-Christov heat flux model to investigate heat transfer and boundary layer flow of a viscoelastic fluid above a stretching plate with velocity slip boundary by using HAM. Mustafa (2015) also used HAM to investigate the rotating flow of UCM fluid through Cattaneo-Christov heat flux model. Khan et al. (2015) studied the boundary layer flow of UCM fluid induced by exponentially stretching sheet using Cattaneo-Christov model. Hayat et al. (2015) discussed the impact of Cattaneo-Christov heat flux in the flow over a stretching sheet with variable thickness.

Abbasi et al. (2016) investigated the Cattaneo-Christov heat flux model for a two-dimensional laminar boundary layer flow of an incompressible Oldroyd-B fluid over a linearly stretching sheet, where the dimensionless velocity and temperature profiles are obtained through optimal homotopy analysis method (OHAM). Mushtaq et al. (2016) studied the Sakiadis flow of Maxwell fluid along a moving plate in a calm fluid by considering the Cattaneo-Christov model. Abbasi and Shehzad (2016) proposed a mathematical model to study the Cattaneo-Christov heat flux model for three-dimensional flow of Maxwell fluid over a bi-directional stretching surface by employing the homotopic procedure. Rubab and Mustafa (2016) used HAM to investigate the magnetohydrodynamic (MHD) three-dimensional flow of UCM fluid over a bi-directional stretching surface.

The wide range of publications revealed that the no-slip boundary condition is mostly studied in the literature. However, the fluids that exhibit the boundary slip have important technological applications such as the polishing of the artificial heart valves

and internal cavities, inexpensive lubricating, refrigeration equipment, optical coatings and in many industrial processes.

Ibrahim and Shankar (2013) analyzed the effects of magnetic field and velocity thermal slips on the boundary layer flow and heat transfer over a permeable stretching sheet due to a nanofluid. Nandy and Mahapatra (2013) investigated the heat transfer rate of MHD stagnation point flow of nanofluid over a stretching or shrinking surface along with the effects of velocity slip and convective boundary conditions. Aman et al. (2013) studied the problem of slip effects on stagnation point flow past a stretching or shrinking sheet in the presence of magnetic field. Bhattacharyya et al. (2013) examined the similarity solution of mixed convective boundary layer flow over a vertical plate along with the velocity and thermal slip effects. Noghrehabadi et al. (2012) observed the slip effects on the flow and heat transfer rate of nanofluid over stretching sheet.

In this section, we now apply the Haar wavelet quasilinearization method to solve coupled flow and heat transfer of boundary layer in viscoelastic fluid with the upper-convected Maxwell model and Cattaneo-Christov heat flux model with velocity slip on boundary. The effects involved on parameters of the velocity and temperature fields are analyzed and discussed.

### 6.1.2 Problem Formulation

The model in this work is the same as that in (Han et al., 2014). Consider the steady two dimensional boundary layer flow of UCM fluid over a plate. The detailed of governing equations expressing conservation of mass and momentum, and the boundary conditions with velocity slip on boundary can be found in work by Han et al. (2014).

$$\frac{\partial u}{\partial x} + \frac{\partial v}{\partial y} = 0, \quad (6.1)$$

$$u \frac{\partial u}{\partial x} + v \frac{\partial u}{\partial y} + \lambda_1 \left( u^2 \frac{\partial^2 u}{\partial x^2} + v^2 \frac{\partial^2 u}{\partial y^2} + 2uv \frac{\partial^2 u}{\partial x \partial y} \right) = \nu \frac{\partial^2 u}{\partial y^2}, \quad (6.2)$$

where  $u$  and  $v$  denote the velocity components along the  $x$ - and  $y$ - directions, respectively,  $\nu$  is the kinematic viscosity and  $\lambda_1$  is the fluid relaxation time.

The equations above are subjected to the boundary conditions with velocity slip on boundary given as

$$u = ax + \lambda_0 \frac{2 - \sigma_v}{\sigma_v} \frac{\partial u}{\partial y} \Big|_{y=0}, \quad v = 0 \quad \text{at} \quad y = 0, \quad (6.3)$$

$$u \rightarrow 0 \quad \text{as} \quad y \rightarrow \infty,$$

where  $a$  is positive constant, the tangential momentum is denoted as  $\sigma_v$  and  $\lambda_0$  is the molecular mean free path.

In this work, Cattaneo-Christov heat flux model is taken into consideration. This model can predict the effects of thermal relaxation time on the boundary layer. The heat flux model is given in the following equation,

$$\mathbf{q} + \lambda_2 \left[ \frac{\partial \mathbf{q}}{\partial t} + \mathbf{V} \cdot \nabla \mathbf{q} - \mathbf{q} \cdot \nabla \mathbf{V} + (\nabla \cdot \mathbf{V}) \mathbf{q} \right] = -k \nabla T, \quad (6.4)$$

in which  $\mathbf{q}$  is the heat flux,  $\lambda_2$  is the thermal relaxation time,  $T$  is the Maxwell fluid temperature,  $k$  is the thermal conductivity of the fluid and  $\mathbf{V} = (u, v)$  is the velocity vector of the Maxwell fluid. Equation (6.4) can be written as,

$$\mathbf{q} + \lambda_2 \left[ \frac{\partial \mathbf{q}}{\partial t} + \mathbf{V} \cdot \nabla \mathbf{q} - \mathbf{q} \cdot \nabla \mathbf{V} \right] = -k \nabla T. \quad (6.5)$$

The energy balance for the steady boundary layer flow can be written as

$$\rho c_p \mathbf{V} \cdot \nabla T = -\nabla \cdot \mathbf{q}. \quad (6.6)$$

To obtain the temperature governing equation for the steady flow,  $\mathbf{q}$  is eliminated between Equations (6.5) and (6.6),

$$u \frac{\partial T}{\partial x} + v \frac{\partial T}{\partial y} + \lambda_2 \left( u \frac{\partial u}{\partial x} \frac{\partial T}{\partial x} + v \frac{\partial v}{\partial y} \frac{\partial T}{\partial y} + u \frac{\partial v}{\partial x} \frac{\partial T}{\partial y} + v \frac{\partial u}{\partial y} \frac{\partial T}{\partial x} \right. \\ \left. + 2uv \frac{\partial^2 T}{\partial x \partial y} + u^2 \frac{\partial^2 T}{\partial x^2} + v^2 \frac{\partial^2 T}{\partial y^2} \right) = \alpha \frac{\partial^2 T}{\partial y^2}, \quad (6.7)$$

where  $\alpha = k / \rho c_p$  is the thermal diffusivity,  $\rho$  is the fluid density and  $c_p$  is the specific heat. The boundary conditions in the present problem are

$$\begin{aligned} T &= T_w \text{ at } y=0, \\ T &\rightarrow T_\infty \text{ as } y \rightarrow \infty. \end{aligned} \quad (6.8)$$

By using these transformations,

$$\eta = \sqrt{\frac{a}{\nu}} y, \quad \psi = \sqrt{va} x f(\eta), \quad \theta = \frac{T - T_\infty}{T_w - T_\infty}, \quad (6.9)$$

in which  $\psi$  is the stream function. Equations (6.2) and (6.7) can be reduced to a system of two coupled ordinary differential equations as follows

$$f''' - f'^2 + ff'' + \beta(2ff'f'' - f^2 f''') = 0, \quad (6.10)$$

and

$$\frac{1}{\text{Pr}} \theta'' + f\theta' - \gamma(ff'\theta' + f^2\theta'') = 0, \quad (6.11)$$

where the prime denotes the derivative with respect to  $\eta$ . Prandtl number is given as  $\text{Pr} = \nu / \alpha$ , where  $\nu$  is the velocity component along  $y$ -direction and  $\alpha$  is thermal diffusivity.  $\beta = \lambda_1 a$  is the Deborah number and  $\gamma = \lambda_2 a$  is the non-dimensional thermal relaxation time, where  $a$  is a positive constant,  $\lambda_1$  is fluid relaxation time and  $\lambda_2$  is thermal relaxation time. The boundary conditions for Equations (6.10) and (6.11) are

$$\begin{aligned} f &= 0, \quad f' = 1 + bf'', \quad \theta = 1 \text{ at } \eta = 0, \\ f' &\rightarrow 0, \quad \theta \rightarrow 0 \text{ as } \eta \rightarrow \infty, \end{aligned} \quad (6.12)$$

where  $b = \lambda_0 \frac{2 - \sigma_v}{\sigma_v} \sqrt{\frac{a}{\nu}}$ .

### 6.1.3 Numerical Solution

Quasilinearization technique is applied to Equations (6.10) and (6.11). We get,

$$\begin{aligned}
 f_{r+1}''' - \frac{1}{1-\beta f_r^2} (2f_r' f_{r+1}' - 2\beta f_r f_r'' f_{r+1}' - f_r f_{r+1}'' - 2\beta f_r f_r' f_{r+1}'') - \frac{1}{(1-\beta f_r^2)^2} \\
 (2\beta f_r f_r'^2 f_{r+1}' - f_r'' f_{r+1}' - \beta f_r^2 f_r'' f_{r+1}' - 2\beta f_r' f_r'' f_{r+1}' - 2\beta^2 f_r^2 f_r' f_r'' f_{r+1}') \\
 = \frac{1}{1-\beta f_r^2} (-f_r'^2 + 2\beta f_r f_r' f_r'') + \frac{1}{(1-\beta f_r^2)^2} (-2\beta f_r^2 f_r'^2 + f_r f_r'' + \beta f_r^3 f_r'' \\
 + 2\beta f_r f_r' f_r'' + 2\beta^2 f_r^3 f_r' f_r''),
 \end{aligned} \tag{6.13}$$

and

$$\begin{aligned}
 \theta_{r+1}'' + \frac{1}{1-\text{Pr} \gamma f_r^2} (\text{Pr} f_r \theta_{r+1}' - \text{Pr} \gamma f_r f_r' \theta_{r+1}' - \text{Pr} \gamma f_r \theta_r' f_{r+1}') + \frac{1}{(1-\text{Pr} \gamma f_r^2)^2} \\
 (\text{Pr} \theta_r' f_{r+1}' + \text{Pr}^2 \gamma f_r^2 \theta_r' f_{r+1}' - \text{Pr} \gamma f_r' \theta_r' f_{r+1}' - \text{Pr}^2 \gamma^2 f_r^2 f_r' \theta_r' f_{r+1}') \\
 = \frac{1}{1-\text{Pr} \gamma f_r^2} (-\text{Pr} \gamma f_r f_r' \theta_r') + \frac{1}{(1-\text{Pr} \gamma f_r^2)^2} (+\text{Pr}^2 \gamma f_r^3 \theta_r' \\
 - \text{Pr} \gamma f_r f_r' \theta_r' + \text{Pr} \theta_r' f_r - \text{Pr}^2 \gamma^2 f_r^3 f_r' \theta_r'),
 \end{aligned} \tag{6.14}$$

respectively. The boundary conditions are

$$\begin{aligned}
 f_{r+1} = 0, \quad f_{r+1}' = 1 + b f_{r+1}'', \quad \theta_{r+1} = 1 \quad \text{at} \quad \eta = 0, \\
 f_{r+1}' \rightarrow 0, \quad \theta_{r+1} \rightarrow 0 \quad \text{as} \quad \eta \rightarrow \infty.
 \end{aligned} \tag{6.15}$$

The Haar wavelet method is applied to Equations (6.13) and (6.14). The higher order derivatives in this problem is similar to problem in Section 5.1.3, as shown in Equations (5.14) and (5.15). The lower order derivatives are obtained by integrating them and use the boundary conditions given.

$$f_{r+1}''(\eta) = \sum_{i=0}^{m-1} a_i \left( p_{i,1}(\eta) - \frac{1}{(L+b)} p_{i,2}(L) \right) - \frac{1}{(L+b)}, \tag{6.16}$$

$$f_{r+1}'(\eta) = \sum_{i=0}^{m-1} a_i \left( p_{i,2}(\eta) + \left( \frac{-\eta-b}{L+b} \right) p_{i,2}(L) \right) + \left( \frac{-\eta-b}{L+b} \right) + 1, \tag{6.17}$$

$$f_{r+1}(\eta) = \sum_{i=0}^{m-1} a_i \left( p_{i,3}(\eta) + \left( \frac{-\eta^2-2b\eta}{2(L+b)} \right) p_{i,2}(L) \right) + \left( \frac{-\eta^2-2b\eta}{2(L+b)} \right) + \eta, \tag{6.18}$$

$$\theta'_{r+1}(\eta) = \sum_{i=0}^{m-1} b_i \left( p_{i,1}(\eta) - \frac{1}{L} p_{i,2}(L) \right) - \frac{1}{L}, \quad (6.19)$$

$$\theta_{r+1}(\eta) = \sum_{i=0}^{m-1} b_i \left( p_{i,2}(\eta) - \frac{\eta}{L} p_{i,2}(L) \right) - \frac{\eta}{L} + 1, \quad (6.20)$$

where  $L$  is sufficiently large number. The values for  $f''_{r+1}(0)$  and  $\theta'_{r+1}(0)$  can be obtained as

$$f''_{r+1}(0) = \frac{1}{(L+b)} \left( - \sum_{i=0}^{m-1} a_i p_{i,2}(L) - 1 \right), \quad (6.21)$$

and

$$\theta'_{r+1}(0) = \frac{1}{L} \left( - \sum_{i=0}^{m-1} b_i p_{i,2}(L) - 1 \right). \quad (6.22)$$

Substitute Equations (6.16) - (6.20) and higher order derivatives into Equations (6.13) and (6.14), we obtain

$$\sum_{i=0}^{m-1} a_i K_1 = L_1, \quad (6.23)$$

and

$$\sum_{i=0}^{m-1} a_i K_2 + \sum_{i=0}^{m-1} b_i K_3 = L_2, \quad (6.24)$$

where

$$\begin{aligned} K_1 = & h_i(\eta) - \frac{1}{1-\beta f_r^2} \left[ 2(f'_r - \beta f_r f_r'') p_{i,2}(\eta) - (f_r + 2\beta f_r f_r') p_{i,1}(\eta) \right. \\ & \left. + \frac{1}{L+b} (2(-\eta-b)f'_r - 2\beta(-\eta-b)f_r f_r'' + f_r + 2\beta f_r f_r') p_{i,2}(L) \right] \\ & - \frac{1}{(1-\beta f_r^2)^2} \left[ (2\beta f_r f_r'^2 - f_r'' - \beta f_r^2 f_r'' - 2\beta f_r' f_r'' - 2\beta^2 f_r^2 f_r' f_r'') p_{i,3}(\eta) \right. \\ & \left. + \left( \frac{-\eta^2 - 2b\eta}{2(L+b)} \right) (2\beta f_r f_r'^2 - f_r'' - \beta f_r^2 f_r'' - 2\beta f_r' f_r'' - 2\beta^2 f_r^2 f_r' f_r'') p_{i,2}(L) \right], \end{aligned}$$

$$K_2 = \frac{\Pr \gamma f_r \theta_r'}{1 - \Pr \gamma f_r^2} \left[ -p_{i,2}(\eta) - \left( \frac{-\eta - b}{L + b} \right) p_{i,2}(L) \right] \\ + \frac{1}{(1 - \Pr \gamma f_r^2)^2} \left[ \Pr \theta_r' (1 + \Pr \gamma f_r^2 - \gamma f_r' - \Pr \gamma^2 f_r^2 f_r') p_{i,3}(\eta) \right. \\ \left. + \left( \frac{-\eta^2 - 2b\eta}{2(L + b)} \right) \Pr \theta_r' (1 + \Pr \gamma f_r^2 - \gamma f_r' - \Pr \gamma^2 f_r^2 f_r') p_{i,2}(L) \right],$$

$$K_3 = h_i(\eta) + \frac{\Pr f_r}{1 - \Pr \gamma f_r^2} \left[ (1 - \gamma f_r') p_{i,1}(\eta) - \frac{1}{L} (1 - \gamma f_r') p_{i,2}(L) \right],$$

$$L_1 = \frac{1}{1 - \beta f_r^2} \left[ 2 \left( \frac{-\eta - b}{L + b} \right) (f_r' - \beta f_r f_r'') + f_r' (-f_r' + 2\beta f_r f_r'' + 2) - 2\beta f_r f_r'' \right. \\ \left. + \frac{1}{L + b} f_r (1 + 2\beta f_r') \right] + \frac{1}{(1 - \beta f_r^2)^2} \left( \frac{-\eta^2 - 2b\eta}{2(L + b)} \right) [2\beta f_r' (f_r f_r' - f_r'' - \beta f_r^2 f_r'') \\ - f_r'' (1 + \beta f_r^2)] + \frac{1}{(1 - \beta f_r^2)^2} [2\beta f_r' (-f_r^2 f_r' + f_r f_r'' + \beta f_r^3 f_r'' + \eta f_r f_r' - \eta f_r'' \\ - \beta \eta f_r^2 f_r'') + f_r'' (f_r + \beta f_r^3 - \eta - \beta \eta f_r^2)],$$

$$L_2 = \frac{1}{1 - \Pr \gamma f_r^2} \left[ \Pr f_r \left( -\gamma f_r' \theta_r' + \frac{1}{L} - \frac{1}{L} \gamma f_r' + \left( \frac{-\eta - b}{L + b} \right) \gamma \theta_r' + \gamma \theta_r' \right) \right] \\ + \frac{1}{(1 - \Pr \gamma f_r^2)^2} \left[ \Pr f_r \theta_r' (1 + \Pr \gamma f_r^2 - \gamma f_r' - \Pr \gamma^2 f_r^2 f_r' - \Pr \gamma \eta f_r + \Pr \gamma^2 \eta f_r f_r') \right. \\ \left. + \left( \frac{-\eta^2 - 2b\eta}{2(L + b)} \right) \Pr \theta_r' (-1 - \Pr \gamma f_r^2 + \gamma f_r' + \Pr \gamma^2 f_r^2 f_r') - \Pr \eta \theta_r' (1 - \gamma f_r') \right].$$

The Equations (6.23) and (6.24) can be solved simultaneously to obtain Haar coefficients,  $a_i$  and  $b_i$ . We chose the initial approximation which satisfy the boundary conditions (6.15) as follow

$$f_0(\eta) = \frac{1 - e^{-\eta}}{1 + b}, \quad (6.25)$$

and

$$\theta_0(\eta) = e^{-\eta}. \quad (6.26)$$

#### 6.1.4 Results and Discussion

This similar problem has been solved by Han et al. (2014). However, they only provided

a graphical results to show the output of their proposed method. All computations of HWQM are performed by MATLAB. Based on Figures 6.1 - 6.6, it is clear that HWQM agrees well with HAM as proposed by Han et al. (2014).

Figures 6.1 and 6.2 show the effects of elasticity number,  $\beta$  on the velocity and temperature distributions. The elastic force disappears when  $\beta = 0$  and the fluid becomes the Newtonian fluid. From Figure 6.1, it is clear that with the increase of  $\beta$ , the value of  $f(\eta)$  become smaller. The impact of elasticity number,  $\beta$  on the velocity distribution is also illustrated in this figure. It is noted that velocity distribution shows decreasing behaviour corresponding to higher values of  $\beta$ . Physically, bigger  $\beta$  indicates stronger viscous force which restricts the fluid motion and subsequently the velocity decreases. Characteristics of  $\beta$  on temperature distribution is displayed in Figure 6.2. Temperature distribution increases for large values of  $\beta$ . The increase in parameter of  $\beta$  corresponds to larger relaxation time which provides resistance to the fluid motion, hence as a result more heat is produced. Therefore, temperature distribution increases.

The influence of velocity slip,  $b$  on the velocity and temperature is delineated in Figures 6.3 and 6.4, respectively. To avoid the crowded plots, both distributions are separated in two figures. The stretching of the sheet causes a descend in the fluid flow, so the velocity of the fluid becomes lessen with the rise of velocity slip as the distance  $\eta$  increase from 0 to 2, but slightly increase from the surface of the sheet in the boundary layer. Physically, with the enhanced velocity slip, as a consequence of decrease in the tendency of fluid to remove the heat away from the plate, there is a rise in temperature profile.

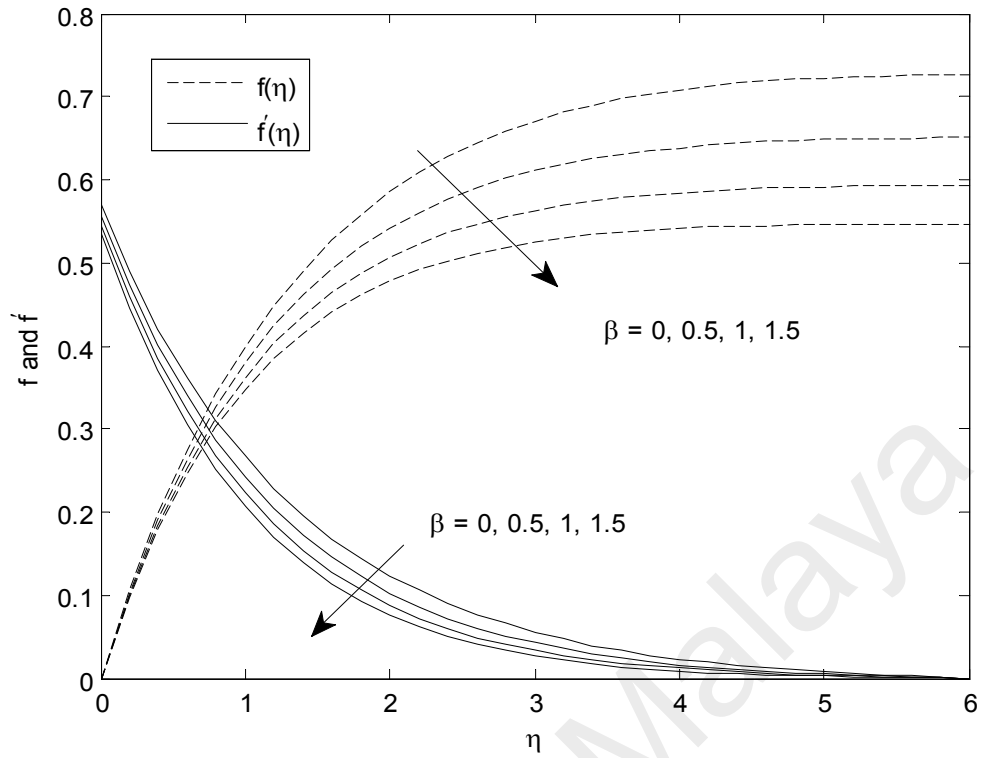


**Figure 6.1:** Profiles of  $f(\eta)$  and  $f'(\eta)$  for different values of  $\beta$  when  $\gamma = \text{Pr} = b = 1$ ,  $m = 256$  and  $L = 6$

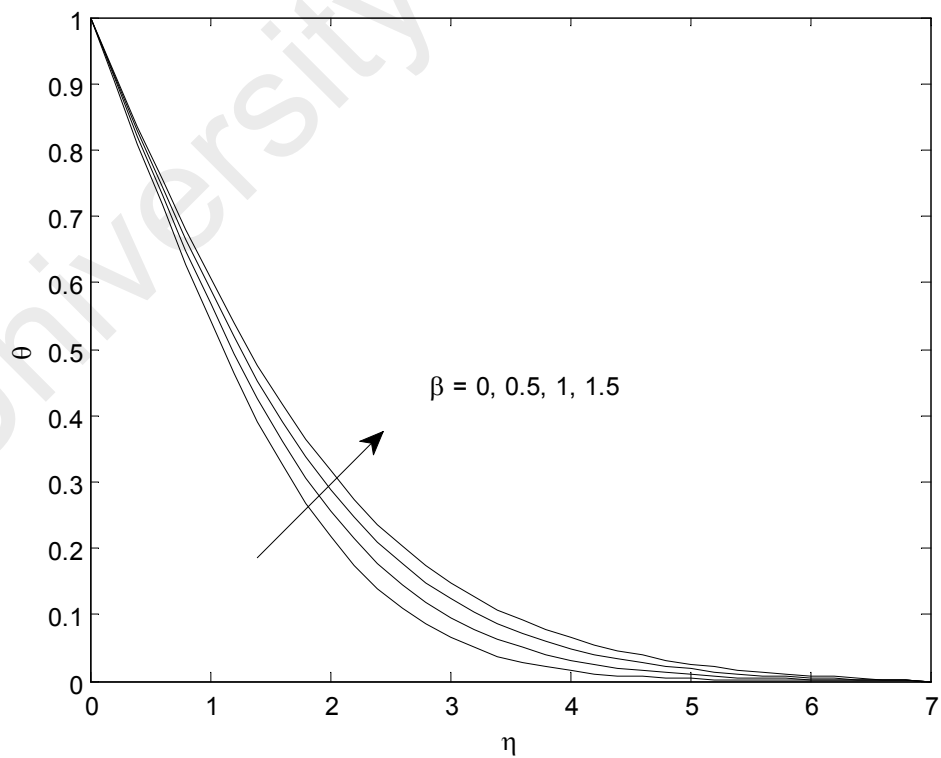


**Figure 6.2:** Profiles of  $\theta(\eta)$  for different values of  $\beta$  when  $\gamma = \text{Pr} = b = 1$ ,  $m = 256$ , and  $L = 7$

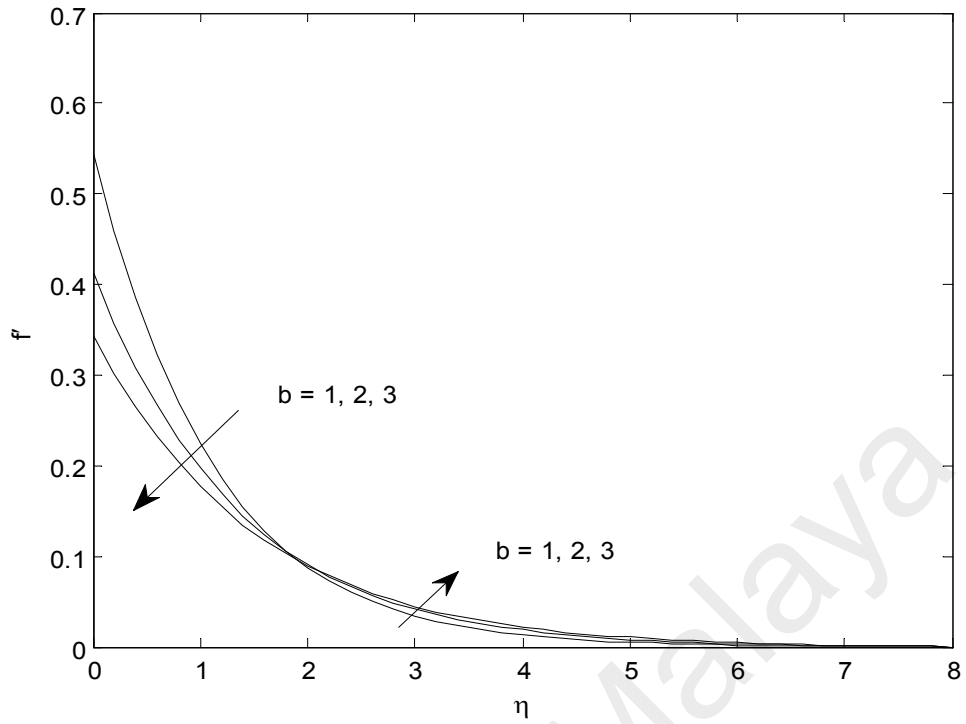


**Figure 6.3:** Profiles of  $f'(\eta)$  for different values of  $b$  when  $\gamma = \text{Pr} = \beta = 1$ ,  $m = 256$  and  $L = 8$

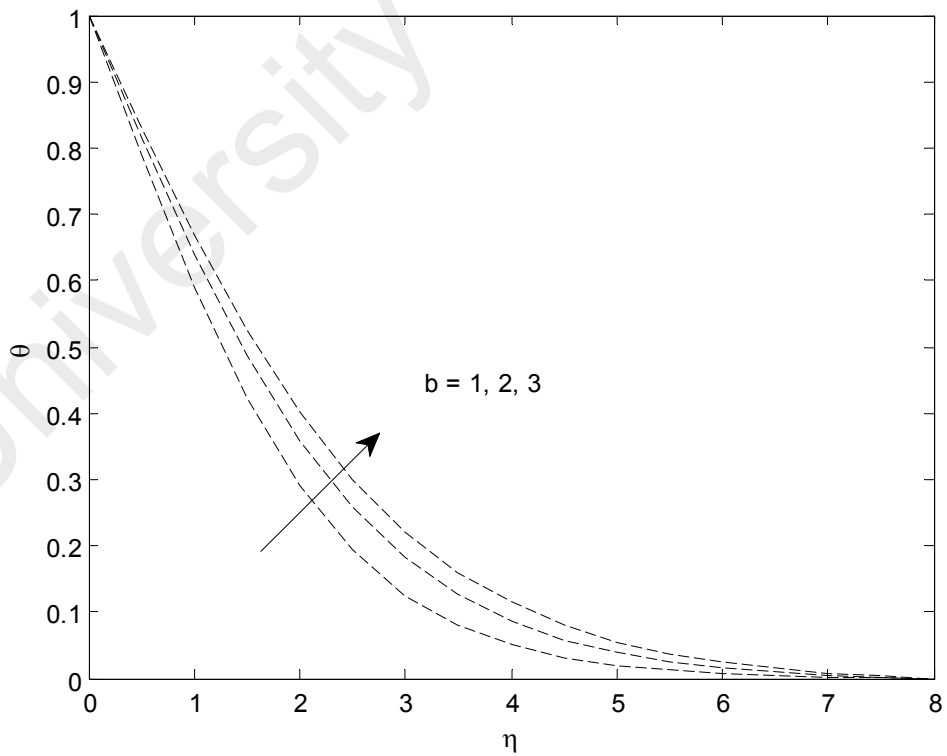


**Figure 6.4:** Profiles of  $\theta(\eta)$  for different values of  $b$  when  $\gamma = \text{Pr} = \beta = 1$ ,  $m = 256$ , and  $L = 8$

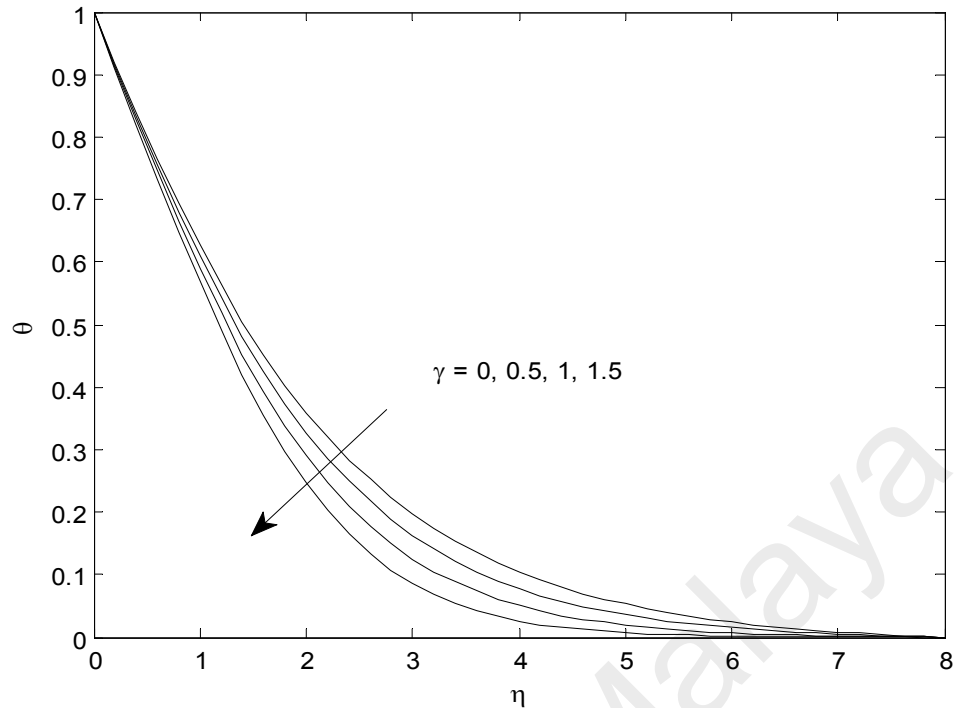


**Figure 6.5:** Profiles of  $\theta(\eta)$  for different values of  $\gamma$  when  $\beta = b = \text{Pr} = 1$ ,  $m = 256$  and  $L = 8$

The Cattaneo-Christov heat flux model is a modified version of the classical Fourier's law that takes into account of thermal relaxation time (Christov, 2009). The impact of non-dimensional heat flux relaxation time  $\gamma$  on temperature can be explained through Figure 6.5. Temperature distribution is a decreasing function of thermal relaxation parameter. It is also analyzed that thermal boundary layer thickness decreases. This due to the fact that as the thermal relaxation parameter increased, particles of the material require more time to transfer heat to its neighboring particles. In other words, a non-conducting behaviour showed by the higher values of thermal relaxation parameter material is responsible in reduction of temperature distribution. Further, it is also noticed that the thermal boundary layer thickness is larger for the classical Fourier's law when the heat transfers instantly throughout the material ( $\gamma = 0$ ) as compared to the Cattaneo-Christov heat flux model.

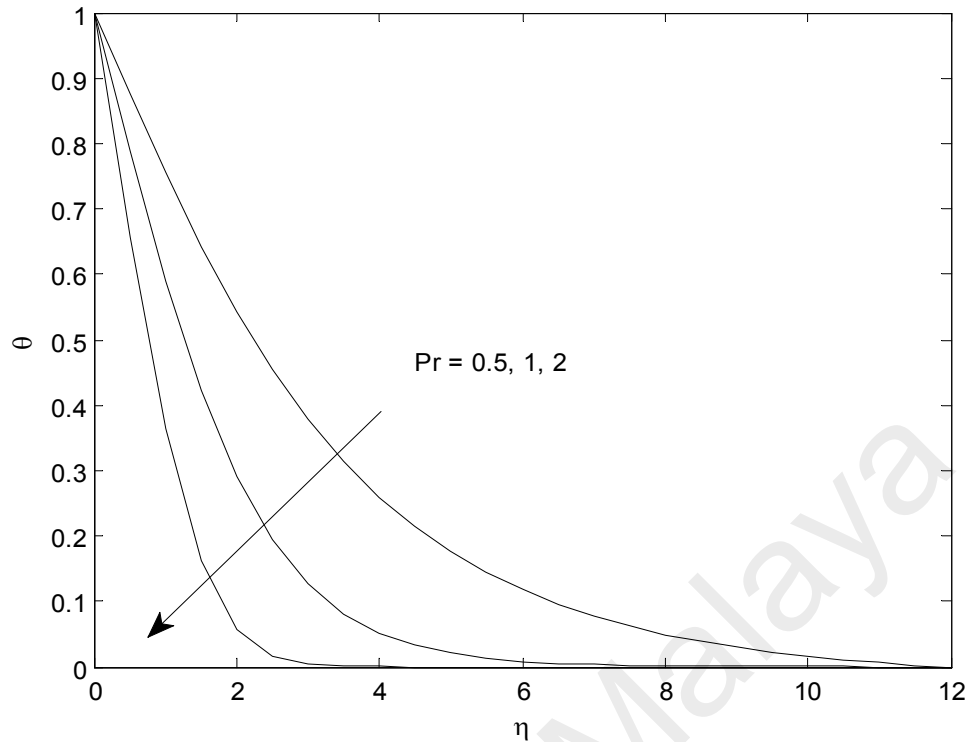


**Figure 6.6:** Profiles of  $\theta(\eta)$  for different values of Pr when  $\beta = b = \gamma = 1$ ,  $m = 256$  and  $L = 12$

Figure 6.6 reveals the effects of Pr on energy boundary. It can be seen that temperature profile as well as thermal boundary layer thickness decrease when Pr is increased. An increase in Pr corresponds to a decrease in thermal diffusivity and hence thinner thermal boundary layer exists for larger Prandtl number fluid.

In order to validate the numerical method used in this work, the elasticity number ( $\beta = 0$ ), heat flux relaxation time ( $\gamma = 0$ ) and slip coefficient ( $b = 0$ ) are considered in Tables 6.1 and 6.2. The results obtained by HWQM are then compared with some previous literature and good agreement is found between these results.

Tables 6.3 and 6.4 contain the numerical values of  $f''(0)$  and  $\theta'(0)$ , respectively for different values of elasticity number,  $\beta$  and non-dimensional heat flux relaxation time,  $\gamma$ . We found that magnitude of  $\theta'(0)$  is directly proportional to the parameter  $\gamma$ . However, it has inverse relationship with the viscoelastic fluid parameter  $\beta$ .

**Table 6.1:** Comparison the values of  $-f''(0)$  between exact solution and HWQM at  $\beta = 0$ ,  $b = 0$ ,  $m = 512$  and  $L = 6$

Exact solution (Magyari & Keller, 2000)	HWQM (Present)
1.0000000	1.0004761

**Table 6.2:** Comparison of local Nusselt number  $-\theta'(0)$  in the case of Newtonian fluid ( $\beta = \gamma = b = 0$ ) with  $m = 512$  and  $L = 6$  for different values of Pr

Pr	Wang (1989)	Gorla and Sidawi (1994)	Khan and Pop (2010)	Malik et al. (2017)	HWQM (Present)
0.70	0.4539	0.5349	0.4539	0.45392	0.453930
2.00	0.9114	0.9114	0.9113	0.91135	0.911345
7.00	1.8954	1.8905	1.8954	1.89543	1.895489
20.0	3.3539	3.3539	3.3539	3.35395	3.353905

**Table 6.3:** The values of HWQM for  $-f''(0)$  with different values of  $\beta$  when Pr = 1,  $b = 1$ ,  $\gamma = 0.1$ ,  $m = 512$  and  $L = 6$

$\beta$	$-f''(0)$
0.10	0.43355
0.15	0.43498
0.20	0.43638
0.30	0.43912
0.50	0.44436

**Table 6.4:** The values of HWQM for  $-\theta'(0)$  with different values of  $\beta$  and  $\gamma$  when  $Pr = 1$ ,  $b = 1$ ,  $m = 512$  and  $L = 6$

$\gamma$	$-\theta'(0)$				
	$\beta = 0.1$	$\beta = 0.15$	$\beta = 0.2$	$\beta = 0.3$	$\beta = 0.5$
0.1	0.44409	0.44211	0.44018	0.43640	0.42925
0.4	0.45242	0.45025	0.44811	0.44396	0.43611
0.5	0.45558	0.45332	0.45111	0.44681	0.43869
0.6	0.45893	0.45659	0.45430	0.44985	0.44144
0.8	0.46624	0.46372	0.46126	0.45647	0.44745
1.0	0.47434	0.47164	0.46899	0.46385	0.45416

## 6.2 Convective Heat Transfer in Maxwell Fluid with Cattaneo-Christov Heat Flux Model Past a Stretching Sheet in the Presence of Suction and Injection

### 6.2.1 Introduction

This problem is extended from Section 6.1 to the case where the presence of suction and injection parameters are taken into account. Related to this presence, Vajravelu (1994) has analyzed the convection flow and heat transfer of a viscous fluid near an infinite, porous and vertical stretching surface by using variable size finite difference method. Muthucumaraswamy (2002) studied the effects of suction on heat and mass transfer along a moving vertical surface in the presence of chemical reaction. El-Arabawy (2009) investigated the effects of suction/injection and chemical reaction on mass transfer over a stretching surface. Elbashaeshy and Bazid (2004) have analyzed the effect of internal heat generation and suction or injection on the heat transfer in a porous medium over a stretching surface. Sultana et al. (2009) discussed the effects of internal heat generation, radiation and suction or injection on the heat transfer in a porous medium over a stretching surface. Rajeswari et al. (2009) studied the effect of chemical reaction, heat

and mass transfer on nonlinear MHD boundary layer flow through vertical porous surface with heat source in the presence of suction. Elbashbeshy et al. (2011) used Runge-Kutta technique to study the effects of suction/injection and variable chemical reaction on mass transfer characteristics over unsteady stretching surface embedded in porous medium.

To the best of our knowledge, no attempt has been made to analyze the effects of both temperature and velocity on the steady, two dimensional, incompressible, laminar flow of Maxwell fluid past a stretching sheet in the presence of suction by using HWQM. The impact of various physical parameters (such as fluid relaxation time, thermal relaxation time, the suction or injection parameter, Pr) on the velocity and temperature profiles is displayed in the form of tables and graphs.

### 6.2.2 Problem Formulation

Consider the steady, two dimensional, incompressible, laminar flow of Maxwell fluid past a stretching sheet with suction. The heat transfer process is studied through the Cattaneo-Christov heat flux theory. In the absence of the gradient of pressure, the governing equations expressing conservation of mass, momentum and energy are given as,

$$\frac{\partial u}{\partial x} + \frac{\partial v}{\partial y} = 0, \quad (6.27)$$

$$u \frac{\partial u}{\partial x} + v \frac{\partial u}{\partial y} + \lambda_1 \left( u^2 \frac{\partial^2 u}{\partial x^2} + v^2 \frac{\partial^2 u}{\partial y^2} + 2uv \frac{\partial^2 u}{\partial x \partial y} \right) = \nu \frac{\partial^2 u}{\partial y^2}, \quad (6.28)$$

$$u \frac{\partial T}{\partial x} + v \frac{\partial T}{\partial y} + \lambda_2 \left( u \frac{\partial u}{\partial x} \frac{\partial T}{\partial x} + v \frac{\partial v}{\partial y} \frac{\partial T}{\partial y} + u \frac{\partial v}{\partial x} \frac{\partial T}{\partial y} + v \frac{\partial u}{\partial y} \frac{\partial T}{\partial x} + 2uv \frac{\partial^2 T}{\partial x \partial y} + u^2 \frac{\partial^2 T}{\partial x^2} + v^2 \frac{\partial^2 T}{\partial y^2} \right) = \alpha \frac{\partial^2 T}{\partial y^2}, \quad (6.29)$$

where  $u$  and  $v$  denote the velocity components along the  $x$ - and  $y$ - directions,

respectively.  $\nu$  is the kinematic viscosity,  $\lambda_1$  is the fluid relaxation time,  $\lambda_2$  is the thermal relaxation time,  $T$  is temperature of the Maxwell fluid and  $\alpha = k / \rho c_p$  is thermal diffusivity, where  $k$  is the thermal conductivity.

The boundary conditions in the present problem are,

$$\begin{aligned} u &= ax, \quad v = v_0, \quad T = T_w \quad \text{at } y = 0, \\ u &\rightarrow 0, \quad T \rightarrow T_\infty \quad \text{as } y \rightarrow \infty. \end{aligned} \quad (6.30)$$

The similarity transformations for Equations (6.28) and (6.29) are as follows,

$$\begin{aligned} \psi &= x\sqrt{av}f(\eta), \quad \eta = y\sqrt{\frac{a}{v}}, \\ u &= axf'(\eta), \quad v = -\sqrt{av}f(\eta), \\ \theta &= \frac{T - T_\infty}{T_w - T_\infty}, \end{aligned} \quad (6.31)$$

where the stream function  $\psi$  is defined by  $u = \partial\psi / \partial y$  and  $v = -\partial\psi / \partial x$ , and  $\theta$  is the dimensionless temperature, thus the continuity Equation (6.27) is satisfied automatically.

In the above and behind equations, the prime denotes the derivative with respect to  $\eta$ . Substituting Equations (6.31) into (6.28) - (6.30), a set of ordinary differential equations with variable coefficients is given by

$$f''' - f'^2 + ff'' + \beta(2ff'f'' - f^2f''') = 0, \quad (6.32)$$

and

$$\frac{1}{\text{Pr}}\theta'' + f\theta' - \gamma(ff'\theta' + f^2\theta'') = 0. \quad (6.33)$$

In the above equations,  $\beta = \lambda_1 a$  is the Deborah number in terms of relaxation time,  $\gamma = \lambda_2 a$  is the non-dimensional thermal relaxation time, where  $a$  is a positive constant. Pr is given as  $\text{Pr} = \nu / \alpha$ , where  $\nu$  is the velocity component along  $y$ -direction and  $\alpha$  is thermal diffusivity.

The boundary conditions for Equations (6.32) and (6.33) are given as

$$\begin{aligned} f &= f_w, \quad f' = 1, \quad \theta = 1 \quad \text{at } \eta = 0, \\ f' &\rightarrow 0, \quad \theta \rightarrow 0 \quad \text{as } \eta \rightarrow \infty, \end{aligned} \quad (6.34)$$

where  $f_w = -\frac{v_w}{\sqrt{c\nu}}$  is the suction parameter. Note that  $f_w > 0$  corresponds to suction,

$f_w < 0$  corresponds to injection and  $f_w = 0$  is impermeable surface.

### 6.2.3 Numerical Solution

Quasilinearization technique is applied to (6.32) and (6.33) implies

$$\begin{aligned} f_{r+1}''' &- \frac{1}{1 - \beta f_r^2} (2f_r' f_{r+1}' - 2\beta f_r f_r'' f_{r+1}' - f_r f_{r+1}'' - 2\beta f_r f_r' f_{r+1}'') \\ &- \frac{1}{(1 - \beta f_r^2)^2} (2\beta f_r f_r'^2 f_{r+1} - \beta f_r^2 f_r'' f_{r+1}' - 2\beta f_r' f_r'' f_{r+1}' \\ &- f_r'' f_{r+1}' - 2\beta^2 f_r^2 f_r' f_r'' f_{r+1}') \\ &= \frac{1}{1 - \beta f_r^2} (-f_r'^2 + 2\beta f_r f_r' f_r'') + \frac{1}{(1 - \beta f_r^2)^2} (-2\beta f_r^2 f_r'^2 \\ &+ \beta f_r^3 f_r'' + 2\beta f_r f_r' f_r'' + f_r f_r'' + 2\beta^2 f_r^3 f_r' f_r''), \end{aligned} \quad (6.35)$$

and

$$\begin{aligned} \theta_{r+1}'' &+ \frac{1}{1 - \text{Pr} \gamma f_r^2} (\text{Pr} f_r \theta_{r+1}' - \text{Pr} \gamma f_r f_r' \theta_{r+1}' - \text{Pr} \gamma f_r \theta_r' f_{r+1}') \\ &+ \frac{1}{(1 - \text{Pr} \gamma f_r^2)^2} (-\text{Pr} \gamma f_r' \theta_r' f_{r+1}' - \text{Pr}^2 \gamma^2 f_r^2 f_r' \theta_r' f_{r+1}' \\ &+ \text{Pr} \theta_r' f_{r+1}' + \text{Pr}^2 \gamma f_r^2 \theta_r' f_{r+1}') \\ &= \frac{1}{1 - \text{Pr} \gamma f_r^2} (-\text{Pr} \gamma f_r f_r' \theta_r') + \frac{1}{(1 - \text{Pr} \gamma f_r^2)^2} (\text{Pr} \theta_r' f_r \\ &+ \text{Pr}^2 \gamma f_r^3 \theta_r' - \text{Pr} \gamma f_r f_r' \theta_r' - \text{Pr}^2 \gamma^2 f_r^3 f_r' \theta_r'), \end{aligned} \quad (6.36)$$

respectively. The boundary conditions are

$$\begin{aligned} f_{r+1} &= f_w, \quad f_{r+1}' = 1, \quad \theta_{r+1} = 1 \quad \text{at } \eta = 0, \\ f_{r+1}' &\rightarrow 0, \quad \theta_{r+1} \rightarrow 0 \quad \text{as } \eta \rightarrow \infty. \end{aligned} \quad (6.37)$$

Now, we apply the Haar wavelet method to Equations (6.35) and (6.36). The lower order derivatives are obtained by integrating Equations (5.14) and (5.15) and use the

boundary conditions (6.37),

$$f_{r+1}''(\eta) = \sum_{i=0}^{m-1} a_i \left( p_{i,1}(\eta) - \frac{1}{L} p_{i,2}(L) \right) - \frac{1}{L}, \quad (6.38)$$

$$f_{r+1}'(\eta) = \sum_{i=0}^{m-1} a_i \left( p_{i,2}(\eta) - \frac{\eta}{L} p_{i,2}(L) \right) - \frac{\eta}{L} + 1, \quad (6.39)$$

$$f_{r+1}(\eta) = \sum_{i=0}^{m-1} a_i \left( p_{i,3}(\eta) - \frac{\eta^2}{2L} p_{i,2}(L) \right) - \frac{\eta^2}{2L} + \eta + f_w, \quad (6.40)$$

$$\theta_{r+1}'(\eta) = \sum_{i=0}^{m-1} b_i \left( p_{i,1}(\eta) - \frac{1}{L} p_{i,2}(L) \right) - \frac{1}{L}, \quad (6.41)$$

$$\theta_{r+1}(\eta) = \sum_{i=0}^{m-1} b_i \left( p_{i,2}(\eta) - \frac{\eta}{L} p_{i,2}(L) \right) - \frac{\eta}{L} + 1. \quad (6.42)$$

Substitute Equations (6.38) - (6.42) and higher order derivatives into Equations (6.35) and (6.36), we obtain

$$\sum_{i=0}^{m-1} a_i K_1 = L_1, \quad (6.43)$$

and

$$\sum_{i=0}^{m-1} a_i K_2 + \sum_{i=0}^{m-1} b_i K_3 = L_2, \quad (6.44)$$

where

$$\begin{aligned} K_1 = & h_i(\eta) - \frac{1}{1 - \beta f_r^2} \left[ 2(f_r' - \beta f_r f_r'') p_{i,2}(\eta) - f_r(1 + 2\beta f_r') p_{i,1}(\eta) \right. \\ & \left. - \frac{2}{L} \left( \eta f_r' - \beta \eta f_r f_r'' - \frac{1}{2} f_r - \beta f_r f_r' \right) p_{i,2}(L) \right] \\ & - \frac{1}{(1 - \beta f_r^2)^2} \left[ 2\beta \left( f_r f_r'^2 - \frac{1}{2\beta} f_r'' - \frac{1}{2} f_r^2 f_r'' - f_r' f_r'' - \beta f_r^2 f_r' f_r'' \right) p_{i,3}(\eta) \right. \\ & \left. + \frac{1}{L} \eta^2 \left( -\beta f_r f_r'^2 + \frac{1}{2} f_r'' + \beta f_r^2 f_r'' + \beta f_r' f_r'' + \beta^2 f_r^2 f_r' f_r'' \right) p_{i,2}(L) \right], \end{aligned}$$

$$\begin{aligned}
K_2 &= \frac{1}{1 - \Pr \gamma f_r^2} \left[ \Pr \gamma f_r \theta_r' \left( -p_{i,2}(\eta) + \frac{1}{L} \eta p_{i,2}(L) \right) \right] \\
&\quad + \frac{1}{(1 - \Pr \gamma f_r^2)^2} \left[ \Pr \theta_r' (1 + \Pr \gamma f_r^2 - \gamma f_r' - \Pr \gamma^2 f_r^2 f_r') p_{i,3}(\eta) \right. \\
&\quad \left. + \frac{\Pr}{2L} \eta^2 \theta_r' (-1 - \Pr \gamma f_r^2 + \gamma f_r' + \Pr \gamma^2 f_r^2 f_r') p_{i,2}(L) \right], \\
K_3 &= h_i(\eta) + \frac{1}{1 - \Pr \gamma f_r^2} \left[ \Pr f_r (1 - \gamma f_r') p_{i,1}(\eta) - \frac{1}{L} \Pr f_r (1 - \gamma f_r') p_{i,2}(L) \right], \\
L_1 &= \frac{1}{1 - \beta f_r^2} \left[ 2 \left( -\frac{1}{2} f_r'^2 + \beta f_r f_r' f_r'' - \frac{1}{L} \eta f_r' + f_r' - \beta f_r f_r'' + \frac{1}{2L} f_r \right) \right. \\
&\quad \left. + \frac{2\beta}{L} (\eta f_r f_r'' + f_r f_r') \right] + \frac{1}{(1 - \beta f_r^2)^2} \left[ 2\beta f_r \left( -f_r f_r'^2 + \frac{1}{2\beta} f_r'' \right) \right. \\
&\quad \left. + \frac{1}{2} f_r^2 f_r'' + f_r' f_r'' + \beta f_r^2 f_r' f_r'' - \frac{1}{2L} \eta^2 f_r'^2 + \eta f_r'^2 + f_w f_r'^2 \right. \\
&\quad \left. + \frac{1}{4L} \eta^2 f_r f_r'' - \frac{1}{2} \eta f_r f_r'' - \frac{1}{2} f_w f_r f_r'' + \frac{\beta}{2L} \eta^2 f_r f_r' f_r'' - \beta \eta f_r f_r' f_r'' \right. \\
&\quad \left. - \beta f_w f_r f_r' f_r'' \right) + \eta f_r'' \left( \frac{1}{2L} \eta - 1 - \frac{f_w}{\eta} + \frac{\beta}{L} \eta f_r' - 2\beta f_r' - \frac{2\beta f_w}{\eta} f_r' \right), \\
L_2 &= \frac{1}{1 - \Pr \gamma f_r^2} \left[ \Pr \gamma f_r \left( -f_r' \theta_r' + \frac{1}{L\gamma} - \frac{1}{L} f_r' - \frac{1}{L} \eta \theta_r' + \theta_r' \right) \right] \\
&\quad + \frac{1}{(1 - \Pr \gamma f_r^2)^2} \left[ \Pr f_r \theta_r' (1 + \Pr \gamma f_r^2 - \gamma f_r' - \Pr \gamma^2 f_r^2 f_r') \right. \\
&\quad \left. + \frac{1}{2L} \Pr \gamma \eta^2 f_r - \Pr \gamma \eta f_r - \Pr \gamma f_w f_r - \frac{1}{2L} \Pr \gamma^2 \eta^2 f_r f_r' \right. \\
&\quad \left. + \Pr \gamma^2 \eta f_r f_r' + \Pr \gamma^2 f_w f_r f_r' \right) + \Pr \eta \theta_r' \left( \frac{1}{2L} \eta - 1 - \frac{1}{\eta} f_w \right. \\
&\quad \left. - \frac{1}{2L} \gamma \eta f_r' + \gamma f_r' + \frac{1}{\eta} \gamma f_w f_r' \right) \right].
\end{aligned}$$

The Equations (6.43) and (6.44) can be solved simultaneously to obtain Haar coefficients,  $a_i$  and  $b_i$ . We chose the initial approximation which satisfy the boundary conditions (6.37) as follow

$$f_0(\eta) = f_w + 1 - e^{-\eta} \quad (6.45)$$

and

$$\theta_0(\eta) = e^{-\eta}. \quad (6.46)$$

In the next section, by using the above method, the detailed results of numerical simulation will be given to show the impact of various physical parameters on  $f''(0)$ ,  $\theta'(0)$ ,  $f'(\eta)$  and  $\theta(\eta)$ .

#### 6.2.4 Results and Discussion

More detailed results are shown in Tables 6.5 - 6.9, which reflects the effect of each parameter on both  $f''(0)$  and  $\theta'(0)$ . And also Figures 6.7 - 6.10 are shown to illustrate the effects of various physical parameters on the velocity and temperature profiles.

Table 6.5 depicts the validation of the present result by comparing with the published result by Magyari and Keller (2000) under some special and limited case where the elasticity number,  $\beta = 0$  with different values of  $f_w$ . We found a favourable agreement of the present result with the published result.

**Table 6.5:** Comparison the values of  $-f''(0)$  between exact solution and HWQM for different values of  $f_w$  at  $\beta = 0$ ,  $Pr = 1$ ,  $L = 5$ ,  $\gamma = 0.1$  and  $m = 512$

$f_w$	Exact solution (Magyari & Keller, 2000)	HWQM (Present)
-1.5	0.5000000	0.5001199
0.0	1.0000000	1.0001623
1.0	1.6180340	1.6180203
1.5	2.0000000	1.9999694

**Table 6.6:** The values of HWQM for  $-f''(0)$  with different values of  $\beta$  when  $Pr = 1, L = 5, f_w = 0, \gamma = 0.1$  and  $m = 512$

$\beta$	$-f''(0)$
0.10	1.02653
0.15	1.03939
0.20	1.05214
0.50	1.12634
0.80	1.19676
1.00	1.24178

**Table 6.7:** The values of HWQM for  $-\theta'(0)$  with different values of  $\beta$  and  $\gamma$  when  $Pr = 1, L = 5, f_w = 0$  and  $m = 512$

$\gamma$	$-\theta'(0)$					
	$\beta = 0.1$	$\beta = 0.15$	$\beta = 0.2$	$\beta = 0.5$	$\beta = 0.8$	$\beta = 1.0$
0.1	0.58379	0.57983	0.57593	0.55398	0.53439	0.52253
0.4	0.61014	0.60554	0.60101	0.57555	0.55293	0.53931
0.5	0.61998	0.61516	0.61042	0.58371	0.55996	0.54567
0.6	0.63029	0.62526	0.62031	0.59234	0.56742	0.55244
0.8	0.65215	0.64673	0.64138	0.61098	0.58368	0.56721
1.0	0.67551	0.66972	0.66400	0.63130	0.60165	0.58364

Tables 6.6 and 6.7 show the values of  $f''(0)$  and  $\theta'(0)$  for various values of heat flux relaxation parameter,  $\gamma$ . From Table 6.6, it is indicated that  $f''(0)$  decreases with the increase in the values of elasticity number,  $\beta$ . The value of  $\gamma$  is keep fix at 0.1 since no effect of changing the value of heat flux relaxation because Equation (6.32) does not has a direct impact on  $\gamma$ .

Table 6.7 shows the values of  $\theta'(0)$  decreases with the increase of heat flux relaxation, but it tends to increase with the enhanced of elasticity number, which is opposite to the effect on  $f''(0)$ . Tables 6.8 and 6.9 are for examining  $f''(0)$  and

$\theta'(0)$  for different values of suction/injection parameter,  $f_w$  and elasticity number,  $\beta$  when  $Pr = 1, \gamma = 0.5, L = 5$  and  $m = 512$ . These tables clearly present that  $f''(0)$  and  $\theta'(0)$  are reduced as parameter of  $f_w$  increases.

**Table 6.8:** The values of HWQM for  $-f''(0)$  and  $-\theta'(0)$  with different values of  $\beta$  and  $f_w$  (impermeable surface and suction) when  $Pr = 1, \gamma = 0.5, L = 5$  and  $m = 512$

$f_w$	$\beta = 0.1$		$\beta = 0.2$		$\beta = 0.3$	
	$-f''(0)$	$-\theta'(0)$	$-f''(0)$	$-\theta'(0)$	$-f''(0)$	$-\theta'(0)$
0	1.02653	0.61998	1.05271	0.61061	1.07776	0.60177
0.2	1.15770	0.79129	1.20962	0.77715	1.26184	0.76338
0.3	1.23064	0.89891	1.30056	0.88164	1.37188	0.86469
0.5	1.39442	1.18255	1.51424	1.15696	1.64127	1.13124
0.6	1.48644	1.37604	1.64070	1.34471	1.80853	1.31269

**Table 6.9:** The values of HWQM for  $-f''(0)$  and  $-\theta'(0)$  with different values of  $\beta$  and  $f_w$  (injection) when  $Pr = 1, \gamma = 0.5, L = 5$  and  $m = 512$

$f_w$	$\beta = 0.1$		$\beta = 0.2$		$\beta = 0.3$	
	$-f''(0)$	$-\theta'(0)$	$-f''(0)$	$-\theta'(0)$	$-f''(0)$	$-\theta'(0)$
-1.0	0.59764	0.16047	0.57485	0.16186	0.55080	0.16331
-0.6	0.73351	0.29864	0.72106	0.29788	0.70828	0.29715
-0.5	0.77402	0.33953	0.76537	0.33788	0.75644	0.33629
-0.3	0.86440	0.43362	0.86568	0.42964	0.86665	0.42582
-0.2	0.91476	0.48852	0.92258	0.48306	0.93003	0.47783

Figure 6.7 depicts the effects of non-dimensional heat flux relaxation time,  $\gamma$  on velocity field and temperature field. As can be seen from this profile, as the distance  $\eta$  increase from 0, there is no effect of changing the values of  $\gamma$  on the velocity. Meanwhile the temperature monotonically decreasing tends to 0. The temperature and

the temperature boundary layer thickness decrease with the increase of  $\gamma$ , and simultaneously the temperature gradient increases. So, the heat transfer rate of surface increases.

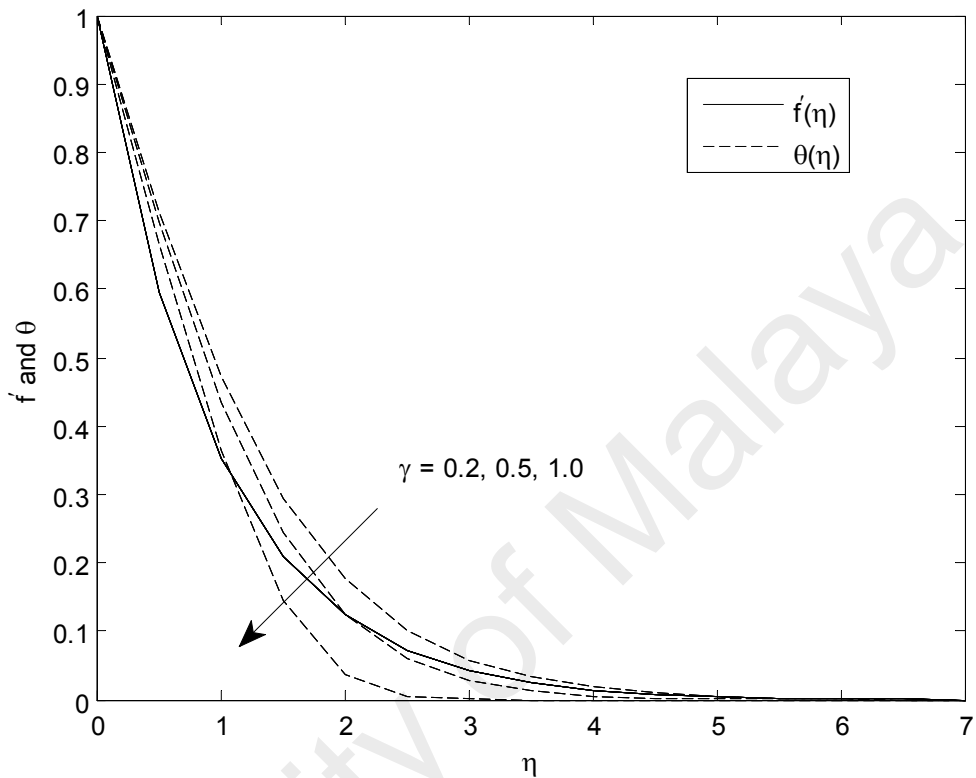


**Figure 6.7:** Velocity and temperature profiles for different values of  $\gamma$  when  $f_w = 0$ ,  $m = 512$ ,  $L = 7$ ,  $Pr = 1$  and  $\beta = 0.1$

Figure 6.8 exhibits the velocity and the temperature profiles for different values of elasticity number  $\beta$ . As  $\beta$  increases, the velocity of the fluid decreases to 0. However, when the parameter  $\beta$  is very small, the temperature decreases to 0 as the distance  $\eta$  increases from 0. The decrease in the values of  $\beta$  has the tendency to decrease the temperature and thermal boundary layer thickness but increase the temperature gradient.

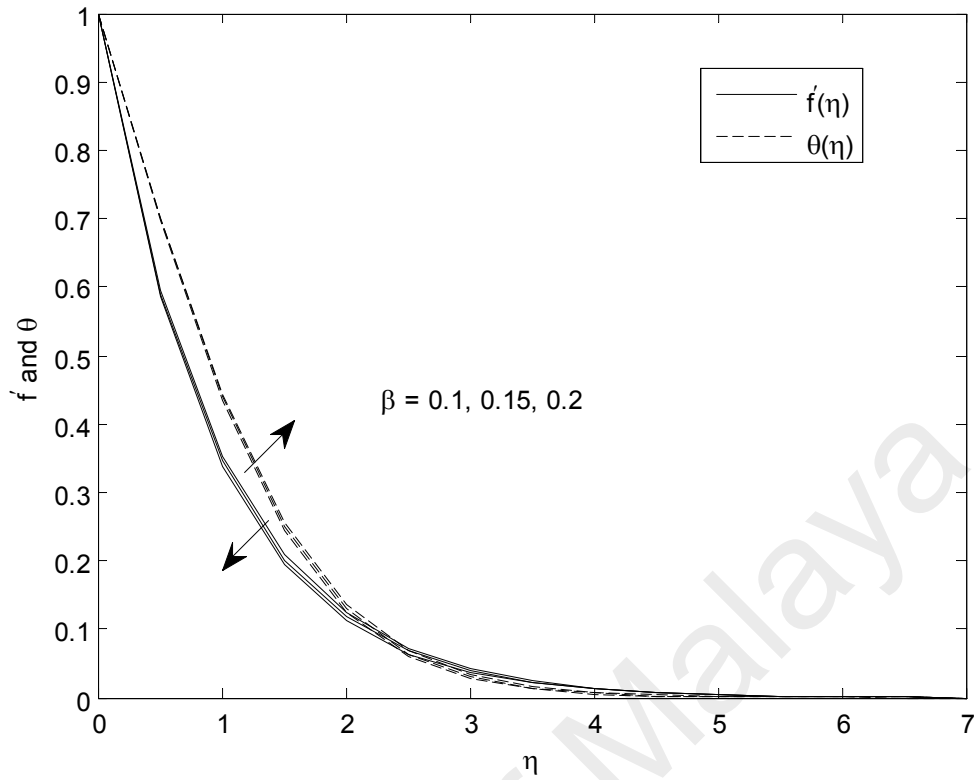


**Figure 6.8:** Velocity and temperature profiles for different values of  $\beta$  when  $f_w = 0$ ,  $m = 512$ ,  $L = 7$ ,  $Pr = 1$  and  $\gamma = 0.5$

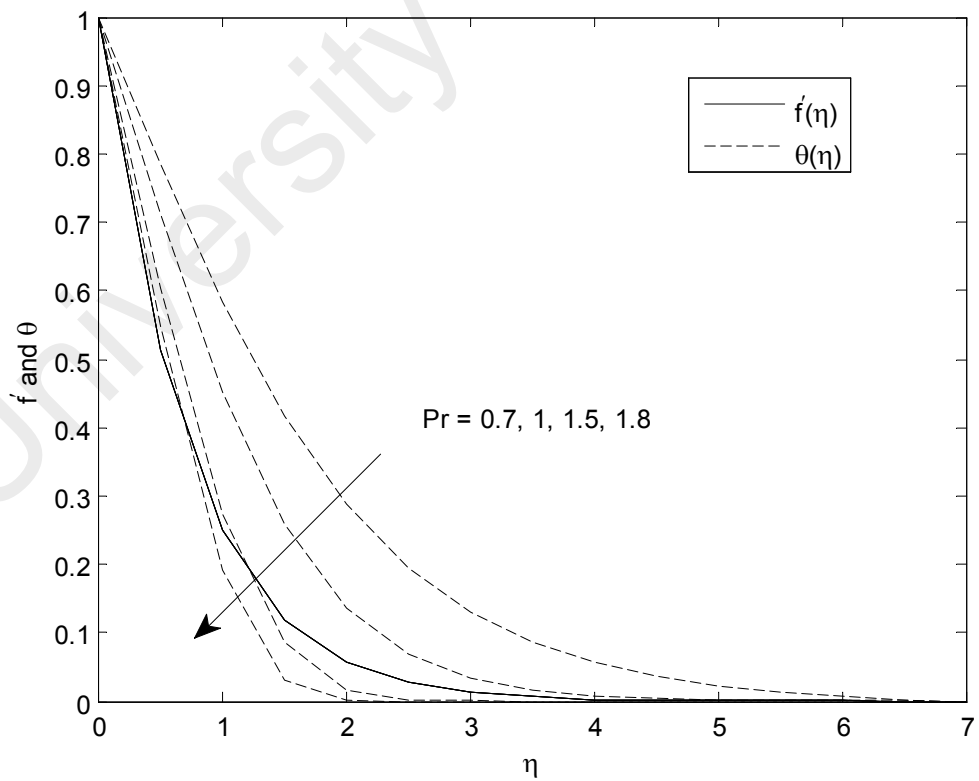


**Figure 6.9:** Velocity and temperature profiles for different values of  $Pr$  when  $f_w = 0$ ,  $m = 512$ ,  $\beta = \gamma = 1$  and  $L = 7$

Figure 6.9 represents the variation of both the velocity and temperature profiles in response to a change in Pr. The graph depicts that there is no effect of changing Pr on  $f'(\eta)$ . But, the temperature decrease monotonically to 0 with the increasing of  $\eta$ . In general, it can be seen from Figure 6.9 that the impact of Pr on the temperature field is more noticeable than that on the velocity field. Meanwhile, this phenomenon can be roughly observed from Equation (6.23). Actually, Pr is the coefficient of the temperature and has a direct impact on the temperature. However, the impact of Pr on the velocity is achieved through the coupling various terms, hence the effect may be weakened.

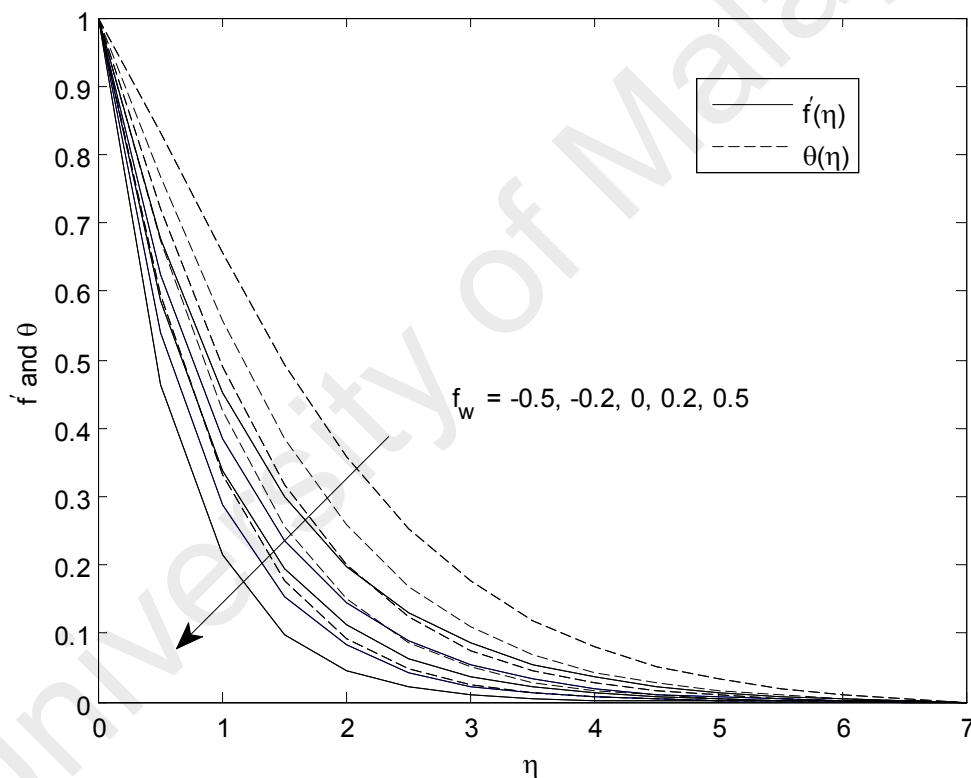


**Figure 6.10:** Velocity and temperature profiles for different values of  $f_w$  when  $m = 512, L = 7, \beta = 0.2, \gamma = 0.1$  and  $Pr = 1$

Figure 6.10 shows the velocity and the temperature profiles with respect to the suction (or injection) parameter,  $f_w$ . The fluid velocity and temperature field are found to decrease with increasing value of  $f_w$ . Suction ( $f_w > 0$ ) causes to decrease the velocity of the fluid in the boundary layer region. This effect acts to decrease the wall

shear stress. On the other hand, increase in suction causes progressive thinning of the boundary layer.

### **6.3 MHD Flow of Cattaneo-Christov Heat Flux Model for Maxwell Fluid Past a Stretching Sheet with Heat Generation/Absorption**

#### **6.3.1 Introduction**

The boundary layer flows induced by a stretching sheet has great importance in the aerodynamic extrusion of plastic sheets, crystal growing, continuous casting, cooling of metallic plate in a bath, glass fiber and paper production, the boundary layer along a liquid film in the condensation process and many others (Vajravelu & Rollins, 1991). Such consideration in the presence of heat transfer has central role in the polymer industry. An exact analytic solution for the two dimensional boundary layer flow of viscous fluid over a linearly stretching surface was firstly presented by Crane (1970).

Later, this problem has been extensively examined through various aspects such as suction/blowing, stretching velocities, magnetohydrodynamics, heat/ mass transfer and so on. Further, the addition of heat generation/absorption term in energy expression is very important in the cases involving underground disposal of radioactive waste material, storage of food stuffs, heat removal from nuclear fuel fragments and packed bed reactors. Some of the studies on such effects can be seen in the work by Vajravelu and Rollins (1991), Zheng et al. (2011), Gireesha et al. (2011), Ramesh et al. (2012), Shehzad et al. (2014) and Cao et al. (2015).

The aim for this section is to propose a mathematical model to study the Cattaneo-Christov heat flux model for Maxwell fluid past a stretching sheet with heat generation/absorption. The impact of heat generation/absorption is incorporated in the energy expression. Another features of this investigation to examine through the aspects

of suction or injection parameter and magnetic field parameter in momentum equation which has not yet been addressed for the Cattaneo-Christov heat flux model.

### 6.3.2 Problem Formulation

Consider the steady, two dimensional, incompressible, laminar flow of Maxwell fluid past a stretching sheet with suction, magnetic and heat generation/absorption. The heat transfer process is studied through the Cattaneo-Christov heat flux theory. In the absence of the gradient of pressure, the governing equations expressing conservation of mass, momentum energy are given as

$$\frac{\partial u}{\partial x} + \frac{\partial v}{\partial y} = 0, \quad (6.47)$$

$$u \frac{\partial u}{\partial x} + v \frac{\partial u}{\partial y} + \lambda_1 \left( u^2 \frac{\partial^2 u}{\partial x^2} + v^2 \frac{\partial^2 u}{\partial y^2} + 2uv \frac{\partial^2 u}{\partial x \partial y} \right) = \nu \frac{\partial^2 u}{\partial y^2} - \frac{\sigma B_0^2}{\rho} u, \quad (6.48)$$

$$u \frac{\partial T}{\partial x} + v \frac{\partial T}{\partial y} + \lambda_2 \left( u \frac{\partial u}{\partial x} \frac{\partial T}{\partial x} + v \frac{\partial v}{\partial y} \frac{\partial T}{\partial y} + u \frac{\partial v}{\partial x} \frac{\partial T}{\partial y} + v \frac{\partial u}{\partial y} \frac{\partial T}{\partial x} + 2uv \frac{\partial^2 T}{\partial x \partial y} + u^2 \frac{\partial^2 T}{\partial x^2} + v^2 \frac{\partial^2 T}{\partial y^2} \right) = \alpha \frac{\partial^2 T}{\partial y^2} + \frac{Q}{\rho c_p} (T - T_\infty), \quad (6.49)$$

where  $u$  and  $v$  denote the velocity components along the  $x$ - and  $y$ - directions, respectively.  $\nu$  is the kinematic viscosity,  $\lambda_1$  is the fluid relaxation time,  $\lambda_2$  is the thermal relaxation time,  $T$  is temperature of the Maxwell fluid,  $\alpha = k / \rho c_p$  is thermal diffusivity, where  $k$  is the thermal conductivity,  $B_0$  is the transverse magnetic field and  $Q_0$  is the heat generation/absorption coefficient.

The boundary conditions in the present problem are,

$$\begin{aligned} u = ax, \quad v = v_w, \quad T = T_w \quad \text{at } y = 0, \\ u \rightarrow 0, \quad T \rightarrow T_\infty \quad \text{as } y \rightarrow \infty. \end{aligned} \quad (6.50)$$

Adopting the suitable transformations as Equation (6.31), the law of conservation of mass is identically satisfied and Equations (6.48) and (6.49) along with the boundary

conditions (6.50) are readily read as ,

$$f''' - f'^2 + ff'' + \beta(2ff'' - f^2 f''') - Mf' = 0, \quad (6.51)$$

and

$$\frac{1}{Pr} \theta'' + f\theta' - \gamma(ff'\theta' + f^2 \theta'') + Q\theta = 0. \quad (6.52)$$

Here,  $\beta = \lambda_1 a$ ,  $\gamma = \lambda_2 a$ ,  $M = \frac{\sigma B_0^2}{\rho a}$ ,  $Q = \frac{Q_0}{\rho c_p a}$  and  $Pr = \frac{\nu}{\alpha}$ , where  $M$  is the magnetic

field parameter and  $Q$  is the heat generation/absorption parameter. The boundary conditions are given as

$$\begin{aligned} f = f_w, \quad f' = 1, \quad \theta = 1 \quad \text{at} \quad \eta = 0, \\ f' \rightarrow 0, \quad \theta \rightarrow 0 \quad \text{as} \quad \eta \rightarrow \infty, \end{aligned} \quad (6.53)$$

where  $f_w = -\frac{v_w}{\sqrt{c\nu}}$  is a suction parameter. In the above equations, the differentiation

with respect to  $\eta$  is represented by primes.

### 6.3.3 Numerical Solution

Quasilinearization technique is applied to Equations (6.51) and (6.52) implies

$$\begin{aligned} f'''_{r+1} - \frac{1}{1 - \beta f_r^2} (2f'_r f'_{r+1} + Mf'_{r+1} - 2\beta f_r f''_r f'_{r+1} - f_r f''_{r+1} - 2\beta f_r f'_r f''_{r+1}) \\ - \frac{1}{(1 - \beta f_r^2)^2} (2\beta f_r f_r'^2 f_{r+1} - f_r'' f_{r+1} - \beta f_r^2 f_r'' f_{r+1} - 2\beta^2 f_r^2 f'_r f_r'' f_{r+1} \\ - 2\beta f'_r f_r'' f_{r+1} + 2M\beta f_r f'_r f_{r+1}) \\ = \frac{1}{1 - \beta f_r^2} (-f_r'^2 + 2\beta f_r f'_r f_r'') + \frac{1}{(1 - \beta f_r^2)^2} (-2\beta f_r^2 f_r'^2 + f_r f_r'' \\ + 2\beta f_r f'_r f_r'' + 2\beta^2 f_r^3 f'_r f_r'' + \beta f_r^3 f_r'' - 2M\beta f_r^2 f'_r), \end{aligned} \quad (6.54)$$

and

$$\begin{aligned}
\theta_{r+1}'' &= \frac{1}{1 - \Pr \gamma f_r^2} \left( -\Pr Q \theta_{r+1} - \Pr f_r \theta_{r+1}' + \Pr \gamma f_r f_r' \theta_{r+1}' + \Pr \gamma f_r \theta_r' f_{r+1}' \right) \\
&= \frac{1}{(1 - \Pr \gamma f_r^2)^2} \left( \Pr^2 \gamma^2 f_r^2 f_r' \theta_r' f_{r+1} - \Pr^2 \gamma f_r^2 \theta_r' f_{r+1} + \Pr \gamma f_r' \theta_r' f_{r+1} \right. \\
&\quad \left. - \Pr \theta_r' f_{r+1} + 2 \Pr^2 \gamma Q f_r \theta_r f_{r+1} \right) \\
&= \frac{1}{1 - \Pr \gamma f_r^2} \left( -\Pr \gamma f_r f_r' \theta_r' \right) + \frac{1}{(1 - \Pr \gamma f_r^2)^2} \left( -\Pr^2 \gamma^2 f_r^3 f_r' \theta_r' \right. \\
&\quad \left. - \Pr \gamma f_r f_r' \theta_r' - 2 \Pr^2 \gamma Q f_r^2 \theta_r + \Pr \theta_r' f_r + \Pr^2 \gamma f_r^3 \theta_r' \right),
\end{aligned} \tag{6.55}$$

respectively. The boundary conditions are

$$\begin{aligned}
f_{r+1} &= f_w, \quad f_{r+1}' = 1, \quad \theta_{r+1} = 1 \quad \text{at} \quad \eta = 0, \\
f_{r+1}' &\rightarrow 0, \quad \theta_{r+1} \rightarrow 0 \quad \text{as} \quad \eta \rightarrow \infty.
\end{aligned} \tag{6.56}$$

Now, we apply the Haar wavelet method to Equations (6.54) and (6.55). The highest order and the boundary conditions for this problem is similar with previous problem.

Hence, the Haar coefficients,  $a_i$  and  $b_i$  are obtained as follow.

$$\sum_{i=0}^{m-1} a_i K_1 = L_1, \tag{6.57}$$

and

$$\sum_{i=0}^{m-1} a_i K_2 + \sum_{i=0}^{m-1} b_i K_3 = L_2, \tag{6.58}$$

where

$$\begin{aligned}
K_1 &= h_i(\eta) - \frac{1}{1 - \beta f_r^2} \left[ (2f_r' - 2\beta f_r f_r'' + M) p_{i,2}(\eta) - f_r (1 + 2\beta f_r') p_{i,1}(\eta) \right. \\
&\quad \left. - \frac{2}{L} \left( \eta f_r' - \beta \eta f_r f_r'' + \frac{1}{2} M \eta - \frac{1}{2} f_r - \beta f_r f_r' \right) p_{i,2}(L) \right] \\
&\quad - \frac{1}{(1 - \beta f_r^2)^2} \left[ 2\beta \left( f_r f_r'^2 - \frac{1}{2\beta} f_r'' - \frac{1}{2} f_r^2 f_r'' - f_r' f_r'' - \beta f_r^2 f_r' f_r'' + M f_r f_r' \right) p_{i,3}(\eta) \right. \\
&\quad \left. + \frac{1}{L} \beta \eta^2 \left( -f_r f_r'^2 + \frac{1}{\beta} f_r'' + \frac{1}{2} f_r^2 f_r'' + f_r' f_r'' + \beta f_r^2 f_r' f_r'' - M f_r f_r' \right) p_{i,2}(L) \right],
\end{aligned}$$

$$\begin{aligned}
K_2 = & \frac{1}{1 - \Pr \gamma f_r^2} \left[ \Pr \gamma f_r \theta_r' \left( -p_{i,2}(\eta) + \frac{1}{L} \eta p_{i,2}(L) \right) \right] \\
& + \frac{1}{(1 - \Pr \gamma f_r^2)^2} \left[ \Pr \theta_r' (1 + \Pr \gamma f_r^2 - \gamma f_r' - \Pr \gamma^2 f_r^2 f_r') p_{i,3}(\eta) \right. \\
& + \frac{\Pr}{2L} \eta^2 \theta_r' (-1 - \Pr \gamma f_r^2 + \gamma f_r' + \Pr \gamma^2 f_r^2 f_r') p_{i,2}(L) \\
& \left. - \Pr^2 \gamma Q f_r \theta_r \left( 2p_{i,3}(\eta) - \frac{1}{L} \eta^2 p_{i,2}(L) \right) \right],
\end{aligned}$$

$$\begin{aligned}
K_3 = & h_i(\eta) + \frac{\Pr}{1 - \Pr \gamma f_r^2} \left( Q p_{i,2}(\eta) - \frac{1}{L} Q \eta p_{i,2}(L) + f_r p_{i,1}(\eta) \right. \\
& \left. - \frac{1}{L} f_r p_{i,2}(L) - \gamma f_r f_r' p_{i,1}(\eta) + \frac{1}{L} \gamma f_r f_r' p_{i,2}(L) \right),
\end{aligned}$$

$$\begin{aligned}
L_1 = & \frac{1}{1 - \beta f_r^2} \left[ f_r' \left( -f_r + 2\beta f_r f_r'' - \frac{2}{L} \eta + 2 + \frac{2\beta}{L} f_r \right) \right. \\
& \left. + \frac{2\beta}{L} \left( \eta f_r f_r'' - L f_r f_r'' - \frac{1}{2\beta} M \eta + \frac{L}{2\beta} M + \frac{1}{2\beta} f_r \right) \right] \\
& + \frac{1}{(1 - \beta f_r^2)^2} \left[ 2\beta \left( -f_r^2 f_r'^2 + \frac{1}{2} f_r^3 f_r'' + f_r f_r' f_r'' + \beta f_r^3 f_r' f_r'' - M f_r^2 f_r' \right. \right. \\
& - \frac{1}{2L} \eta^2 f_r f_r'^2 + \eta f_r f_r'^2 + f_w f_r f_r'^2 + \frac{1}{4L} \eta^2 f_r^2 f_r'' - \frac{1}{2} \eta f_r^2 f_r'' - \frac{1}{2} f_w f_r^2 f_r'' \\
& + \frac{1}{2L} \eta^2 f_r' f_r'' - \eta f_r' f_r'' - f_w f_r' f_r'' + \frac{\beta}{2L} \eta^2 f_r^2 f_r' f_r'' - \beta \eta f_r^2 f_r' f_r'' \\
& \left. \left. - \beta f_w f_r^2 f_r' f_r'' - \frac{1}{2L} M \eta^2 f_r f_r' + M \eta f_r f_r' + M f_w f_r f_r' \right) \right. \\
& \left. + f_r'' \left( f_r + \frac{1}{2L} \eta^2 - \eta - f_w \right) \right],
\end{aligned}$$

$$\begin{aligned}
L_2 = & \frac{\Pr}{1 - \Pr \gamma f_r^2} \left( -\gamma f_r f_r' \theta_r' + \frac{1}{L} Q \eta - Q + \frac{1}{L} f_r - \frac{1}{L} \gamma f_r f_r' - \frac{1}{L} \gamma \eta f_r \theta_r' + \gamma f_r \theta_r' \right) \\
& + \frac{\Pr}{(1 - \Pr \gamma f_r^2)^2} \left( f_r \theta_r' + \Pr \gamma f_r^3 \theta_r' - \gamma f_r f_r' \theta_r' - \Pr \gamma^2 f_r^3 f_r' \theta_r' - 2 \Pr \gamma Q f_r^2 \theta_r' \right. \\
& + \frac{1}{2L} \eta^2 \theta_r' - \eta \theta_r' - f_w \theta_r' + \frac{1}{2L} \Pr \gamma \eta^2 f_r^2 \theta_r' - \Pr \gamma \eta f_r^2 \theta_r' - \Pr \gamma f_w f_r^2 \theta_r' \\
& - \frac{1}{2L} \gamma \eta^2 f_r' \theta_r' + \gamma \eta f_r' \theta_r' + \gamma f_w f_r' \theta_r' - \frac{1}{2L} \Pr \gamma^2 \eta^2 f_r^2 f_r' \theta_r' + \Pr \gamma^2 \eta f_r^2 f_r' \theta_r' \\
& \left. + \Pr \gamma^2 f_w f_r^2 f_r' \theta_r' - \frac{1}{2L} \Pr \gamma Q \eta^2 f_r \theta_r' + 2 \Pr \gamma Q \eta f_r \theta_r' + 2 \Pr \gamma Q f_w f_r \theta_r' \right).
\end{aligned}$$

The Equations (6.57) and (6.58) can be solved simultaneously to obtain Haar coefficients,  $a_i$  and  $b_i$ . The initial approximations are similar as in Equations (6.45) and (6.46).

### 6.3.4 Results and Discussion

In order to validate the Haar wavelet method, ignoring the effects of magnetic field parameter, ( $M = 0$ ) and with  $f_w = 0$  for different values of elasticity number,  $\beta$ , the model in this section for Equations (6.51) and (6.52) are similar as proposed by Sadeghy et al. (2006), Abel et al. (2012), Mukhopadhyay (2012), Megahed (2013) and Abbasi et al. (2016). The comparison of numerical results among them as shown in Tables 6.10 and 6.11 for  $f''(0)$  and  $\theta'(0)$ , respectively. The comparison between HWQM and previously reported are found to be in good agreement.

**Table 6.10:** Comparison the values of  $-f''(0)$  with previous studies for different values of  $\beta$  when  $f_w = 0, M = 0, L = 7, Pr = 1, Q = 0, \gamma = 0.2$  and  $m = 512$

$\beta$	Sadeghy et al. (2006)	Abel et al. (2012)	Mukhopadhyay (2012)	Megahed (2013)	Abbasi et al. (2016)	HWQM (Present)
0	1.00000	0.999962	0.999996	0.999978	1.00000	1.000162
0.2	1.05490	1.051948	1.051949	1.051945	1.05189	1.051966
0.4	1.10084	1.101850	1.101851	1.101848	1.10190	1.101942
0.6	1.15016	1.150163	1.150162	1.150160	1.15014	1.150160
0.8	1.19872	1.196692	1.196693	1.196690	1.19671	1.196728

**Table 6.11:** Comparison the values of  $-\theta'(0)$  with previous study when  $f_w = 0, M = 0, Q = 0, Pr = 1, \beta = 0.5, \gamma = 0.3, L = 7$  and  $m = 512$

Abbasi et al. (2016)	HWQM (Present)
0.56621	0.56678

**Table 6.12:** Comparison the values of  $-f''(0)$  with previous study for different values of  $M$  when  $f_w = 0$ ,  $\beta = 0$ ,  $\gamma = 0.2$ ,  $Pr = 1$ ,  $L = 8$  and  $m = 512$

$M$	Mahmoud (2010)	HWQM (Present)
0.1	1.04881	1.04882
0.3	1.14018	1.14016
0.5	1.22474	1.22472
0.7	1.30384	1.30381
1.0	1.41421	1.41417

Meanwhile Table 6.12 shows the comparative values of  $f''(0)$  for various values of magnetic field parameter,  $M$  given by present method and previous study as reported by Mahmoud (2010). This table clearly indicates that our present analytical solutions are in good agreement with the solutions of Mahmoud (2010).

**Table 6.13:** The values of HWQM for  $-f''(0)$  and  $-\theta'(0)$  when  $Pr = 2$ ,  $\beta = 0.1$ ,  $\gamma = 0.2$ ,  $m = 512$  and  $L = 5$

$f_w$	$Q$	$M$	$-f''(0)$	$-\theta'(0)$
		0	1.15769	1.14909
0.2	0.1	0.1	1.20459	1.13787
		0.2	1.24965	1.12709
		0.3	1.29305	1.11672
	0		1.20459	1.23648
0.2	0.1	0.1	1.20459	1.13787
		0.2	1.20459	1.02951
		0.3	1.20459	0.90822
0.1			1.13708	0.84680
0.2	0.2	0.1	1.20459	1.02951
0.3			1.27729	1.23239

Table 6.13 is tabulated to examine  $f''(0)$  and  $\theta'(0)$  for different values of  $f_w$ ,  $Q$  and  $M$  when  $Pr = 2$ ,  $\beta = 0.1$  and  $\gamma = 0.2$ . Here we can see that the values of  $f''(0)$  and  $\theta'(0)$  decrease with the increase of suction/injection parameter,  $f_w$ . The value of  $\theta'(0)$  increases for larger heat generation/absorption parameter,  $Q$  and magnetic field parameter,  $M$ . It is observed that rising the values of magnetic field declines the value of  $f''(0)$  but an increase of heat generation/absorption gives a constant result.

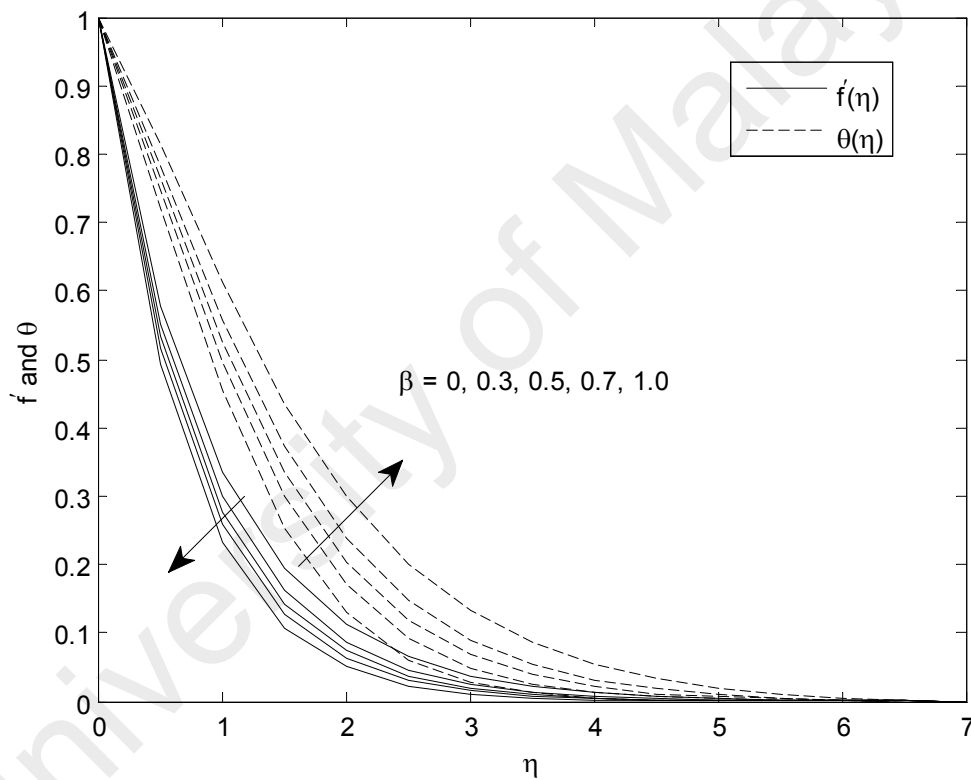


**Figure 6.11:** Velocity and temperature profiles for different values of  $\beta$  when  $m = 512$ ,  $L = 7$ ,  $M = 0.2$ ,  $f_w = 0$ ,  $Q = 0.2$ ,  $\gamma = 0.3$  and  $Pr = 1.4$

Figure 6.11 is drawn to examine the influences of Deborah number,  $\beta$  with respect to the relaxation time on the dimensionless velocity field and temperature profile. From Figure 6.11, we find that the velocity field and the momentum boundary layer thickness are decreasing functions of  $\beta$ . The Deborah number,  $\beta$  appears due to the relaxation time. The larger  $\beta$  corresponds to longer relaxation time and such longer relaxation time

resists the fluid flow due to lower velocity and thinner momentum boundary layer. On the other hand, an increase in  $\beta$  gives reverse effects on the temperature profile and the thermal boundary layer thickness. The temperature profile is enhanced with the increase of the Deborah number. The involvement with the relaxation time is responsible for the reduction and enhancement of the temperature profile and the thermal boundary layer thickness.

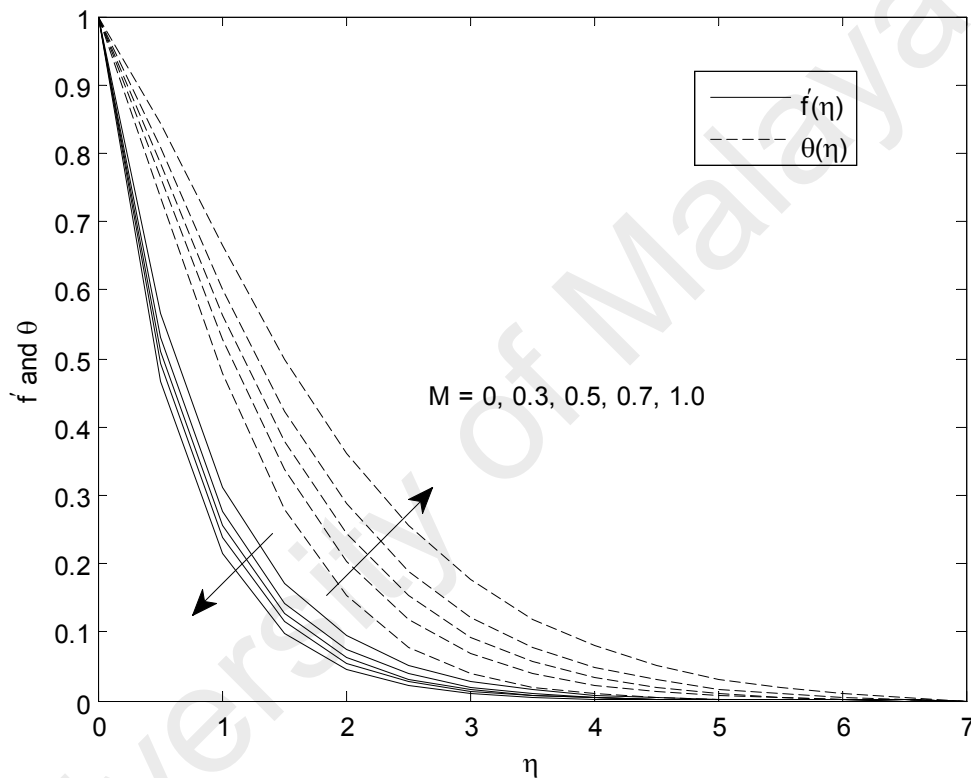


**Figure 6.12:** Velocity and temperature profiles for different values of  $M$  when  $m = 512$ ,  $L = 7$ ,  $\beta = 0.4$ ,  $f_w = 0$ ,  $Q = 0.2$ ,  $\gamma = 0.3$  and  $Pr = 1.4$

Figure 6.12 portrays the effect of magnetic field parameter,  $M$  on velocity and temperature fields. It is evident that the influence of increase in the strength of magnetic field is to diminish the velocity. This reduction can be attributed to the fact that the magnetic field provides a resisting type of force, where this force tends to lessen the motion of the fluid and as a consequence the velocity depreciates. It is observed that the velocity along the sheet decreases with  $M$  accompanied by a reduction in the thickness of the boundary layer. Meanwhile, the temperature is found to enhance with magnetic

field, the frictional resistance on account of the magnetic field resulting in the reduction of velocity and thereby enhances the temperature in the thermal boundary layer. Hence, there is an increase in the thickness of thermal boundary layer.

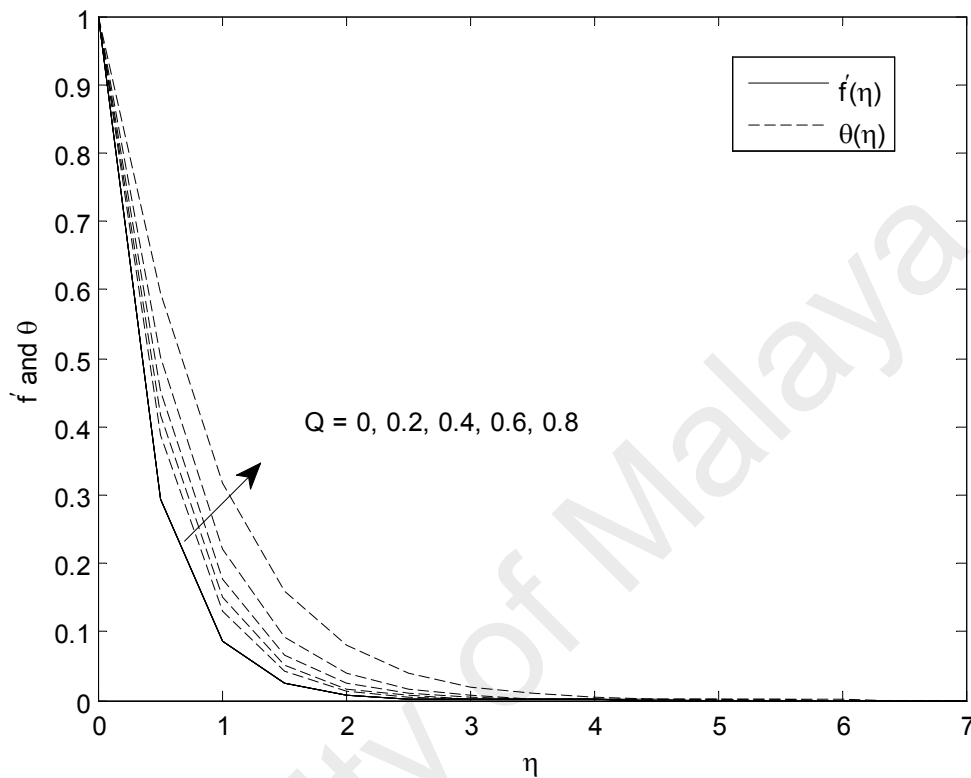


**Figure 6.13:** Velocity and temperature profiles for different values of  $Q$  when  $m = 512$ ,  $L = 7$ ,  $\beta = 0.2$ ,  $f_w = 1$ ,  $M = 0.2$ ,  $\gamma = 0.2$  and  $Pr = 1$

The effects of heat generation parameter,  $Q$  on the velocity and the temperature profiles are revealed in Figure 6.13. The graph depicts that there is no effect of changing  $Q$  on  $f'(\eta)$ . However, the heat generation parameter gives rise to the temperature and thermal boundary layer thickness. For  $Q > 0$ , the heat generation phenomenon occurs. As the values of heat generation increase, more heat is absorbed by the fluid due to temperature of fluid is enhanced.

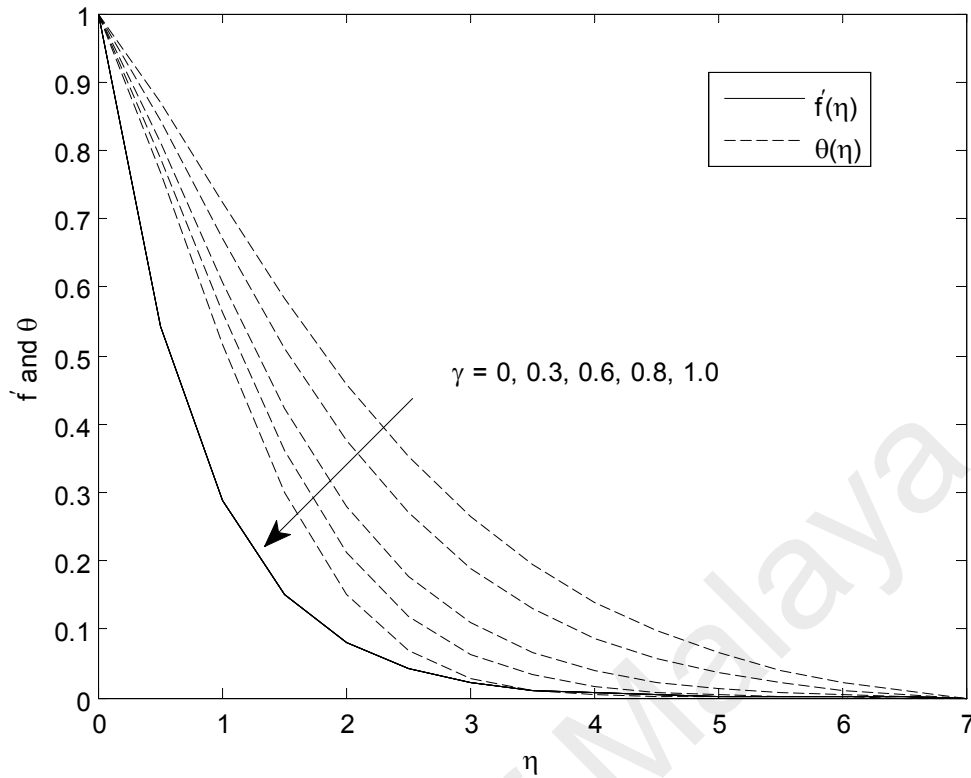


**Figure 6.14:** Velocity and temperature profiles for different values of  $\gamma$  when  $m = 512$ ,  $L = 7$ ,  $\beta = 0.4$ ,  $f_w = 0$ ,  $M = 0.2$ ,  $Q = 0.2$  and  $Pr = 1$

Figure 6.14 depicts the effects of non-dimensional heat flux relaxation time,  $\gamma$  on velocity and temperature fields. It shows that there is no effect of changing the values of  $\gamma$  on the velocity. However, the temperature profile and the thermal boundary layer thickness are lower for larger  $\gamma$ . The Deborah number  $\gamma$  arises due to the heat flux relaxation time. The fluid with longer heat flux relaxation time has lower temperature and the fluid with shorter heat flux relaxation time corresponds to higher temperature.

The effects of  $Pr$  on the velocity and temperature profiles are explored in Figure 6.15. The suitable Prandtl numbers are quite essential in the industrial processes since they are used to control the heat transfer rate during the final product (Abbasi et al., 2016). It is observed that an increase in the  $Pr$  leads to a reduction in the temperature and thermal boundary layer thickness. The  $Pr$  is the ratio of momentum to the thermal diffusivity. The thermal diffusivity is weaker for larger  $Pr$  due to the fact that the rate of

diffusion decreases. Such a reduction in the diffusion rate acts as an agent showing a reduction in temperature and thermal boundary layer thickness. The graph also depicts that there is no effect of changing Pr on  $f'(\eta)$ . This is similar to previous problem where Pr is the coefficient of the temperature and has a direct impact on the temperature. But, the impact of Pr on the velocity is attained through the combination various terms, hence the effect may be debilitated.

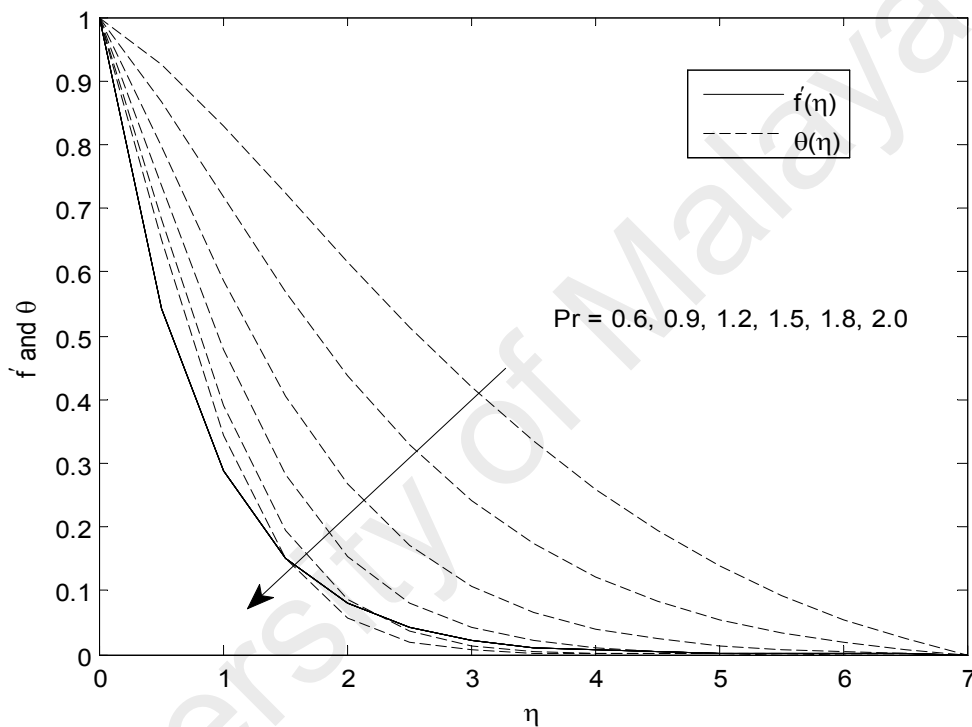


**Figure 6.15:** Velocity and temperature profiles for different values of Pr when  $m = 512$ ,  $L = 7$ ,  $\beta = 0.4$ ,  $f_w = 0$ ,  $M = 0.2$ ,  $Q = 0.2$  and  $\gamma = 0.3$

Figure 6.16 illustrates the behaviour of suction (or injection) parameter,  $f_w$  on the velocity and temperature fields. As shown in this graph, both of the profiles decrease with the increase of suction/injection parameter. Since suction leads to draw the amount of fluid particles therefore the velocity field and temperature field are decreased.

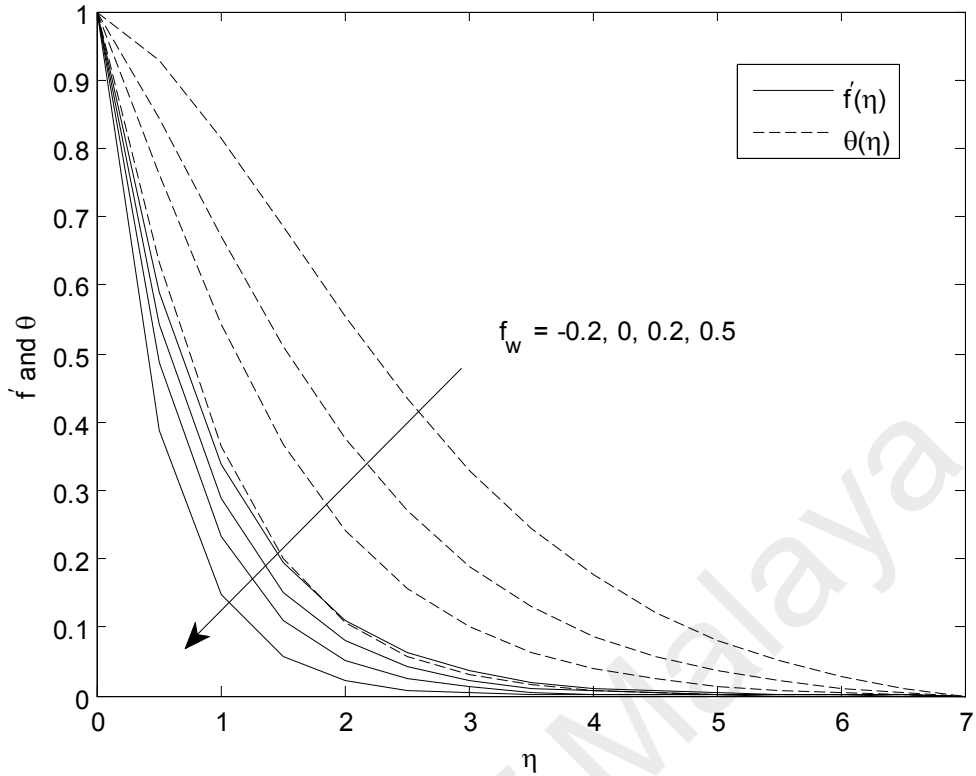


**Figure 6.16:** Velocity and temperature profiles for different values of  $f_w$  when  $m = 512$ ,  $L = 7$ ,  $\beta = 0.4$ ,  $M = 0.2$ ,  $Q = 0.2$ ,  $Pr = 1$  and  $\gamma = 0.3$

#### 6.4 Conclusions

In Section 6.1, the UCM model is examined with the consideration of Cattaneo-Christov heat flux model to investigate heat transfer and boundary layer flow of a viscoelastic fluid above a stretching plate with velocity slip boundary. Highly accurate solutions of the coupled nonlinear ODEs (6.10) and (6.11) with boundary conditions (6.12) are computed by employing HWQM. The main observations are summarized as follows:

- (a) the velocity field decreases while the temperature profile increases as the elasticity number,  $\beta$  increases,
- (b) the velocity profile was decreased as the distance,  $\eta$  increase from 0 to 2, but increases far away from the surface of the sheet in the boundary layer, whereas the temperature profile was increased with the velocity slip parameter,

- (c) the temperature profile decreases smoothly descend to zero at a distance  $\eta = 8$  from the sheet when thermal relaxation parameter,  $\gamma$  is incremented. This indicates that there will be thinner thermal boundary layer when relaxation time for heat flux is larger,
- (d) Pr has inverse relationship with thermal diffusivity, therefore an increase in Pr reduces conduction and hence causes a reduction in the penetration depth of temperature,
- (e) temperature distribution is higher in the case of Fourier's law compared to Cattaneo-Christov heat flux model,
- (f) with the increase of Pr, the value of  $\theta'(0)$  increase, where the increase is very slow,
- (g) an increment in the thermal relaxation parameter,  $\gamma$  leads to the constantly result in the surface friction coefficient,  $f''(0)$  whereas the value of  $\theta'(0)$  was decreased.

In Section 6.2, numerical solution has been obtained for the effects of suction/injection, non-dimensional heat flux relaxation time,  $\gamma$ , elasticity number,  $\beta$  and Pr on heat transfer characteristics over the steady, two dimensional, incompressible, laminar flow of Maxwell fluid past a stretching sheet. The obtained key features are listed below:

- (a) the impact of the heat flux relaxation time,  $\gamma$  on the temperature field is more noticeable than that on the velocity field, where the result of temperature field decreases as  $\gamma$  increases,
- (b) the elasticity number,  $\beta$  has quite opposite effects on the velocity field and the temperature profile,
- (c) no effect of changing Pr on velocity field, while the temperature profile decreases with an increase in Pr and the temperature boundary layer becomes thinner. The influence of Pr on the temperature field is more prominent than that on the velocity

field,

- (d) the varies of suction/injection parameter,  $f_w$  affected both velocity and temperature fields. The larger number of  $f_w$  leads to a reduction in the velocity and temperature distributions,
- (e)  $f''(0)$  is found to decrease upon increasing the suction/injection parameter,  $f_w$ ,
- (f) no effect of changing the value of heat flux relaxation,  $\gamma$  on the surface friction coefficient,  $f''(0)$ ,
- (g)  $\theta'(0)$  decreases with the increase of heat flux relaxation,  $\gamma$ , but it tends to increase with the enhanced of elasticity number,  $\beta$ .

Section 6.3 investigates the impact of heat generation/absorption parameter,  $Q$ , suction/injection parameter,  $f_w$ , magnetic field parameter,  $M$ , elasticity number,  $\beta$ , non-dimensional heat flux relaxation time,  $\gamma$  and Prandtl number, Pr. Some novel numerical results are obtained as follows:

- (a) the velocity field decreases while the temperature profile increase as the elasticity number,  $\beta$  increases,
- (b) velocity distribution shows decreasing behaviour whereas the increase of temperature profile as the magnetic field parameter increases,
- (c) an increment in the heat generation/absorption leads to the increase of temperature field whereas no effect of velocity profile,
- (d) the larger thermal relaxation time,  $\gamma$  leads to a reduction in the temperature profile, but the velocity distribution remains constant,
- (e) the temperature profile is highly influenced by the Prandtl number compared to the velocity distribution,
- (f) the velocity and temperature profiles decrease as the values of suction/injection,

$f_w$  increases,

- (g)  $f''(0)$  was decreased with the magnetic parameter whereas  $\theta'(0)$  was decreased,
- (h)  $f''(0)$  remains constant, while  $\theta'(0)$  increases as the heat generation/absorption parameter increases,
- (i)  $f''(0)$  and  $\theta'(0)$  decrease as the values of suction/injection increases.

University of Malaya

## CHAPTER 7: CONCLUSIONS AND FUTURE WORK

### 7.1 Conclusions

Broadly speaking, efficient numerical methods are needed for numerical solution of highly nonlinear system of ODEs, where the analytical solutions appear infeasible. Thus, many researchers aim to solve these types of ODEs mostly by using the perturbation techniques. However, these techniques have their own limitations such as (He, 1999b)

- (a) all the perturbation techniques are based on small or large parameters, so that at least one unknown must be expressed in a series of small parameter, based on an assumption that a small parameter must exist in the equation. This will restrict the applications of perturbation techniques,
- (b) an appropriate choice of small parameter contributes to ideal results, but inappropriate choice of small parameter leads to bad effects.

In this thesis, an extended HWQM is proposed for solving boundary value problems; single nonlinear ODEs and systems of coupled nonlinear ODEs. In the beginning of the study, the understanding mathematical background of Haar wavelet is needed, as shown in Chapter 3. Many scholars whom proposed numerical method based on Haar wavelet basis usually defined it in the interval from zero to one. This gives limitations to our ultimate goal as the integration involved in Haar wavelet series does not necessarily lie only in the interval between zero to one. Moreover, the boundary layer fluid flow problems and heat and mass transfer problems deal with sufficiently large number of infinite intervals. Therefore, it is convenient to derive the Haar wavelet functions and their integration that can cover the whole domain of Haar series expansion.

We also set up a MATLAB program for combination of Haar wavelet functions and its integration. This will lead to smaller computational time. In this study, we also used

the quasilinearization procedure in which replaces the original nonlinear equation by a sequence of linear equations. This technique treats the nonlinear terms by a series of a nonperturbative iterations and it is not based on the existence of some kind of small parameter. The major way that the quasilinearization differs from other approximate techniques is at every iterative stage, the differential operator changes significantly to account for nonlinearity. Thus, this technique provides extremely accurate and numerically stable answers for a wide range of nonlinear physics problems. The remainder of the chapter we proposed an efficient new algorithm and step by step for easy understanding the numerical technique of HWQM.

In Chapter 4, the solutions of three problems of single nonlinear ODEs, namely Bratu equation, Falkner-Skan equation and Blasius equation are presented. To justify the proposed method, the result in the present study are compared with existing solutions or exact results. The results show that suggested method provides excellent approximations to the solution and its derivatives of the nonlinear system with high accuracy. Based on the findings presented in Chapter 4, HWQM ensured a very rapid convergence after only one iteration. This procedure is a powerful approach for solving single nonlinear problems without depending on small parameter only.

Chapter 5 presented a methodology for three different types of coupled nonlinear ODEs that related to the natural convection boundary layer fluid flow problems, namely; BLFHTSS, LFC and NCBLF. The effects of variation of Pr on heat transfer are investigated. We obtained the promising results and compared with those obtained by another researcher's work. To the best of our knowledge, this is the first effort to solve coupled nonlinear ODEs through this method. It is worth mentioning that the proposed method is straightforward and concise, and can be applied to another nonlinear problems.

In Chapter 6, numerical tested for three different types of coupled nonlinear

differential equations with some additional parameters that are related to heat and mass transfer problems are discussed. The last two problems are the new problems in the presence of suction/injection and heat generation/absorption, respectively. In this chapter, convective heat transfer in Maxwell fluid with Cattaneo-Christov heat flux model are employed. The numerical solutions are compared with published results that shared similar limited case.

Through this method, we found that;

- (a) the HWQM provides excellent approximation to the solution,
- (b) HWQM suitable for the numerical solution of boundary value problems defined on small and long intervals,
- (c) it provides smaller computational time since universal subprogram is applied to calculate Haar wavelet and its integration,
- (d) unlike RKM, HWQM does not require conversion of boundary value problems into initial value problem,
- (e) the boundary value problem of HWQM need not to be reduced into a system of first order ODE,
- (f) variety of boundary conditions can be handle with equal ease,
- (g) in order for achieving a very accurate solution, HWQM ensured a very rapid convergence after only one iteration and by increasing level of resolution,
- (h) to recuperate the approximation of original function, the highest order derivative of Haar wavelet is approximated by Haar functions using integral approach,
- (i) HWQM allow simplicity, fast and small computation cost.

## **7.2 Future Work**

Suggestions for future research are summarized as following:

- (a) In this thesis, to justify the accuracy of the numerical results, a comparison with

analytical solutions given by others is being employed. We did not go in depth into mathematically proving the numerical stability and convergence of the method. So that in the future work, we are interested in calculating the error bound in order to analyze the convergence of our results, since we can not claim that this approximation solution is good or bad unless we are able to determine the error bound. Therefore, it is necessary for us to introduce the process of estimating the error function when the exact solution is unknown.

- (b) To find the convergence criteria for HWQM, hence to establish a new theorem for convergence criteria.
- (c) Most of the previous studies are solved only quadratic nonlinearity terms. Therefore, we suggest extending this work to the case of nonlinear ODEs contain not only quadratic nonlinear terms, but various other forms of nonlinearity, and not only first, but also higher order derivatives, and not only deal with linear boundary conditions, but also the nonlinear boundary conditions, and not only coupled nonlinear ODEs, but also more than two nonlinear ODEs.
- (d) Given that Haar wavelet method is relatively easy to implement and computationally inexpensive, we would like to extend the use of this method to solve directly partial differential equations or governing equations expressing conservation of mass, momentum and energy.
- (e) Apart from applications in physics and engineering fields, HWQM can also be applied in other field such as medicine.

## REFERENCES

- Abbasbandy, S. (2007). A numerical solution of Blasius equation by Adomian decomposition method and comparison with homotopy perturbation method. *Chaos, Solitons and Fractals*, 31(1), 257-260.
- Abbasbandy, S., & Hayat, T. (2009a). Solution of the MHD Falkner-Skan flow by homotopy analysis method. *Communications in Nonlinear Science and Numerical Simulation*, 14(9-10), 3591-3598.
- Abbasbandy, S., & Hayat, T. (2009b). Solution of the MHD Falkner-Skan flow by Hankel-Pade method. *Physics Letters A: General Atomic and Solid State Physics*, 373(7), 731-734.
- Abbasbandy, S., Hashemi, M.S. & Liu, C.S. (2011). The Lie-group shooting method for solving Bratu equation. *Communications in Nonlinear Science and Numerical Simulation*, 16(11), 4238-4249.
- Abbasi, F. M., Mustafa, M., Shehzad, S. A., Alhuthali, M. S., & Hayat, T. (2016). Analytical study of Cattaneo-Christov heat flux model for a boundary layer flow of Oldroyd-B fluid. *Chinese Physics B*, 25(1), Article ID 014701.
- Abbasi, F. M., & Shehzad, S. A. (2016). Heat transfer analysis for three-dimensional flow of Maxwell fluid with temperature dependent thermal conductivity: Application of Cattaneo-Christov heat flux model. *Journal of Molecular Liquids*, 220, 848-854.
- Abel, M. S., Tawade, J. V., & Nandeppanavar, M. M. (2012). MHD flow and heat transfer for the upper-convected Maxwell fluid over a stretching sheet. *Meccanica*, 47, 385-393.
- Abel-Halim Hassan, I. H. & Erturk, V.S. (2007). Applying differential transformation method to the one-dimensional planar Bratu problem. *International Journal of Contemporary Mathematical Sciences*, 2(29), 1493-1504.
- Ahmad, F. (2007). Degeneracy in the Blasius problem. *Electronic Journal of Differential Equations*, 79, 1-8.
- Ahmed, N., Siddique, Z. U. & Mishra, M.K. (2010). Boundary layer flow and heat transfer past a stretching plate with variable thermal conductivity. *International Journal of Nonlinear Mechanics*, 45(3), 306-309.
- Ahmet, Y. (2009). The solutions of Bratu-type problems by He's homotopy perturbation method. *Journal of Applied Functional Analysis*, 4(2), 265-272.
- Al-Bayati, A. Y., Ibraheem, K. I. & Ahmed, G. I. (2011). A modified wavelet algorithm to solve BVPs with an infinite number of boundary conditions. *International Journal of Open Problems in Computer Science and Mathematics*, 4(2), 141-154.

- Alizadeh, E., Farhadi, M., Sedighi, K., Ebrahimi-Kebria, H. R., & Ghafourian, A. (2009). Solution of the Falkner-Skan equation for wedge by adomian decomposition method. *Communications in Nonlinear Science and Numerical Simulation*, 14(3), 724-733.
- Allame, M., Maleki, M., & Kajani, M. T. (2014). Solution of Falkner-Skan equation with heat transfer using a Legendre collocation method. *American Institute of Physics Conference Proceedings*, 1629(1), 394-399.
- Aman, F., Ishak, A., & Pop, I. (2013). Magnetohydrodynamic stagnation-point flow towards a stretching/shrinking sheet with slip effects. *International Communications in Heat and Mass Transfer*, 47, 68-72.
- Aminikhah, H. (2009). An analytical approximation for solving nonlinear Blasius equation by NHPM. *Numerical Methods for Partial Differential Equations*, 26(6), 1291-1299.
- Aminikhah, H. (2012). Analytical approximation to the solution of nonlinear Blasius' viscous flow equation by LTNHPM. *Hindawi (International Scholarly Research Network) in ISRN Mathematical Analysis*, 2012, 1-10.
- Aregbesola, Y. A. S. (2003). Numerical solution of Bratu problem using the method of weighted residual. *Electronic Journal of Southern African Mathematical Sciences*, 3(1), 1-7.
- Ariel, P. D. (2009). The homotopy perturbation method and analytical solution of the problem of flow past a rotating disk. *Computers and Mathematics with Applications*, 58(11-12), 2504-2513.
- Asaithambi, A. (1997). A numerical method for the solution of the Falkner-Skan equation. *Applied Mathematics and Computation*, 81(2-3), 259-264.
- Asaithambi, A. (1998). A finite-difference method for the solution of the Falkner-Skan equation. *Applied Mathematics and Computation*, 92(2), 135-141.
- Asaithambi, A. (2004a). A second-order finite-difference method for the Falkner-Skan equation. *Applied Mathematics and Computation*, 156(3), 779-786.
- Asaithambi, A. (2004b). Numerical solution of the Falkner-Skan equation using piecewise linear functions. *Applied Mathematics and Computation*, 159(1), 267-273.
- Asaithambi, A. (2005). Solution of the Falkner-Skan equation by recursive evaluation of Taylor coefficients. *Journal of Computational and Applied Mathematics*, 176(1), 203-214.
- Babolian, E., & Fattahzadeh, F. (2007). Numerical computation method in solving integral equations by using Chebyshev wavelet operational matrix of integration. *Applied Mathematics and Computation*, 188(1), 1016-1022.

- Babolian, E., & Shahsavaran, A. (2009). Numerical solution of nonlinear Fredholm integral equations of the second kind using Haar wavelets. *Journal of Computational and Applied Mathematics*, 225(1), 87-95.
- Batiha, B. (2010). Numerical solution of Bratu-type equations by the variational iteration method. *Hacettepe Journal of Mathematics and Statistics*, 39(1), 23-29.
- Beckett, P. M. (1983). Finite-difference solution of boundary-layer type equations. *International Journal of Computational Mathematics*, 14(2), 183-190.
- Bellman, R. E. & Kalaba, R. E. (1965). *Quasilinearization and nonlinear boundary value problems*. New York: American Elsevier Pub. Co.
- Bellman, R. E. & Roth, R. (1983). *Quasilinearization and the identification problem*. Republic of Singapore: World Scientific Publishing Company.
- Bhattacharyya, K., Mukhopadhyay, S., & Layek, G. C. (2013). Similarity solution of mixed convective boundary layer slip flow over a vertical plate. *Ain Shams Engineering Journal*, 4(2), 299-305.
- Blasius, H. (1950). The boundary layers in fluid with little friction. *Journal of Mathematics and Physics*, 56(1), 1-37.
- Boyd, J. P. (2000). *Chebyshev and fourier spectral methods* (2<sup>nd</sup> Ed.). New York: Dover Publishers.
- Boyd, J. P. (2003). Chebyshev polynomial expansions for simultaneous approximation of two branches of a function with application to the one dimensional Bratu equation. *Applied Mathematics and Computation*, 142, 189-200.
- Boyd, J. P. (2011). One-point pseudospectral collocation for the one dimensional Bratu equation. *Applied Mathematics and Computation*, 217(12), 5553-5565.
- Bromely, L. A. (1952). Effect of heat capacity of condensate. *Industrial & Engineering Chemistry*, 44(12), 2966-2969.
- Brouwers, H. J. H. (1989). Film condensation on nonisothermal vertical plates. *International Journal of Heat and Mass Transfer*, 32(4), 655-663.
- Buckmire, R. (2004). Application of Mickens finite-difference scheme to the cylindrical Bratu-Gelfand problem. *Numerical Methods for Partial Differential Equations*, 20(3), 327-337.
- Caglar, N. & Caglar, H. (2009). B-spline method for solving linear system of second order boundary value problems. *Computers and Mathematics with Applications*, 57(5), 757-762.
- Caglar, H., Caglar, N., Ozer, M., Valaristos, A. & Anagnostopoulos, A. N. (2010). B-Spline method for solving Bratu's problem. *International Journal of Computer Mathematics*, 87(8), 1885-1891.

- Cao, L., Si, X., Zheng, L., & Pang, H. (2015). Lie group analysis for MHD effects on the convectively heated stretching porous surface with the heat source/sink. *Boundary Value Problems*, 2015(63), 1-18.
- Carragher, P., & Crane, L. J. (1982). Heat transfer on a continuous stretching sheet. *Journal of Applied Mathematics and Mechanics*, 62(10), 564–565.
- Cattaneo, C. (1948). On heat conduction. *Atti of the Mathematical and Physical Seminary of the University of Modena and Reggio Emilia*, 3, 83-101.
- Cattani, C. (2001). Haar wavelet spline. *Journal of Interdisciplinary Mathematics*, 4(1), 35-47.
- Cattani, C. (2004). Haar wavelets based technique in evolution problems. *Proceedings of the Estonian Academy of Sciences, Physics, Mathematics*, 53(1), 45-63.
- Cebici, T., & Keller, H. B. (1971). Shooting and parallel shooting methods for solving the Falkner-Skan boundary-layer equation. *Journal of Computational Physics*, 7(2), 289-300.
- Chang, C. W., Chang, J. R., & Liu, C. S. (2006). The Lie-group shooting method for boundary layer equations in fluid mechanics. *Journal of Hydrodynamics, Series B*, 18(3), 103-108.
- Chang, P., & Piau, P. (2008). Simple procedure for the designation of Haar wavelet matrices for differential equations. *International Multi Conference of Engineers and Computer Scientists*, 2, 19-21.
- Changqing, Y. & Jianhua, H. (2013). Chebyshev wavelets method for solving Bratu's problem. *Boundary Value Problems*, 2013(142), 1-9.
- Chen, C., & Char, M. I. (1988). Heat transfer of a continuous, stretching surface with suction or blowing. *Journal of Mathematical Analysis and Applications*, 135(2), 568–580.
- Chen, C. F., & Hsiao, C. H. (1975). A Walsh series direct method for solving variational problems. *Journal of the Franklin Institute*, 300(4), 265-280.
- Chen, C. F., & Hsiao, C. H. (1997). Haar wavelet method for solving lumped and distributed parameter systems. *IEEE Proceedings on Control Theory and Applications*, 144(1), 87-94.
- Chen, M. M. (1961). An analytical study of laminar film condensation: Part 1-Flat Plates. *Journal of Heat Transfer*, 83(1), 48-54.
- Cheng, B., & Hsu, N. S. (1982). Analysis and parameter estimation of bilinear systems via block pulse function. *International Journal of Control*, 36(1), 53-65.
- Chi-Hsu, W. (1983). On the generalization of block pulse operational matrices for fractional and operational calculus. *Journal of the Franklin Institute*, 315(2), 91-102.

- Christov, C. I. (2009). On frame indifferent formulation of the Maxwell-Cattaneo model of finite speed heat conduction. *Mechanics Research Communications*, 36(4), 481-486.
- Ciarletta, M., & Straughan, B. (2010). Uniqueness and structural stability for the Cattaneo-Christov equations. *Mechanics Research Communications*, 37(5), 445-447.
- Coppel, W. A. (1960). On a differential equation of boundary layer theory. *Philosophical Transactions of the Royal Society of London, Series A*, 253(1023), 101-136.
- Cortell, R. (2005). Numerical solution of the Blasius flat-plate problem. *Applied Mathematics and Computation*, 170(1), 706-710.
- Cortell, R. (2007). Flow and heat transfer in a moving fluid over a moving flat surface. *Theoretical and Computational Fluid Dynamics*, 21(6), 435-446.
- Crane, L. J. (1970). Flow past a stretching plate. *Journal of Applied Mathematics and Physics*, 21(4), 645-647.
- Dai, R., & Cochran, J. E. (2009). Wavelet collocation method for optimal control problems. *Journal of Optimization Theory and Applications*, 143(2), 265-278.
- Daubechies, I. (1988). Orthonormal bases of compactly supported wavelets. *Communications on Pure and Applied Mathematics*, 41, 909-996.
- Deeba, E., Khuri, S. A. & Xie, S. (2000). An algorithm for solving boundary value problems. *Journal of Computational Physics*, 159(2), 125-138.
- Dehghan, M. & Saadatmandi, A. (2007). The numerical solution of a nonlinear system of second-order boundary value problems using the sinc-collocation method. *Mathematical and Computer Modelling*, 46(11), 1434-1441.
- Derili, H., Sohrabi, S., & Arzhang, A. (2012). Two-dimensional wavelets for numerical solution of integral equations. *Mathematical Sciences*, 6(5), 1-4.
- Dinarvand, S., Doosthoseini, A., Doosthoseini, E., & Rashidi, M. M. (2010). Series solutions for unsteady laminar MHD flow near forward stagnation point of an impulsively rotating and translating sphere in presence of bouyancy forces. *Nonlinear Analysis: Real World Applications*, 11(2), 1159-1169.
- Dremin, I. M., Ivanov, O. V., & Nechitailo, V. A. (2001). Wavelets and their use. *Physics-Uspekhi*, 44(5), 1-63.
- Dutta, B. K., Roy, P., & Gupta, A. S. (1985). Temperature field in flow over a stretching sheet with uniform heat flux. *International Communications in Heat and Mass Transfer*, 12(1), 89-94.
- Eckert, E. R. G. and Soehngen, E. E. (1948). Studies on heat transfer in laminar free convection with Zehnder-Mach interferometer. *UASF Technical Report 5747*, 7-19.

- Eckert, E. R. G. (1963). *Introduction to heat and mass transfer*. New York: McGraw-Hill.
- Elbarbary, E. M. E. (2005). Chebyshev finite difference method for the solution of boundary-layer equations. *Applied Mathematics and Computation*, 160(2), 487-498.
- Elbashbeshy, E. M. A. (1998). Heat transfer over a stretching surface with variable surface a heat flux. *Journal of Physics D*, 31(16), 1951–1954.
- Elbashbeshy, E. M. A., & Bazid, M. A. A. (2004). Heat transfer in a porous medium over a stretching surface with internal heat generation and suction or injection. *Applied Mathematics and Computation*, 158(3), 799-807.
- Elbashbeshy, E. M. A., Emam, T. G., & Abdel-wahed, M. S. (2011). Mass transfer over unsteady stretching surface embedded in porous medium in the presence of variable chemical reaction and suction/injection. *Applied Mathematics Sciences*, 5(12), 557-571.
- El-Arabawy, H. A. M. (2009). Exact solution of mass transfer over a stretching surface with chemical reaction and suction/injection. *Journal of Mathematics and Statistics*, 5(3), 159-166.
- Elgazery, N. S. (2008). Numerical solution for the Falkner-Skan equation. *Chaos, Solitons and Fractals*, 35(4), 738-746.
- Esmailpour, M., & Ganji, D. D. (2007). Application of He's homotopy perturbation method to boundary layer flow and convection heat transfer over a flat plate. *Physics Letters A*, 372(1), 33-38.
- Falkner, V. M., & Skan, S. W. (1931). Some approximate solutions of the boundary layer equations. *Philosophical Magazine*, 12, 865-896.
- Fang, T. (2003a). Further study on a moving-wall boundary-layer problem with mass transfer. *Acta Mechanica*, 163(3-4), 183-188.
- Fang, T. (2003b). Similarity solutions for a moving-flat plate thermal boundary layer. *Acta Mechanica*, 163(3-4), 161-172.
- Fang, T., Guo, F., & Lee, C. F. (2006). A note on the extended Blasius problem. *Applied Mathematics Letters*, 19(7), 613-617.
- Fazal-i-Haq, Aziz, I., & Islam, S. U. (2010). A Haar wavelets based numerical method for eight-order boundary problems. *International Journal of Mathematical and Computer Sciences*, 6(1), 25-31.
- Fazal-i-Haq, Aziz, I., & Islam, S. U. (2011). Numerical solution of singularly perturbed two-point BVPs using nonuniform Haar wavelets. *International Journal for Computational Methods in Engineering Science and Mechanics*, 12(4), 168-175.
- Fazio, R. (1994). The Falkner-Skan equation: Numerical solutions within group invariance theory. *Calcolo*, 31(1), 115-124.

- Fazio, R. (1996). A novel approach to the numerical solution of boundary value problems on infinite intervals. *SIAM Journal on Numerical Analysis*, 33(4), 1473-1483.
- Feng, X., He, Y., & Meng, J. (2008). Application of homotopy perturbation method to the Bratu-type equations. *Topological Methods in Nonlinear Analysis*, 31(2), 243-252.
- Fourier, J. B. J. (1822). *Analytical theory of heat*. Paris: Chez Firmin Didot.
- Gahan, B., Miller, J. J. H., & Shishkin, G. I. (2000). Accurate numerical method for Blasius' problem for flow past a flat-plate with mass transfer. *Proceedings of the Conference Finite Difference Schemes Theory and Applications-2000*, 1-10.
- Geng, F. & Cui, M. (2007). Solving a nonlinear system of second order boundary value problems. *Journal of Mathematical Analysis and Applications*, 327(2), 1167-1181.
- Geng, W., Chen, Y., Li, Y., & Wang, D. (2011). Wavelet method for nonlinear partial differential equations of fractional order. *Computer and Information Science*, 4(5), 28-35.
- Ghani, C. N. A. (2012). *Numerical solution of elliptic partial differential equations by Haar wavelet operational matrix method* (Master's thesis). University of Malaya, Kuala Lumpur, Malaysia.
- Ghani, C. N. A., Hussin, A., & Siri, Z. (2014). *Analysis of three different Haar wavelet methods for solving boundary value problems*. Paper presented at the 22<sup>nd</sup> National Symposium on Mathematical Sciences Conference, Shah Alam, Malaysia.
- Ghasemi, M., & Tavassoli Kajani, M. (2011). Numerical solution of time-varying delay systems by Chebyshev wavelets. *Applied Mathematical Modelling*, 35(11), 5235-5244.
- Ghazanfari, B. & Sefvandezadeh, A. (2014). Adomian decomposition method for solving fractional Bratu-type equations. *Journal of Mathematics and Computer Science*, 8, 236-244.
- Ghazanfari, B. & Sefvandezadeh, A. (2015a). Solving fractional Bratu-type equations by modified variational iteration method. *Selcuk Journal of Applied Mathematics*, 15(1), in press.
- Ghazanfari, B. & Sefvandezadeh, A. (2015b). Homotopy perturbation method for solving fractional Bratu-type equation. *Journal of Mathematical Modeling*, 2(2), 143-155.
- Ghotbi, A. R., Bararnia, H., Domairry, G., & Barari, A. (2009). Investigation of a powerful analytical method into natural convection boundary layer flow. *Communications in Nonlinear Science and Numerical Simulation*, 14(5), 2222-2228.

- Gireesha, B. J., Ramesh, G. K., Abel, M. S., & Bagewadi, C. S. (2011). Boundary layer flow and heat transfer of a dusty fluid flow over a stretching sheet with non-uniform heat source/sink. *International Journal of Multiphase Flow*, 37(8), 977-982.
- Gorla, R. S. R., & Sidawi, I. (1994). Free convection on a vertical stretching surface with suction and blowing. *Applied Scientific Research*, 52(3), 247-257.
- Grubka, L. J., & Bobba, K. M. (1985). Heat transfer characteristic of a continuous surface with variable temperature. *Journal of Heat Transfer*, 107(1), 248-255.
- Gu, J. S., & Jiang, W. S. (1996). The Haar wavelets operational matrix of integration. *International Journal of Systems Science*, 27(7), 623-628.
- Gupta, P. S., & Gupta, A. S. (1977). Heat and mass transfer on a stretching sheet with suction and blowing. *Canadian Journal of Chemistry*, 55(6), 744-746.
- Han, S., Zheng, L., Li, L., & Zhang, X. (2014). Coupled flow and heat transfer in viscoelastic fluid with Cattaneo-Christov heat flux model. *Applied Mathematics Letters*, 38, 87-93.
- Hariharan, G., & Kannan, K. (2011). A comparative study of Haar wavelet method and homotopy perturbation method for solving one-dimensional reaction-diffusion equations. *International Journal of Applied Mathematics and Computation*, 3(1), 21-34.
- Hariharan, G., Kannan, K., & Sharma, K. R. (2009). Haar wavelet method for solving Fisher's equation. *Applied Mathematics and Computation*, 211 (2), 284-292.
- Hartree, D. R. (1937). On an equation occurring in Falkner-Skan approximate treatment of the equations of the boundary layer. *Mathematical Proceedings of the Cambridge Philosophical Society*, 33(2), 223-239.
- Hayat, T., Abbas, Z., Pop, I., & Asghar, S. (2010). Effects of radiation and magnetic field on the mixed convection stagnation-point flow over a vertical stretching sheet in a porous medium. *International Journal of Heat and Mass Transfer*, 53, 466-474.
- Hayat, T., Farooq, M., Alsaedi, A., & Falleh Al-Solamy. (2015). Impact of Cattaneo-Christov heat flux in the flow over a stretching sheet with variable thickness. *American Institute of Physics Advances*, 5(8), 1-13.
- He, J. H. (1999a). Approximate analytical solution of Blasius' equation. *Communications in Nonlinear Science and Numerical Simulation*, 4(1), 75-80.
- He, J. H. (1999b). Homotopy perturbation technique. *Computer Methods in Applied Mechanics and Engineering*, 178, 257-262.
- He, J. H. (2004). Comparison of homotopy perturbation method and homotopy analysis method. *Applied Mathematics and Computation*, 156(2), 527-539.

- He, J. H., Kong, H. Y., Chen, R. X., Hu, M. S., Chen, Q. L. (2014). Variational iteration method for Bratu-like equation arising in electrospinning. *Carbohydrate Polymers*, 105, 229-230.
- Hendi, F. A., & Hussain, M. (2012). Analytic solution for MHD Falkner-Skan flow over a porous surface. *Journal of Applied Mathematics*, 2012, Article ID 123185.
- Howarth, L. (1938). On the solution of the laminar boundary layer equations. *Proceedings of the Royal Society of London, Series A, Mathematical and Physical Sciences*, 164(919), 547-579.
- Hsiao, C. H. (1997). State analysis of linear time delayed systems via Haar wavelets. *Mathematics and Computers in Simulation*, 44(5), 457-470.
- Hsiao, C. H. (2004). Haar wavelet direct method for solving variational problems. *Mathematics and Computers in Simulation*, 64(5), 569-585.
- Hsiao, C. H. (2008). Wavelets approach to time varying functional differential equations. *International Journal of Computer Mathematics*, 87(3), 528-540.
- Hsiao, C. H., & Wang, W. J. (2001). Haar wavelet approach to nonlinear stiff systems. *Mathematics and Computers in Simulation*, 57(6), 347-353.
- Hussaini, M. Y., & Lakin, W. D. (1986). Existence and non-uniqueness of similarity solutions of a boundary-layer problem. *The Quarterly Journal of Mechanics and Applied Mathematics*, 39(1), 15-24.
- Hwang, C. C. (1997). Numerical modeling of lightning based on the traveling wave equations. *IEEE Transactions on Magnetics*, 33(2), 1520-1523.
- Ibrahim, W., & Shankar, B. (2011). Unsteady boundary layer flow and heat transfer due to a stretching sheet by quasilinearization technique. *World Journal of Mechanics*, 2011(1), 288-293.
- Ibrahim, W., & Shankar, B. (2013). MHD boundary layer flow and heat transfer of a nanofluid past a permeable stretching sheet with velocity, thermal and solutal slip boundary conditions. *Computers and Fluids*, 75, 1-10.
- Inc, M., Akgül, A., & Gery, F. (2015). Reproducing kernel Hilbert space method for solving Bratu's problem. *Bulletin of The Malaysian Mathematical Sciences Society*, 38(1), 271-287.
- Ishak, A., Nazar, R., & Pop, I. (2009). Boundary layer flow and heat transfer over an unsteady stretching vertical surface. *Meccanica*, 44(4), 369-375.
- Islam, S. U., Aziz, I., & Šarler, B. (2010). The numerical solution of second-order boundary value problems by collocation method with the Haar wavelets. *Mathematical and Computer Modelling*, 52(9), 1577-1590.
- Islam, S. U., Šarler, B., Aziz, I., & Haq, F. (2011). Haar wavelet collocation method for the numerical solution of boundary layer fluid flow problems. *International Journal of Thermal Sciences*, 50(5), 686-697.

- Islam, S. U., Aziz, I., & Fayyaz, M. (2013). A new approach for numerical solution of integro-differential equations via Haar wavelets. *International Journal of Computer Mathematics*, 90(9), 1971-1989.
- Jalilian, R. (2010). Non-polynomial spline method for solving Bratu's problem. *Computer Physics Communications*, 181(11), 1868-1872.
- Jiwari, R. (2012). A Haar wavelet quasilinearization approach for numerical simulation of Burgers' equation. *Computer Physics Communications*, 183(11), 2413-2423.
- Kajani, M. T., Maleki, M., & Allame, M. (2014). A numerical solution of Falkner-Skan equation via a shifted Chebyshev collocation method. *AIP Conference Proceedings*, 1629(1), 381-386.
- Kaur, H., Mittal, R.C. & Mishra, V. (2011). Haar wavelet quasilinearization approach for solving nonlinear boundary value problem. *American Journal of Computational Mathematics*, 1(3),176-182.
- Kaur, H., Mishra, V. & Mittal, R. C. (2013). Numerical solution of a laminar viscous flow boundary layer equation using uniform Haar wavelet-quasilinearization method. *World Academy of Science, Engineering and Technology*, 79(79), 1410-1415.
- Khan, J. A., Mustafa, M., Hayat, T., & Alsaedi, A. (2015). Numerical study of Cattaneo-Christov heat flux model for viscoelastic flow due to an exponentially stretching surface. *PLoS ONE*, 10, Article ID 0137363.
- Khan, W. A., & Pop, I. (2010). Boundary-layer flow of a nanofluid past a stretching sheet. *International Journal of Heat and Mass Transfer*, 53, 2477-2483.
- Khellat, F., & Yousefi, S. A. (2006). The linear Legendre mother wavelets operational matrix of integration and its application. *Journal of the Franklin Institute*, 343(2), 181-190.
- Khuri, S. A. (2004). A new approach to Bratu's problem. *Applied Mathematics and Computation*, 147(1), 131-136.
- Klemp, J. B., & Acrivos, A. (1976). A moving-wall boundary layer with reverse flow. *Journal of Fluid Mechanics*, 76(2), 363-381.
- Koh, J. C. Y., Sparrow, E. M., & Hartnett, J. P. (1961). The two-phase boundary layer in laminar film condensation. *International Journal of Heat and Mass Transfer*, 2(1-2), 69-82.
- Kumar, M. & Yadav, N. (2015). Numerical solution of Bratu's problem using multilayer perception neural network method. *National Academy Science Letters*, 38(5), 425-428.
- Kuo, B. L. (2003). Application of the differential transformation method to the solutions of the Falkner-Skan wedge flow. *Acta Mechanica*, 164(3), 161-174.

- Lakestani, M. (2011). Numerical solution for the Falkner-Skan equation using Chebyshev cardinal functions. *Acta Universitatis Apulensis*, 27, 229-238.
- Lee, E.S. (1968). *Quasilinearization and invariant embedding with applications to chemical engineering and adaptive control*. New York: Academic Press.
- Lee, J., & Kim, D. H. (2005). An improved shooting method for computation of effectiveness factors in porous catalysts. *Chemical Engineering Science*, 60(20), 5569-5573.
- Lepik, Ü. (2005). Numerical solution of differential equations using Haar wavelets. *Mathematics and Computers in Simulation*, 68(2), 127-143.
- Lepik, Ü. (2007). Numerical solution of evolution equations by the Haar wavelet method. *Applied Mathematics and Computation*, 185(1), 695-704.
- Lepik, Ü. (2011). Solving PDEs with the aid of two-dimensional Haar wavelets. *Computers and Mathematics with Applications*, 61(7), 1873-1879.
- Lepik, Ü., & Tamme, E. (2004). Application of the Haar wavelets for solution of linear integral equations. *Dynamical Systems and Application Proceedings*, 494-507.
- Li, Y., & Zhao, W. (2010). Haar wavelet operational matrix of fractional order integration and applications in solving the fractional order differential equations. *Applied Mathematics and Computation*, 216(8), 2276-2285.
- Liao, S. J. (1997). A kind of approximate solution technique which does not depend upon small parameters-II. An application in fluid mechanics. *International Journal of Non-Linear Mechanics*, 32(5), 815-822.
- Liao, S. J. (1998). An explicit, totally analytic solution of laminar viscous flow over a semi-infinite flat plate. *Communications in Nonlinear Science and Numerical Simulation*, 3(2), 53-57.
- Liao, S. J., & Pop, I. (2004). Explicit analytic solution for similarity boundary layer equations. *International Journal of Heat and Mass Transfer*, 47(1), 75-85.
- Lin, C. R., & Chen, C. K. (1998). Exact solution of heat transfer from a stretching surface with variable heat flux. *Heat and Mass Transfer*, 33(5), 477-480.
- Lin, J. (1999). A new approximate iteration solution of Blasius equation. *Communications in Nonlinear Science and Numerical Simulation*, 4(2), 91-94.
- Liu, C. S., & Chang, J. R. (2008). The Lie-group shooting method for multiple-solutions of Falkner-Skan equation under suction-injection conditions. *International Journal of Non-Linear Mechanics*, 43(9), 844-851.
- Lu, J. (2007). Variational iteration method for solving a nonlinear system of a second order boundary value problems. *Computers and Mathematics with Applications*, 54(7-8), 1133-1138.

- Magyari, E., & Keller, B. (1999). Heat and mass transfer in the boundary layers on an exponentially stretching continuous surface. *Journal of Physics D: Applied Physics*, 32(5), 577–585.
- Magyari, E., & Keller, B. (2000). Exact solutions for self-similar boundary-layer flows induced by permeable stretching walls. *European Journal of Mechanics B/Fluids*, 19(1), 109-122.
- Mahdy, A. and Hady, F. (2009). Effects of thermophoretic particle deposition in non-newtonian free convection flow over a vertical plate with magnetic field effect. *Journal of non-Newtonian Fluid Mechanics*, 161(1), 37-41.
- Mahmoud, M. A. A. (2010). Chemical reaction and variable viscosity effects on flow and mass transfer of a non-Newtonian visco-elastic fluid past a stretching surface embedded in a porous medium. *Meccanica*, 45, 835-846.
- Maleknejad, K., & Mirzaee, F. (2005). Using rationalized Haar wavelet for solving linear integral equations. *Applied Mathematics and Computation*, 160(2), 579-587.
- Malik, R., Khan, M., Shafiq, A., Mushtaq, M., & Hussain, M. (2017). An analysis of Cattaneo-Christov double-diffusion model for Sisko fluid flow with velocity slip. *Results in Physics*, 7, 1232-1237.
- Mandelzweig, V. B. & Tabakin, F. (2001). Quasilinearization approach to nonlinear problems in physics with application to nonlinear ODEs. *Computer Physics Communications*, 141(2), 268-281.
- Marinca, V., Ene, R. D., & Marinca, B. (2014). Analytic approximate solution for Falkner-Skan equation. *The Scientific World Journal*, 2014, 1-22.
- Megahed, A. M. (2013). Variable fluid properties and variable heat flux effects on the flow and heat transfer in a non-Newtonian Maxwell fluid over an unsteady stretching sheet with slip velocity. *Chinese Physics B*, 22(9), 094701.
- Méndez, F., & Treviño, C. (1996). Longitudinal heat conduction effects on a vertical thin plate in a steady laminar condensation process. *International Journal of Heat and Fluid Flow*, 17(5), 517-525.
- Merkin, J. H. (1985). A note on the similarity solutions for free convection on a vertical plate. *Journal of Engineering Mathematics*, 19(3), 189–201.
- Michalik, C., Hannemann, R., & Marquardt, W. (2009). Incremental single shooting - a robust method for the estimation of parameters in dynamical systems. *Computers and Chemical Engineering*, 33(7), 1298-1305.
- Miele, A., & Wang, T. (1993). Parallel computation of two-point boundary value problems via particular solutions. *Journal of Optimization Theory and Applications*, 79(1), 5-29.
- Mohammed, M. A., Mohammed, M. E., & Khidir, A. A. (2014). A successive linearization method approach for solving general boundary layer problems. *International Journal of Applied Mathematics and Mechanics*, 10(4), 55-72.

- Mounim, A.S., & de Dormale, B.M. (2006). From the fitting techniques to accurate schemes for the Liouville-Bratu-Gelfand problem. *Numerical Methods for Partial Differential Equations*, 22(4), 761-775.
- Mouroutsos, S. G., & Paraskevopoulos, P. N. (1985). Identification of time-varying linear systems using orthogonal functions. *Journal of the Franklin Institute*, 320(5), 249-258.
- Mukhopadhyay, S. (2012). Heat transfer analysis of the unsteady flow of a Maxwell fluid over a stretching surface in the presence of a heat source/sink. *Chinese Physics Letters*, 29(5), Article ID 054703.
- Murty, K. N., Srinivas, M.A.S. & Prasad, K. R. (1990). On the use of the quasilinearization method in the growth of a pathogenic bacteria. *Journal of Mathematical Analysis and Applications*, 149(2), 576-582.
- Mushtaq, A., Abbasbandy, S., Mustafa, M., Hayat, T., & Alsaedi, A. (2016). Numerical solution for Sakiadis flow of upper-convected Maxwell fluid using Cattaneo-Christov heat flux model. *AIP Advances*, 6(1), Article ID 015208.
- Mustafa, M. (2015). Cattaneo-Christov heat flux model for rotating flow and heat transfer of upper-convected Maxwell fluid. *AIP Advances*, 5(4), Article ID 047109.
- Muthucumaraswamy, R. (2002). Effects of suction on heat and mass transfer along a moving vertical surface in the presence of a chemical reaction. *Forsch Ingenieurwes*, 67, 129-132.
- Na, T. Y. (1979). *Computational methods in engineering boundary value problems*. New York: Academic Press.
- Nandy, S. K., & Mahapatra, T. R. (2013). Effects of slip and heat generation/absorption on MHD stagnation flow of nanofluid past a stretching/shrinking surface with convective boundary conditions. *International Journal of Heat and Mass Transfer*, 64, 1091-1100.
- Nasr, H., Hassanien, I. A., & El-Hawary, H. M. (1990). Chebyshev solution of laminar boundary-layer flow. *International Journal of Computational Mathematics*, 33(1-2), 127-132.
- Noghrehabadi, A., Pourrajab, R., & Ghalambaz, M. (2012). Effect of partial slip boundary condition on the flow and heat transfer of nanofluids past stretching sheet prescribed constant wall temperature. *International Journal of Thermal Sciences*, 54, 253-261.
- Nusselt, W. (1916). Die oberflächenkondensation des wasserdampfes. *Zeitschrift des Vereines Deutscher Ingenieure*, 60, 541-569.
- Oosthuizen, P., & Naylor, D. (1999). *An introduction to convective heat transfer analysis*. New York: WCB/McGraw-Hill.

- Oskam, B., & Veldman, A. E. P. (1982). Branching of the Falkner-Skan solutions for  $\lambda < 0$ . *Journal of Engineering Mathematics*, 16, 295-308.
- Ostrach, S. (1953). New aspects of natural convection heat transfer. *Transactions of the American Society of Mechanical Engineers*, 75, 1287-1290.
- Parand, K., Pakniat, N., & Delafkar, Z. (2011). Numerical solution of the Falkner-Skan equation with stretching boundary by collocation method. *International Journal of Nonlinear Science*, 11(3), 275-283.
- Paraskevopoulos, P. N. (1987). The operational matrices of integration and differentiation for the Fourier sine-cosine and exponential series. *Automatic Control, IEEE Transactions*, 32(7), 648-651.
- Patankar, S. V., & Sparrow, E. M. (1979). Condensation on an extended surface. *Journal of Heat Transfer*, 101(3), 434-440.
- Pop, S., Grosan, T., & Pop, I. (2004). Radiation effects on the flow near the stagnation point of a stretching sheet. *Technische Mechanik*, 25(2), 100-106.
- Rach, R. (2008). A new definition of the Adomian polynomials. *Kybernetes*, 37(7), 910-955.
- Raja, M. A. Z. & Islam, S. U. (2012). Numerical treatment for solving one-dimensional Bratu problem using neural networks. *Neural Computing and Applications*, 24(3), 549-561.
- Rajeswari, R., Jothiram, B., & Nelson, V. K. (2009). Chemical reaction, heat and mass transfer on nonlinear MHD boundary layer flow through a vertical porous surface in the presence of suction. *Journal of Applied Mathematical Science*, 3(50), 2469-2480.
- Ramesh, G. K., Gireesha, B. J., & Bagewadi, C. S. (2012). MHD flow of a dusty fluid near the stagnation point over a permeable stretching sheet with non-uniform source/sink. *International Journal of Heat and Mass Transfer*, 55(17-18), 4900-4907.
- Rashidi Kouchi, M., Khosravi, M., & Bahmani, J. (2011). A numerical solution of homogeneous and inhomogeneous harmonic differential equation with Haar wavelet. *International Journal of Contemporary Mathematical Sciences*, 6(41), 2009-2018.
- Rashidi, M. & Pour, S. (2010). Analytical approximation solutions for unsteady boundary-layer flow and heat transfer due to a stretching sheet by homotopy analysis method. *Nonlinear Analysis: Modelling and Control*, 15(1), 83-95.
- Razzaghi, M., & Ordokhani, Y. (2001). An application of rationalized Haar functions for variational problems. *Applied Mathematics and Computation*, 122(3), 353-364.
- Rohsenow, W. M. (1956). Heat transfer and temperature distribution in laminar-film condensation. *Transactions of the American Society of Mechanical Engineers*, 78, 1645-1648.

- Rose, J. W. (1988). Fundamentals of condensation heat transfer: Laminar film condensation. *International Journal of Japan Society of Mechanical Engineer*, 31(3), 357-375.
- Rubab, K., & Mustafa, M. (2016). Cattaneo-Christov heat flux model for MHD three-dimensional flow of Maxwell fluid over a stretching sheet. *PLoS ONE*, 11(4), Article ID 0153481.
- Saadatmandi, A. & Farsangi, J. A. (2007). Chebyshev finite difference method for a nonlinear system of second order boundary value problems. *Applied Mathematics and Computation*, 192(2), 586-591.
- Sadeghy, K., Hajibeygi, H., & Taghavi, S. M. (2006). Stagnation point flow of upper-convected Maxwell fluids. *International Journal of Non-Linear Mechanics*, 41(10), 1242-1247.
- Saeed, U. & Rehman, M. U. (2013). Haar wavelet-quasilinearization technique for fractional nonlinear differential equations. *Applied Mathematics and Computation*, 220, 630-648.
- Saeedi, H., Mollahasani, N., Mohseni Moghadam, M. & Chuev, N. G. (2011). An operational Haar wavelet method for solving fractional Volterra integral equations. *International Journal of Applied Mathematics and Computer Science*, 21(3), 535-547.
- Sakiadis, B. C. (1961). Boundary-layer behavior on continuous solid surface: I. Boundary-layer equations for two-dimensional and axisymmetric flow. *AIChE Journal*, 7, 26-28.
- Saravi, M., Herman, M. & Kaiser, D. (2013). Solution of Bratu's equation by He's variational iteration method. *American Journal of Computational and Applied Mathematics*, 3(1), 46-48.
- Shang, D. Y. (1997). An extended study on steady-state laminar film condensation of a superheated vapour on an isothermal vertical plate. *International Journal of Heat and Mass Transfer*, 40(4), 931-941.
- Sharidan, S., Mahmood, T. & Pop, I. (2006). Similarity solutions for the unsteady boundary layer flow and heat transfer due to a stretching sheet. *International Journal of Applied Mechanics and Engineering*, 11(3), 647-654.
- Shehzad, S. A., Alsaedi, A., Hayat, T., & Alhuthali, M. S. (2014). Three-dimensional flow of an Oldroyd-B fluid with variable thermal conductivity and heat generation/absorption. *PLoS ONE*, 9(1), Article ID 0078240.
- Sher, I., & Yakhot, A. (2001). New approach to the solution of the Falkner-Skan equation. *American Institute of Aeronautics and Astronautics Journal*, 39(5), 965-967.
- Shi, Z., Deng, L. Y., & Chen, Q. J. (2007). Numerical solution of differential equations by using Haar wavelets. *Proceedings of The 2007 International Conference on*

- Shu, J. J. (2012). Laminar film condensation heat transfer on a vertical, non-isothermal, semi-infinite plate. *Arabian Journal for Science and Engineering*, 37(6), 1711-1721.
- Sparrow, E. M., & Gregg, J. L. (1959). A boundary-layer treatment of laminar film condensation. *Transactions of the American Society of Mechanical Engineers*, 81, 13-17.
- Stewart, W. E. (1971). Asymptotic calculation of free convection in laminar three-dimensional systems. *International Journal of Heat Mass Transfer*, 14(8), 1013–1031.
- Straughan, B. S. (2010). Thermal convection with the Cattaneo-Christov model. *International Journal of Heat and Mass Transfer*, 53, 95-98.
- Sultana, T., Saha, S., Rahman, M. M., & Saha, G. (2009). Heat transfer in a porous medium over a stretching surface with internal heat generation and suction or injection in the presence of radiation. *Journal of Mechanical Engineering*, 40(1), 22-28.
- Sunmonu, A. (2012). Implementation of wavelet solutions to second order differential equations with Maple. *Applied Mathematical Sciences*, 6(127), 6311-6326.
- Suwono, A. (1980). Laminar free convection boundary layer in three-dimensional systems. *International Journal of Heat Mass Transfer*, 23(1), 53–61.
- Swaidan, W., & Hussin, A. (2013). Feedback control method using Haar wavelet operational matrices for solving optimal control problems. *Abstract and Applied Analysis*, 2013, Article ID 240352.
- Tajvidi, M., Razzaghi, M., & Dehghan, M. (2008). Modified rational Legendre approach to laminar viscous flow over a semi-infinite flat plate. *Chaos, Solitons and Fractals*, 35(1), 59-66.
- Tibullo, V., & Zampoli, V. (2011). A uniqueness result for the Cattaneo-Christov heat conduction model applied to incompressible fluids. *Mechanics Research Communications*, 38(1), 77-79.
- Vajravelu, K. (1994). Convection heat transfer at a stretching sheet with suction or blowing. *Journal of Mathematical Analysis and Applications*, 188(12), 1002-1011.
- Vajravelu, K., & Mohapatra, R. N. (1990). On fluid dynamic drag reduction in some boundary layer flows. *Acta Mechanica*, 81(1), 59-68.
- Vajravelu, K., & Rollins, D. (1991). Heat transfer in a viscoelastic fluid over a stretching sheet. *Journal of Mathematical Analysis and Applications*, 158(1), 241-255.

- Veldman, A. E. P., & van de Vooren, A. I. (1980). On a generalized Falkner-Skan equation. *Journal of Mathematical Analysis and Applications*, 75(1), 102-111.
- Wang, C. Y. (1989). Free convection on a vertical stretching surface. *Journal of Applied Mathematics and Mechanics*, 69(11), 418-420.
- Wang, L. (2004). A new algorithm for solving classical Blasius equation. *Applied Mathematics and Computation*, 157(1), 1-9.
- Wazwaz, A. M. (1999). A reliable modification of the Adomian decomposition method. *Applied Mathematics and Computation*, 102(1), 77-86.
- Wazwaz, A. M. (2005). Adomian decomposition method for a reliable treatment of the Bratu-type equations. *Applied Mathematics and Computation*, 166(3), 652-663.
- Wazwaz, A. M. (2007). The variational iteration method for solving two forms of Blasius equation on a half-infinite domain. *Applied Mathematics and Computation*, 188(1), 485-491.
- Wazwaz, A. M. (2016). The successive differentiation method for solving Bratu equation and Bratu-type equations. *Romanian Journal of Physics*, 61(5-6), 774-783.
- Weyl, H. (1942). On the differential equations of the simplest boundary-layer problem. *Annals of Mathematics*, 43(2), 381-407.
- White, F. M. (2005). *Viscous fluid flow*. New York: McGraw-Hill.
- Wilkins, J. E. (1980). Condensation on an extended surface. *Journal of Heat Transfer*, 102(1), 180-187.
- Wu, J. L. (2009). A wavelet operational method for solving fractional partial differential equations numerically. *Applied Mathematics and Computation*, 214(1), 31-40.
- Xu, H. (2004). An explicit analytic solution for free convection about a vertical flat plate embedded in a porous medium by means of homotopy analysis method. *Applied Mathematics and Computation*, 158(2), 433-443.
- Xu, H., You, X. C. and Pop, I. (2008). Analytical approximation for laminar film condensation of saturated stream on an isothermal vertical plate. *Applied Mathematical Modeling*, 32(5), 738-748.
- Yao, B. (2009). Approximate analytical solution to the Falkner-skan wedge flow with the permeable wall of uniform suction. *Communications in Nonlinear Science and Numerical Simulation*, 14(8), 3320-3326.
- Zarebnia, M. & Sarvari, Z. (2013). Numerical solution of the boundary value problems in calculus of variations using parametric cubic spline method. *Journal of Information and Computing Science*, 8(4), 275-282.
- Zheng, L., Wang L., & Zhang, X. (2011). Analytic solutions of unsteady boundary flow and heat transfer on a permeable stretching sheet with non-uniform heat

source/sink. *Communications in Nonlinear Science and Numerical Simulation*, 16(2), 731-740.

Zhu, S., Wu, Q., & Cheng, X. (2009). Numerical solution of the Falkner-Skan equation based on quasilinearization. *Applied Mathematics and Computation*, 215(7), 2472-2485.

University of Malaya

## LIST OF PUBLICATIONS AND PAPERS PRESENTED

### **Publications:**

- 1- Nor Artisham Che Ghani, Zailan Siri and Ruhaila Md. Kasmani. Heat transfer over steady stretching surface in the presence of suction. Accepted for publication in Boundary Value Problems.

### **Paper Presented:**

- 1- Nor Artisham Che Ghani, Amran Hussin and Zailan Siri. (2014, November). Analysis of three different Haar wavelet methods for solving boundary value problems. Paper presented at the 22nd National Symposium on Mathematical Sciences, Shah Alam, Malaysia.

University of Malaysia